UNIVERSITAT DE BARCELONA

Study of new strategies for steatotic liver disease: SIRT1-mediated modulation of VLDLR levels and evaluation of a soluble epoxyde hydrolase-targeted PROTAC

Mona Peyman

University of Barcelona

Faculty of Pharmacy and Food Sciences

Department of Pharmacology, Toxicology and Therapeutic Chemistry

Study of new strategies for steatotic liver disease: SIRT1-mediated modulation of VLDLR levels and evaluation of a soluble epoxyde hydrolase-targeted PROTAC

Mona Peyman

2024

UNIVERSITAT DE BARCELONA

University of Barcelona
Faculty of Pharmacy and Food Sciences
Department of Pharmacology, Toxicology and Therapeutic Chemistry

PhD Program in Biotechnology

Study of new strategies for steatotic liver disease: SIRT1-mediated modulation of VLDLR levels and evaluation of a soluble epoxyde hydrolase-targeted PROTAC

Dissertation presented by Mona Peyman to apply for the doctorate degree from the University of Barcelona

Directors

Dr. Manuel Vázquez Carrera
Dr. Emma Barroso Fernández

PhD Student

Mona Peyman

Mona Peyman

2024

The present doctoral thesis has generated two original scientific papers, one of them published (attached in the annex section) and the other one pending to submit:

Article 1:

Peyman, M., Barroso, E., Turcu, A. L., Estrany, F., Jr, Smith, D., Jurado-Aguilar, J., Rada, P., Morisseau, C., Hammock, B. D., Valverde, Á. M., Palomer, X., Galdeano, C., Vázquez, S., & Vázquez-Carrera, M. (2023). **Soluble epoxide hydrolase-targeting PROTAC activates AMPK and inhibits endoplasmic reticulum stress.** *Biomedicine & pharmacotherapy = Biomedecine & pharmacotherapie*, *168*,115667. https://doi.org/10.1016/j.biopha.2023.115667

Article 2:

Peyman, M., Babin-Ebell, A., Rodríguez-Rodríguez, R., Rigon, M., Aguilar-Recarte, D., Villarroya, J., Planavila, A., Villarroya, F., Palomer, X., Barroso, E., & Vázquez-Carrera, M. **SIRT1 REGULATES HEPATIC VLDLR LEVELS THROUGH HIF-1α.** (Pending to submit)

Additionally, extra scientific paper has been published during the development of the doctoral thesis and is attached in the annex section. These were obtained as a result of participating in other projects that do not correspond to the scope of the results presented in this thesis:

Barroso, Emma, Marta Díaz, Ana Cristina Reguera, **Mona Peyman**, Jesús Balsinde, Javier Jurado-Aguilar, Meijian Zhang et al. "**CHOP upregulation and dysregulation of the mature form of the SNAT2 amino acid transporter in the placentas from small for gestational age newborns**." *Cell Communication and Signaling* 21, no. 1 (**2023**): 326. https://doi.org/10.1186/s12964-023-01352-5

INDEX

Abbreviations

AA	Arachidonic Acid
AASLD	American Association for the Study of Liver Diseases
ADH	Alcohol Dehydrogenase
ALD	Alcohol-associated/related Liver Disease
ALDH	Aldehyde Dehydrogenase
AMPK	AMP-activated Protein Kinase
AR	Androgen Receptor
ATF4	Activating Transcription Factor 4
ATF6	Activating Transcription Factor 6
ATGL	Adipose Triglyceride Lipase
ATP	Adenosine Triphosphate
BiP	Binding immunoglobulin Protein
BMI	Body Mass Index
BP	Blood Pressure
CALR	Calreticulin
CaMKK2	Ca2+/calmodulin-dependent Kinase 2
CaMKKβ	Ca2+/calmodulin-dependent protein Kinase β
CCL20	Chemokine CC Ligand 20
CHB	Chronic Hepatitis B
CHC	Chronic Hepatitis C
CHOP	C/EBP Homologous Protein
ChREBP	Carbohydrate Response Element-Binding Protein

CKD	Chronic Kidney Disease
CLD	Chronic Liver Disease
CMC	Carboxymethylcellulose
CMRF	Cardiometabolic Risk Factor
COX	Cyclooxygenase
CRE	cAMP Response Elements
CRL4–CRBN	Cullin–RING Ligase 4–Cereblon
CT	Control
CVD	Cardiovascular Disease
CYP2E1	Cytochrome P4502E1
CYP450	Cytochrome P450
DAG	Diacylglycerol
DHA	Docosahexaenoic Acid
DHET	Dihydroxyeicosatrienoic Acid
DNL	*de novo* Lipogenesis
EASL	European Association for the Study of the Liver
EET	Epoxyeicosatrienoic acid
eIF2α	Eukaryotic Initiation Factor 2α
ELF	Enhanced Liver Fibrosis
EMA	European Medicines Agency
EpFAs	Epoxidized Fatty Acids
ER	Endoplasmic Reticulum
ER	Estrogen Receptor
ERAD	ER-associated protein Degradation

ERK1/2	Extracellular-signal-Regulated Kinase 1/2
ERO	ER Oxidoreductin
ERSE	ER Stress Elements
FABPs	FA Binding Proteins
FAO	Fatty Acid Oxidation
FAS	Fatty Acid Synthase
FAs	Fatty Acids
FATPs	Fatty Acid Transport Proteins
FFAs	Free Fatty Acids
FGF21	Fibroblast Growth Factor 21
FIB-4	Fibrosis-4 Index
FOXOs	Forkhead box proteins
FR	Fructose
G6Pase	Glucose 6-phosphatase
GADD34	Growth Arrest and DNA Damage-inducible protein 34
GAPD	Glyceraldehyde 3-Phosphate Dehydrogenase
GCKR	Glucokinase Regulator
GCN2	General Control non-derepressible kinase 2
GLUT1	Glucose Transporter 1
GRP78	Glucose-Regulating Protein 78 kDa
GTT	Glucose Tolerance Test
HCC	Hepatocellular Carcinoma
HDL	High-Density Lipoprotein
HFD	High Fat Diet

HIF	Hypoxia-Inducible Factors
HIF1α	Hypoxia-Inducible Factor 1α
HOMA-IR	Homeostatic Model Assessment for Insulin Resistance
HRI	Heme-Regulated Inhibitor Kinase
HSC	Hepatic Stellate Cells
hsCRP	High sensitivity C-reactive Protein
IL-32	Interleukin-32
INASL	Indian National Association for the Study of the Liver
IR	Insulin Resistance
IRE1	Inositol-Requiring Enzyme 1
IRE1α	Inositol-Requiring Enzyme 1α
IRs	Insulin Receptors
IRS	Integrated Stress Response
IRS1	Insulin Receptor Substrate 1
JNK	Jun N-terminal Kinase
KCs	Kupffer Cells
LFTs	Liver Function Tests
LKB1	Liver Kinase B1
LOX	Lipoxygenase
LPS	Lipopolysaccharide
MAFL	Metabolic dysfunction–Associated Fatty Liver Disease
MAPK	Mitogen Activated Protein Kinase
MASH	Metabolic dysfunction-Associated Steatohepatitis
MASLD	Metabolic dysfunction-Associated Steatotic Liver Disease

MCP-1	Monocyte Chemoattractant Protein-1
MRI	Magnetic Resonance Imaging
NAD^+	Nicotinamide Adenine Dinucleotide
NADPH	Nicotinamide Adenine Dinucleotide Phosphate
NAFLD	Non-alcoholic Fatty Liver Disease
NASH	Non-alcoholic Steatohepatitis
NF-κB	Nuclear Factor kappa-B
NK	Natural Killer
NRF2	Nuclear Factor-erythroid 2 Related Factor 2
p- eIF2α	phosphorylation of eukaryotic Initiation Factor 2α
PA	Palmitic Acid
PAMPs	Pathogen-Associated Molecular Patterns
PEPCK	Phosphoenolpyruvate Carboxykinase
PERK	PKR-like ER Kinase
PGC-1α	PPARγ co-activator 1 α
PHD	Prolyl Hydroxylase Domain
PKR	Protein Kinase R
PNPLA3	Patatin-like Phospholipase Domain Containing 3
POI	Protein of Interest
PPAR-α	Peroxisome Proliferator-Activated Receptor-α
PROTAC	Proteolysis Targeting Chimera
PUFAs	Polyunsaturated Fatty Acids
qPCR	Quantitative PCR
RIDD	Ire1 dependent decay

RNS	Reactive Nitrogen Species
ROS	Reactive Oxygen Species
SCFAs	Short-Chain Fatty Acids
sEH	Soluble Epoxide Hydrolase
SFAs	Saturated Fatty Acids
SIRT1	Sirtuin 1
SLD	Steatotic Liver Disease
SNPs	Single-Nucleotide Polymorphisms
SOCS3	Suppressor Of Cytokine Signaling 3
SREBP	Sterol Regulatory Element-Binding Protein
SSBs	Sugar-Sweetened Beverages
SSI3	STAT-induced STAT inhibitor
STAT3	Signal Transducer and Activator of Transcription 3
sXBP1	spliced XBP1
T2DM	Type 2 Diabetes Mellitus
TAK1	Transforming Activated Kinase 1
TBP	TATA-Binding Protein
TG	Triglycerides
TGF-β1	Transforming Growth Factor β1
TLRs	Toll-Like Receptors
TM	Tunicamycin
TM6SF2	Transmembrane 6 Superfamily 2
TNFα	Tumor Necrosis Factor α

TPD	Targeted Protein Degradation
TRAF2	Receptor-Associated Factor 2
TRAIL	TNF-related apoptosis inducing ligand
TRB3	Tribbles homolog 3
TSP-1	Thrombospondin 1
UPR	Unfolded Protein Response
USFDA	United States Food and Drug Administration
VAT	Visceral adipose tissue
VEGF	Vascular Endothelial Growth Factor
VLDL	Very Low-density Lipoproteins
VLDLR	VLDL Receptor
WC	Waist Circumference
XBP1	X box-Binding Protein 1

SUMMARY

Metabolic dysfunction-associated steatotic liver disease (MASLD) is the most common cause of chronic liver disease (CLD). The first stage in the development of MASLD is metabolic dysfunction-associated fatty liver (MASL), which is defined as a condition where excessive levels of triglycerides (TG) accumulate in the liver. Little is known about the role played by the uptake of lipoproteins, such as very low-density lipoproteins (VLDL) that predominantly transport TG in plasma, in the development of hepatic steatosis. Interestingly, endoplasmic reticulum (ER) stress-mediated increase in the levels of the VLDL receptor (VLDLR) results in remarkable hepatic steatosis via enhanced triglyceride-rich lipoprotein delivery to the liver. A better understanding of how hepatic VLDLR is regulated might help to develop new effective therapies against MASLD. On the other hand, soluble epoxide hydrolase (sEH), an enzyme highly expressed in the liver, converts epoxyeicosatrienoic acids (EETs) and other epoxy fatty acids (EpFAs) to their corresponding diols. These diols are much less bioactive than their parents' epoxides. As a result, compounds that inhibit sEH increase the levels of EETs and other EpFAs, which are opposing counterparts to the largely pro-inflammatory prostanoids and leukotrienes, thereby providing therapeutic efficacy for the treatment of several diseases, including hepatic steatosis. An additional new strategy for targeting sEH might be the use of proteolysis-targeting chimeras (PROTACs), due to its capacity to induce its degradation.

In the present thesis, we show that induction of hepatic steatosis by fructose-drinking water in rats caused a reduction in the levels of hepatic sirtuin 1 (SIRT1), a NAD $(^{+})$-dependent deacetylase, and upregulation of VLDLR, suggesting a potential relationship between these two proteins. Consistent with this, $Sirt1^{-/-}$ mice displayed increased hepatic VLDLR levels and enhanced expression of HIF-1α-target genes. Likewise, the increase in VLDLR protein levels induced by pharmacological inhibition or gene knockdown of SIRT1 in a human hepatic cell line was abolished by a HIF-1α inhibitor. Moreover, SIRT1

activation in mice prevented the increase in hepatic VLDLR protein levels caused by ER stress. Additionally, we report that the sEH-targeting PROTAC ALT-PG2 degrades this protein in the human hepatoma-derived Huh-7 cell line and in primary mouse hepatocytes as well as in the liver of mice. PROTAC-mediated degradation of the sEH protein in cells resulted in adenosine monophosphate-activated protein kinase (AMPK) activation, while phosphorylated extracellular-signal-regulated kinase 1/2 (ERK1/2) was reduced. Consistent with the role of these two kinases in ER stress, ALT-PG2 reduced both ER stress and inflammatory markers.

Altogether, the findings of the present doctoral thesis shed light on a new mechanism of VLDLR regulation and its contribution to hepatic steatosis and demonstrate that targeting sEH with a PROTAC molecule is an effective strategy to activate AMPK and to prevent ER stress and inflammation in hepatic cells.

RESUMEN

La causa más común de enfermedad crónica del hígado (CLD) es la enfermedad del hígado graso asociada a disfunción metabólica (MASLD, por sus siglas en inglés). El hígado graso asociado a la disfunción metabólica (MASL, por sus siglas en inglés), que se define como una condición donde se acumulan niveles excesivos de triglicéridos (TG) en el hígado, es la primera etapa en el desarrollo de MASLD. La captación de lipoproteínas, como las lipoproteínas de muy baja densidad (VLDL), que transportan principalmente TG en el plasma, es poco conocida por su papel en el desarrollo de la esteatosis hepática. Es destacable que el aumento de los niveles del receptor de VLDL (VLDLR) mediado por el estrés del retículo endoplásmico (ER) contribuye significativamente a la esteatosis hepática a través de un aumento en la captación de lipoproteínas ricas en triglicéridos por el hígado. Entender mejor cómo se regulan los niveles de VLDLR hepático podría ayudar en el desarrollo de nuevas terapias contra el MASLD. Por otro lado, la epóxido hidrolasa (sEH, de su acrónimo en inglés *soluble epoxide hydrolase*), una enzima que se expresa de forma abundante en el hígado, convierte ácidos eicosatrienoicos epóxicos (EETs, *epoxyeicosatrienoic acids*) y epoxiácidos (EpFA, *epoxy fatty acids*) en sus correspondientes dioles. Estos dioles son menos bioactivos que sus precursores epóxidos. El resultado de la inhibición de la sEH es un aumento de los niveles de EETs y otros EpFAs, que son antagónicos de prostanoides y leucotrienos proinflamatorios. El aumento de estos compuestos proporciona eficacia terapéutica para el tratamiento de varias enfermedades, incluida la esteatosis hepática. Debido a su capacidad para inducir su degradación, las quimeras de direccionamiento de proteólisis (PROTACs, *proteolysis-targeting chimeras*) podrían ser una nueva estrategia para degradar la sEH. En esta tesis demostramos que el consumo de fructosa en ratas causó esteatosis hepática, reduciendo los niveles de sirtuina 1 hepática (SIRT1), una deacetilasa dependiente de NAD $^{(+)}$, y aumentando los de VLDLR, lo que sugería una relación potencial entre estas dos proteínas. . De hecho, los ratones deficientes en SIRT1 presentaban niveles más altos de

VLDLR hepático y mayor expresión de los genes diana de HIF-1α. Asimismo, el aumento de los niveles de VLDLR inducidos mediante inhibición farmacológica o la inactivación del gen de SIRT1 en una línea celular hepática humana se contrarrestó con un inhibidor HIF-1α. Además, la activación de SIRT1 en ratones impidió el aumento de los niveles de proteína VLDLR hepático provocado por el estrés del ER. Adicionalmente, demostramos que un PROTAC dirigido contra la sEH, ALT-PG2, degrada esta proteína en hepatocitos primarios de ratón, en la línea celular de hepatoma humano Huh7 así como en hígado de ratón. La degradación de la sEH causada por el PROTAC en células activó la proteína quinasa activada por monofosfato de adenosina (AMPK), mientras que los niveles de la quinasa regulada por señales extracelulares 1/2 (ERK1/2) disminuyeron. En consonancia con el papel que estas dos quinasas desempeñan en el estrés del RE, ALT-PG2 disminuyó tanto los niveles de marcadores de estrés del RE como inflamatorios.

Los resultados generales de la tesis doctoral desvelan un nuevo mecanismo de regulación de VLDLR y su papel en la esteatosis hepática, y asimismo demuestran que la degradación de la proteína sEH con una molécula PROTAC es un método efectivo para activar AMPK y prevenir el estrés y la inflamación en las células hepáticas.

I. INTRODUCTION

I.1. Steatotic Liver Diseases (SLD) and the new nomenclature

The term "chronic liver disease" (CLD) refers to a progressive decline in liver function that lasts longer than six months. This decline affects the liver's ability to synthesise clotting factors and other proteins, detoxify toxic metabolic products, and excrete bile. Fibrosis and cirrhosis are the results of the ongoing inflammation, destruction, and regeneration of the liver parenchyma in CLD. CLD has many different etiologies, such as exposure to toxins, long-term alcohol misuse, infections, autoimmune diseases, genetic disorders, and metabolic problems. The last stage of CLD, known as cirrhosis, is characterized by disruption of the architecture of the liver, formation of widespread nodules, vascular reorganization, neo-angiogenesis, and extracellular matrix deposition. At the cellular level, fibrosis and cirrhosis are caused by the recruitment of fibroblasts and stellate cells, whereas parenchymal regeneration is dependent on hepatic stem cells (Sharma, and Shivaraj.2023, Casey,2016). CLD which affects 800 million people worldwide and results in 2 million deaths annually, includes alcoholic liver disease (ALD), chronic hepatitis B (CHB), and non-alcoholic fatty liver disease (NAFLD) (Jerez, et al.2023). NAFLD affects 25% of the global population and is mainly characterized by hepatic steatosis (Younossi et al., 2016). A severe form of NAFLD known as non-alcoholic steatohepatitis (NASH), which is characterized by increased inflammation and hepatocyte injury, affects roughly 10% to 15% of patients suffering NAFLD (Torres, et al.2021).

Although excess fat deposition in the liver has been known for centuries, there were several reasons why it was time for the nomenclature to be updated. The first time the term NAFLD was used was when von Rokitansky described the visceral and subcutaneous adiposity in overfed children in 1849. Since then, the field has struggled to come up with appropriate nomenclature (Ludwig, et al.1980).

Subsequently, the liver histology linked to excess liver fat without a history of heavy alcohol use was initially referred to as NASH. The researchers used the term "non-alcoholic" because, at the time, there was little understanding of the pathophysiological basis of alcohol-related liver disease, and the histopathological findings mirrored those of individuals with this condition. Since the term NAFLD was added to the medical compendium because there were no other options, there have been talks about renaming the condition to more accurately describe the disease process and go beyond the apparent histopathological similarities to alcohol-related liver disease (Bedossa, et al. ,2012). In fact, it is now understood that ALD and NAFLD may be caused by similar biological mechanisms (Israelsen, et al.2024). In 2020 it was proposed to refer to patients with a fatty liver regardless of the quantity and pattern of alcohol intake under the term metabolic dysfunction–associated fatty liver disease (MAFLD) (Eslam, et al.2020). While some people accepted MAFLD, others expressed concerns about the confluence of etiologies due to.

The new terminology for liver disease was developed and finalized by the members of the American Association for the Study of Liver Diseases (AASLD) in June 2023 (Rinella, et al.2023). The general term for all steatosis aetiologies was chosen to be steatotic liver disease (SLD) (Figure 1). It was believed that the term "steatohepatitis" was a crucial pathophysiological idea that ought to be kept. The term metabolic dysfunction-associated steatotic liver disease (MASLD) will now be used to refer NAFLD. Patients with hepatic steatosis with at least one of the five cardiometabolic risk factors are classified as having MASLD (Fouad,.2023).

Beyond pure MASLD, a new category called MetALD (pronounced Met A-L-D) was chosen to characterize MASLD patients who drink more alcohol on a weekly basis (140 g/week for females and 210 g/week for males, respectively). NASH has been replaced with metabolic dysfunction-associated steatohepatitis (MASH). Cryptogenic SLD is characterized by the absence of metabolic parameters and an unknown cause (Rinella, et al.2023).

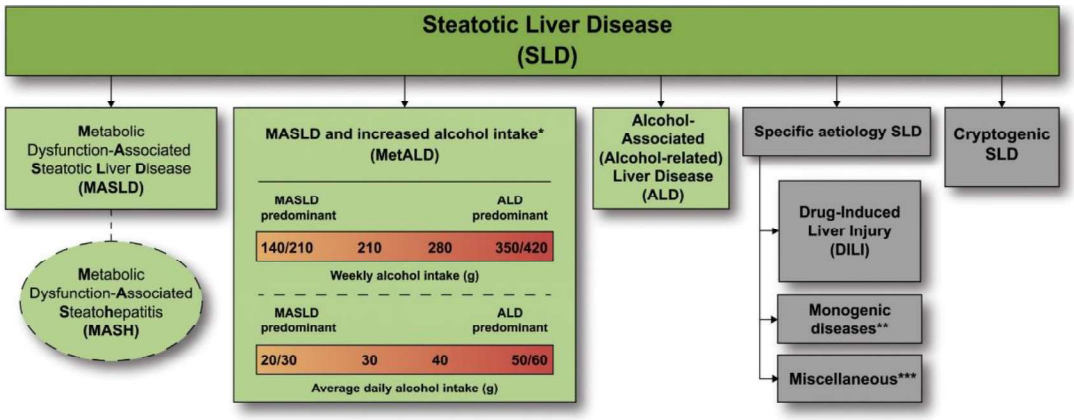

Figure 1. This figure shows the SLD schema along with its subcategories. Although there are many causes of SLD, MASLD, ALD, and their combination (MetALD) are the most common. Hepatic steatosis plus one cardiometabolic risk factor without additional apparent causes is what defines MASLD, and individuals who have both MASLD and steatohepatitis are referred to as MASH. The MetALD category represents a range of ALD and MASLD influence, so specific recommendations for alcohol consumption must be made based on each person's susceptibility. Moreover, different pathophysiological circumstances demand separate investigation for alternative causes of SLD, highlighting the significance of comprehensive diagnostic assessments for metabolic dysfunction or cryptogenic SLD. With the help of this method, early MASLD detection is made easier, coexisting liver conditions can be acknowledged, and intake recommendations can be modified to reduce risk (Rinella, et al.2023).

I.1.1. MASLD and MASH

MASLD is the leading cause of liver disease worldwide and its global incidence and prevalence is increasing every year due to its link with obesity and type 2 diabetes mellitus (T2DM) (Chan, et al.2023). In USA, is the only liver disease that has been systematically rising over the past three decades (Kalligeros, et al.2023). Moreover, the past 20 years have seen a rise in the prevalence of MASLD in the Asian population (Yang, et al.2023), which can be attributed to the rise in sedentary lifestyles, overweight, and T2DM.

In our country, a study on the prevalence and risk factors of MASLD among the prison population of Catalonia shows that one-third of this population had at least one metabolic disorder. The percentage of inmates with MASLD was found to be 33.9%; of them, 16.4% and 9.4% had significant fibrosis and MASLD-associated significant fibrosis, respectively. The population under study had higher alcohol-induced liver injury (ALT) values, metabolic syndrome, T2DM, and waist circumference (WC) as independent risk factors for MASLD and MASLD-associated significant fibrosis (Rivera-Esteban, et al.2023).

Initially, MASLD may progress without apparent symptoms and be considered a silent disease. The first stage in the development of MASLD is SLD, which is defined as a condition where excessive levels of triglycerides accumulate (TG) in the liver (at least 5% of liver weight) without evidence of significant hepatocyte ballooning indicative of hepatocellular damage in the absence of competing liver disease etiologies (Polyzos, et al. 2019). The underlying mechanisms for the accumulation of fat in the liver in MASLD include excess dietary fat, increased delivery of free fatty acids (FFAs) to the liver, and *de novo* lipogenesis (DNL) (Bugianesi, et al.2010).

On the other hand, it should be noted that it has been suggested that the buildup of inert TGs in the liver is an adaptive reaction to an excess of FFAs, shielding hepatocytes from the lipotoxic effects of excess toxic FFAs or from the synthesis of lipotoxic species derived from fatty acids (FAs), such as ceramide and diacylglycerol (DAG) as well as lysophosphatidylcholine (Bril, et al.2017, Kawano, et al.2015). After the physiologically adaptive mechanisms are overridden, an excess of FAs causes lipotoxicity, which is a set of detrimental effects that include mitochondrial dysfunction and reactive oxygen species (ROS) production, stress on the endoplasmic reticulum (ER), and inflammation pathways being activated as well as cell death and hepatocellular damage (Tsuchida, and Friedman.2017).

After years of MASLD progression, it can lead to MASH, a severe disease in which hepatic steatosis is accompanied by inflammation, hepatocellular ballooning and may also include varying degrees of fibrosis (Manne, et al. 2018). A key mechanism driving fibrosis is the activation of hepatic stellate cells, producing highly proliferative extracellular matrix–myofibroblasts once activated and differentiated (Wiering, et al.2023). Eventually, in an advanced stage, MASH can manifest in liver cirrhosis and hepatocellular carcinoma (HCC) (Musio, et al.2023). Related to this, the prognosis of MASLD, has a certain degree of uncertainty, while the progression of MASLD from steatohepatitis to fibrosis in some patients is known to take a long time, others experience a quicker transition from cirrhosis to HCC. (Nath and Shivaram. 2018). In addition to these complications, MASLD/MASH presents a major factor in several systemic complications, including T2DM, cardiovascular disease (CVD), and chronic kidney disease (CKD). So, patients with MASH have a mortality rate of 11.77 per 1000 person-years for liver-specific causes and a 25.56 annual all-cause mortality rate per 1000 person-years for other causes, which is significantly higher than the general population or patients without this inflammatory subtype of MASLD (Sheka, et al.2020) (Figure 2).

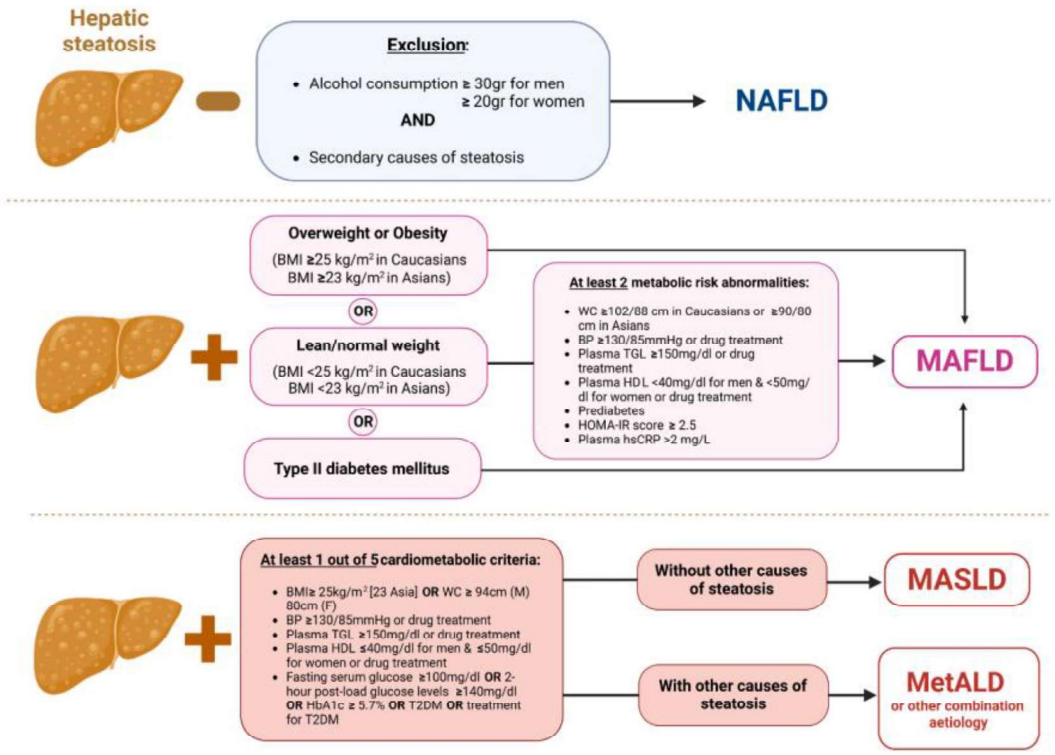

Figure 2. The terms metabolic NAFLD, MAFLD, MASLD are defined. Body mass index (BMI), waist circumference (WC), triglyceride lipid (TGL), blood pressure (BP), and high-density lipoprotein (HDL), insulin resistance (IR) measured by the homeostasis model assessment (HOMA-IR), high sensitivity C-reactive protein (hsCRP), type 2 diabetes mellitus (T2DM) (Lekakis and George .2023)

The most definitive method for diagnosis is liver biopsy, which is considered the gold standard. However, liver biopsy is invasive and carries certain risks, making it less ideal for routine diagnosis. This limitation underscores the need for developing safer, non-invasive diagnostic methods that can reliably detect and assess the severity of MASLD (Castera.2018) (Figure 3).

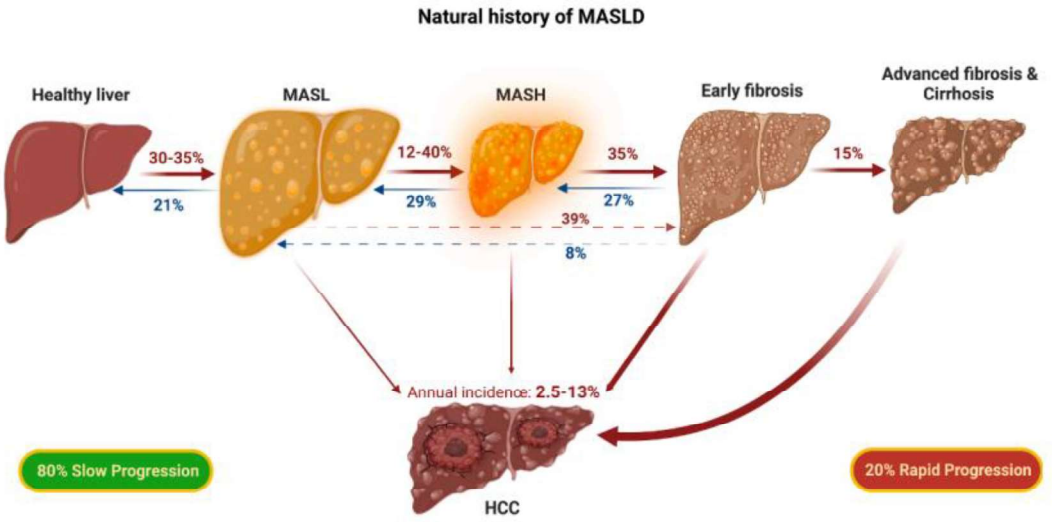

Figure 3. Untreated metabolic liver disease can result in irreversible conditions that requires liver transplantation. Since the natural history data that are currently available mostly comprise of patients who have been selected for further evaluation, they most likely overestimate the rates of progression among MASLD patients (Lekakis and George.2023).

Due to the complexity of the disease and how it progresses, non-invasive and, less frequently, invasive methods are used in the diagnosis of MAFLD and its more severe form, MASH. Assessing the degree of liver fat accumulation, inflammation, and fibrosis is the main objective in the diagnosis of MASLD. It is also important to distinguish between MASH and simple steatosis, as the latter has a greater propensity to develop into cirrhosis and HCC. Biochemical testing, imaging methods, and the application of particular biomarkers are examples of diagnostic approaches. Conventional liver function tests (LFTs), like AST and ALT, are frequently performed. However, in many MASLD cases, their results may be normal. To more precisely assess liver fibrosis and steatosis levels without requiring a liver biopsy, more targeted non-invasive tests and biomarkers have been developed, such as the MASLD liver fat score, fibrosis-4 index (FIB-4), and the enhanced liver fibrosis (ELF) panel (Martinou, et al.2022, Piazzolla, et al.2020).

Imaging methods are essential for both diagnosing and tracking MASLD. Although ultrasound is frequently used to identify steatosis, its sensitivity is limited, particularly in obese patients and those with less severe fat accumulation. More accurate measurements of liver fibrosis and fat are possible with advanced imaging techniques like magnetic resonance imaging (MRI) and elastography, which includes FibroScan. Particularly with MRI, liver fat content can be accurately quantified (Tincopa, and Rohit.2023). New "omics" technologies such as proteomics, metabolomics, and genomics are being investigated to find novel biomarkers that could help with MASLD pathogenesis understanding, risk assessment, and diagnosis. These methods seek to identify the molecular changes linked to MASLD and MASH, potentially leading to the development of personalized medicine techniques in the future (Martinou, et al.2022). Finally, a suggested diagnostic algorithm aims to lessen the need for liver biopsies, which are currently the gold standard for diagnosis but have risks and limitations. It suggests a tiered approach using non- or minimally invasive markers to identify and differentiate between MASLD and MASH (Figure 4) (Piazzolla, et al.2020).

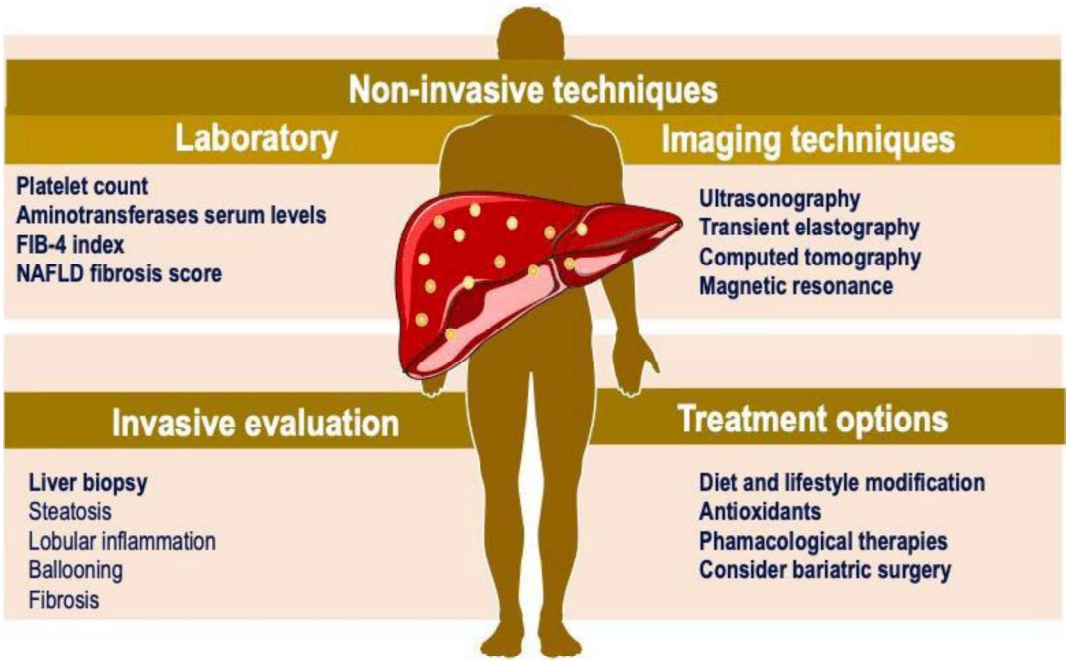

Figure 4. MASLD diagnosis and therapeutic strategy. Non-invasive methods, invasive assessment, and therapeutic choices (Salva-Pastor, et al.2019).

I.1.1.1. The “multiple- hit” pathogenesis in the development of MASLD/MASH

Complex and multifactorial mechanisms underlie the onset and progression of MASLD/MASH. Several theories have been proposed, which first gave rise to the "two-hit hypothesis." This suggests that a first hit such as a sedentary lifestyle, a high-fat diet, obesity, and IR acts to promote hepatic accumulation of lipids. Then a "second hit" sensitizes the liver to additional insults. Fibrogenesis and inflammatory cascades are triggered by the "second hit." However, it quickly became evident that this perspective is too reductionist to fully capture the intricacy of human MASLD/MASH, where several concurrent factors, working in concert with one another in genetically predisposed individuals, are responsible for the onset and advancement of the illness. Thus, for the progression of MASLD/MASH, a multiple-hit hypothesis (Figure 5) has now replaced the antiquated two-hit hypothesis (Filipovic, et al.2023, Rupasinghe, et al.2023). Next, we will describe some of the reported hits that promote MASLD/MASH progression as well as some additional pathways and strategies involved in MASLD development and prevention.

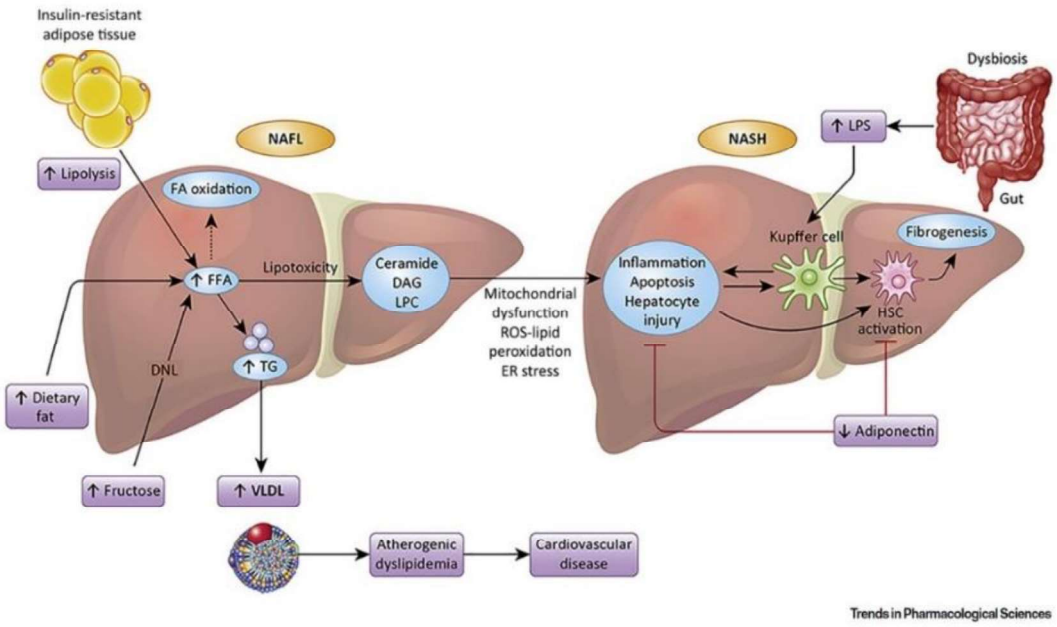

Figure 5. Schematic Summary of the Pathophysiology of MASH. very low-density lipoproteins (VLDL), lipopolysaccharide (LPS), hepatic stellate cells (HSC) and diacylglycerol (DAG) (Zarei, et al.2020).

I.1.1.1.1. Genetic Factors

Genetic and epigenetic factors play significant roles in MASLD and MASH. Several single-nucleotide polymorphisms (SNPs) have been linked to MAFLD through genome-wide and exome-wide association studies. These SNPs include well-known SNPs in genes like Patatin-like Phospholipase Domain Containing 3 (*PNPLA3*), transmembrane 6 superfamily 2 (*TM6SF2*), and Glucokinase Regulator (*GCKR*), as well as some more recently found SNPs linked to liver steatosis (Zhu, et al.2016).

The development of MASLD and MASH has been closely linked to the *PNPLA3* gene. There is a correlation between the I148M variant of this gene and a higher risk of liver fibrosis as well as increased accumulation of liver fat (Cherubini, et al.2021). Increased hepatic lipid content is associated with I148M, a non-synonymous cytosine to guanine mutation that results in isoleucine to methionine conversion.

This mutation also predisposes to fatty liver-associated liver disease, which includes fibrosis, hepatocellular carcinoma, and simple steatosis (Schwartz, et al.2020).

The function of the 481 amino acid protein that *PNPLA3* encodes is still unknown. Acting on triacylglycerol, diacylglycerol, and monoacylglycerol, it appears to have an acylglycerol hydrolase function. Further data suggests that PNPLA3 functions as an acetyltransferase of lysophosphatidic acid (Caligiuri, et al.2016). Increased fatty acid synthesis, decreased triacylglycerol hydrolysis, and triacylglycerol accumulation are all caused by overexpression of the I148M variant in the mouse liver (Smagris, et al.2015). Additionally, it has been observed that the *PNPLA3* genotype affects the amount of retinol stored in the liver and the amount of retinol in serum in obese individuals, indicating a possible function of PNPLA3 in controlling the metabolism of retinol and the biology of hepatic stellate cells (HSCs) (Kovarova, et al.2015). According to reports, PNPLA3 could perform both anabolic and catabolic enzymatic tasks by acting as a transacylase or TG hydrolase. Hepatic steatosis is linked to the L148M mutant of *PNPLA3*. However, it is unclear if this is because of a gain-of-function mutation that results in overexpression of the enzyme or a loss of function mutation that reduces the hydrolyc function of the enzyme (Manne, et al.2018).

Additionally, mutations in *TM6SF2* have been linked to reduce hepatic TG secretion causing steatosis in mouse models. TM6SF2 has also a significant role in the promotion of hepatocellular cancer and hepatic fibrosis (Luo, et al.2022). These gene's variants that cause changes in lipid metabolism in liver cells are linked to increased fat storage and liver damage (Xue, et al.2022).

Likewise, the *GCKR* gene, which is involved in glucose metabolism, linked to MAFLD. Variants in this gene may affect the liver's metabolism of lipids and carbohydrates, which may result in the buildup of fat (Lin, et al.2014).

I.1.1.1.2. Dietary Factors

As an essential characteristic of MASLD, increased hepatic steatosis has been linked to specific dietary patterns. These eating habits usually include consuming large amounts of particular foods and nutrients, which can lead to the buildup of fat in the liver. The following are some of the main food habits connected to elevated hepatic steatosis.

High Sugar and High Fructose Diets. Hepatic steatosis and sugar-rich diets, particularly those high in fructose, are closely related. Fat synthesis, or lipogenesis, is stimulate by fructose, which the liver directly metabolizes. These diets increase lipogenesis and decrease fat oxidation, which are two mechanisms that lead to the buildup of fat in the liver. (Jensen, et al.2018). A major factor in this process is the liver's metabolism of fructose. Fructose metabolism produces uric acid and ATP depletion, both of which contribute to the buildup of fat in the liver. In addition to increase DNL, this process can result in liver inflammation, IR and other cardiometabolic diseases. It was discovered that fructose from fruit juice and sugar-sweetened beverages (SSBs) was independently linked to increased intrahepatic lipid content, but fructose from whole fruits did not exhibit the same correlation. This suggests that the way fructose is ingested can affect how it is metabolized (Malik, and Frank.2022). Fructose is used as a sweetener in liquid beverages, and epidemiological evidence points to a causal relationship between human populations' consumption of sugar-sweetened beverages and SLD. It has been suggested that the high energy intake, insufficient energy compensation, and unique fructose metabolism account for this association. Consuming fructose is also linked to the development of hypertriglyceridemia (Rebollo, et al.2014). Due to insufficient expression in the gut's cells of glucose transporter 5, the transporter responsible for fructose uptake, fructose is difficult to absorb through the gastrointestinal tract (Song, et al.2023, Smith, et al.2022). Through the portal vein, fructose is transported to the liver for initial metabolism after being absorbed from the intestine (Manne, et al.2018).

Diets high in fructose have the potential to precipitously progress nearly all basic metabolic syndrome diseases. Obesity, arterial hypertension, high serum sugar/impaired glucose tolerance, elevated serum TG, and decreased HDL are all linked to this condition (Figure 6) (Roeb, and Weiskirchen,2021).

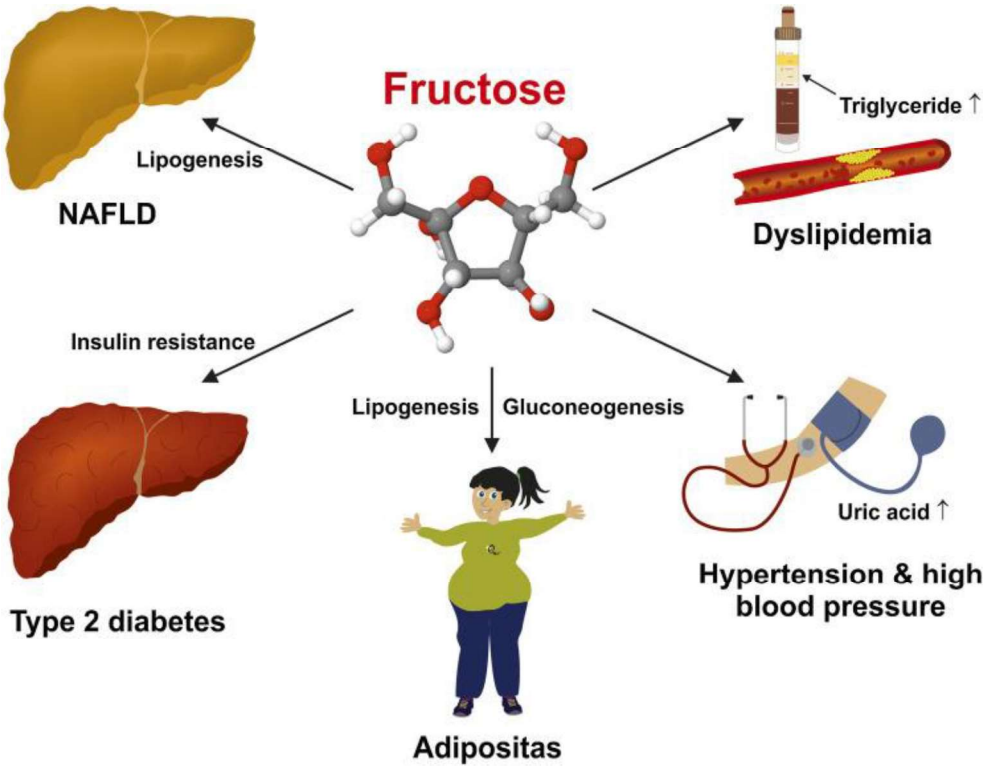

Figure 6. Negative health effects of consuming large amounts of fructose. Overconsumption of fructose raises the risk of a number of chronic conditions, such as obesity, dyslipidemia, IR/TD2, hyperuricemia, and MASLD (NAFLD) (Roeb, Elke, and Ralf Weiskirchen,2021).

Increased consumption of fructose in the diet has also been connected to changes in the composition of the gut microbiome, including a shift toward the depletion of helpful microbial species. Fructose, but not glucose, adds to the impairment of mitochondrial function in the liver when combined with a high-fat diet (HFD). Dietary fructose has been connected to the indirect development of hepatic IR through disruption of these pathways, and as a result, it may play a significant role in the pathophysiology of MASLD (Figure 7) (Johanna, and Q Shaibi.2021).

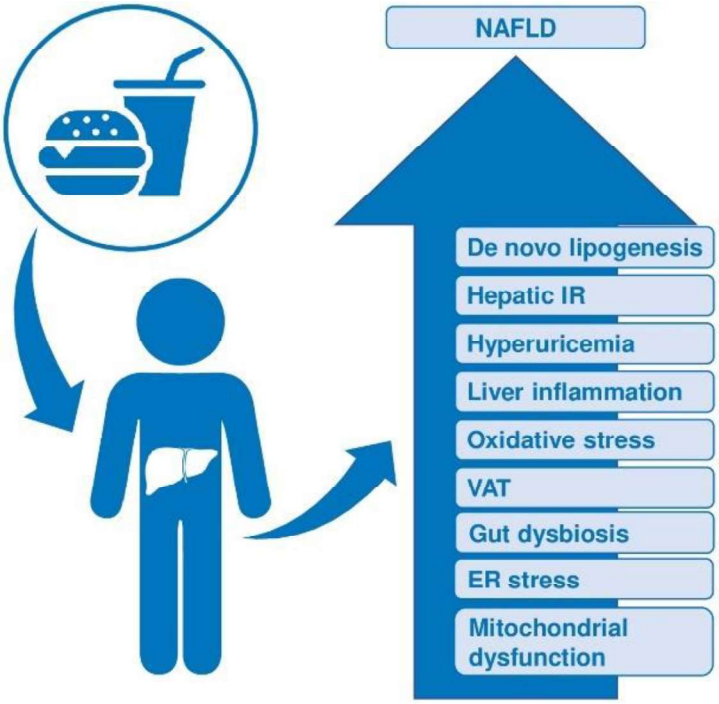

Figure 7. Effects of high fructose consumption on biological pathways in developing and progressing NAFLD. High intake of fructose or added sugar has been linked to increased visceral adiposity, oxidative stress, hepatic inflammation, hyperuricemia, DNL, and IR. Intestinal dysbiosis has also been linked to high fructose consumption (Johanna, and Q Shaibi.2021).

High Fat and High Calorie Diets. Hepatic steatosis can arise as a result of diets heavy in trans and saturated fats, which are frequently found in fried, processed, and fast food. Whatever the source, an excessive calorie diet can also cause the liver to become overweight (Parra-Vargas, et al.2020). Research on both humans and animals has shown how the HFD affects hepatic steatosis. The composition of the diet affects how the HFD affects the histology of MASLD. In particular, studies have shown that polyunsaturated fatty acids (PUFAs) improve hepatic steatosis and raise insulin sensitivity while saturated fatty acids (SFAs) have been shown to promote obesity and hepatic steatosis (Žáček, et al.2019, Lian, et al.2020).

Western Diet. An increased risk of MASLD and hepatic steatosis is linked to the typical Western diet, which is defined by a high intake of red and processed meats, refined grains, and sugary desserts and a low intake of fruits, vegetables, and whole grains (Gerges, et al.2021). A Western diet can raise the risk of MASLD by as much as 56%, according to studies. Healthy eating habits, on the other hand, such as the Prudent or Mediterranean diets, which are high in whole grains, fruits, vegetables, and healthy fats, are linked to a 22% and 23% lower risk of NAFLD, respectively (Cartland, et al.2020, Hassani Zadeh, et al.2020).

Low Fiber Diet. Fiber-poor diets may be a factor in MASLD. Dietary fiber, particularly that which comes from fruits, vegetables, and whole grains, is essential for sustaining gut health, enhancing insulin sensitivity, and controlling body weight, all of which are critical for liver health (Zhao, et al.2020). Furthermore, through fermentation in the gut, dietary fiber aids in the short-chain fatty acids (SCFAs). SCFAs are known to be beneficial for conditions related to obesity, such as MASLD. They may have an indirect effect on liver health by influencing the gut-liver axis. This emphasizes how crucial a well-balanced diet high in dietary fiber is for liver function and general metabolic health (Zhang, et al.2021, Zhu, et al.2023).

Alcohol Consumption. Excessive alcohol consumption is a well-known cause of liver damage and fat accumulation in the liver, even though it is not a dietary pattern per se. Moderate to high alcohol consumption can exacerbate the MetALD (Hajifathalian, et al.2019, Weng and Winston.2019). Furthermore, studies have demonstrated that mild alcohol consumption among MASLD patients is associated with a reduction in all-cause mortality, whereas higher levels of consumption (more than 1.5 drinks per day) are linked to an increase in mortality. This points to a complex link between alcohol consumption and the development of liver disease in MASLD patients (Oh, et al.2023).

I.1.1.1.3. Lipid metabolism in MASLD/MASH

An organ crucial to the metabolism of lipids is the liver. The liver is in charge of coordinating the production of new FAs, their export and subsequent redistribution to other tissues, as well as their use as energy substrates. It is a central regulator of lipid homeostasis. Hepatic lipid homeostasis is tightly controlled by these processes, which are governed by intricate interactions between nuclear receptors, transcription factors, and hormones. The retention of fat in the liver and the subsequent onset of MASLD may be accelerated by the disruption of one or more of these pathways. An imbalance between the uptake and disposal of lipids leads to hepatic fat accumulation. This imbalance is regulated by four main pathways: the uptake of circulating lipids, DNL, FAO, and export of lipids in very low-density lipoproteins (VLDL) (Figure 8). Nevertheless, the molecular processes that underlie the abnormal accumulation of fat in the liver remain incompletely understood (Ipsen, et al.2018).

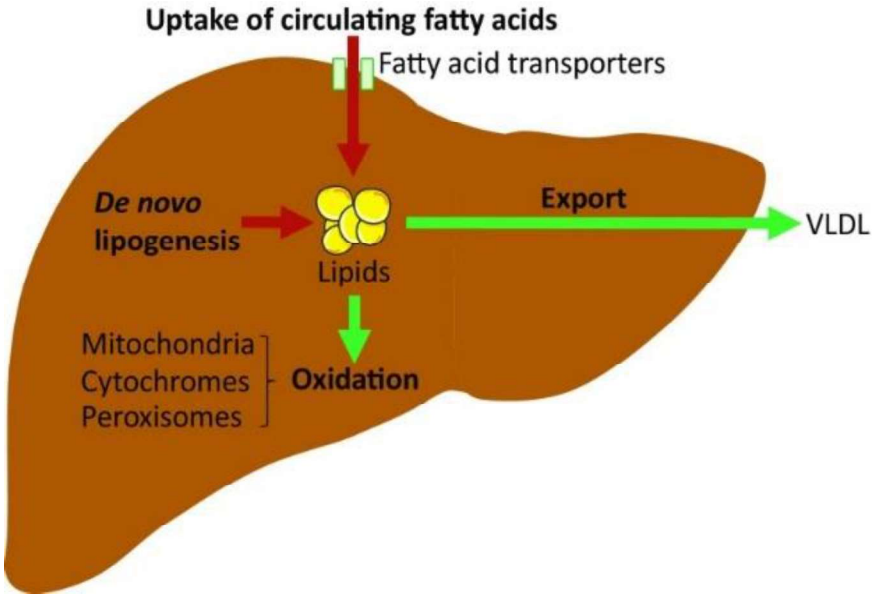

Figure 8. Hepatic lipid uptake and excretion. The balance between lipid acquisition and disposal, which make up the four main pathways of hepatic lipid homeostasis, controls intrahepatic lipid levels. The liver gets its lipids from DNL and from the uptake of circulating fatty acids. On the other hand, lipids can be eliminated by export as VLDL particles and by oxidation (in the mitochondria, peroxisomes, and cytochromes). Thus, if lipid acquisition pathways outweigh lipid disposal pathways, lipid accumulation results (Ipsen, et al.2018).

The hepatic uptake of excess FFA is usually derived from adipocytes via lipolysis. The release of FAs from adipose tissue occurs under the control of adipose triglyceride lipase (ATGL), hormone-sensitive lipase, and monoglyceride lipase (Nassir, 2022). One study reported the importance of FA uptake in the pathogenesis of MASLD, stating that approximately 60% of hepatic TG in human subjects is derived from plasma non-esterified FAs (Manne, et al. 2018). The liver takes up FAs from the circulation through both passive diffusion and active transport. Different proteins take part in FA uptake in the liver, including the FA translocase CD36, the FA transport proteins (FATPs), and the FA binding proteins (FABPs) (Nassir, 2022).

Specific FA transporters found in the hepatocyte plasma membrane facilitate the uptake of circulating lipids, and Peroxisome Proliferator-Activated Receptor (PPAR)-γ regulates this process. Hydrophobic FAs are more easily transported by FABP1 to the various cytoplasmic compartments of cells. Acetyl-CoA, which is produced from surplus carbohydrates, is transformed into new fatty acids by de novo lipogenesis. These fatty acids can then be esterified and stored as TGs. The intricate regulation of DNL is predominantly governed by two pivotal transcription factors, namely SREBP1c and ChREBP. PPARα regulates fatty acid oxidation, which uses lipids as an energy source to lower intrahepatic fat levels. Although the process mostly takes place in the mitochondria, lipid overload and/or impaired mitochondrial function necessitate a greater degree of FAO in the cytochromes and peroxisomes, which produces ROS. Lipids can be exported by the liver in the form of water-soluble VLDL particles, which can subsequently be stored or used by other tissues. ROS, PPAR (peroxisome proliferator-activated receptor), SREBP1c, VLDL, and ChREBP (carbohydrate regulatory element binding protein) are some examples of the proteins involved in this process (Ipsen, et al.2018).

Therefore, the amount of intrahepatic lipids is the result of the balance between processes promoting FA synthesis/uptake and export/oxidation.

Compared to healthy subjects, where DNL contributes 5% to the accumulation of TGs, DNL in MASLD patients contributes 26% to the increase in TGs (Basaranoglu, et al 2015). Transport of endogenously synthesized TG and cholesterol from the liver into the bloodstream and to other parts of the body is mainly carried out by VLDLs that contain apoB100 as an obligatory structural component that requires progressive lipidation (Ramms, et al.2019).

Patients with NAFLD have higher levels of VLDL secretion, and there is a direct correlation between liver triglyceride content and VLDL-TG secretion rates. The secretion of VLDL-TG, however, peaks when the hepatic fat content surpasses 10%, exceeding the compensatory capacity to prevent the increase in hepatic lipid accumulation.

This contrasted with the export of VLDL-TG, which increased with intrahepatic lipid content. VLDL-apoB100 secretion remains unchanged in patients with hepatic steatosis, despite higher VLDL-TG secretion relative to healthy individuals. This suggests that NAFLD patients do not secrete more VLDL particles, but rather larger and more triglyceride rich VLDL particles (Kanda, et al. 2018).

Finally, resident hepatic macrophages, known as Kupffer cells (KCs), can contribute to hepatic steatosis and the progression of MASDL due to a dual effect. Polarization of macrophages to the M1 phenotype, the pro-inflammatory subtype, can lead to increased hepatic steatosis via increased activity of DAG transferase, which converts DAG to TG. In addition, the macrophage M1 phenotype also plays an important role in modulating FAO through inhibition of PPAR-α (Manne, et al 2018).

I.1.1.1.4. Inflammation, IR and gut microbiota in MASLD/MASH

An important factor in the development of MASLD and MASH is the inflammatory process. Toxic lipid overload, mainly FFA, causes cellular stress and induces specific signals that trigger hepatocyte apoptosis, the predominant mechanism of cell death in MASH, correlating with the degree of inflammation and liver fibrosis. (Caligiuri, et al 2016). Research has been done on how particular molecules in MASLD cause fibrosis and inflammation. For example, it has been demonstrated that interleukin-32 (IL-32) and chemokine CC ligand 20 (CCL20) can be expressed in vitro when palmitic acid (PA) is present and the development of fibrosis in MASLD is associated with these molecules. The molecular mechanisms through which dietary components may influence the inflammatory process in MASLD are highlighted by the fact that the expression of IL-32 and CCL20 is mediated by signaling pathways such as Extracellular-signal-Regulated Kinase 1/2 (Erk1/2) and p38/ERK-mitogen activated protein kinase (MAPK) (Schilcher, et al.2023).

Additionally, there is a great deal of crosstalk between the gut, liver, and adipose tissue during the immune and inflammatory response in MASH. Adipocytes and macrophages in adipose tissue release a variety of adipokines, which contribute to liver inflammation. Adipokines are peptides with autocrine, paracrine, and endocrine functions regulating systemic metabolism and energy homeostasis are secreted by adipose (Boutari, et al.2018). These adipokines include adiponectin, interleukin-6 (IL-6), leptin, tumor necrosis factor α (TNFα), and monocyte chemoattractant protein-1 (MCP-1). Further factors that contribute to liver inflammation and steatosis include lipopolysaccharides (LPS) and FAs, which are produced because of increased gut permeability and bacterial overgrowth (Mzimela, et al.2024, Wang, et al.2023, Li, and Hakkak.2023, Nadine et al.2023).

Furthermore, there is a positive correlation between the presence of IR, the main contributing factor to the development of MASLD/MASH, and elevated levels of inflammatory markers, including hsCRP, IL-6, TNFα, serum amyloid substance A, intercellular adhesion molecule 1-soluble, and CD40L (Gonzáliez et al 2006).

IR increases the number of FFAs that enter the liver through increased hepatic DNL and impaired inhibition of adipose tissue lipolysis. IR also encourages dysfunction of adipose tissue, which leads to changes in adipokine and inflammatory cytokine secretion and production (Kountouras, et al.2023, Xian, et al.2020). Among these, leptin has been found to be a profibrogenic adipokine, and adiponectin is implicated in the pathophysiology of MASLD and its progression to MASH. In general, adiponectin is beneficial for MASLD. While TNF-α increases IR and has pro-inflammatory effects, adiponectin decreases IR and exhibits anti-steatotic and anti-inflammatory qualities (Caligiuri, et al.2016).

In addition, TNF-α activate Jun N-terminal kinase (JNK) in visceral adipose tissue which results in IR (Fernández-Veledo et al., 2009). This kinase phosphorylates of IR Substrate 1 (IRS-1) in serine residues and decreases tyrosine phosphorylation, thereby negatively regulating IRS-1's functions (Bouzakri and Zierath, 2007).

Since it is commonly known that inhibiting or eliminating nuclear factor kappa-B (NF-κB) improves insulin sensitivity, NF-κB is a frequently used target for treating IR. Deficiency of IKKβ, the kinase that activates NF-κB signaling by phosphorylating the inhibitor I-κBα, causes adipocytes to express less TNF-α and IL-6 in response to FFA (Yekollu et al., 2011).

On the other hand, it has been shown that changes in the gut microbiota can trigger intestinal inflammation and impair the gut barrier. Microbial products can reach the liver, induce hepatic inflammation and contribute to MASLD and MASH progression (Brandl and Schandl, 2017).

The released microbial metabolites consist of LPS, endotoxins, bacterial DNAs, and SCFAs. Endotoxin and LPS, for instance, can raise the release of inflammatory factors like TNF-α, which, is crucial for the emergence of MASLD. In the meantime, cholic acid have direct antibacterial qualities and can reduce inflammation by blocking NF-κB signalling and macrophage cytokine production (Pan, et al.2020).

The canonical NF-κB signaling pathway, which is mainly triggered by pathogens and inflammatory mediators, places a great deal of importance on the p65 subunit. When pathological stimuli activate this pathway and activate NF-κB, the most prevalent form of the protein is the p65: p50 heterodimer (Giridharan, and Mythily.2018). In patients with HCC who had inflammation-related hepatic injury, NF-κBp65 phosphorylation was significantly elevated, as was the case in mouse models of liver inflammation (Xu et al.,2021). There is increasing proof that T2DM, obesity, and MASLD are all influenced by changes in and dysfunction of the gut microbiome. Ethanol levels are elevated in patients with these comorbidities due to higher proportions of ethanol-producing Gram-negative bacteria like *Escherichia coli* and *Proteobacteria*. The ethanol and the bacteria themselves cause the liver to produce more TNF and Toll-like receptors (TLRs), which may accelerate the development of MASLD (Shen, et al.2022).

Although inflammation is an important mechanism of pathogenesis, patients tend to be mostly asymptomatic with respect to their liver disease at the earlier stages of MASLD because the incidence for clinical symptoms increases with fibrosis stages. This is in line with the findings that histopathologic inflammation alone is not a reliable predictor of MASLD progression. Fibrosis severity is the critical indicator of mortality during MASH, with higher risk of liver-related complications and death in MASH patients with F3 or F4 stage fibrosis (Wiering et al 2023) (Figure9).

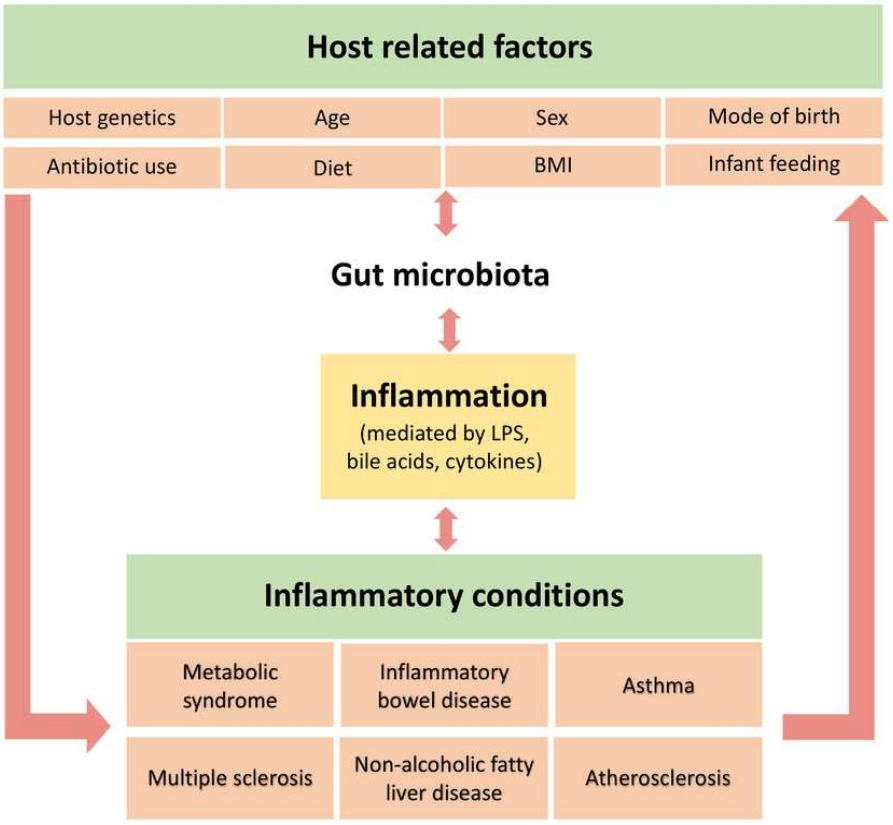

Figure 9. Relationships among inflammatory conditions, inflammation, and the gut microbiota. The gut microbiota is influenced by a number of variables and is inversely correlated with BMI and diet. It also interacts with inflammation in both directions, and depending on its makeup, it may either stimulate or inhibit inflammatory pathways. These in turn may facilitate the start of different inflammatory diseases (Al Bander et al.2020).

I.1.1.1.5. Apoptosis in MASLD/MASH

Cell death, including apoptosis, seems very important in the progression of MASLD and MASH. Activation of caspases, Bcl-2 family proteins, and JNK-induced hepatocyte apoptosis plays a role in the activation of MASLD/MASH. Apoptotic hepatocytes stimulate immune cells and hepatic stellate cells toward the progression of fibrosis in the liver through the production of inflammasomes and cytokines (Kanda, Tatsuo et al 2018).

In addition, oxidative stress brought on by the disruption of mitochondrial function results in cell damage and apoptosis. Increased lipid accumulation in hepatocytes in MASLD can cause mild to severe mitochondrial damage, which can affect the fate of the cell. This may set off a series of events that lead to the production of more ROS and reactive nitrogen species (RNS) within the cell, thereby accelerating the disease's progression from mild steatosis to more severe stages of MASLD/MASH, resulting in fibrosis and inflammation (Bagherieh, Molood et al.2023, Karkucinska-Wieckowska, Agnieszka et al.2022).

The extrinsic cell death pathway depends heavily on death receptors like FAS, TNF receptors, and TNF-related apoptosis inducing ligand (TRAIL) receptors. TRAIL receptor signaling was also found to be involved in the pathogenesis of NASH in mice with a genetic deletion of the TRAIL receptor. Furthermore, patients with NASH had significantly reduced plasma TRAIL concentrations compared to controls, patients with simple steatosis, or obese individuals (Kanda, Tatsuo et al 2018). The development of MASLD/MASH is significantly influenced by caspase activation. Caspases-dependent pathways, both intrinsic and extrinsic, mediate apoptosis and are activated by various factors such as ER stress, cytokines, mitochondrial dysfunction, and elevated FFA (Wilson, Claire H, and Sharad Kumar.2018).

Moreover, in MASH, the energy sensor AMPK is inhibited, which causes caspase-6 to be activated, thereby exacerbating liver damage. As affecting these pathways improved liver damage and fibrosis in animal models, targeting the AMPK-caspase-6 axis may be a therapeutic strategy for treating MASH (Zhao, et al.2020).

Understanding regulators of cell survival, or Bcl-2 family proteins, plays an important role in the context of MASLD and has a major impact on the regulation of apoptosis. These proteins have roles that are both pro- and anti-apoptotic.

They play a key role in the intrinsic apoptosis pathway, which is especially important in the pathophysiology of MASLD because it involves ER stress and mitochondrial dysfunction. Gaining knowledge about the function and control of Bcl-2 family proteins in MASLD may help identify possible targets for treatment (Hatok, and Racay.2016).

I.2. ER stress in the development of MASLD

FFA supply excesses or disposal is compromised due to IR, which provides substrates for the production of lipotoxic species that cause hepatocellular injury and ER stress. An unfolded protein response (UPR) signaling network is triggered when there is an accumulation of unfolded proteins in the ER, a condition known as ER stress (Brown, et al.2020).

One of the main characteristics of metabolic disorders is ER stress, which is brought on by abnormal ER function. This phenomenon is caused by glucotoxicity, lipotoxicity, and/or proteotoxicity, which impacts a number of metabolic and cellular processes. A number of important processes, such as altered calcium homeostasis, lipid and carbohydrate metabolism, inflammation, and protein quality control are linked to ER stress in MASLD.

Particularly in cells like hepatocytes, adipocytes, muscle cells, and neurons, the ER functions as a vital platform for nutrient sensing. When adaptive programs like the UPR, ER-associated protein degradation (ERAD), or autophagy are activated, the temporary state of functional imbalance that ER stress represents in these cells is typically rectified. However, disturbances to proteostasis also affect metabolism of fat and glucose, and vice versa; when ER is unable to adjust, this can result in metabolic dysfunction, inflammation, and IR (Imke et al.2021). All these processes and the accumulation of lipotoxic compounds seems to be one possible link connecting ER stress and MASH (Manne, et al 2018).

Three essential ER transmembrane proteins initiate the UPR, leading to downstream responses that are dynamic and interconnected. Therefore, understanding these pathways is necessary to investigate the complex role of ER stress in the development of MASLD and MASH.

These three main pathways are (1) the Protein Kinase R-like ER Kinase (PERK), (2) the Activating Transcription Factor 6 (ATF6), and (3) the Inositol-Requiring Enzyme 1 (IRE1). Each of these pathways has a distinct function in identifying and reacting to protein misfolding in the ER. Numerous cellular reactions are triggered by their activation, all of which are intended to preserve cellular homeostasis and restore ER function (Ajoolabady, et al.2022) (Figure 10).

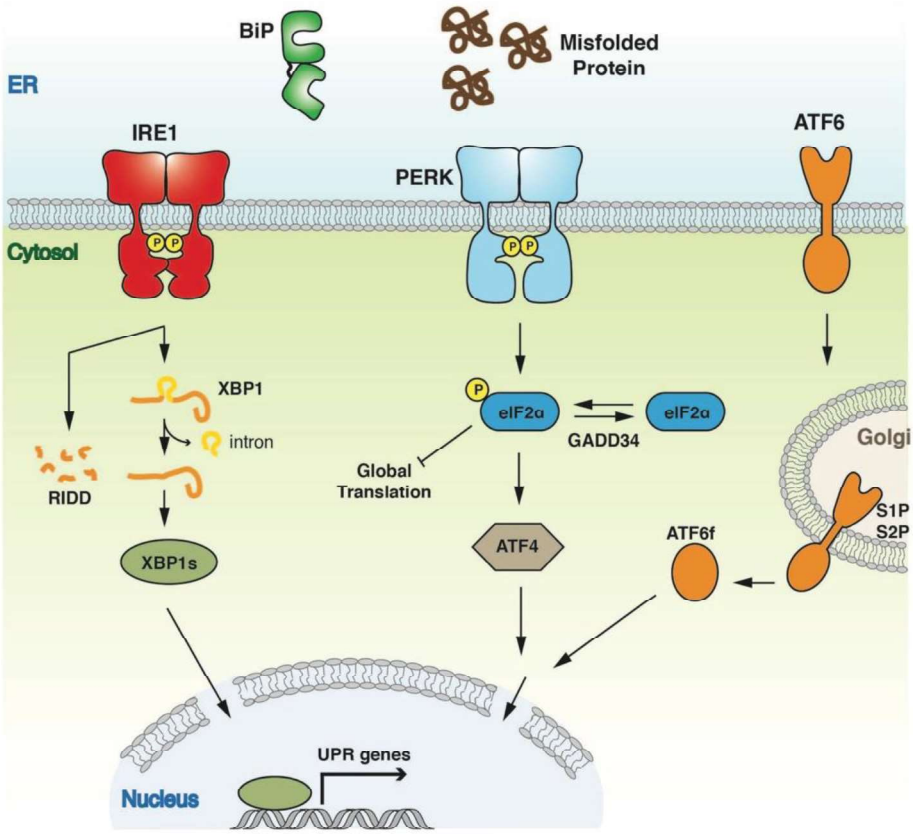

Figure 10. Overview of UPR signaling pathways. In response to ER stress, the UPR triggers a transcriptional and translational response. Three distinct branches of the response are triggered by the three UPR activator proteins (IRE1, PERK, and ATF6) and their shared goals are to successfully maintain ER protein homeostasis and lessen the burden of misfolded protein (Christopher et al.2019).

I.2.1. PERK

The PERK pathway is one of three major branches in the UPR, and it is the only one to modulate protein synthesis as an adaptive response (Bell. et al 2016). Activation of eukaryotic translation initiation factor 2 (eIF2α) occurs through phosphorylation of the Ser51 residue of the α subunit by PERK. As a result, there are fewer newly synthesized proteins because the mRNA translation rate decreases.

Additionally, phosphorylated eIF2α (p-eIF2α) interacts with ATF4, which stimulates the transcription of genes related to apoptosis or protein synthesis, such as binding immunoglobulin protein (BiP/ GRP78), CHOP, and TRB3 (Flamment et al., 2012). Furthermore, p-eIF2α can trigger the NF-κB pro-inflammatory pathway (Salvado et al., 2015). Several factors can also regulate this branch of the UPR. Three kinases, namely protein kinase R (PKR), general control non-derepressible kinase 2 (GCN2), and heme-regulated inhibitor kinase (HRI), can phosphorylate the serine residue of eIF2α (Ron and Walter, 2007; Schröder and Kaufman, 2005).

This pathway is also known as the integrated stress response (IRS) because it can be activated by non-UPR mechanisms that also affect the eIF2α/ATF4 branch (Dey, et al.2012, Vasudevan, et al.2020)

Under circumstances of hyperinsulinemia, the p-eIF2α and the upregulation of CHOP expression cause the overproduction of glucose in the liver and the upregulation of the gluconeogenic genes glucose 6-phosphatase (G6Pase) and phosphoenolpyruvate carboxykinase (PEPCK) (Choudhury et al.,2011).

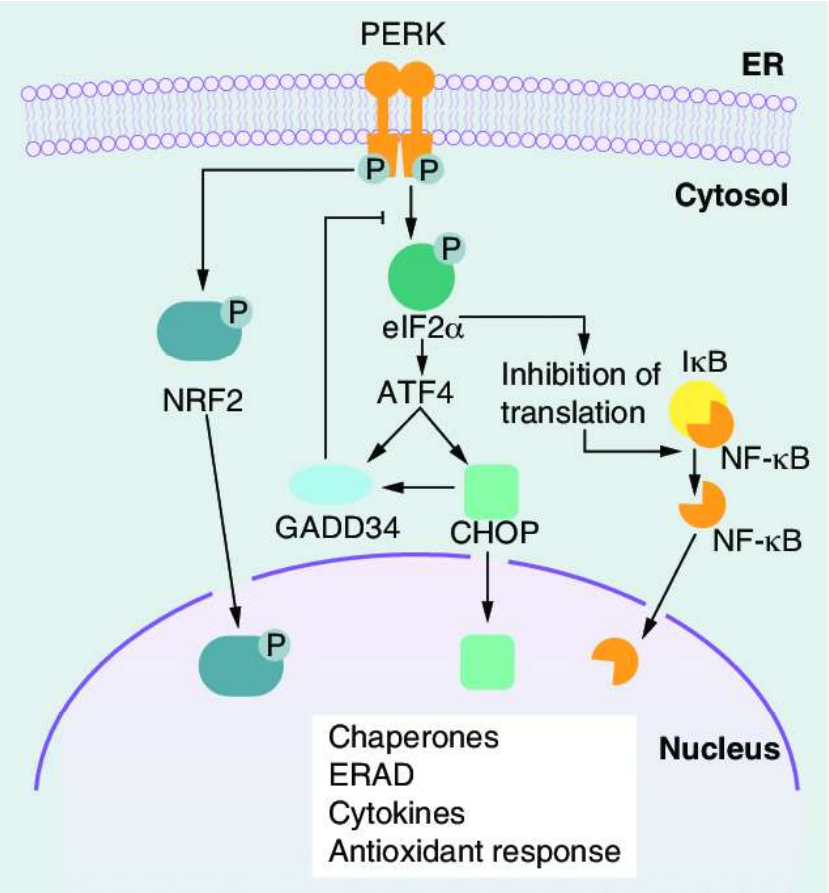

Figure 11. PERK signaling in the unfolded protein response. A transmembrane kinase called PERK is triggered by autophosphorylation and oligomerization. Protein translation is generally inhibited when PERK phosphorylates eIF2α. By using a different translation initiation site, the transcription factor ATF4 can evade translation inhibition. ATF4 stimulates the production of CHOP and GADD34, a phosphatase that controls the p-eIF2α. Additionally, NRF2, a transcription factor that promotes the expression of genes involved in the antioxidant response, can be phosphorylated, and activated by PERK. PERK-induced p-eIF2α and the ensuing reduction in translation can encourage NF-κB activation because IκB, the inhibitor of NF-κB, has a much shorter half-life (Galluzzi, et al.2017).

I.2.2. ATF6

To increase ER folding capacity, ATF6 is activated, cleaved by regulated intramembrane proteolysis, ultimately leading to its translocation into the nucleus where it increases the transcription of genes regulated by cAMP response elements (CRE) and ER stress elements (ERSE) activation (Scheuner et al.,2005). ATF6 also transactivates genes encoding ER chaperones, ERAD components, and protein foldases. Besides, it controls the expression of the apoptotic transcription factor CHOP, which regulates the expression of various proapoptotic genes (Flamment et al., 2012) (Figure 12).

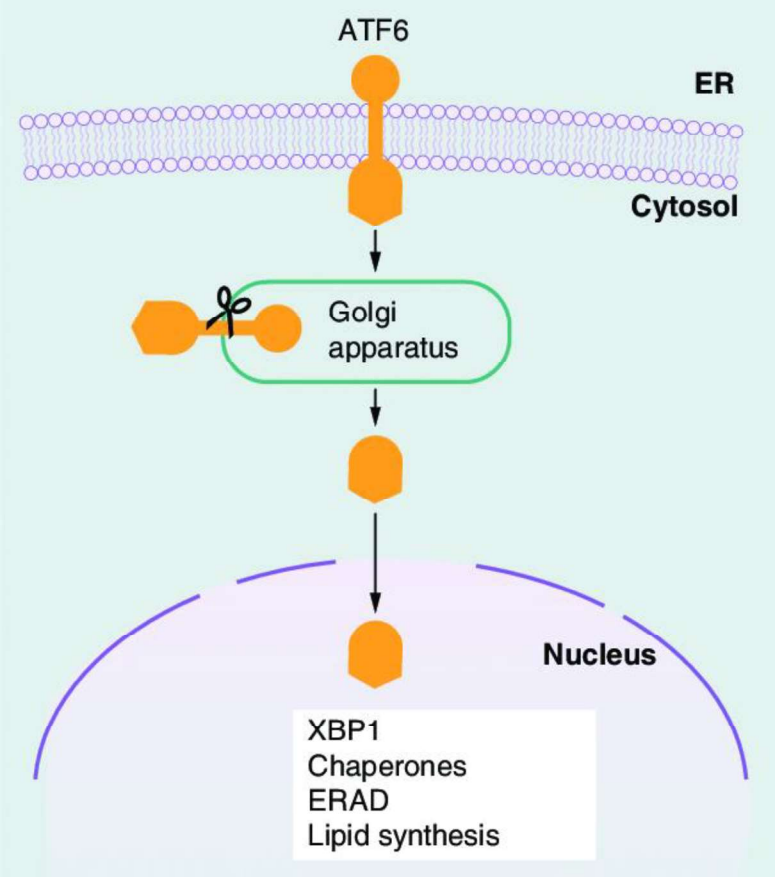

Figure 12. ATF6 signaling in the unfolded protein response. In unstressed cells, ATF6 is found at the ER. ATF6 is shipped to the Golgi apparatus, where it undergoes proteolysis. This releases its cytosolic bZIP-containing transcription factor domain that moves to the nucleus, where it regulates the upregulation of XBP1 and several genes involved in lipid synthesis, ERAD, and protein folding (Galluzzi, et al.2017).

ATF6 plays critical roles in preventing tissue damage and promoting repair processes by encouraging the expression of protective and adaptive genes. This helps cells deal with the burden of misfolded proteins (Blackwood et al.2019).

I.2.3. IRE1

When the ER is under stress, IRE1, a kinase that can function as an endoribonuclease to carry out alternative splicing of the X box-binding protein 1 (XBP1) mRNA, gets auto phosphorylated. This results in spliced XBP1 (sXBP1), an unusual form of XBP1 that can function as a transcription factor following translation (Flamment et al., 2012). The production of chaperones and proteins involved in ER biogenesis, or the degradation and exportation of proteins can be regulated by sXBP1 in conjunction with ATF6, which activates the most significant UPR pathways to restore the ER folding capacity during stress (Hotamisligil, 2010). Additionally, by binding to the TNF receptor-associated factor 2 (TRAF2), IRE1 activates c- JNK (Schröder and Kaufman, 2005) and triggers pathways that are both pro-inflammatory and pro-apoptotic. IR is directly linked to the activation of the JNK pathway because IRE1α-dependent JNK activation results in the subsequent phosphorylation on serine residues of IRS-1 (Kim et al., 2015a).

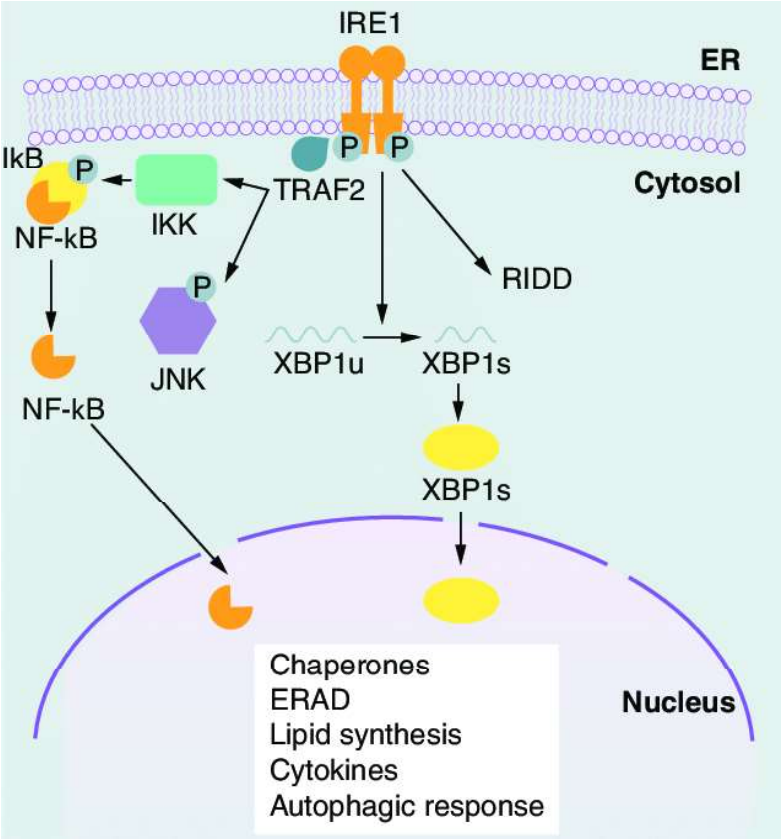

Figure 13. IRE1 signaling in the unfolded protein response. The endoribonuclease domain of IRE1 is activated by oligomerization and autophosphorylation, leading to the cleavage of XBP1 mRNA and the subsequent generation of XBP1s mRNA, which facilitates the translation of the active XBP1s transcription factor. Through a process called Ire1 dependent decay (RIDD), IRE1 can also aid in the degradation of mRNAs linked to ribosomes at the ER. Additionally, phosphorylated IRE1α controls the activation of the two main inflammatory transcription factors, NF-κB and AP-1, by interacting with IKK and JNK through the recruitment of TRAF2 (Galluzzi, et al.2017).

ER stress can cause inflammation via several pathways, including direct triggering of key inflammatory pathways like IRE1α-NF-κB and ATF4-CHOP-Growth Arrest and DNA Damage-inducible protein 34 (GADD34)/ ER Oxidoreductin (ERO)-1α, as well as by acting as both a cause and a result of chronic inflammation (Chen, et al.2023).

These pathways exacerbate the inflammatory response by promoting the synthesis and release of proinflammatory cytokines and other mediators. Comprehending these mechanisms is essential for formulating therapeutic approaches to address ailments linked to endogenous stress and inflammation (He, et al.2024, Bowen et al.2023) (Figure 14).

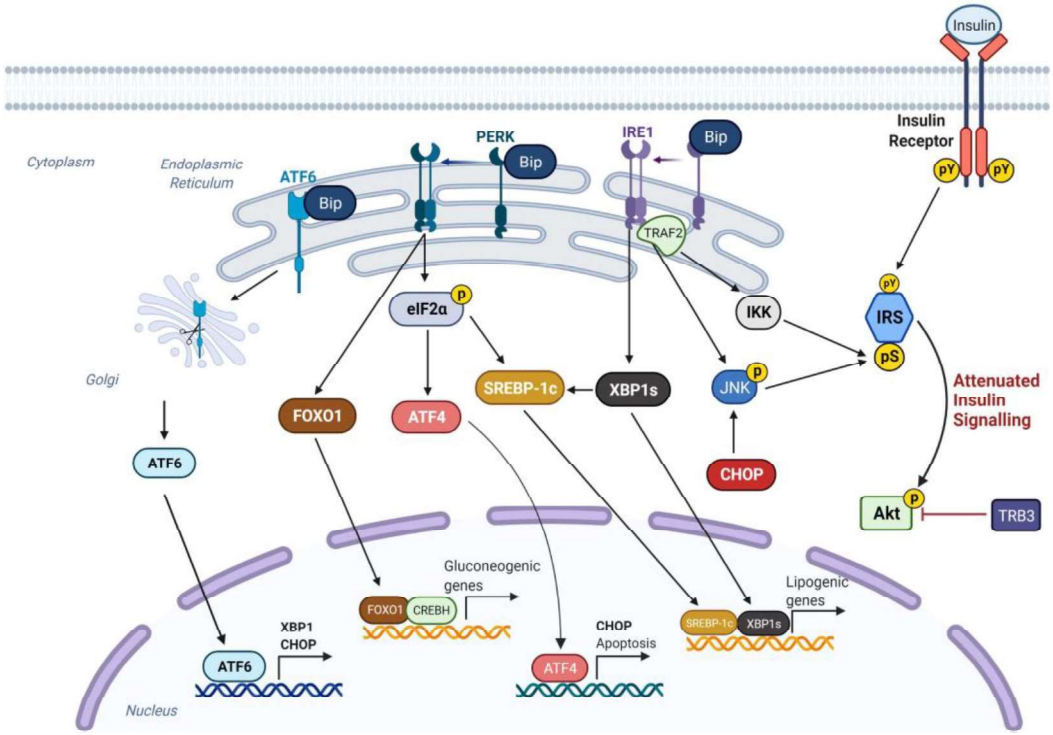

Figure 14. ER stress molecular pathways involved in IR. Hepatic FOXO1 increases because of PERK activation, and the FOXO1-CREBH complex is formed, upregulating gluconeogenic genes**.** Concurrently, eIF2α is turned on by PERK,which in turn activates SREBP-1c, leading to the upregulation of lipogenic genes. IRE1 promotes the splicing of XBP1 and subsequent activation of IKK and JNK, eventually causing an increase IRS phosphorylation serine residues and reduction in insulin signaling routes. The escalation of CHOP resulting from distinct UPR pathways intensifies these impacts and collectively aid in the emergence of IR in various tissues. Taken from (Salvado et al., 2015).

I.3. Role of VLDL Receptor (VLDLR) in MASLD/MASH

Overexpression of VLDL in hepatocytes has been reported to have pro-inflammatory effects, raising ER stress and the risk of hepatic steatosis. Thus, the VLDLR appears to be involved in the processes leading to MASLD influencing. For this reason, delineating how VLDLR regulation impacts MASLD may help to develop future strategies for the treatment of these conditions (Huang, and Hsiang-Chun,2022). Lipoproteins like chylomicrons and VLDL primarily transport TGs in plasma. Remarkably, it has been documented that increased TG-enriched lipoprotein delivery to the liver causes a notable hepatic steatosis through the ER stress-mediated elevation of VLDLR levels (Hyunsun et al.2013). While VLDLR expression is very low in the liver under normal circumstances, it is widely expressed in the brain, heart, skeletal muscle, and adipose tissue (Webb et al.1994, Oka et al.1994). Furthermore, it was discovered that elevated VLDLR expression in macrophages encouraged inflammation of the adipose tissue and decreased glucose tolerance in obese mice. VLDLR expression has been linked to adipose tissue inflammation, according to a different study, and this inflammation was only lessened in obese VLDLR-deficient mice fed HFD. Moreover, it has been discovered that VLDLR increases inflammation by modifying fibrin-dependent leukocyte (Krauss, et al.2023).

Consequently, a connection between plasma TG levels and VLDLR levels has been found. Leaner, with normal blood lipid levels, VLDLR-null mice are also shielded against obesity brought on by a HFD feeding or leptin deficiency. However, these animals display elevated plasma TG levels after fasting or exposure to HFD. As mentioned above, ER stress increases the expression of VLDLR, and this is a key event in ER stress-dependent hepatic steatosis. Hepatic VLDLR expression upregulation in the presence of ER stress is mediated by the PERK–ATF4 signaling (Oshio, et al.2021).

Apolipoprotein E (apoE) TG-rich lipoproteins like chylomicrons and VLDL are bound by VLDLR, a member of the low-density lipoprotein (LDL) receptor family, which facilitates lipid entry into the cell via receptor-mediated endocytosis or lipoprotein lipase-dependent lipolysis (Huang, and Hsiang-Chun.,2022 Takahashi,.2017). Furthermore, VLDLR and APOE-deficient mice exhibit significantly reduced ER stress-dependent hepatic steatosis. In addition, several transcription factors, such as hypoxia-inducible factor 1α (HIF1α), regulate VLDLR, which in turn contributes to lipid deposition in tissues (Zarei et al,2018). Likewise, the increase in the levels of hepatic VLDLR caused by fenofibrate through PPARα activation plays an essential role in the triglyceride-lowering effect of this drug (Yang et al.2014) (Figure 15).

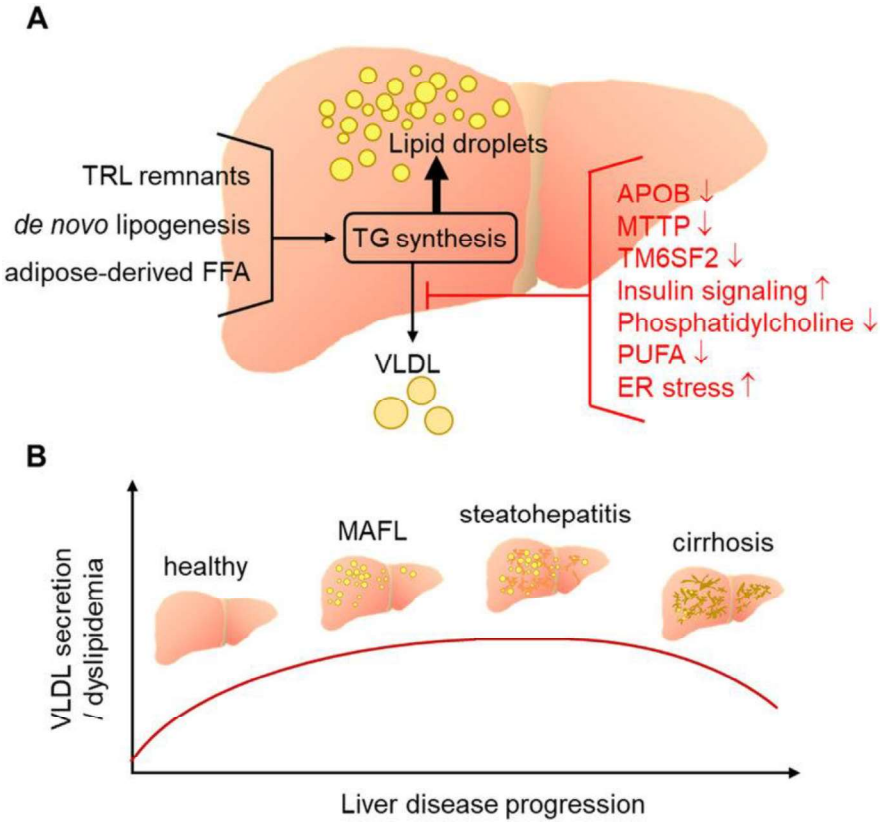

Figure 15. liver steatosis and the VLDL secretory pathway's connection. The capacity of hepatocytes to effectively export extra TG and other lipids as VLDL is one of their key characteristics. (A) The degree of steatosis increases and TGs are redirected to lipid droplets if the rate of VLDL assembly and secretion is limited. (B) Clinical research indicates that when MAFLD progresses and liver steatosis occurs, there is a corresponding rise in VLDL secretion and dyslipidemia (Heeren and Ludger.2021).

I.4. Sirtuin 1 (Sirt1) as a target for MASLD and MASH treatment

SIRTs are a family of seven members (SIRT1–7) with different cellular localization that represent potential targets for treating MASLD due to their role in hepatic lipid and carbohydrate metabolism, insulin signalling, redox signalling and inflammation.

Among them, SIRT1 and SIRT3 are NAD $^{(+)-}$ dependent deacetylases regulated by cellular NAD $^{(+)}$/NADH ratio and are upregulated by fasting, calorie restriction, exercise, and polyphenols and downregulated by nutrient overload. The involvement of SIRTs in MASLD, particularly SIRT1, has been demonstrated in both human and animal models of MASLD (Nassir, 2022). SIRT1 has been reported to be downregulated in humans with NAFLD, and this was associated with increased expression of lipogenic proteins, such as SREBP1, ACC and FAS. In obese patients, SIRT1 levels were lower compared to lean patients and lower in obese patients with severe hepatic steatosis compared to obese patients with mild hepatic steatosis. Moreover, SIRT1 overexpression reduces oxygen consumption in MASLD and relieves oxidative stress (Ji Yong et al.2022, Yunshu et al.2022) (Figure 16).

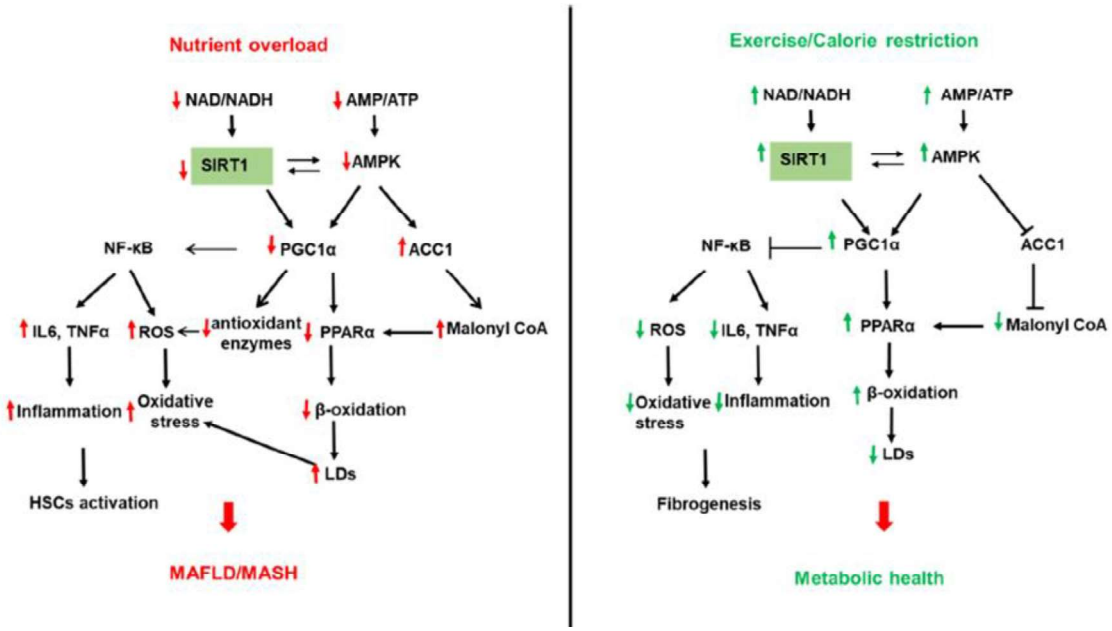

Figure 16. SIRT1's function in NAFLD. Left pannel,Through a series of events involving SIRT1, PGC1α, and AMPK, nutrient overload can disturb metabolic homeostasis. This can result in increased lipid accumulation, oxidative stress, and inflammation in the liver, all of which can contribute to hepatic steatosis. Right panel, Exercise, calorie restriction, and fasting all upregulate SIRT1, which has the opposite effect on β-oxidation, inflammation, and ROS generation from chronic nutrient overload. This results in a healthier liver (Nassir.2022).

SIRT1 plays a wide range of biological roles, most of which are mediated by its ability to deacetylate target proteins, which can be either histones or non-histone proteins (Yunshu et al.2022) (Figure 17).

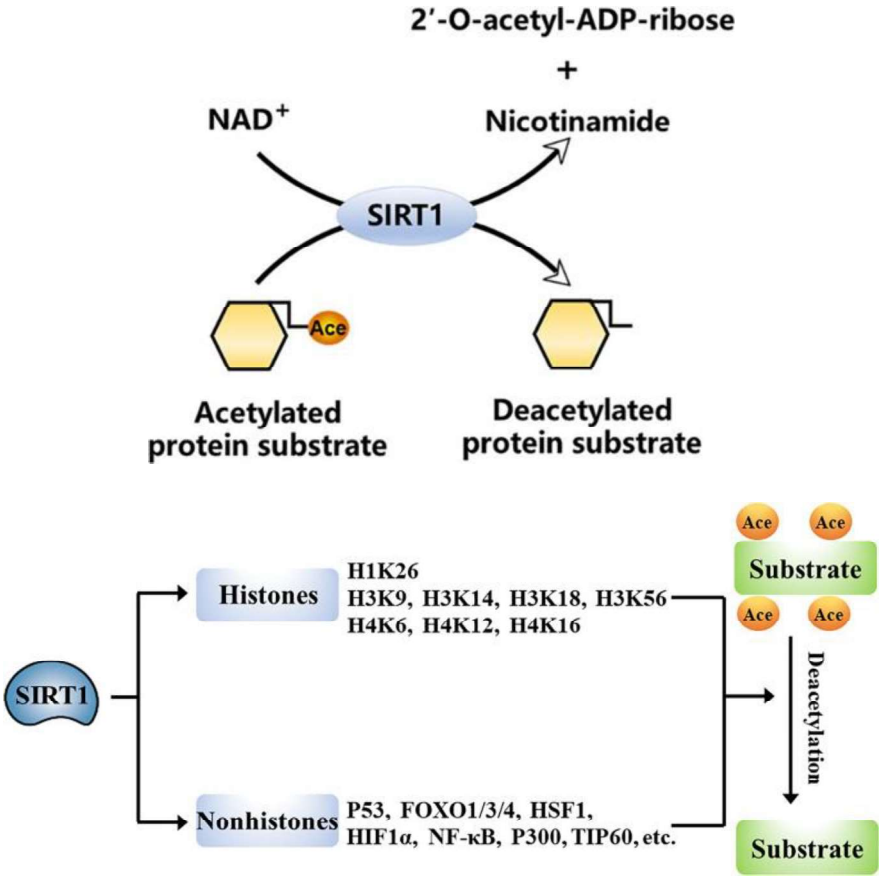

Figure 17. SIRT1 deacetylase reaction dependent on NAD (+). Diagram showing the genes that SIRT1 is trying to deacetylate (Yunshu et al.2022).

Transcription factors p53 is one of the many transcription factors and co-factors that control SIRT1 transcription. In addition, P53 acetylation influences its transcriptional activity and SIRT1 directly deacetylates p53's lysine 382. By attaching to the p53 response element in the SIRT1 promoter, p53 can create a negative feedback loop that prevents SIRT1 transcription (Ong and Ramasamy.2018).

Proinflammatory gene expression rises in alcohol-induced inflammation and oxidative stress, while SIRT1 activity and cellular NAD^+ levels concurrently reduce (Kang, et al.2021). SIRT1 has been shown to directly suppress the expression of inflammatory genes. Specifically, Yeung et al. showed that SIRT1 deacetylates the NF-κB P65 subunit, thereby suppressing NF-κB activity. Further research has verified that SIRT1 suppresses the expression of inflammatory cytokines mediated by NF-κB by reducing P65's acetylation due to its deacetylation at lysine 310, which has anti-inflammatory properties (Tshivhase, et al.2024, Jing et al.2023). In addition, the selective SIRT1 activator SRT1720 attenuates HFD-induced liver steatosis (Long The et al.2018) Alternatively, by controlling the expression of mediator proteins like AMPK and PPARs, SIRT1 can indirectly inhibit NF-κB signaling. The way that SIRT1 and AMPK interact is crucial for the inflammatory response. An essential NF-κB inhibitor is AMPK, and SIRT1 can activate AMPK, which in turn can have an indirect impact on NF-κB (Salminen, et al.2011).

An increasing amount of evidence points to SIRT1 as having a major protective role against liver inflammation and associated injuries (Zhou, et al.2020). For example, Yin et al. discovered that mice with a liver-specific deletion of SIRT1 exhibited hypersensitivity when challenged with ethanol. SIRT1 deletion in the liver increased fibrosis, inflammation, and steatosis. The authors proposed that SIRT1 modification of lipin-1 mRNA splicing contributed to the onset of inflammation and alcoholic steatosis, which may lead to the development of new treatments for alcoholic fatty liver disease (Huquan et al.2014). Additionally numerous investigations have documented how SIRT1 activation reduces DNL. Furthermore, the expression of SREBP1c is decreased by SIRT1 activity, whereas the expression of ChREBP in HepG2 cells has been reported to be elevated in SIRT1 knockout mice.

This indicates how crucial SIRT1 is for controlling lipid metabolism in general and DNL in particular (Anggreini, et al.2023). On the other hand, protecting the liver from oxidative stress is one of SIRT1's primary functions. It accomplishes this by boosting antioxidant capacities through PPARγ co-activator 1 α (PGC-1α) deacetylation and forkhead box proteins (FOXOs) (Hongdong et al.2024).

Consistent with these actions, SIRT1 heterozygous knockout (*Sirt1*$^{+/-}$ mice) fed HFD exhibited hepatic steatosis with significant increase in lipid content and liver inflammation (Xu, et al.2010, Nguyen, et al.2020). However, it is currently unknown if SIRT1 regulates hepatic lipid accumulation by modulating the levels of VLDLR and the subsequent uptake of triglyceride-enriched lipoproteins.

I.5. HIF1α

HIF1α plays a crucial transcriptional role in pro-inflammatory and oxidative stress responses. During hypoxia, HIF1α protein stability requires SIRT1's direct deacetylation. Another important factor in the immunologic homeostasis of immune cells is glucose metabolism.

Cellular machinery depends so heavily on oxygen that a shortage of it necessitates a fast reaction for the cell to adjust to its new circumstances and the HIFs mediate this response. HIFα and HIFβ are the two subunits that make up HIFα; the best characterized HIFα subunits are HIF1α and HIF2α. Two particular prolyl residues in the HIFα subunit can be hydroxylated by three different iron-dependent enzymes known as "prolyl hydroxylase domain" (PHD) proteins under normal oxygen conditions (Mengqiu et al.2022).

In addition to hypoxia, HIF-1α is activated by non-canonical pathways, including insulin, LPS, growth factors, oxidative stress, and TNF-α (Mingxiao et al.2023). It has been reported that both MASLD and SLD are associated with elevated liver HIF expression. While studies have shown that SLD is associated with HIF-1α upregulation, the significance of hepatocyte-specific HIF-1α in the development of SLD is still under debate (Qingfei et al.2022). When macrophages in MASH are exposed to HIF-1α, it results in a decrease in autophagic flux. Moreover, it has been reported that treating macrophages with saturated FAs inhibits autophagy by activating HIF-1α (Xiaojing et al.2019).

HIF1α and HIF2α are upregulated in the liver by hypoxia, which may lead to an increase in hepatic steatosis through the induction of DNL and FFA uptake as well as the repression of FAO. However, the exact role of HIFs in the pathophysiology of intermittent hypoxia-induced MASLD remains unclear (Isaza et al, 2023) (Figure 18).

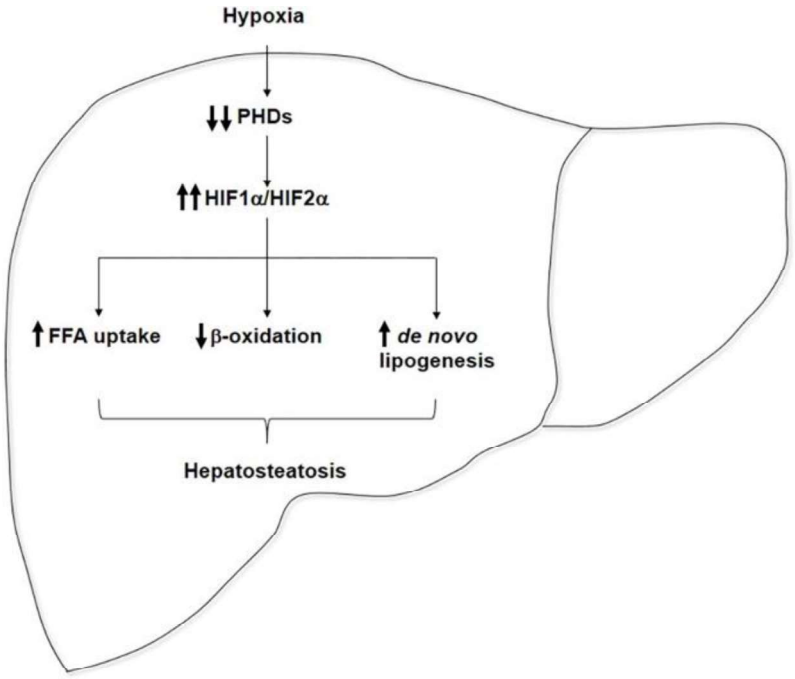

Figure 18. The pathophysiological role of hypoxia in the hepatic steatosis onset. Hypoxia deactivates PHDs and increases the expression of HIF1α and HIF2α in the liver. This may help promote hepat steatosis by increasing the uptake of FFAs, suppressing FFA β-oxidation, and stimulating DNL.

On the other hand, both HIF-1α and HIF-2α control thrombospondin 1 (TSP-1), matrix metalloproteinases, and vascular endothelial growth factor (VEGF) in hepatocytes. These factors help transform latent transforming growth factor β1 (TGF-β1) into its active form, one of the most relevant fibrogenic mediators that may be involved in MASLD progression (Yiwei et al.2021).

It has also been demonstrated that overexpressing HIF1α reduces the upregulation of the ER stress indicators, BiP/GRP78 and CHOP, whereas HIF1α knockdown raises the amount of CHOP (Wonbaek et al.2014). These results suggest that reduced HIF1α expression is linked to hepatocyte lipotoxicity. In fact, apoptosis, inflammation, and fibrosis are attenuated by CHOP deficiency, whereas NF-κB activation by CHOP has been demonstrated to cause apoptosis and inflammatory responses in hepatocytes (Kanda al 2018).

In spite of the findings reported above, silencing of HIF-1α may worsen MASLD. In fact, silencing of this transcription factor has been reported to increase TGs and apolipoprotein B, and to promote lipid accumulation in an *in vitro* model using HepG2 cells stimulated with oleic acid and PA. Moreover, this silencing exacerbated inflammation in cells by raising oxidative stress and pro-inflammatory cytokines. These results imply that HIF-1α, by activating the PPAR-α/ANGPTL4 signaling pathway in MASLD, plays a crucial role in controlling lipid metabolism (Yan et al.2021). The loss of HIF-1α inhibited the nuclear accumulation of Lipin1, a protein involved in lipid metabolism, and decreased the expression of PPARα/RXRα co-activators in a diet deficient in choline that produced a fatty liver model (Takatomo et al.2018). Overall, these findings seem to indicate that both overactivation or inhibition of HIF1α can contribute to MASLD, suggesting that proper activation of this transcription factor is required to maintain a healthy liver.

Hepatocyte vascular endothelial growth factor A (VEGFA) is involved in angionesis and its upregulation by HIF1, is a critical component of HCC and MASLD. Mice with hepatocyte specific *Vegfa* deletion showed a significant reduction in the progression from MASLD to HCC.

Moreover, human HSCs are activated by *Vegfa* into a fibrogenic phenotype, which is a crucial stage in the development of MASLD into HCC (Hao et al.2022).

Another gene that may be upregulated by HIF is glucose transporter 1 (GLUT1). In MASLD, *Glut1* plays a crucial role as a biomarker to differentiate between simple SLD and MASH. Likewise, hepatogenic exosomes containing *Glut1* can act as molecular biomarkers for early warning of MASH. *Glut1* is also used as a non-invasive diagnostic biomarker for liver fibrosis stage. Compared to patients with early-stage MASH, those with advanced MASH had a significantly higher percentage of hepatogenic exosomes *Glut1* (Wenyan et al.2023).

I.6. Soluble Epoxide Hydrolase (sEH) as a target for MASLD/MASH

Several therapeutic strategies for MASH have been studied in clinical trials without achieving the expected results, mainly because the expected benefit remains uncertain and does not sufficiently compensate for the potential risks. Based on this and the multifactorial complexity of MASLD/MASH, it is clear that successful therapeutic efficacy requires the use of multiple modes of action. In this line, several preclinical studies suggest that sEH inhibition is a promising strategy for treating MASH due to the resulting anti-inflammatory and anti-fibrotic activities (Yan et al. 2012; Todd et al 2015 and Jeffrey et al 2020).

sEH is a bifunctional enzyme that exhibits lipid epoxide hydrolase (sEH-H) and lipid phosphatase (sEH-P) activity encoded by the *Ephx2* gene. The C-terminus is in charge of breaking down epoxy fatty acids (EpFAs) into their corresponding 1,2-diols, whereas the N-terminal domain is a lipid phosphatase. Inhibition of sEH hydrolase activity by small molecules could be beneficial for the treatment of various diseases related to inflammation, pain, cancer, and metabolic alterations such as MASLD by reducing the levels of dihydroxyeicosatrienoic acid (DHET) levels, while the levels of endogenous epoxyeicosatrienoic acid (EET) can be effectively maintained (Yuxin et al.2023) (Figure 19).

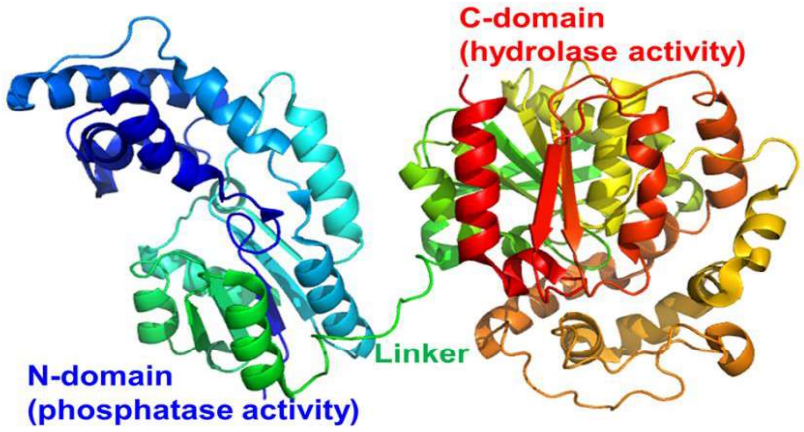

Figure 19. X-ray cocrystal structure of a single subunit of the human sEH. This sEH is a bifunctional enzyme that possesses an N-terminal phosphatase region and a C-terminal hydrolase domain (Cheng-Peng et al.2021).

It is still unknown what the N-terminal phosphatase domain does. While its physiological and possibly pathophysiological roles remain unclear, Cronin et al. and Newman et al. found that the N-terminal domain of sEH exhibits phosphatase activity to hydrolyse diverse lipid phosphates in vitro, including farnesyl pyrophosphate, sphingosine 1-phosphate, and lysophosphatidic acid (Annette, et al.2003). In addition, recent investigation has demonstrated that sEH-P plays a crucial role in the metabolism of fat and energy and works in tandem with sEH-H to regulate cardiometabolic homeostasis. This suggests that using sEH to inhibit hydrolase activity alone may not always yield the same results as reducing phosphatase and hydrolase activity (Matthieu, et al.2023).

One strategy to inhibit both hydrolase and phosphatase activity of sEH is to use the proteolysis-targeting chimera (PROTAC) technology, a new technology based on the event-driven pharmacological model of action that will be discussed in a next section.

I.6.1. sEH inbibitors

T-TUCB is a sEH inhibitor that has been investigated for its potential applications in a range of physiological settings. For instance, studies show that sEH inhibition by t-TUCB can increase brown adipogenesis and lower serum TGs in diet-induced obesity. According to this, sEH may be important for brown adipogenesis, and inhibitors such as t-TUCB may help improve lipid metabolism in brown adipose tissue. These findings may have implications for obesity prevention and treatment (Haley et al.2020). Furthermore, the cardioprotective qualities of t-TUCB have also been investigated. It has been demonstrated to protect against myocardial ischemia injury in rats, indicating that sEH inhibitors may be a useful therapeutic approach to lessen myocardial ischemia damage (Shrestha et al.2014) (Figure 20).

Collectively, these results demonstrate the therapeutic potential of sEH inhibitors, like t-TUCB, in the treatment of obesity and heart disease. They also highlight the increasing interest in this class of drugs for the management of chronic illnesses.

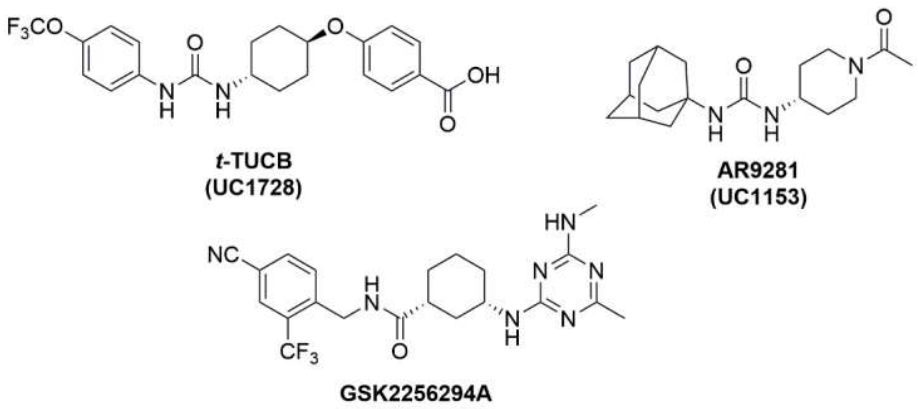

Figure 20. Structures of several sEH inhibitors (*t*-TUCB, TPPU, GSK2256294A, AR9281) (Sean D et al.2018).

I.6.2. Epoxidized fatty acids and EETs

An important class of sEH substrates are the cytochrome P450 (CYP450) monooxygenated products of the omega-3 and omega-6 PUFA including epoxyeicosatrienoic acids (EETs, products of arachidonic acid (AA)) (Jeffery et al 2020).

CYP450 enzymes are involved in the third pathway of cascade and they metabolize AA to produce EETs. These metabolites have a variety of biological roles, but their opposing effects on the vasculature where EETs are vasodilators and 20-hydroxyeicosatetraenoic acid is a vasoconstrictor—make them especially interesting. Because changes in these eicosanoids' levels are linked to pathological conditions, the balance between these eicosanoids is critical, and the enzymes involved in their formation and degradation may be targets for therapeutic intervention (Deanna and Zeldin.2002).

EETs present anti-inflammatory, vasodilator, anti-thrombotic, and cardioprotective properties (El-Kadi, et al. 2010). Particularly because of their anti-inflammatory, anti-apoptotic, and antioxidant properties, EETs can reduce ER stress by stabilizing mitochondria and reducing ROS's effects.

It has been discovered that the metabolites derived from CY P450 play a complex role in diseases like diabetes and diabetic cardiomyopathy, impacting cardiovascular health. Thus, targeting theses pathways could be an effective therapeutic intervention for diabetes and related cardiomyopathies (Fadumo Ahmed et al.2022) (Figure 21). In addition, CYP450 convert FA into bioactive lipids that have hepatoprotective properties.

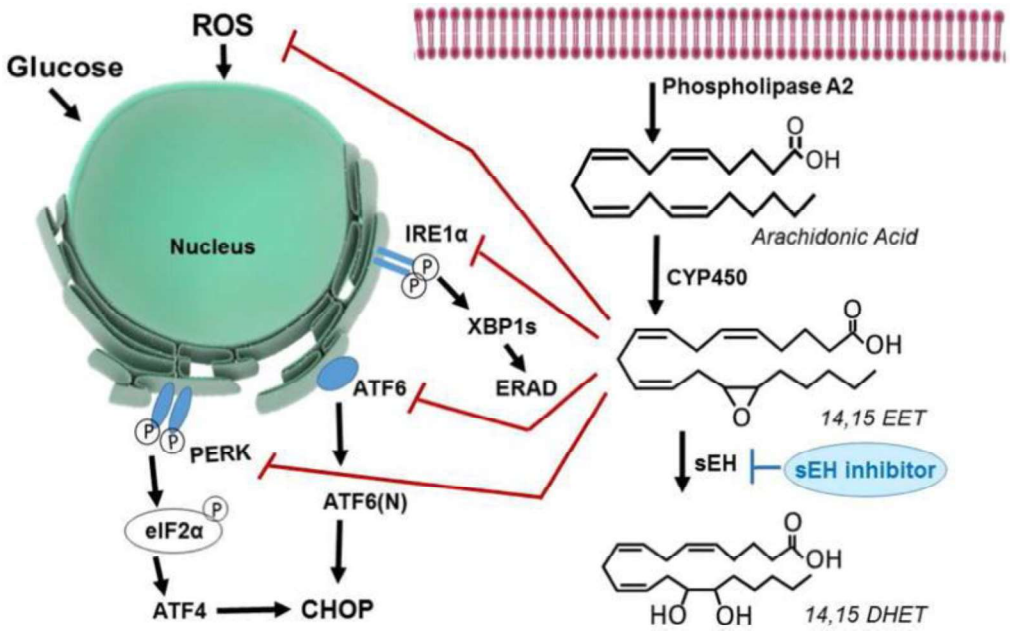

Figure 21. sEH inhibition and EpFA block ER Stress. Phospholipase A2 releases ARA from the phospholipid bilayer, which CYP450 epoxygenase acts upon to form 14,15 EET. The sEH then metabolizes the 14,15 EET into a less active 14,15 DHET. By blocking sEH, EpFA is maintained, which prevents phosphorylation of IRE1α, elF2α, and PERK and dramatically lowers the expression of ATF6(N) and XBP1s. Furthermore, phospho-p38 and phospho-JNK, kinase mediators (ElKhatib, et al.2023).

AA is converted by the epoxygenases CYP2C and CYP2J into EET regioisomers, mainly 11,12- and 14,15-EET. sEH then breaks these EET regioisomers down into less active DHET. Accredited biomarkers of CYP epoxygenase and sEH function are total EET (11,12, and 14,15 EET) plus total DHET (11,12, and 14,15 DHET), as well as the ratio of 14,15 EET to 14,15 DHET11, 12. New preclinical research indicates that EET might offer protection against MASH (Arvind, et al.2020). Cyclooxygenases, lipoxygenases, and CYP metabolize AA to biologically active eicosanoids, which are important modulators of many biological processes, including inflammation. The liver as a rich expression site for CYP enzymes, catalyze the oxidative biotransformation of xenobiotics. Furthermore, some CYP isoforms metabolize natural substrates. The CYP2C and CYP2J subfamilies of CYP epoxygenase enzymes are notable for their ability to metabolize AA into physiologically active EETs. Nevertheless, sEH quickly hydrolyzes EETs to DHETs, typically less biologically active. Previous research has demonstrated that hepatic CYP epoxygenase expression and EET biosynthesis are suppressed by acute, LPS-evoked activation of the innate immune response. Increased endothelial EET biosynthesis or reduced global sEH-mediated EET hydrolysis also attenuates the acute vascular and systemic inflammatory response to LPS and NF-κB activation (Schuck, et al.2014).

Therefore, in accordance with all this data, inhibitors of sEH may be considered a promising strategy to stop EET metabolism and increase their advantageous effects (Figure 22).

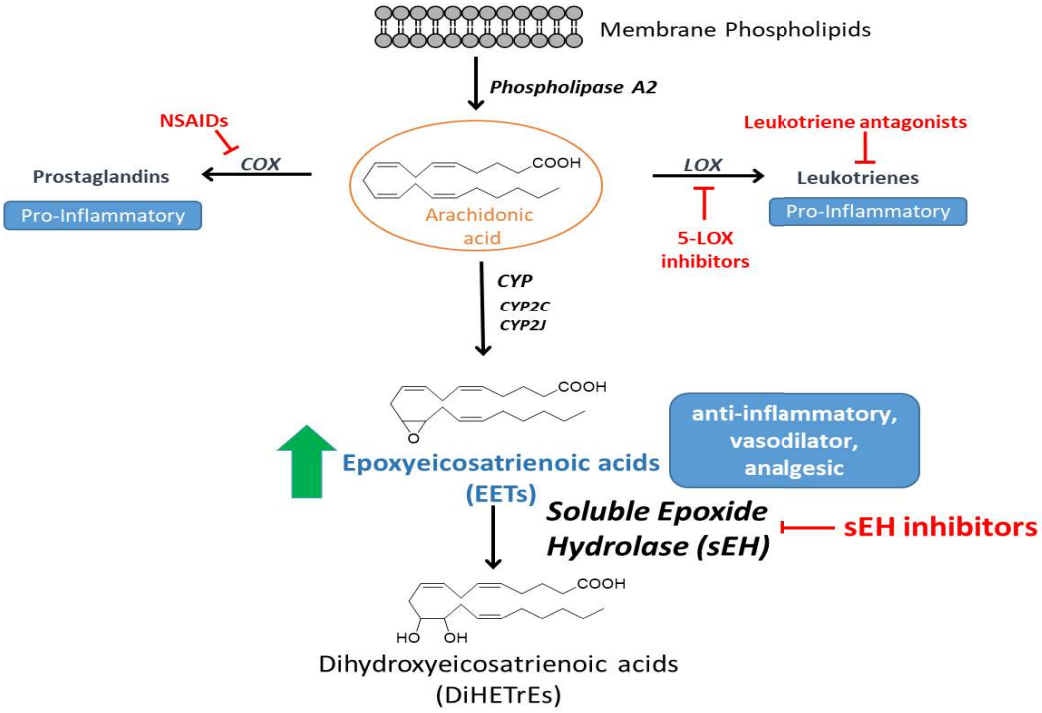

Figure 22. AA cascade pathway. The liver is the primary site of expression for sEH, an enzyme that is mostly cytosolic and functions in the AA cascade. The anti-inflammatory EETs and other EpFAs are hydrolyzed by sEH to produce DHET and related fatty acid diols, which are either less biologically active or even proinflammatory. The hydrolysis of EpFAs, such as EETs, from AA to their less active corresponding diols, such as DHET, is catalyzed by the C-terminal hydrolase (Wang, et al.2021).

I.6.3. AMPK

AMPK regulates metabolic homeostasis and is a crucial energy sensor. Several studies have shown a strong link between reduced AMPK activity and the incidence of metabolic diseases such as obesity, diabetes and MASLD. AMPK activity is substantially attenuated in obese patients and human subjects, mainly due to excessive calorie intake, lack of exercise and increased inflammation and in particular, in both MASLD and MASH.

In addition, although the loss of AMPK activity does not affect lipid accumulation in the liver, it substantially exacerbates liver injury and fibrosis, promoting the transition from MASLD to cirrhosis and HCC (Zhao, Peng and Saltiel, Alan R. 2020). The adenosine triphosphate (ATP) system in the body is responsible for preserving energy balance. The AMPK pathway is triggered when cellular ATP levels are lowered, phosphorylating proteins and growth-regulating enzymes to produce ATP and reduce ATP consumption (Sharma, Ankita et al.2023). AMPK is thought to be the master regulator of many proteins involved in redox, aging, inflammation, and the metabolism of glucose and lipids (Wang, Doudou et al.2022). AMPK is a trimeric complex made up of two regulatory subunits, β and γ, and a catalytic α subunit, according to the protein's crystal structure (Kanagaki, Shuhei et al.2023). Multiple factors regulate AMPK activity through the modulation of different subunits. Phosphorylation of Thr172 in the catalytic domain of the subunit is required for AMPK activation. Three central kinases, liver kinase B1 (LKB1), Ca2+/calmodulin-dependent protein kinase β (CaMKKβ) and transforming growth factor β (TGFβ)-activated kinase 1 (TAK1), have been shown to phosphorylate the Thr172 residue (Zhao, Peng and Saltiel, Alan R. 2020). AMPK binds to glycogen through a carbohydrate binding site found in the β subunit**.** The γ subunit also serves as a sensor for variations in the AMP/ADP ratio (Kanagaki, Shuhei et al.2023).

AMPK suppresses the NF-κB pathway to produce anti-inflammatory effects in a SIRT1-dependent manner. In fact, it has been reported that by upregulating NF-κB, SIRT1 deficiency accelerated the worsening of hepatic inflammation. AMPK regulates aberrant lipid metabolism and inflammation. Thus AMPK/SIRT1/NF-κB pathway plays a crucial role in the progression of MASLD (Anggreini, Putri et al.2023).

In addition to being essential regulatory proteins in metabolic disorders like T2DM, obesity, and cardiovascular diseases, AMPK and SIRT1 are also critical in controlling the DNL and for this reason they show promise as targets for the treatment of MASLD. AMPK activation reduces hepatic steatosis by controlling hepatic lipogenesis and FAO through the AMPK/Sirt1 pathway.

Specific substances can trigger these pathways, resulting in decreased body and liver weight, improved hepatic steatosis, and lessened liver damage in mice fed a HFD (Anggreini, Putri et al.2023). However, others have reported that activated AMPK can suppress PPARα transcriptional activity in hepatoma cells. This implies a complex interaction wherein the function of PPARα in lipid metabolism may be modulated by AMPK activation (Li, Songtao et al.2020) (Figure 23).

FFA treatment caused modifications in the synthesis of glycogen, an increase in the accumulation of lipid droplets, and changes in a number of metabolic markers (Huang, Cheng et al.2022).

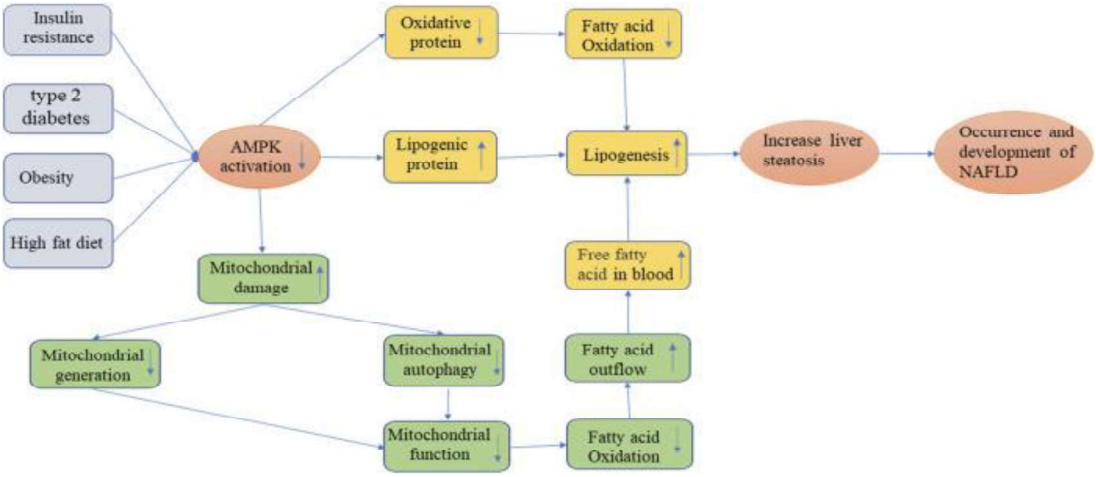

Figure 23. Role of AMPK in MASLD development (Fang, Chunqiu et al.2022).

Excessive ER stress contributes to the development of IR and T2DMs and activation of AMPK has been reported to protect against IR by reducing ER stress. In addition, the presence of an inhibitory crosstalk between AMPK and ERK1/2 contributes to the development of ER stress, since inhibition of ERK1/2 was found to improve AMPK pathway and to reverse ER stress-induced IR (Salvadó, Laia et al.2014, Hwang, Seung-Lark et al.2013).

ERK1/2 belongs to the family of serine-threonine kinases known as mitogen-activated protein (MAP) kinases, formerly called extracellular related kinase (ERK), and is involved in the proliferation and progression of the cell cycle. TNF-α, IL-1β, ER stress, and SFAs activate JNK and other MAP kinases (Wu and Ballantyne, 2020).

The inhibitory crosstalk between the ERK and AMPK pathways in skeletal muscle shows how interactions between these pathways can cause IR when ER stress is present. This interaction was found in L6 muscle cells treated with thapsigargin or tunicamycin (TM). It affected insulin signaling and glucose uptake by altering the phosphorylation levels of IRS-1, Akt, AMPK, and ACC (Hwang, Seung-Lark et al.2013).

I.7. Diet, lifestyle changes and pharmacotherapy for MASLD/MASH

Although diet and lifestyle modifications are essential for the management of MASLD, they might not be adequate for all patients. The best course of treatment for MASLD is significant weight loss, which can be attained with diet, lifestyle modifications, bariatric surgery, or medication (Kim, et al.2019). It has been shown that losing weight, whether by medication or lifestyle modifications, improves liver biomarkers and may even reverse fibrosis. However, for optimal liver outcomes, especially in cases where lifestyle changes do not lead to the desired weight loss or metabolic improvements, pharmacotherapies are increasingly being considered (Tsankof, et al.2022). These therapies might include anti-obesity medications, either alone or in combination with lifestyle interventions, to achieve a reversal of obesity comparable to weight-loss surgery. For effective treatment, weight management services should be incorporated within hepatology care to ensure comprehensive support for patients with MASLD (Finer,.2022).

The European Medicines Agency (EMA) and the United States Food and Drug Administration (USFDA) have not yet approved a medication to treat MASLD.

Therefore, using any medication to treat MASLD for this indication must currently be regarded as "off-label use." However, MASLD patients frequently have other metabolic syndrome-related conditions. For instance, patients with MASLD who also diabetes mellitus or dyslipidemia have frequently taken medications for these conditions that have been approved by these regulatory bodies (Deepu, and Eapen.2020). The overwhelming need for pharmacological therapies in the global MASLD epidemic and emerging data of their efficacy to treat MASLD have translated into recommendations for use of currently available drugs to treat MASLD in clinical practice guidelines issued by the AASLD, even though US and European drug regulatory agencies have not approved any drug to be used to treat MASLD (Chalasani, et al.2018),European Association for the Study of the Liver (EASL) (EASL et al.,2016), and Indian National Association for the Study of the Liver (INASL) (Duseja, et al.2015).

Recommendation to treat NAFLD				
Mechanism of action	**Side effects**	**AASLD**	**EASL**	
Pioglitazone	PPARγ agonist, decreases IR	Weight gain, fractures, may precipitate heart failure	Yes (use in patients with biopsy proven MASH, with/without T2DM)	Yes (use in patients with MASH, especially in diabetics)
Vitamin E	Antioxidant	Increase in overall mortality, hemorrhagic stroke, prostat cancer	Yes (use in nondiabetic patients with biopsy proven MASH)	Yes (use in nondiabetic, noncirrhotic patients with MASH)
Statins	HMG CoA reductase inhibitor	Hepatitis (serious live injury is rare)	No (can use to treat dsyslipidemia. Avoid in decompensated cirrhosis)	NO (can use to treat dsyslipidemia)
Metformin	Decrease IR	Lactic acidosis	No	No
Ursodeoxycholic acid	Decreases TNF-α, reduce oxidative stress and IR	Headache, GI side effects	No	No

Table1. PPARγ: peroxisome proliferator activated receptor gamma; HMG CoA: 3 hydroxy 3 methyl glutaryl coenzyme A; TNF-α: tumor necrosis factor alpha (Deepu, and Eapen.2020).

Numerous MASLD treatments, including dapagliflozin, semaglutide, resmetirom, obeticholic acid, and aramchol, are undergoing phase 3 trials. Additional treatments are being developed. According to the current trajectory, drug therapies for different stages of MASLD are probably being customized.

For example, patients with simple steatosis may benefit from using aramchol or NGM282, while patients with fibrosis may benefit more from dapagliflozin. Moreover, phase 2 trials are investigating combination therapies as well. These regimens will probably also work because of the intricate pathophysiology of MASLD, but more research is needed to determine the best drug combination, safety profile, and tolerability (Shen, et al.2022).

Thus, the failure of the proposed therapies and the increasing prevalence of the disease highlight the urgent need to identify new targets that represent potential opportunities for developing drug treatments for MASH.

I.8. Proteolysis-targeting chimeras (PROTAC) and targeted protein degradation

Proteolysis-targeting chimeras (PROTAC) technology was created in 2001 with the idea of targeting the binding of two proteins that do not usually form a complex. This makes it possible not only to attack original biological targets, but also to potentially counteract possible resistance mechanisms established, for example, by cancer cells against classical chemotherapies, thanks to the event-driven pharmacological model (Guedeney, et al 2023). In addition, the catalytic mechanism of action of PROTACs represents a new pharmacodynamic modality with several potential advantages over traditional inhibitors that may be adapted to many target proteins. For this reason, the design of a PROTAC directed to a therapeutic target with a relevant role in metabolic disorders or the development of MASLD is of great interest.

Structurally, PROTACs consist in heterobifunctional molecules made up of two distinct ligands joined by a linker. One key component of proteasome-mediated protein degradation is the E3 ligase. There are more than 600 known E3 ligases in the human body, but the most widely used are cereblon (CRBN), VHL, MDM2, cIAP, etc. (Xu, 2023).

The PROTAC is formed when one ligand binds to the protein of interest (POI) and the other ligand binds to an E3 ligase. This makes it possible for the E3 ligase to polyubiquitinate the POI based on proximity, leading to the target protein's non-natural degradation (Figure 24) (Sandeep, et al.2021).

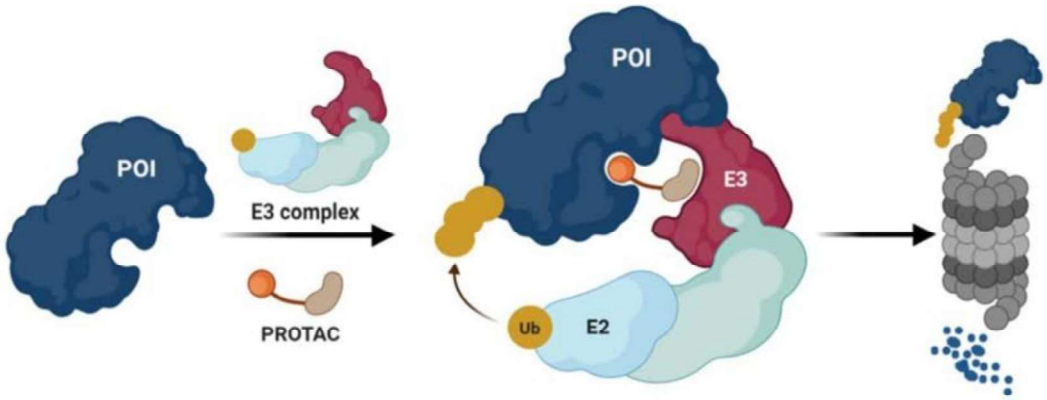

Figure 24. Targeted Protein Degradation (TPD) by PROTACs. Heterobifunctional molecules known as PROTACs bind to an E3 ubiquitin ligase complex and POI at the same time. This process ubiquitinates the POI and causes its degradation by the ubiquitin proteasome system. Ub: Uniquitin. Ub conjugating enzyme (E2) and substrate adaptor protein (E3) are E3 ligases (Nalawansha and Craig.2020).

Targeted protein degradation (TPD) therapy has advanced significantly with the development of PROTACs. This system attaches a tag to certain proteins so that the ubiquitin-proteasome system can destroy them. TPD presents a number of potential benefits over conventional small-molecule inhibitors. Even at low doses, PROTACs have the ability to degrade proteins rather than just inhibit them, which may result in long-lasting and significant pharmacological effects. Their ability to target particular protein isoforms adds another layer of selectivity, and they can have cumulative effects by delaying the degradation of the target proteins. Moreover, proteins that have historically been regarded as "undruggable," such as those without an active site where an inhibitor can bind, may be targeted by PROTACs (Qi, et al.2021) (Figure 25).

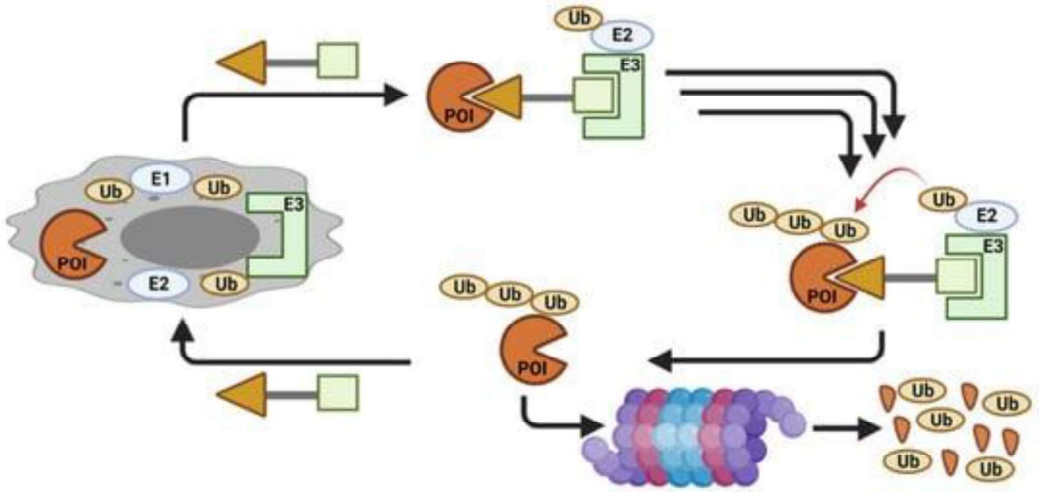

Figure 25. Schematic cartoon showing a PROTAC mechanism of action (Sandeep, et al.2021).

PROTACs have an exciting future in precision medicine, which is highlighted by their distinct mode of action and the increasing amount of clinical data demonstrating their effectiveness. PROTACs have the potential to transform the treatment of many different diseases as research in this area advances, providing new hope for ailments that have proven challenging to treat with current therapies (Liu, et al.2022).

The technology has moved from academia to industry in the 20 years since the first small-molecule PROTAC was reported in the literature. Several biotech and pharmaceutical companies have disclosed preclinical and early clinical development programs using this technology (Figure 26). The first PROTAC molecules were tested in clinical settings in 2019. These trials yielded the modality's first clinical proof-of-concept against two well-known cancer targets, the androgen receptor (AR) and the estrogen receptor (ER), in 2020 (Békés, et al.2022).

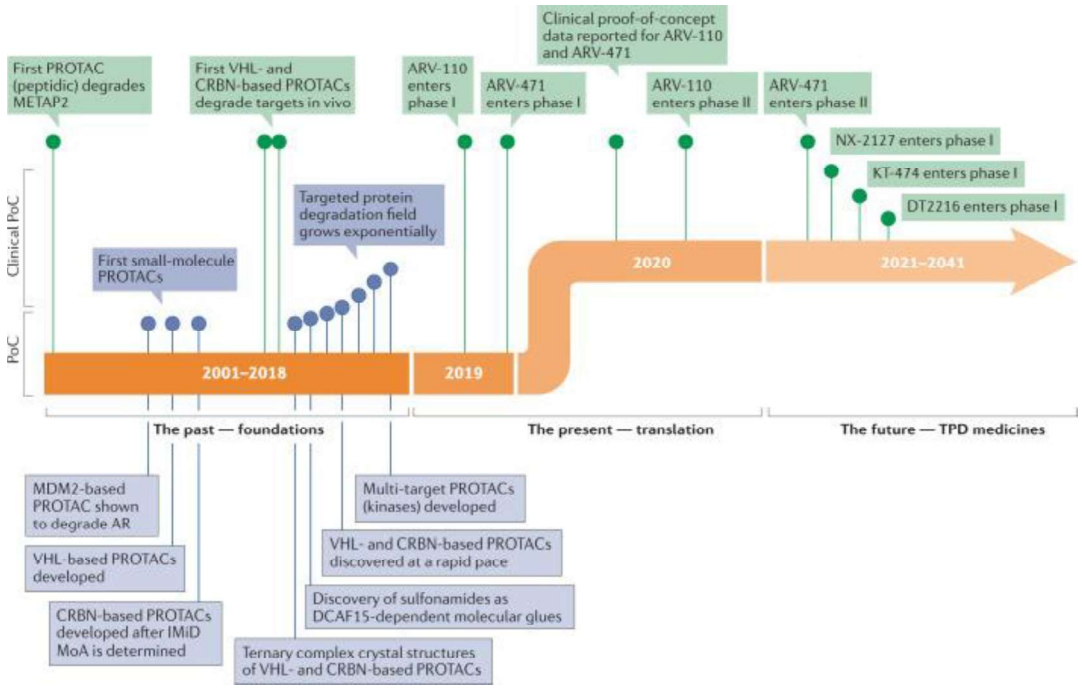

Figure 26. Timeline of PROTAC discoveries.

The crucial PROTAC paper by Sakamoto et al., published in 2001(Sakamoto, et al.2001), marked the beginning of the first era of TPD. This paper was the first to demonstrate the idea that protein targets could be purposefully dragged to a ubiquitin ligase to induce their degradation using chemical tools. Since then, the field has expanded rapidly, going from peptide-based tool degraders to several classes of fully synthetic small molecules that can cause a ligase to come into proximity with a target protein, ultimately resulting in the protein's degradation. The first rational heterobifunctional PROTAC degrader, ARV-110, which targets the AR by recruiting it to the Cullin–RING ligase 4–cereblon (CRL4–CRBN) ligase complex, entered clinical trials in 2019. This marked the culmination of the foundational era of TPD. The current TPD era can be thought of as its first translational phase, during which a number of drugs intended to break down disease-causing proteins are making their way into the clinic in the hopes of offering patients significant therapeutic benefits (Békés, et al.2022).

The ideal targets for PROTAC therapy, which we have named "Tenets of PROTAC targets" can share a number of traits, such as: a departure from the natural state that causes a gain of function that causes the disease, via overexpression, mutation, aggregation, isoform expression, or localization; a binding surface that an E3 ligase can approach; and ideally, an unstructured region to thread into the proteasome (Davis, et al.2021).

Highly suitable PROTAC targets can also include proteins with scaffolding functions, proteins that have evolved resistance mutations to targeted therapies, and proteins that are deemed "undruggable" with other modalities.

II.OBJECTIVES

The disorder known as MASLD is complex and consists of multiple metabolic dysfunctions that mainly affect the liver (Younossi, et al.,2018). The effectiveness of the MASLD treatments currently in use is limited due to the disease's rising prevalence, and they frequently have noticeable side effects that are not fully mitigated (McPherson, et al.,2022). Therefore, it is imperative to discover new therapeutic targets that are capable of effectively handling the complexities associated with MASLD. The study of new mechanisms involved in the development of MASLD as well as new pharmacological strategies to attenuate its progression may provide new insights about how this condition progresses and how to develop new pharmacological strategies to reduce its incidence.

ER stress has been identified as a critical factor affecting insulin signaling pathways, inflammatory responses, and lipid metabolism in the context of MASLD (Flessa, et al.2021). In agreement with this, there has been promise in treating MASLD by addressing ER stress (Koo, and Chang,2021). ER stress-mediated increase in the levels of the VLDLR results in remarkable hepatic steatosis via enhanced triglyceride-rich lipoprotein delivery to the liver (Hepatology 57, 1366-1377.). Moreover, SIRT1 is a NAD $^{(+)}$-dependent deacetylase, and a key regulator of MASLD through the regulation of lipid metabolism, oxidative stress and inflammation in the liver (Nature 460, 587-591). However, it is currently unknown if SIRT1 regulates hepatic lipid accumulation by modulating the levels of VLDLR and the subsequent uptake of TG-rich lipoproteins.

Targeting sEH also attenuates ER stress, converting this enzyme in a drug target with the potential for therapeutic utility in MASLD. Interestingly, PROTACs molecules offer new opportunities for targeting sEH, due to its capacity to induce its degradation. How targeted protein degradation of she by a PROTACs affects ER stress in hepatocytes and in the liver remains to be evaluated.

Considering this, the general aim of the present doctoral thesis has been to assess if SIRT1 attenuates fatty liver development by modulating hepatic VLDLR levels and as to whether targeting sEH with degraders is a promising pharmacological strategy to reduce hepatic ER stress. To accomplish this aim, the following objectives were set up and divided into two differentiated parts:

Part one: SIRT1 REGULATES HEPATIC VLDLR LEVELS THROUGH HIF-1α

- To evaluate how hepatic SIRT1 and VLDLR are regulated in a rat model of MASLD induced by fructose-drinking water.

- To examine if hepatic VLDLR levels are upregulated in $Sirt1^{-/-}$ mice or following pharmacological inhibition or gene knockdown of SIRT1 in Huh-7 cells, and the potential molecular mechanisms involved.

- To assess if SIRT1 activation prevents the increase in hepatic VLDLR protein levels in mice treated with the ER stressor tunicamycin.

Part two: Soluble epoxide hydrolase-targeting PROTAC activates AMPK and inhibits ER stress

- To characterize a new PROTAC for sEH protein degradation in the human hepatic Huh-7 cell line, in isolated mouse primary hepatocytes, and in the liver of mice.

- To assess the effect of the design PROTAC on ER stress and inflammation in hepatocytes and the liver.

- To delineate the molecular mechanisms by which PROTAC-mediated sEH degradation may inhibit ER stress and inflammation *in vitro* and *in vivo*.

III. Materials and Methods

III.1. Regents

The chemicals, compounds, reagents, commercial detection kits and recombinant proteins used in the present thesis are summarized in the next table:

Product	Manufacturer	Reference
Compound C	Santa Cruz	sc-200689
siRNA Control	Santa Cruz	sc-37007
Triglyceride determination kit	Spinreact	41031
Dil VLDL	Alfa Aesar	J65568
SIRT1 siRNA	Santa Cruz	sc-40986
PX-478	Apexbio	B6004
SRT1720	Apexbio	A4180
Tunicamycin	Tocris	268632
EX-527	RayBiotech	3RAY8

Table2. List of reagents used for cell and *in vivo* experiments.

III.2. In vivo experiments

Male Sprague-Dawley rats (Envigo, Barcelona, Spain) and male C57BL/6 mice were housed and maintained under constant conditions of light (12 hours light-dark cycles), temperature (22 ± 2°C) and humidity (55%). The animals were constantly fed a standard diet and supplied with freshwater *ad libitum* and were randomly distributed into different groups in cages after 1 week of acclimatization.

Animal experimentation complied with the Guide for the Care and Use of Laboratory Animals published by the US National Institutes of Health (8th edition: National Academies Press; 2011). All procedures were approved by the Bioethics Committee of the University of Barcelona, as stated in Law 5/21 July 1995 passed by the Generalitat de Catalunya. The animals were treated humanely, and all efforts were made to minimize both animal numbers and suffering.

III.2.1. Fructose-fed rats' treatment

Three-month-old male Sprague-Dawley rats (Envigo, Barcelona, Spain) were housed under conditions of constant humidity (40-60%) and temperature (20-24 °C), with a light/dark cycle of 12 h. Rats were randomly assigned to two groups: control (CT) and fructose (FR) (n = 5 in each). In addition to normal chow, the rats had free access to a 10% (w/v) FR solution or plain tap water for 3 weeks. In the FR group, one rat was euthanized before the end of the experimental period, due to a growing tumor; thus, the final n for the fructose group was 4. Following the treatment, the mice were anesthetized with isoflurane (IsoFlo, Esteve) and sacrificed by cervical dislocation. Samples of liver and blood were collected; the serum was to be extracted later, and the blood was kept in tubes for separation. After being frozen in liquid nitrogen, the tissue samples were kept at -80°C.

III.2.2. Assessment of Liver Responses in Wild-Type and *Sirt1*-Deficient Mice

Livers from male *Sirt1* knockout (*Sirt1*$^{-/-}$) mice (4-weeks-old; 129Sv:B6) and their wild-type littermates (*Sirt1*$^{+/+}$) were used (Planavila, A et al.2012).

III.2.3. Methods and Design of the Experiment to Assess the Impact of TM and SRT1720 on ER Stress in a MASLD- Mouse Model

Three-month-old male mice fed standard chow were randomly assigned to three groups [CT, TM and TM + SRT1720] (n = 4 in each). Mice received one daily p.o. dose of 200 mg/kg/day of the SIRT1 activator SRT1720 (Yamazaki, Yu et al.2009) or carboxymethylcellulose (CMC) (volume administered 1 mL/kg) as vehicle for 5 days, and before the sacrifice mice were treated for 24 h through i.p. injection with DMSO (vehicle, control, CT) or TM (3 mg/kg body weight). After the treatment, mice were sacrificed by cervical dislocation under the effects of isoflurane (IsoFlo, Esteve) anesthesia. Blood and liver samples were taken, and the blood was stored in tubes to be separated and the serum extracted later. The tissue samples were liquid nitrogen-snapped and then stored at -80°C.

III.2.4. Proof of concept: ALT-PG2 Efficacy Experiment in Male C57BL/6 Mice

Male C57BL/6 mice (10-12 weeks old), purchased from Envigo (Barcelona, Spain), were randomly distributed into two experimental groups (n = 5 each). One of the groups received one i.p. injection of vehicle (0.9% NaCl containing 5% DMSO and 10% castor oil) and the other ALT-PG2 (30 mg/kg, i.p., twice a day for 1 day) dissolved in the vehicle. Mice were sacrificed, and liver samples were frozen in liquid nitrogen and then stored at -80ºC.

III.3. Glucose Tolerance Test (GTT)

For the glucose tolerance test (GTT), animals received 2 g/kg body weight of glucose by an intraperitoneal injection and blood was collected from the tail vein after 0, 15, 30, 60 and 120 min.

III.4. Liver triglyceride content

Liver TGs were extracted according to Bligh & Dyer (BLIGH, E G, and W J DYER.1959). The lipid extract was evaporated under a stream of nitrogen gas, redissolved in absolute ethanol, and quantified using a commercial kit (SpinReact SA). In the last step, the Bradford assay was used to standardize it according to the concentration of protein.

III.5. Liver histology

For histological staining studies, samples were formalin fixed, paraffin embedded and 4 μm sections obtained. Oil Red staining (Sigma Aldrich) was performed in 10 μm frozen liver sections. Fifteen images at 20x magnification were captured.

III.6. In vitro experiments

III.6.1. Huh7

Human Huh-7 hepatoma cells (kindly donated by Dr. Mayka Sanchez from the Josep Carreras Leukemia Research Institute, Barcelona) were cultured in DMEM supplemented with 10% fetal bovine serum and 1% penicillin-streptomycin, at 37°C under 5% CO_2. Cell passages were carried out every three to four days, always prior to confluence when cells reached 80–90% confluency.

III.6.2. Primary hepatocytes

Primary mouse hepatocytes were isolated from non-fasting male C57BL/6 mice (10–12 weeks old) by perfusion with collagenase as described elsewhere (Benveniste et al., 1988).

Following the appropriate treatment, cells were extracted using a cell scraper from plate wells in PBS 1X (Sigma) and centrifuged for two minutes at 4°C and 10,000 *g*. Pellet was preserved for protein extraction, and supernatant was disposed of. In order to extract RNA, cells were directly homogenized and then treated with Trisure (Bioline) reagent.

III.6.3. Cell treatments

SIRT1 siRNA

Huh-7 cells were transiently transfected using Lipofectamine 2000 (Invitrogen, Carlsbad, CA) in Opti-MEM medium (Thermo Fisher, MA) with 100 nM siRNA against SIRT1 or siRNA control (Santa Cruz), in accordance with the manufacturer's instructions. Compounds were examined 24 hours following transfection.

EX-527, PX-478, TM

Huh-7 were exposed to 10 μM EX-527, 20 μM PX-478, 10 μM TM and 10 mM SRT1720 (Fiorentino, Teresa Vanessa et al.2015) for 24 h.

Compound C

The AMPK inhibitor Compound C (Santa Cruz) was used at a final concentration of 30 μM and incubated alone or co-incubated with ALT-PG2 for 24h.

Synthesis of ALT-PG2

For the synthesis of ALT-PG2 to a solution of trans-4-[4-(3-trifluoromethoxyphenyl-1-ureido) cyclohexyloxy] benzoic acid (t-TUCB) (26 mg, 0.055 mmol) in dimethylformamide (DMF) (0.5 mL) was added the recruiter molecule (thalidomide-PEG3-NH2·HCl, 25 mg, 0.046 mmol), and the solution was stirred at room temperature. N, N- diisopropylethylamine (DIPEA) (24 μl, 0.138 mmol) was added dropwise, and the mixture was stirred for 5 min at room temperature. Hexafluorophosphate azabenzotriazole tetramethyl uronium (HATU) (35 mg, 0.092 mmol) was added, and the mixture was stirred at room temperature overnight.

Water was added, and the mixture was extracted with ethyl acetate (3 ×). The combined organic phases were washed with NaHCO3 (twice), dried over anhydrous Na2SO4, filtered, and evaporated under reduced pressure to give a crude. Column chromatography [SiO2, 100% dichloromethane (DCM) to 90% DCM / 10% methanol mixtures] yielded ALT-PG2 (23 mg, 54% yield) as a white solid. 1H-RMN (400 MHz, DMSO-d6) δ: 1.32 – 1.40 (cs, 2 H), 1.44 – 1.53 (cs, 2 H), 1.91 – 1.95 (cs, 2 H), 2.00 – 2.06 (cs, 3 H), 2.51 – 2.50 (cs, 2 H), 2.89 (ddd, J =17.6, J'=13.9, J'' =5.5 Hz, 1 H), 3.30 (s, 2 H), 3.38 (q, J =6.0 Hz, 2 H), 3.44 (t, J =5.6 Hz, 2 H), 3.48–3.50 (cs, 12 H), 4.42 (m, 1 H), 4.78 (s, 2 H), 5.11 (dd, J =13.2 Hz, J′ =3.6 Hz, 1 H), 6.18 (d, J =7.4 Hz, 1 H), 6.99 (d, J =8.8 Hz, 2 H), 7.21 (d, J =8.4 Hz, 2 H), 7.39 (d, J = 8.4 Hz, 1 H), 7.45–7.50 (cs, 3 H), 7.77–7.82 (cs, 3 H), 8.00 (t, J =5.6 Hz, 1 H), 8.32 (t, J =5.6 Hz, 1 H), 8.5 (s, 1 H), 11.11 (brs, 1 H). 13C-RMN (100.6 MHz, DMSO-d6) δ: 22.0, 29.7, 30.0, 30.9, 38.4, 47.2, 48.8, 67.5, 68.8, 69.0, 69.6, 69.7, 74.1, 114.8, 116.0, 116.8, 118.5, 120.3, 121.6, 126.4, 129.0, 133.0, 136.9, 139.8, 141.9, 154.4, 155.0, 159.7, 165.4, 165.7, 166.7, 166.9, 169.9, 172.8. HRMS-ESI- m/z [M-]- calcd for [C44H48F3N6O13]-: 925.3237, found: 925.3225.

siRNA transfection

To prevent interference with the siRNAs the medium of differentiated Huh-7 cells was switched to DMEM without serum or antibiotics one day prior to transfection. Following the manufacturer's instructions, Lipofectamine 2000 (7 µl/1.5 ml well, Thermo- Fisher) was used as the transfection agent to conjugate the siRNA oligomers or the control siRNA (Santa Cruz) against SIRT1 (70 µM, Santa Cruz) in Opti-MEM medium (Sigma) at a final volume of 500 µl for each well. Following a 30-minute room temperature incubation period, these complexes were added to wells holding one millilitre of incubation medium. The transfection medium was changed to DMEM containing antibiotics after 8 hours, and treatments using the various compounds assayed were carried out after 24 hours of transfection, for a total duration of 48 hours after starting the process. There was a 60–70% guarantee of gene expression knockdown with this method.

III.7. Tissue processing

Liver

After the mice were sacrificed for the various experimental procedures, their whole livers were removed and snap-frozen in liquid nitrogen to be stored at -80°C later. A liver section weighing 30 mg was placed in glass test tubes filled with cold PBS 1X (Sigma) for additional processing. After that, the tissue was put into a 1.5 ml Eppendorf tube and homogenized using a Polytron homogenizer (Fisher Scientific). After all samples had been homogenized, they were centrifuged for two minutes at 4°C at 10,000g, and the supernatant was taken out. The tissue had been processed and was ready to extract proteins or RNA.

III.8. Immunoblotting

Total protein extraction

The RIPA buffer (Sigma) was mixed with a cocktail of protease and phosphatase inhibitors, which included 1 mM sodium orthovanadate (OvNa), 0.2 mM phenylmethylsulfonyl fluoride (PMSF), 5 mM sodium fluoride (NaF), 2.78 ml/ml aprotinin, and 20 mM leupeptin, before resuspending the cell or tissue pellets. On a microtube rotating system set to 30 rpm and 4°C, this was incubated for either 1 hour (for cell samples) or 2 hours (for tissue samples). Following that, samples were centrifuged at 10,000 *g* for 20 minutes at 4°C. The entire protein extract was found in the supernatant fraction, which was gathered and preserved.

Nuclear and cytosolic protein extraction

The extraction process involved two steps for the isolation of cytosolic and nuclear proteins. Initially, the pellet was again suspended in a mixture that included the previously mentioned ingredients along with 10 mM HEPES, 1.5 mM MgCl2, 10 mM KCl, and 0.5 mM DTT. Samples were incubated for 45 minutes at 4°C and 30 rpm on a microtube rotating system. Following this, they were centrifuged for 10 minutes at 4°C at 10,000 *g*. The cytosolic fraction-containing supernatant was gathered and kept cold at -80°C. After being resuspended in a second buffer with 25% glycerol, 420 mM NaCl, and 0.2 mM EDTA, the leftover pellet was incubated for a further 30 minutes at 4°C and 30 rpm on a microtube rotating system. Samples were then centrifuged for 10 minutes at 4°C at 10,000 g. Finally, the nuclear fraction was found in the supernatant, which was collected and kept at -80°C.

Protein quantification

Bradford-based colorimetric technique was used to quantify proteins, and a protein assay kit (Bio-Rad) was utilized. A 1:20 dilution of the dye reagent was added to the diluted samples, along with bovine serum albumin (BSA) standards, and the mixture was incubated for five minutes. The protein content of every sample was determined by extrapolating the BSA standard curve, which ranges from 0.1 to 0.6 mg/ml, and the absorbance was measured at 595 nM.

SDS-PAGE

Isolation of total protein extracts was performed as described elsewhere (Aguilar-Recarte, David et al.2021). Protein extracts, whether nuclear, cytosolic, or total, were divided based on molecular weight using sodium-dodecyl sulphate (SDS, Sigma) polyacrylamide gel electrophoresis (PAGE). 8–12% of polyacrylamide, SDS, and tris were present in the gel solution of HCl. Depending on the protein type and source, 20–40 μg of the protein extract were run into the gel on an electrophoresis at 120 volts for 70–90 minutes, contingent on the protein size and the percentage of polyacrylamide used.

Once migrated, the proteins were moved to a PVDF (polyvinylidene difluoride) membrane (Bio-Rad), which had been activated earlier by a one-minute methanol rinse and a further one-minute washing in distilled water. To prevent non-specific protein binding, the membrane's proteins were incubated in the commercial solution WestVisionTM Block and Diluent Solution (Cat. No: SP-7000, Vector Labs, CA) for one hour following transfer. After soaking the membrane for five minutes at 4°C in West Vision solution (dilutions listed in Table 5) and washing it three times in Tris-buffered saline (TBS) solution containing 0.1% Tween® 20 detergent (Sigma), the membrane was incubated with a secondary antibody solution (1:5000 to 1:10000 dilution) that was species-specific and able to bind the primary antibody used in TBS solution containing 5% of BSA and 0.1% Tween® 20 detergent. The size of the detected proteins was estimated using protein molecular mass standards (Bio-Rad, Barcelona, Spain). Signal acquisition was performed using the Bio-Rad ChemiDoc apparatus and quantification of immunoblot signal was performed with the Bio-Rad Image Lab software. The results for protein quantification were normalized to the levels of a control protein to avoid unwanted sources of variation. Glyceraldehyde 3-phosphate dehydrogenase (GAPDH), β-actin, α-tubulin (total and cytosolic protein), TATA-binding protein (TBP), or histone H3 (nuclear protein) were used as loading controls to normalize the levels of the proteins detected. Precision Plus Protein Dual Color Standard (Bio-Rad) was used as a protein marker to assess the molecular weight to the bands detected.

Antibody	**Manufacture**	**Reference**	**WB dillution**
ATF4	Cell Signalling	1185	1:500
β-Actin	Sigma	A5441	1:2000
BiP	Cell Signalling	3183	1:1000
CHOP	Genetex	GTX112827	1:1000
FGF21	Santa Cruz	sc-22920	1:1000
HIF-1α	Santa Cruz	sc-10790	1:1000
NQO1	Santa Cruz	sc-393736	1:1000
Ac-p53	Cell Signalling	2525	1:1000
SIRT1	Abcam	ab189494	1:1000
TRB3	Santa Cruz	sc-365842	1:1000
tubulin	Sigma	T6074	1:1000
VLDLR	R&D Systems	AF2258	1:1000
AMPKα	Cell Signaling	2532	1:1000
phosphorylated AMPK^{T172}	Cell Signaling	2531	1:1000
eIF2α	Cell Signalling	9722	1:1000
phosphorylated eIF2α Ser^{51}	Cell Signalling	9721	1:1000
ERK1/2	Cell Signaling	9102	1:1000
phosphorylated ERK1/2	Cell Signalling,	9101	1:1000
IRβ	Cell Signaling	3025	1:1000
IRS-1	Cell Signaling	2382	1:1000
NF-κB p65	Santa Cruz	sc-109	
phosphorylated NF-κB p65	Cell Signalling	3036s	1:1000
PP2A	Cell Signaling	2259	1:1000

p53	Cell Signaling	2524T	1:1000
sEH	Santa Cruz	sc-25797	1:1000
SOCS3	Santa Cruz	sc-9023	1:1000
STAT3	Santa Cruz	sc-482X	1:1000
phosphorylated STAT3-Tyr^{705}	Cell Signaling	9131	1:1000
TNF-α	R&D Systems	AF410-NA	1:1000
vinculin	Santa Cruz	sc-25336	1:1000
Secondary Anti-goat	Santa Cruz	sc-2020	1:5000
Secondary Anti-mouse	Thermo Fisher	A-11001	1:10000
Secondary Anti-rabbit	Thermo Fisher	A-11034	1:5000

Table3. List of antibodies used for immunoblotting

III.9. VLDL uptake assay

VLDLs labelled with DiI (1,1′-dioctadecyl-3,3,3′-tetramethyl-indocarbocyanine perchlorate) were from Alfa Aesar (Cat. No. J65568). Huh-7 cells were pretreated in serum-free media with 10 μM EX-527 or with this compound plus 20 μM PX-478 for 24 h prior to a 1 h incubation with 10 μg/ml DiI-VLDL. Surface-bound DiI-VLDL was removed with acid-wash buffer (0.5 M acetic acid with 150 mM NaCl, pH 2.5). Cells were washed with DPBS with calcium and magnesium, lysed in 1% SDS and 0.1 M NaOH, transferred to a black 96-well half-area plate (Greiner Bio-One), and assessed using a Varioscan micro plate reader (Ex/Em: 520/580 nm; Molecular Devices). Fluorescence was corrected for protein amount.

III.10. Quantitative PCR (qPCR)

RNA extraction

Utilizing the TRIsureTM reagent (Bioline) and the protocol outlined by Chomczynski et al. (Chomczynski and Sacchi, 1987), total RNA extraction was carried out for tissue samples (liver) and cell culture samples (HUH7). Isopropanol was added to precipitate RNA after RNA was separated from proteins and DNA using chloroform. To get rid of salts, 75% ethanol was used to wash the resulting pellet. RNA was quantified using Thermo Scientific's NanoDrop 1000, and its purity was evaluated by dividing its absorbance at 260 and 280 nm (A260/280) by A260/230. Ratios exceeding 1.8–1.9 were deemed appropriate.

Reverse transcription

Using random hexamers (Thermo Scientific), a 10 mM deoxynucleotid (dNTP) mix, and reverse transcriptase enzyme derived from the Moloney murine leukemia virus (MMLV, Thermo Fisher), isolated RNA was reverse transcribed to produce 1 µg of complementary DNA (cDNA). The protocol involved running a program with various steps and temperatures in a thermocycler (BioRad): 65°C for 5 minutes, 4°C for 5 minutes, 37°C for 2 minutes, 25°C for 10 minutes, 37°C for 50 minutes, and 70°C for 15 minutes.

Real time quantitative polymerase chain reaction (qPCR)

Using SYBR Green Master Mix (Applied Biosystems) and a Mini-48 well T100TM heat cycler (Bio-Rad), real-time PCR was used to assess the quantitative gene expression of mouse tissues and cell culture samples. The samples included 10 µl of 2x SYBR Green master mix, 0.9 µM of primer mix, and 25 ng of total cDNA in a final volume of 20 µl. For real-time PCR, the thermal cycler protocol comprised three steps for primer annealing, amplification, and denaturation: 95°C for 15 s, 60°C for 30 s, and 72°C for 30 s. The first step of denaturation was carried out at 95°C for 10 min. There were 40 repetitive cycles total. To determine the best primers for amplification, primer sequences were created using the NCBI's Primer-BLAST tool. These primers were then assessed using Integrated DNA Technologies' Oligo-Analyzer tool to guarantee the ideal melting temperature (Tm) and prevent the formation of homo/heterodimers or nonspecific structures that could impede the interpretation of the results. Table 3 shows that the primer sequences were specifically created to span the junction between exons.

GENE	Primer sequence	
mGapdh	for	5'-TGTGTCCGTCGTGGATCTGA-3'
	rev	5'-CCTGCTTCACCACCTTCTTGA-3'
mVldlr	for	5'-TCCAATGGCCTAATGGAATTACA-3'
	rev	5'-AGCATGTGCAACTTGGAATCC-3'
mVegfa	for	5'- GTTCAGAGCGGAGAAAGCATTTG-3'
	rev	5'- CACATCTGCAAG-TACGTTCGTT-3'
mGlut1	for	5'-GCCCCCAGAAGGTTATTGA-3'
	rev	5'- CGTGGTGAGTGTGGTGGAT-3'
hVLDL	*for*	5'-CAAGAGGAAGTTCCTGTTTAACTCTGA-3'
	rev	5'-TGACCAGTAAACAAAGCCAGACA-3'

Table4. Primer sequences designed for qPCR. h: human genes, m: mouse genes.

III.11. Statistical Analysis

Results are expressed as the mean ± SEM. Significant differences were assessed by either Student's t-test or one-way ANOVA, according to the number of groups compared, using the GraphPad Prism program (version 9.0.2) (GraphPad Software Inc., San Diego, CA, USA). When significant variations were found by ANOVA, Tukey's post-hoc test for multiple comparisons was performed only if F achieved a p value < 0.05. Differences were considered significant at $p < 0.05$.

IV.RESULTS

IV.1. Part 1: SIRT1 REGULATES HEPATIC VLDLR LEVELS THROUGH HIF-1α.

IV.1.1. VLDLR is increased and SIRT1 protein levels are reduced in the liver of rats supplemented with liquid fructose.

To examine a potential relationship between VLDLR and SIRT1, we examined the protein levels of VLDLR in the liver of rats supplemented with fructose, a well-known model of fatty liver (DiNicolantonio, et al.2017). Supplementation with a 10% liquid fructose for 21 days did not affect either body weight (Figure 1A) or epididymal fat depot (Figure 1B), but it resulted in glucose intolerance as demonstrated by the GTT (Figure 1C and D). In addition, fructose ingestion increased plasma TG levels (Figure 1E) and caused hepatic steatosis as determined by the quantification of triglyceride accumulation in the liver (Figure 1F) and hematoxylin & eosin (H&E) staining (Figure 1G). Interestingly, even the induction of a mild liver steatosis with a low percentage of fructose for a relatively short period of time resulted in an increase in the protein levels of VLDLR (Figure 1H), while the protein levels of SIRT1 were reduced (Figure 1I).

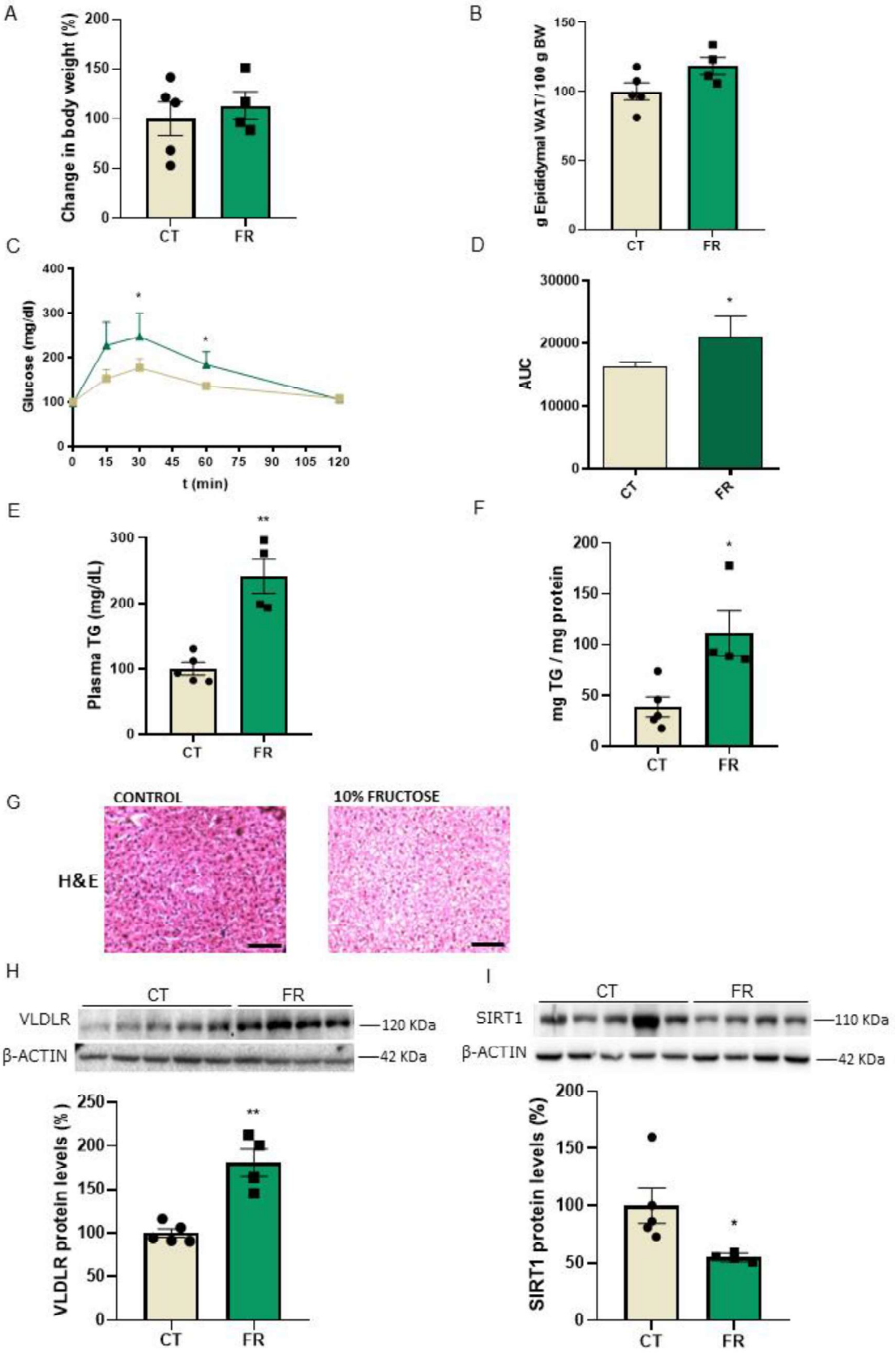
A
Change in body weight (%)
200
150
100
50
0
CT
FR
B
g Epididymal WAT/100 g BW
150
100
50
0
CT
FR
C
Glucose (mg/dl)
400
300
200
100
0
0 15 30 45 60 75 90 105 120
t (min)
*
*
D
AUC
30000
20000
10000
0
CT
FR
*
E
Plasma TG (mg/dL)
300
200
100
0
CT
FR
**
F
mg TG / mg protein
200
150
100
50
0
CT
FR
*
G
CONTROL
10% FRUCTOSE
H&E
H
CT
FR
VLDLR
β-ACTIN
120 KDa
42 KDa
VLDLR protein levels (%)
250
200
150
100
50
0
CT
FR
**
I
CT
FR
SIRT1
β-ACTIN
110 KDa
42 KDa
SIRT1 protein levels (%)
200
150
100
50
0
CT
FR
*

Fig. 1. Hepatic steatosis induced by liquid fructose in rats' results in an increase in VLDLR and a reduction in SIRT1 protein levels. (**A**) Change in body weight in rats with free access to plain tap water (Control, CT) or to a 10% (w/v) fructose (FR) solution for 3 weeks. (**B**) Epididymal adipose tissue. Glucose tolerance test (GTT) (**C**) and area under the curve (AUC) (**D**) in CT and FR rats. (**E**) Plasma triglyceride (TG) levels. (**F**) Hepatic TG levels. (**G**) Representative images of liver sections of hematoxylin–eosin (H&E) staining in CT and FR rats**.** Scale bar: 100 μm**.** Immunoblot analysis of VLDLR (**H**) and SIRT1 (**I**) in the liver of CT and FR rats. Data are presented as the mean ± SEM. Significant differences were established by Student's t-test. *p < 0.05 and **p < 0.01 *vs.* CT. n = 4 or 5 per group.

IV.1.2. *Sirt1*$^{-/-}$ mice show increased hepatic protein levels of VLDLR in the absence of ER stress.

To demonstrate that SIRT1 regulates VLDLR levels we used the livers from wild-type and *Sirt1*$^{-/-}$ mice that survived to adulthood, since only 24% of the *Sirt1*$^{-/-}$ mice pups born survive the first week of life (Planavila, et al.2012). In the liver of these mice, we assessed the protein levels of acetylated p53, a target of SIRT1 (Vaziri, et al.2001). As expected, *Sirt1* deficiency resulted in increased levels of acetylated p53 (Figure 2A). Remarkably, the mRNA (Figure 2B) and protein levels (Figure 2C) of VLDLR were increased in the livers of *Sirt1*$^{-/-}$ mice compared to wild-type mice, indicating that the absence of this deacetylase might increase the VLDLR levels through a transcriptional mechanism. Since VLDLR expression has been reported to be upregulated by the transcription factor ATF4 in liver during ER stress (Jo, et al.2013), we determined the levels of ATF4 as well as other markers of ER stress. No changes were observed in the protein levels of ATF4 in the liver of *Sirt1*$^{-/-}$ mice (Figure 2D). Likewise, no differences were detected in the protein levels of the ER stress markers BiP/GRP78, TRB3 (Figure 2D) or FGF21 (Figure 2E), the latter reported to be upregulated by ATF4 (De Sousa-Coelho, Ana Luísa et al.2012).

However, the protein levels of CHOP were upregulated in the liver of *Sirt1*$^{-/-}$ mice (Figure 2F). The increase in CHOP might be related, not to the presence of ER stress, but to the upregulation of VLDLR, since a previous study reported that the absence of VLDLR in white adipose tissue is accompanied by a reduction of CHOP (Nguyen, et al.2014), suggesting that VLDLR regulates CHOP levels.

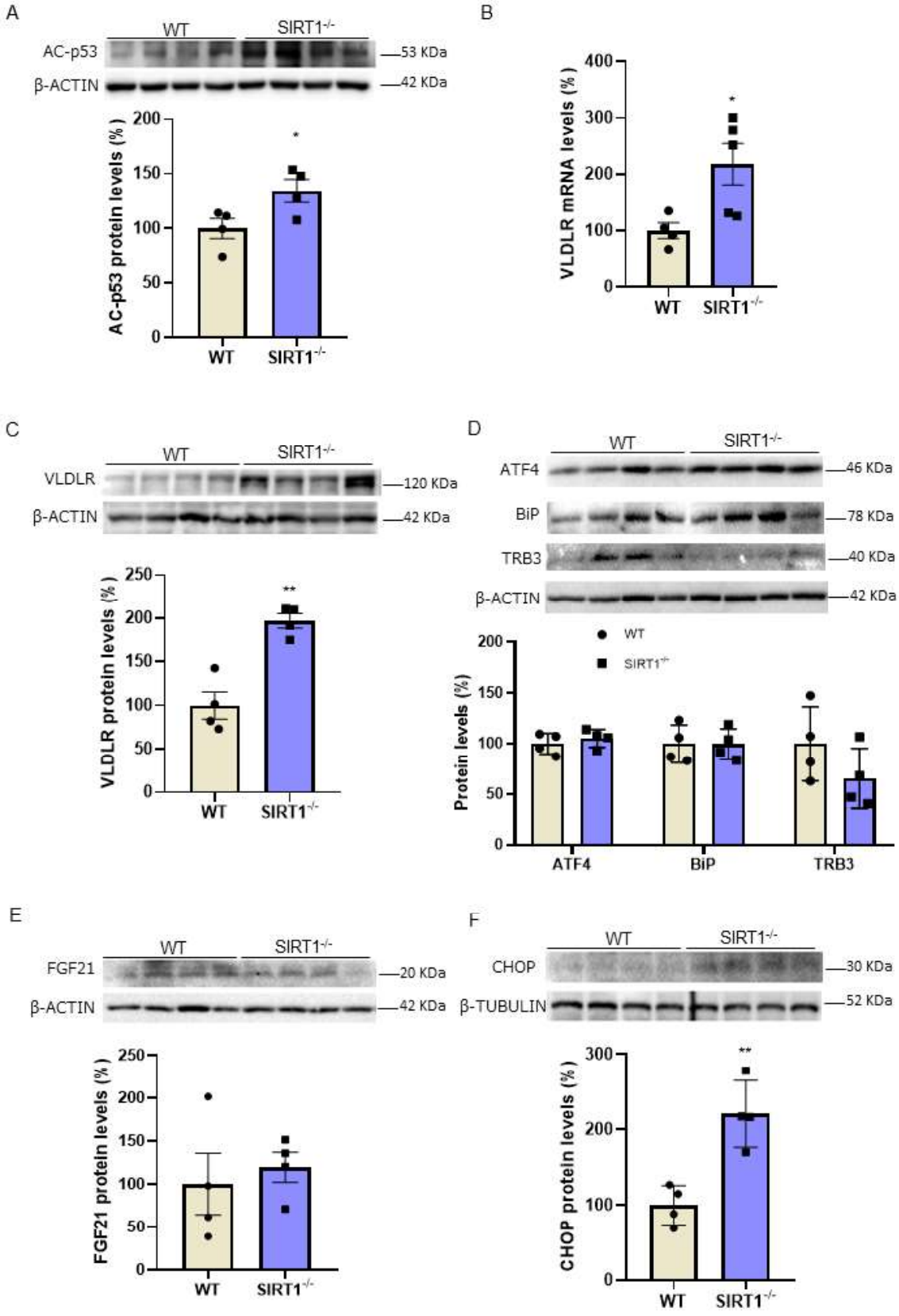
A
WT
SIRT1-/-
AC-p53
β-ACTIN
53 KDa
42 KDa
AC-p53 protein levels (%)
200
150
100
50
0
*
WT
SIRT1-/-
B
VLDLR mRNA levels (%)
400
300
200
100
0
*
WT
SIRT1-/-
C
WT
SIRT1-/-
VLDLR
β-ACTIN
120 KDa
42 KDa
VLDLR protein levels (%)
250
200
150
100
50
0
**
WT
SIRT1-/-
D
WT
SIRT1-/-
ATF4
BiP
TRB3
β-ACTIN
46 KDa
78 KDa
40 KDa
42 KDa
WT
SIRT1-/-
Protein levels (%)
200
150
100
50
0
ATF4
BiP
TRB3
E
WT
SIRT1-/-
FGF21
β-ACTIN
20 KDa
42 KDa
FGF21 protein levels (%)
250
200
150
100
50
0
WT
SIRT1-/-
F
WT
SIRT1-/-
CHOP
β-TUBULIN
30 KDa
52 KDa
CHOP protein levels (%)
300
200
100
0
**
WT
SIRT1-/-

Fig. 2. VLDLR is increased in the liver of *Sirt1*$^{-/-}$ mice. (**A**) Immunoblot analysis of acetylated (Ac)-p53 in the liver of WT and *Sirt1*$^{-/-}$ mice. (**B**) mRNA levels of *Vldlr*. Immunoblot analysis of VLDLR (**C**), ATF4, BiP/GRP78, TRB3 (**D**), FGF21 (**E**) and CHOP (**F**) in the liver of WT and *Sirt1*$^{-/-}$ mice. Data are presented as the mean ± SEM. Significant differences were established by Student's t-test. *p < 0.05 and **p < 0.01 *vs.* CT. n = 4 or 5 per group.

IV.1.3. SIRT1 inhibition leads to the upregulation of VLDLR via HIF-1α in hepatic cells.

Since VLDLR has been reported to be under the transcriptional control of Nrf2 (Wang, et al.2014), we also examined the protein levels of its target gene NAD(P)H quinone dehydrogenase 1 (NQO1). No changes were observed in the NQO1 protein levels in the liver of *Sirt1*$^{-/-}$ mice (Figure 3A), making unlikely the contribution of Nrf2 to the increase in VLDLR in these mice. Another transcription factor regulating VLDLR expression is HIF-1α (Klevstig, et al.2016). Although no changes were observed in HIF-1α protein levels in the liver of *Sirt1*$^{-/-}$ mice compared to wild-type mice (Figure 3B), its transcriptional activity seemed to be upregulated, since the hepatic expression of its target genes, *Glut1* (Figure 3C) and *Vegfa* (Figure 3D), was increased in *Sirt1*$^{-/-}$ mice. These findings suggested that the increased transcriptional activity of HIF-1α might also contribute to elevating VLDLR levels in the liver of *Sirt1*$^{-/-}$ mice. To demonstrate that reduced SIRT1 activity leads to VLDLR upregulation through HIF-1α, we used both a pharmacological and a genetic approach in the human hepatoma cell line Huh-7. First, we used a potent and selective SIRT1 inhibitor, EX-527 (Napper, et al.2005, Broussy, et al.2020). Exposure of Huh-7 cells to EX-527 increased both the expression (Figure 4A) and the protein levels (Figure 4B) of VLDLR, supporting the findings obtained in *Sirt1*$^{-/-}$ mice.

Interestingly, co-incubation of the cells with EX-527 and the HIF-1α inhibitor PX-478 (Welsh, Sarah et al.2004) abrogated the increase in VLDLR protein levels caused by EX-527 (Figure 4C), indicating that HIF-1α was responsible for the upregulation of VLDLR under reduced SIRT1 activity conditions. Next, we assessed whether the changes in VLDLR levels affected the uptake of VLDL. Consistent with the increase in VLDLR caused by EX-527, this compound upregulated VLDL uptake, while in the presence of PX-478 the effect of EX-527 was blunted (Figure 4D).

To further demonstrate that SIRT1 downregulation increases VLDLR via HIF-1α, we knocked down *SIRT1* expression by transfecting cells with siRNA targeting the *SIRT1* gene. The knockdown of *SIRT1* reduced its protein levels and increased those of VLDLR (Figure 4E). However, incubation with PX-478 completely abolished the increase in VLDLR. Collectively, these findings indicate that the reduction in the activity or in the levels of SIRT1 in human Huh-7 hepatic cells results in the upregulation of VLDLR through HIF-1α.

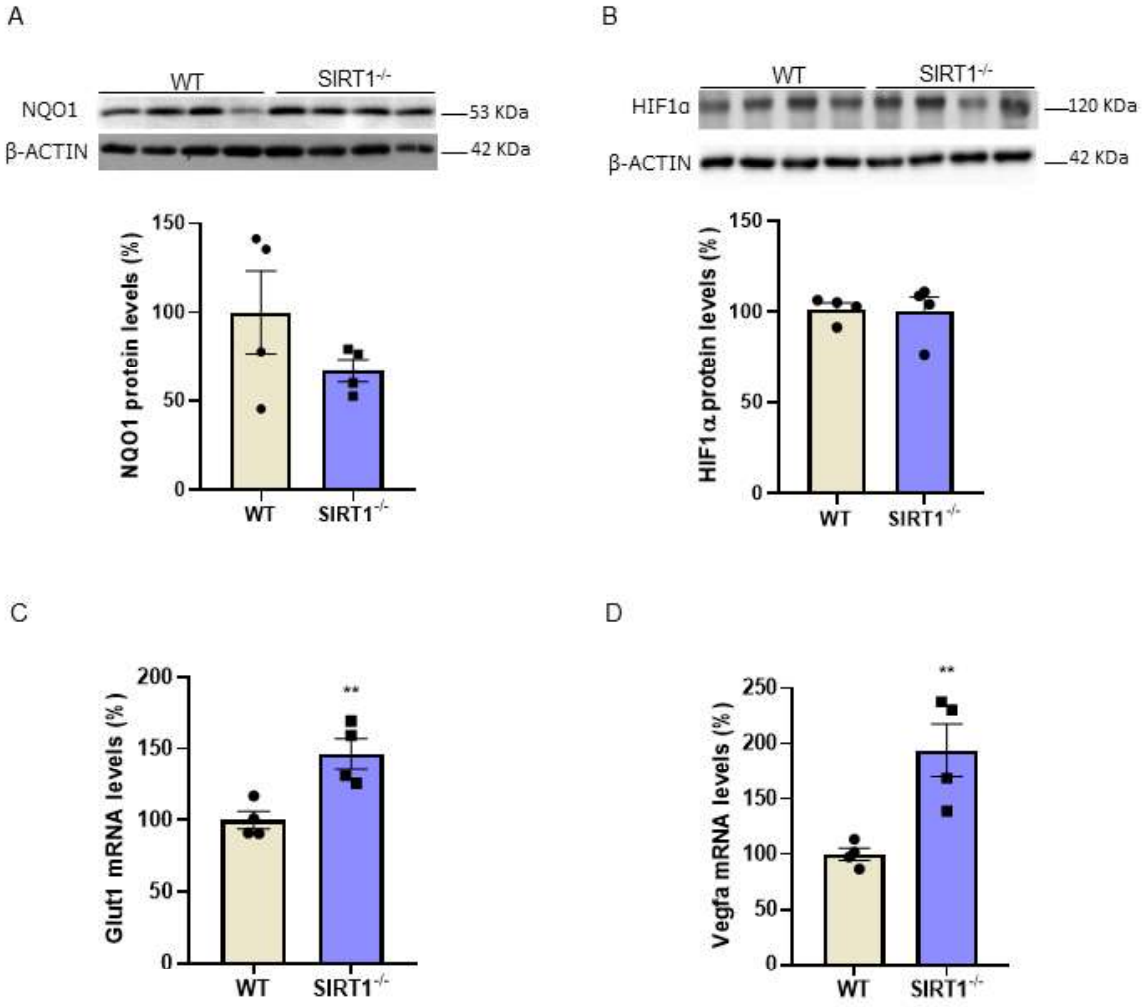

Fig. 3. HIF-1α target genes are increased in the liver of *Sirt1*$^{-/-}$ mice. Immunoblot analysis of and NQO1 (**A**) HIF-1α (**B**) in the liver of WT and *Sirt1*$^{-/-}$ mice. mRNA levels of *Glut1* (**C**) and *Vegfa* (**D**) in the liver of WT and *Sirt1*$^{-/-}$ mice. Data are presented as the mean ± SEM. Significant differences were established by Student's t-test. *$p < 0.05$ and **$p < 0.01$ *vs.* CT. n = 4 per group.

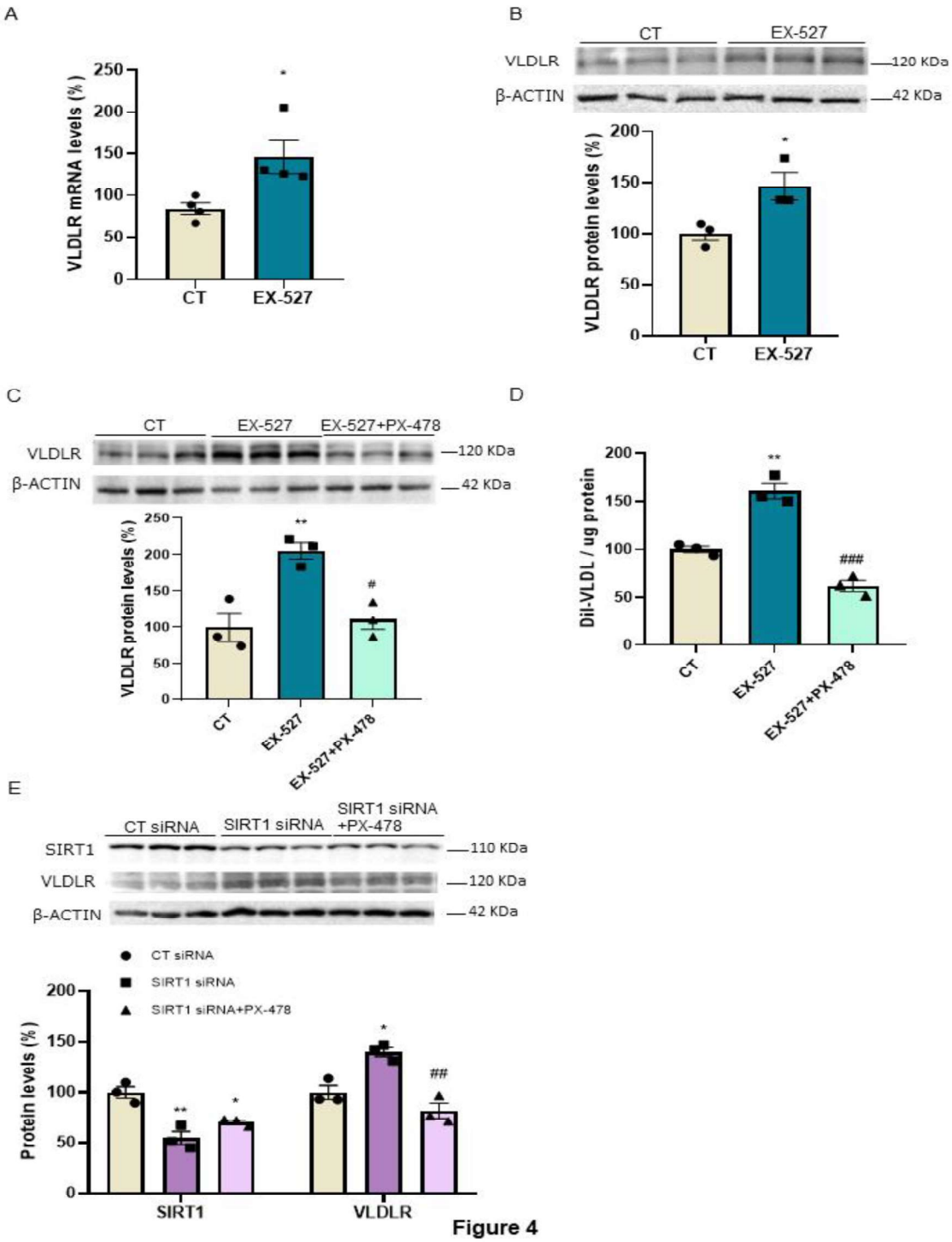
A
VLDLR mRNA levels (%)
250
200
150
100
50
0
CT
EX-527
B
CT
EX-527
VLDLR
β-ACTIN
120 KDa
42 KDa
VLDLR protein levels (%)
200
150
100
50
0
CT
EX-527
C
CT
EX-527
EX-527+PX-478
VLDLR
β-ACTIN
120 KDa
42 KDa
VLDLR protein levels (%)
250
200
150
100
50
0
**
#
CT
EX-527
EX-527+PX-478
D
Dil-VLDL / ug protein
200
150
100
50
0
**
###
CT
EX-527
EX-527+PX-478
E
CT siRNA
SIRT1 siRNA
SIRT1 siRNA +PX-478
SIRT1
VLDLR
β-ACTIN
110 KDa
120 KDa
42 KDa
CT siRNA
SIRT1 siRNA
SIRT1 siRNA+PX-478
Protein levels (%)
200
150
100
50
0
**
*
*
##
SIRT1
VLDLR

Figure 4

Fig. 4. SIRT1 inhibition increases VLDLR levels and VLDL uptake via HIF-1α in human Huh-7 cells. mRNA (A) and immunoblot analysis (B) of VLDLR in human Huh-7 cells in the absence (control, CT) or presence of 10 μM EX-527 for 24 h. Immunoblot analysis of VLDLR (C) and VLDL uptake (D) in human Huh-7 cells in the absence (control, CT), the presence of 10 μM EX-527, or the combination of 10 μM EX-527 and 20 μM PX-478 for 24 h. (E) Immunoblot analysis of SIRT1 and VLDLR in Huh-7 cells transfected with control siRNA or SIRT1 siRNA in the absence or the presence of 20 μM PX-478. Data are presented as the mean ± SEM. Significant differences were established by Student's t-test or one-way ANOVA with Tukey's post-hoc test. *$p < 0.05$ and **$p < 0.01$ *vs.* CT. $^{\#}p < 0.05$, $^{\#\#}p < 0.01$, and $^{\#\#\#}p < 0.001$ *versus* EX-527 or SIRT1 siRNA. n = 3 or 4 per group.

IV.1.4. SIRT1 activation ameliorates fatty liver and abolishes the increase in hepatic VLDLR caused by ER stress

Since hepatic VLDLR is elevated in response to ER stress and it contributes to ER stress-dependent hepatic steatosis (Hyunsun et al.2013), we next evaluated whether SIRT1 activation attenuated VLDLR upregulation and hepatic steatosis caused by the ER stressor TM. First, we treated Huh-7 cells with TM in the presence or in the absence of the SIRT1 activator SRT1720 (Gano, et al.2014). As expected, TM increased the protein levels of VLDLR, but this increase was completely prevented in cells co-incubated with SRT1720 (Figure 5A). We then treated mice with TM with either vehicle or SRT1720. TM treatment resulted in a decrease in serum TG, which is likely to be the result of the higher uptake of circulating TG-enriched lipoproteins by VLDLR, while SRT1720 attenuated this reduction (Figure 5B). This suggests that the uptake of VLDLs by VLDLR is attenuated. TM also led to a clear increase in hepatic triglyceride accumulation as demonstrated by the H&E and ORO staining (Figure 5C) and the quantification of this neutral lipid (Figure 5D). However, treatment with SRT1720 strongly alleviated fatty liver.

Consistent with a higher uptake of circulating triglyceride-enriched lipoproteins VLDLR protein levels were increased in mice treated with TM (Figure 5E), whereas the SIRT1 activator abolished this increase. Overall, these findings indicate that SIRT1 activation contributes to preventing ER stress-induced fatty liver by reducing the levels of VLDLR and modulating serum and hepatic levels of TGs.

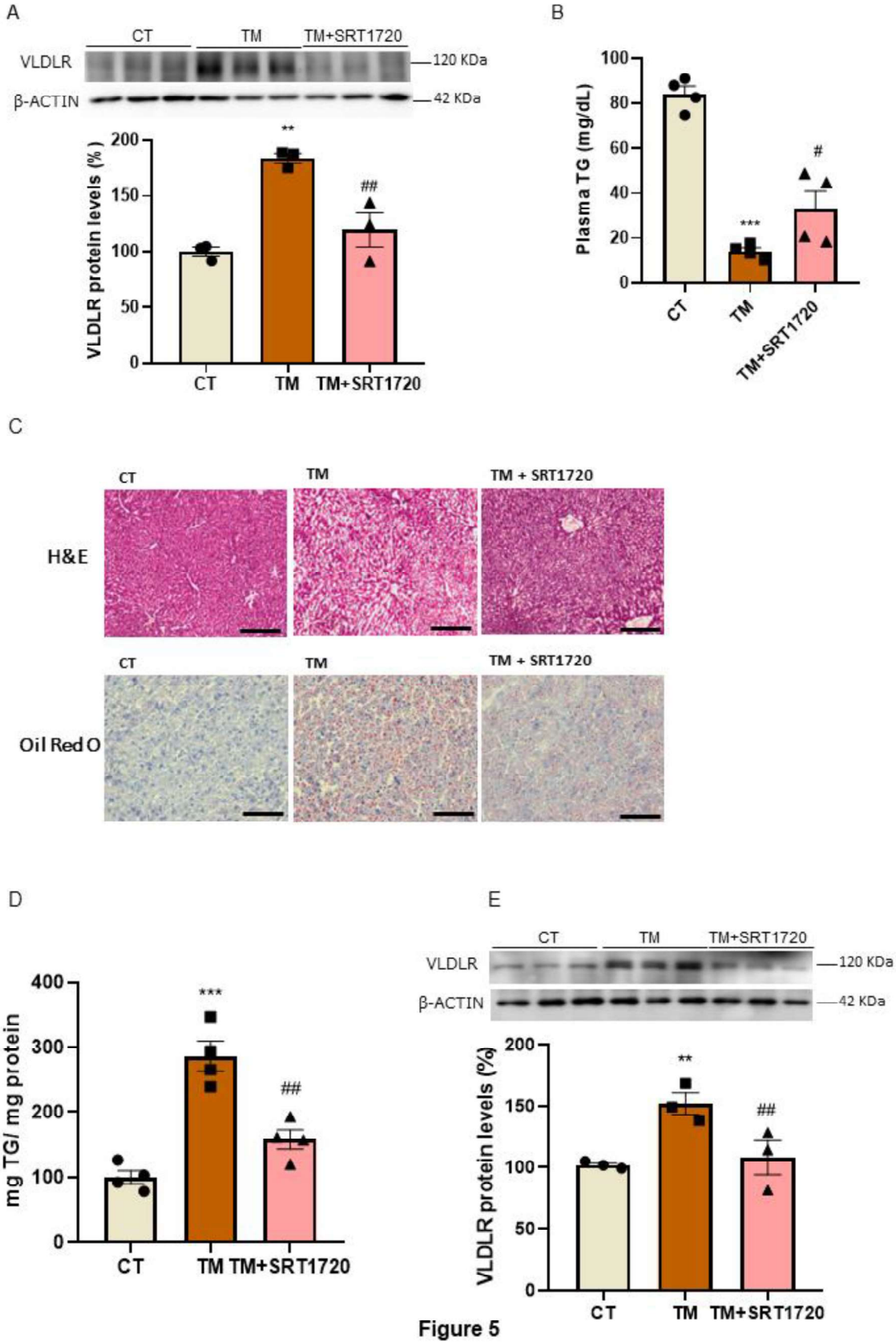
A
CT
TM
TM+SRT1720
VLDLR
120 KDa
β-ACTIN
42 KDa
VLDLR protein levels (%)
200
150
100
50
0
**
##
CT
TM
TM+SRT1720
B
Plasma TG (mg/dL)
100
80
60
40
20
0
***
#
CT
TM
TM+SRT1720
C
CT
TM
TM + SRT1720
H&E
CT
TM
TM + SRT1720
Oil Red O
D
mg TG/ mg protein
400
300
200
100
0
***
##
CT
TM
TM+SRT1720
E
CT
TM
TM+SRT1720
VLDLR
120 KDa
β-ACTIN
42 KDa
VLDLR protein levels (%)
200
150
100
50
0
**
##
CT
TM
TM+SRT1720

Figure 5

Fig. 5 SIRT1 activation prevents the increase in VLDLR caused by the ER stressor TM. (A) Immunoblot analysis of VLDLR in human Huh-7 cells in the absence (control, CT), the presence of TM or the combination of TM plus SRT1720 for 24 h. (n = 3) (**B**) Plasma TG levels in mice treated with the SIRT1 activator SRT1720 for 5 days that received an injection of vehicle or TM the last 24 h. (n = 4 animals) (**C**) Representative images of liver sections of hematoxylin-eosin (H&E) and Oil Red O (ORO) staining**.** Scale bar: 100 μm**.** (**D**) Hepatic TG levels. (**E**) Immunoblot analysis of VLDLR in the liver of mice. Data are presented as the mean ± SEM. Significant differences were established by one-way ANOVA with Tukey's post-hoc test. **p < 0.01 and ***p < 0.001 *vs.* CT. #p < 0.05 and ##p < 0.01 *versus* TM.

IV.2. Part 2: Soluble epoxide hydrolase-targeting PROTAC activates AMPK and inhibits ER stress

IV.2.1. Characterization of the sEH PROTAC ALT-PG2

In this second part, we evaluated two sEH PROTACs against sEH, ALT-PG2 and ALT-PG3. These compounds consist of the sEH inhibitor *trans*-4-[4-(3-trifluoromethoxyphenyl-1-ureido)-cy-clohexyloxy]-benzoic acid (*t*-TUCB) (Table 1) as binder to the enzyme, while incorporate the thalidomide-based cereblon ligand (as E3 ligase ligand) and two different polyethylene glycol (PEG) linkers. PEG3 was the linker incorporated in ALT-PG2 and PEG4 in ALT-PG3 (Table 1). Both compounds showed equal inhibitory potency against human sEH, but that of ALT-PG3 was higher for murine sEH (Table 1). As a control, we first examined the effects of different concentrations of the sEH inhibitor *t*-TUCB on the protein levels of sEH in the human hepatoma-derived Huh-7 cell line. As expected, exposure to this compound did not cause sEH degradation (Figure 1A). In contrast, ALT-PG2 caused a robust degradation of sEH protein levels at concentrations ranging from 1 nM to 1 μM (Figure 1B).

At 1 μM concentration some U-shaped concentration-response curve or hook effect was observed, a known phenomenon for other PROTACs (Pettersson, and Crews., 2019). This effect was not observed with ALT-PG3, although it caused a weaker degradation of sEH, thereby suggesting a lower degradation potency. Thus, we selected the ALT-PG2 PROTAC at 10 nM for further study. When we conducted a time-course study, we observed that significant sEH degradation occurred after only 1 h of treatment, but exposure for longer periods (8, 12 and 24 h) provided greater degradation (Figure 1D). To determine whether ALT-PG2-induced ubiquitination led to sEH degradation via the ubiquitin-proteasome system, cells were treated with the proteasome inhibitor MG132 prior PROTAC application. Inhibition of proteasome with MG132 completely abrogated the ALT-PG2-mediated degradation of sEH (Figure 2A), indicating that this degradation depends on the ubiquitin-proteasome system. Moreover, addition of the cereblon ligand lenalidomide effectively rescued the degradation of sEH by ALT-PG2, confirming that it requires the binding of ALT-PG2 to cereblon (Figure 2B). One of the potential advantages of PROTACs over inhibitors is the potential development of cumulative efficacy after repeating administration when the target protein is slowly synthesized in cells. To assess the presence of this potential effect for ALT-PG2, repeated administrations were conducted in cells. Exposure to 2 concentrations for 24 h or 4 concentrations for 12 h of 10 nM ALT-PG2 yielded similar degradations of sEH (Figure 2C), suggesting that ALT-PG2 does not develop cumulative efficacy following repeated administrations, at least during the time periods assessed.

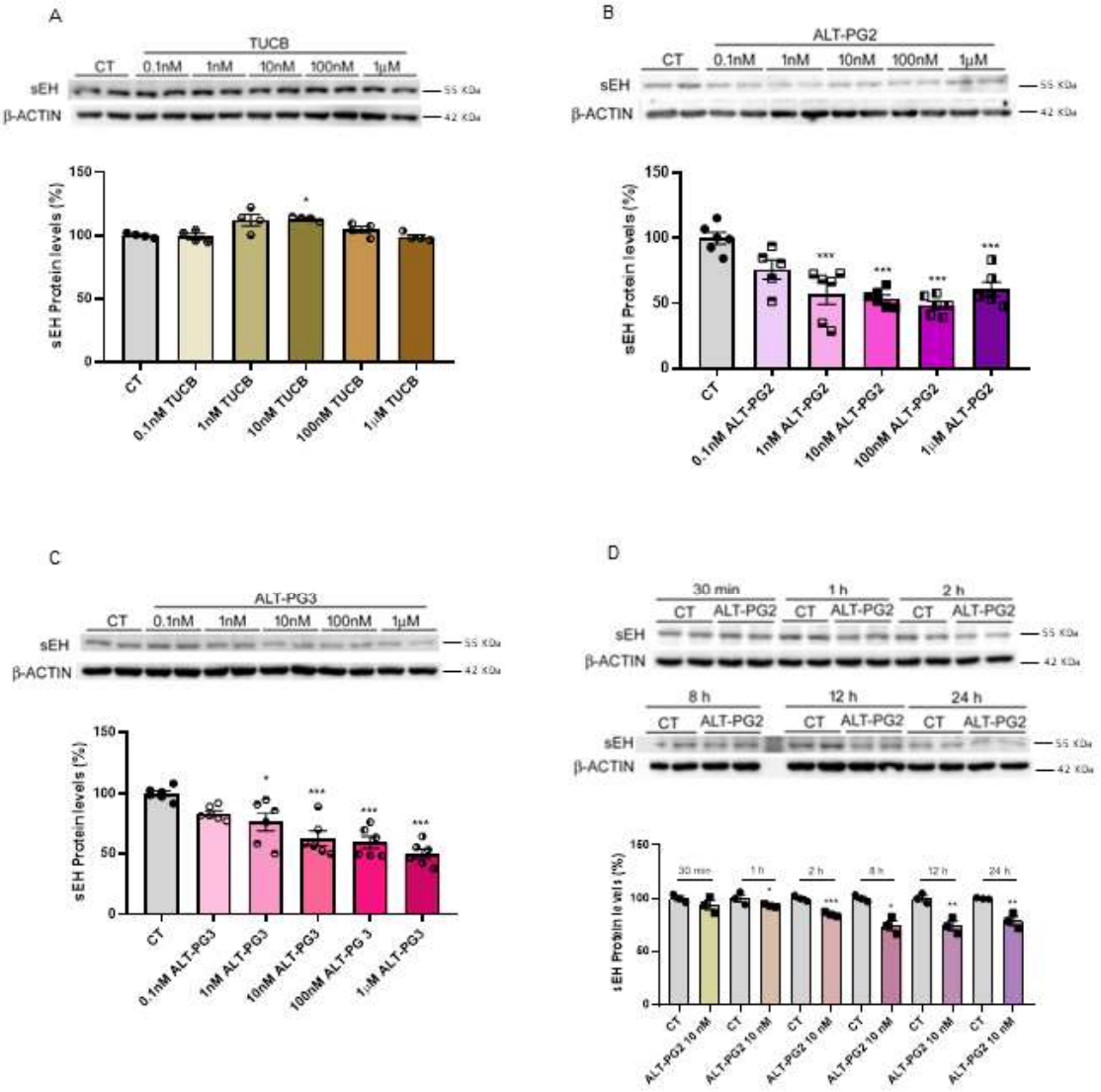

Figure 1. ALT-PG2 PROTAC degrades sEH in Huh-7 hepatic cells. (**A**) Immunoblot analysis of sEH in Huh-7 hepatic cells exposed to different concentrations of *t*-TUCB for 24 h. Immunoblot analysis of sEH in Huh-7 hepatic cells exposed to different concentrations of (**B**) ALT-PG2 or (**C**) ALT-PG3 for 24 h. (**D**) Time-course of the effects of 10 nM ALT-PG2 on sEH protein levels. Data are presented as the mean ± SEM. one-way ANOVA with Tukey's post hoc test. *p < 0.05, **p < 0.01 and ***p < 0.001 *vs.* CT.

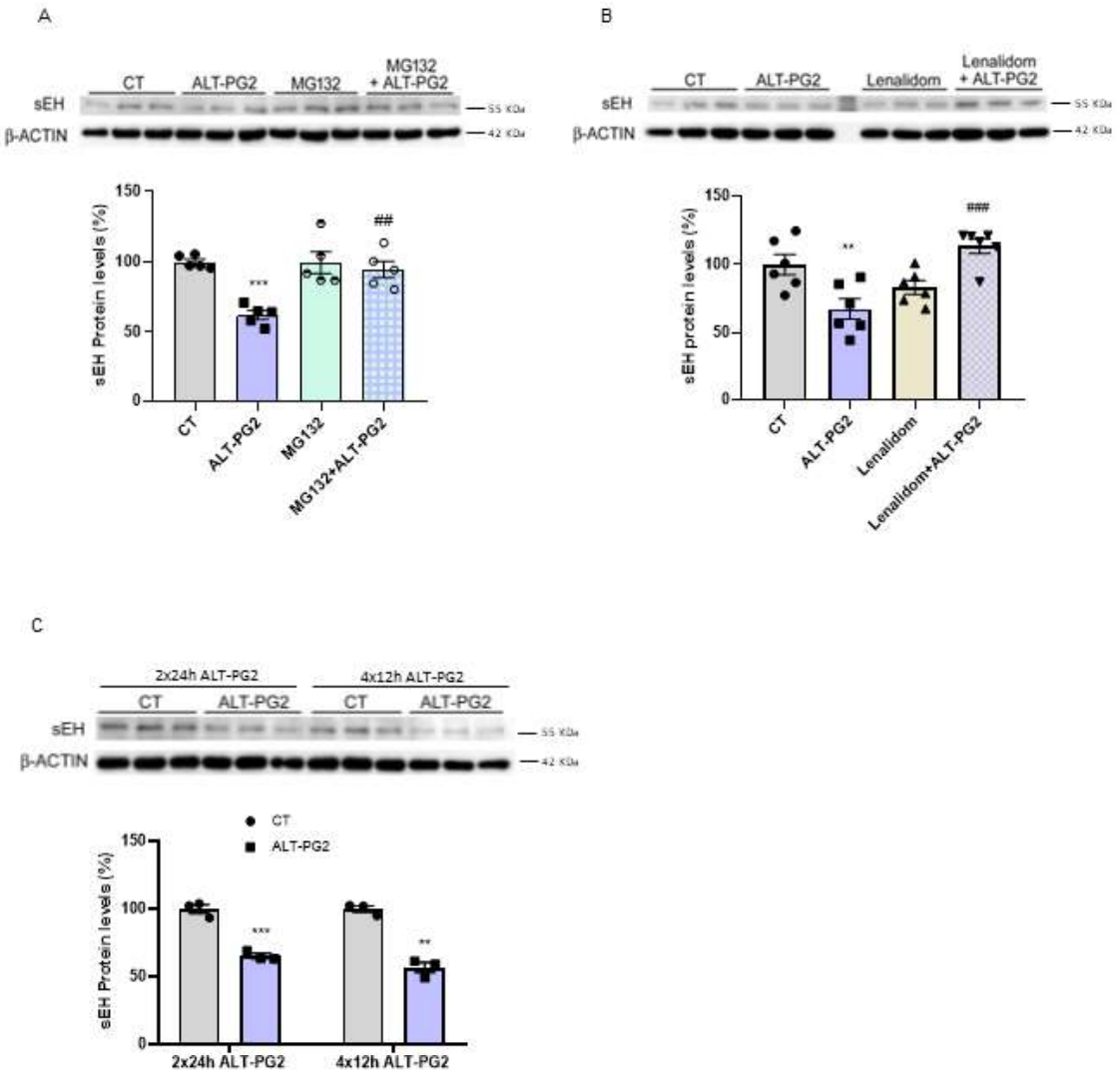

Figure 2. ALT-PG2 degrades sEH via the ubiquitin–proteasome system in Huh-7 hepatic cells. (**A**) Immunoblot analysis of sEH in Huh-7 hepatic cells exposed to 10 nM ALT-PG2 for 24 h in the presence or in the absence of 10 μM of the proteasome inhibitor MG132 (added 3 h prior ALT-PG2). (**B**) Immunoblot analysis of sEH in Huh-7 hepatic cells exposed to 10 nM ALT-PG2 for 24 h in the presence or in the absence of 10 μM of the cereblon ligand lenalidomide (added 3 h prior ALT-PG2). (**C**) sEH protein levels in Huh-7 hepatic cells exposed to the addition of 2 concentrations of ALT-PG2, each one every 24 h, and 4 concentrations of ATL-PG2, each one every 12 h. Data are presented as the mean ± SEM. Significant differences were established by Student's-t test or one-way ANOVA with Tukey's post hoc test. *$p < 0.05$, **$p < 0.01$ and ***$p < 0.001$ *vs.* CT. ##$p < 0.01$ *vs.* ALT-PG2.

IV.2.2. sEH degradation by ALT-PG2 activates AMPK and reduces the levels of ER stress markers in human Huh-7 hepatic cells

Previous studies have reported that the reduction in cardiac AMPK caused by a HFD is prevented in sEH knockout mice (Wang, et al., 2021), that hepatocytes from sEH knockout mice show activation of AMPK (Mangels, et al., 2016), as well as that sEH inhibition significantly attenuates the HFD-induced renal injury, partially by activating AMPK (Luo, et al., 2019). Since these findings suggested that both the absence of sEH or its inhibition resulted in AMPK activation, we next examined whether sEH degradation by ALT-PG2 activated AMPK in human Huh-7 hepatic cells. Moreover, given that AMPK activation mitigates ER stress (Hwang, et al.., 2013; Salvadó, et al., 2014), we also examined if ALT-PG2 attenuated ER stress and inflammatory markers. Exposure of cells to 10 nM ALT-PG2 for 16 h caused a rapid and robust degradation of sEH (Figure 3A). This was accompanied by AMPK activation (Figure 3B), and consistent with the reported inhibitory crosstalk between AMPK and ERK1/2, the phosphorylated levels of the latter kinase were reduced (Figure 3C). The fact that the sEH inhibitor *t*-TUCB increased the phosphorylated levels of AMPK (Figure 3D) suggests that AMPK activation caused by ALT-PG2 is mediated by the reduction of the hydrolase activity, while further studies are needed to evaluate whether the phosphatase activity of the enzyme contributes to AMPK activation. AMPK is known to inhibit the p53 negative regulator, murine double minute X (MDMX), resulting in increased p53 levels (Aguilar-Recarte, et al., 2021). Consistent with this, AMPK activation caused by ALT-PG2 was accompanied by an increase in p53 protein levels (Figure 3E), supporting that ALT-PG2 activates AMPK. Likewise, treatment with ALT-PG2 reduced the levels of ER stress marker p-eIF2α (Figure 3F), while no changes were observed in the levels of inflammatory transcription factor NF-κB or in its phosphorylation status (Figure 3G).

Despite this latter finding, the levels of phosphorylated STAT3, which is activated by ER stress (Meares *et al.*, 2014) and is primary downstream regulator of interleukin (IL)-6 signaling with a prominent role in regulating inflammation (Matsuda,. 2023), were attenuated by ALT-PG2 (Figure 3H). Since activation of the STAT3 pathway has been reported to reduce IRS1 protein levels in hepatocytes (Serrano-Marco, et al., 2012) and ER stress reduces the levels of insulin receptor β (IRβ) Zhou, Lijun et al., 2009), we examined the levels of these two proteins involved in the insulin signaling pathway. Remarkably, the protein amount of both IRβ and IRS1 were upregulated by ALT-PG2 (Figure 3I). Collectively, these findings indicate that the degradation of sEH by ALT-PG2 activates AMPK, reduces ER stress and inflammatory markers, and increases the levels of proteins involved in the insulin signaling pathway in hepatocytes.

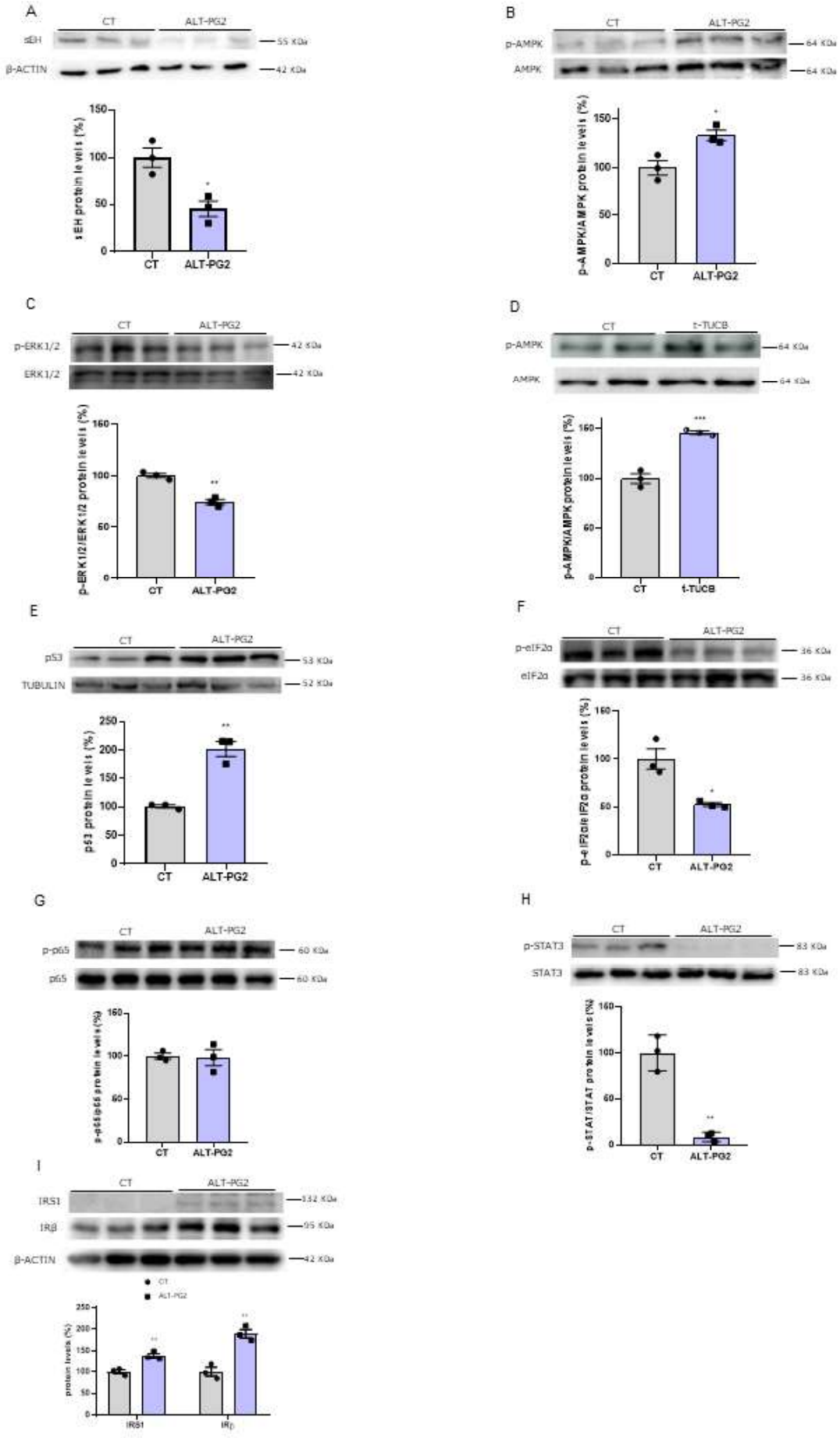
A
CT
ALT-PG2
sEH
β-ACTIN
55 KDa
42 KDa
sEH protein levels (%)
B
p-AMPK
AMPK
64 KDa
p-AMPK/AMPK protein levels (%)
C
p-ERK1/2
ERK1/2
42 KDa
p-ERK1/2/ERK1/2 protein levels (%)
D
t-TUCB
p-AMPK/AMPK protein levels (%)
E
p53
TUBULIN
53 KDa
52 KDa
p53 protein levels (%)
F
p-eIF2α
eIF2α
36 KDa
p-eIF2α/eIF2α protein levels (%)
G
p-p65
p65
60 KDa
p-p65/p65 protein levels (%)
H
p-STAT3
STAT3
83 KDa
p-STAT/STAT protein levels (%)
I
IRS1
IRβ
132 KDa
95 KDa
protein levels (%)

Figure 3. sEH degradation by ALT-PG2 activates AMPK and reduces basal levels of ER stress markers in Huh-7 hepatic cells. Immunoblot analysis of (**A**) sEH in Huh-7 hepatic cells exposed to 10 nM ALT-PG2 for 16 h. (**B**) Total and phosphorylated AMPK and (**C**) total and phosphorylated ERK1/2 in Huh-7 hepatic cells exposed to 10 nM ALT-PG2 for 48 h.(**D**) Immunoblot analysis of total and phosphorylated AMPK in Huh-7 hepatic cells exposed to 1 μM *t*-TUCB for 4 h. Immunoblot analysis of (**E**) p53, (**F**) total and p-eIF2α, (**G**) total and phosphorylated levels of the p65 subunit of NF-κB, (**H**) total and phosphorylated (Tyr^{705}) levels of STAT3 and (**I**) IRβ and IRS1 in Huh-7 hepatic cells exposed to 10 nM ALT-PG2 for 16 h. Significant differences were established by Student's-t test. *$p < 0.05$, **$p < 0.01$ and ***$p < 0.001$ *vs.* CT.

IV.2.3. sEH degradation by ALT-PG2 attenuates thapsigargin-induced ER stress in human Huh-7 hepatic cells

To confirm that ALT-PG2 ameliorates ER stress, we used the ER stressor thapsigargin. Exposure of Huh-7 cells to thapsigargin did not significantly increase sEH protein levels, but co-incubation with thapsigargin and ALT-PG2 resulted in sEH degradation (Figure 4A). Interestingly, ALT-PG2 abolished the increase in the ER stress markers CHOP (Figure 4A), p-eIF2α (Figure 4B), TRB3 and very low-density lipoprotein receptor (VLDLR) (Figure 4C). Consistent with these effects of ALT-PG2, this compound prevented the increase in the levels of SOCS3 (Figure 4A), a STAT3-target gene, and of the inflammatory markers NF-κB (p65 subunit of this transcription factor) and TNF-α (Figure 4C). These findings indicate that ALT-PG2 reduces the levels of ER stress and inflammatory markers in thapsigargin-stimulated cells. Since AMPK activation prevents ER stress (Hwang *et al.*, 2013; Salvado *et al.*, 2014), we examined whether the increase in AMPK activity caused by ALT-PG2 was responsible for the reduction of ER stress by using the AMPK inhibitor compound C.

Remarkably, the reduction in CHOP protein levels caused by ALT-PG2 in thapsigargin-stimulated cells was prevented when cells were co-incubated with compound C (Figure 4D). This finding suggests that the inhibition of ER stress provoked by ALT-PG2 is mediated by AMPK.

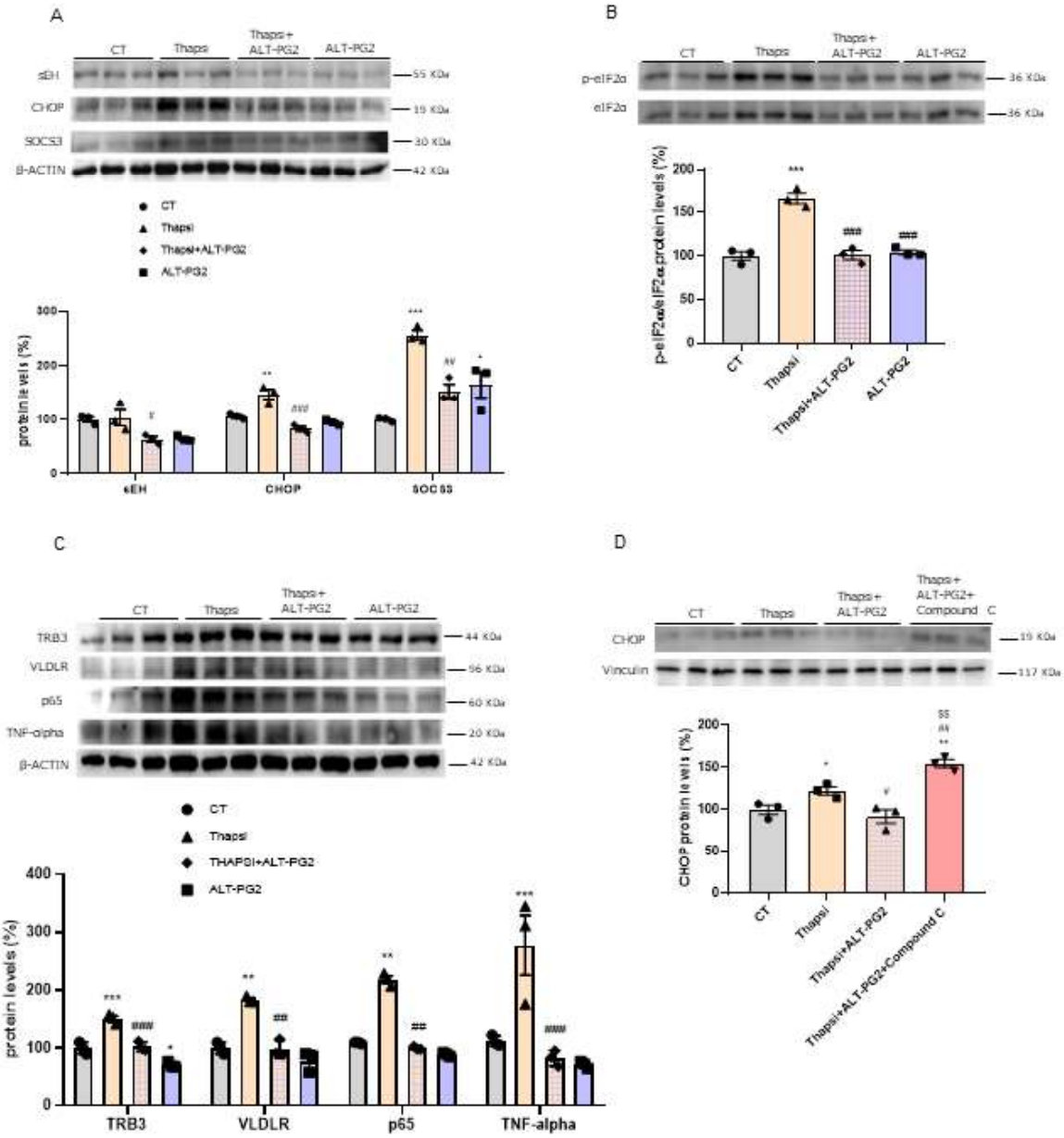

Figure 4. sEH degradation by ALT-PG2 attenuates thapsigargin-induced ER stress in Huh-7 hepatic cells. Immunoblot analysis of (**A**) sEH, CHOP, SOCS3 and (**B**) total and p-eIF2α in Huh-7 hepatic cells exposed to 10 nM ALT-PG2 for 48 h co-incubated with vehicle or the ER stressor thapsigargin (1 μM) for the last 24 h. (**C**) TRB3, VLDLR, p65 and TNF-α in Huh-7 hepatic cells exposed to 10 nM ALT-PG2 for 48 h co-incubated with vehicle or the ER stressor thapsigargin (1 μM) for the last 24 h. (**D**) Immunoblot analysis of CHOP in Huh-7 hepatic cells exposed to 10 nM ALT-PG2 for 48 h co-incubated with vehicle or the ER stressor thapsigargin (1 μM) for the last 24 h with or without the AMPK inhibitor compound C (15 μM). Data are presented as the mean ± SEM. Significant differences were established by one-way ANOVA with Tukey's post hoc test. *$p < 0.05$, **$p < 0.01$ and ***$p < 0.001$ *vs.* CT. $^{\#}p < 0.05$, $^{\#\#}p < 0.01$ and $^{\#\#\#}p < 0.001$ *vs.* thapsigargin.

IV.2.4. sEH degradation by ALT-PG2 activates AMPK and reduces the levels of ER stress markers in mouse primary hepatocytes

Since primary hepatocytes are the gold standard for physiologically relevant *in vitro* liver models as they retain *in vivo*-like functions and morphologies, we next evaluated the effects of the ALT-PG2 PROTAC in this model. Exposure of mouse primary hepatocytes to ALT-PG2 led to significant sEH degradation (Figure 5A), which was accompanied by an increase in phosphorylated AMPK (Figure 5B). Likewise, and in agreement with the activation of AMPK, phosphorylated ERK1/2 was reduced (Figure 5C). In addition, ALT-PG2 reduced basal CHOP protein levels (Figure 5D), as well as the levels of SOCS3, while the protein levels of IRβ were increased (Figure 5E). Likewise, when mouse primary hepatocytes were stimulated with thapsigargin, co-incubation of the cells with ALT-PG2 attenuated the increase in CHOP caused by the ER stressor (Figure 5F). In agreement with the reduction in ER stress, ALT-PG2 also reduced the levels of the inflammatory marker TNF-α (Figure 5G).

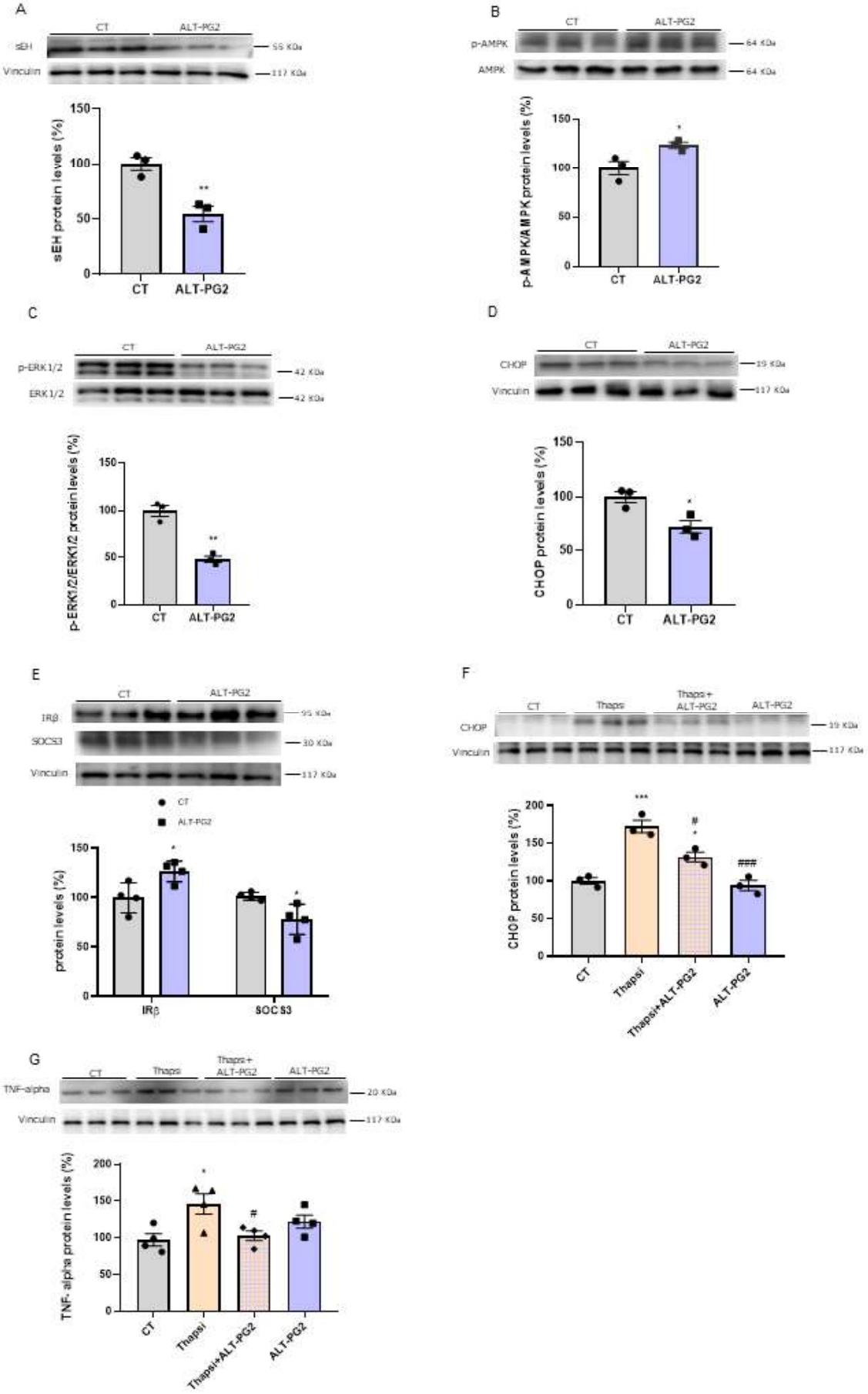
A
CT
ALT-PG2
sEH
Vinculin
55 KDa
117 KDa
sEH protein levels (%)
B
p-AMPK
AMPK
64 KDa
p-AMPK/AMPK protein levels (%)
C
p-ERK1/2
ERK1/2
42 KDa
p-ERK1/2/ERK1/2 protein levels (%)
D
CHOP
Vinculin
19 KDa
CHOP protein levels (%)
E
IRβ
SOCS3
95 KDa
30 KDa
protein levels (%)
F
Thaps
Thaps+ ALT-PG2
CHOP protein levels (%)
G
TNF-alpha
20 KDa
TNF- alpha protein levels (%)

Figure 5. sEH degradation by ALT-PG2 attenuates ER stress in mouse primary hepatocytes. Immunoblot analysis of (**A**) sEH, (**B**) total and phosphorylated AMPK, (**C**) total and phosphorylated ERK1/2, (**D**) CHOP, (**E**) IRβ and SOCS3 in mouse primary hepatocytes exposed to 10 nM ALT-PG2 for 48 h. Immunoblot analysis of (**F**) CHOP and (**G**) TNF-α in mouse primary hepatocytes exposed to 10 nM ALT-PG2 for 48 h co-incubated with vehicle or the ER stressor thapsigargin (1 μM) for the last 24 h. Data are presented as the mean ± SEM. Significant differences were established by Student's-t test or one-way ANOVA with Tukey's post hoc test. *p < 0.05, **p < 0.01 and ***p < 0.001 *vs.* CT. #p < 0.05 *vs.* thapsigargin.

IV.2.5. ALT-PG2 leads to sEH degradation in the liver of mice

Finally, due to limited amounts of the ALT-PG2 compound, we conducted a first approach to evaluate the effect of ALT-PG2 on sEH degradation *in vivo*. Mice treated with ALT-PG2 (30 mg/kg, twice a day for 1 day) showed a significant degradation in hepatic sEH protein levels (Figure 6A). Consistent with previous studies *in vitro*, ALT-PG2 increased the phosphorylated levels of AMPK in the liver (Figure 6B). The activation of AMPK was confirmed by the reduction in phosphorylated ERK1/2 (Figure 6C) and SOCS3 (Figure 6D). Collectively, these findings suggest that the PROTAC ALT-PG2 causes a potent and rapid degradation of sHE *in vivo* after only 24 h that results in the activation of AMPK.

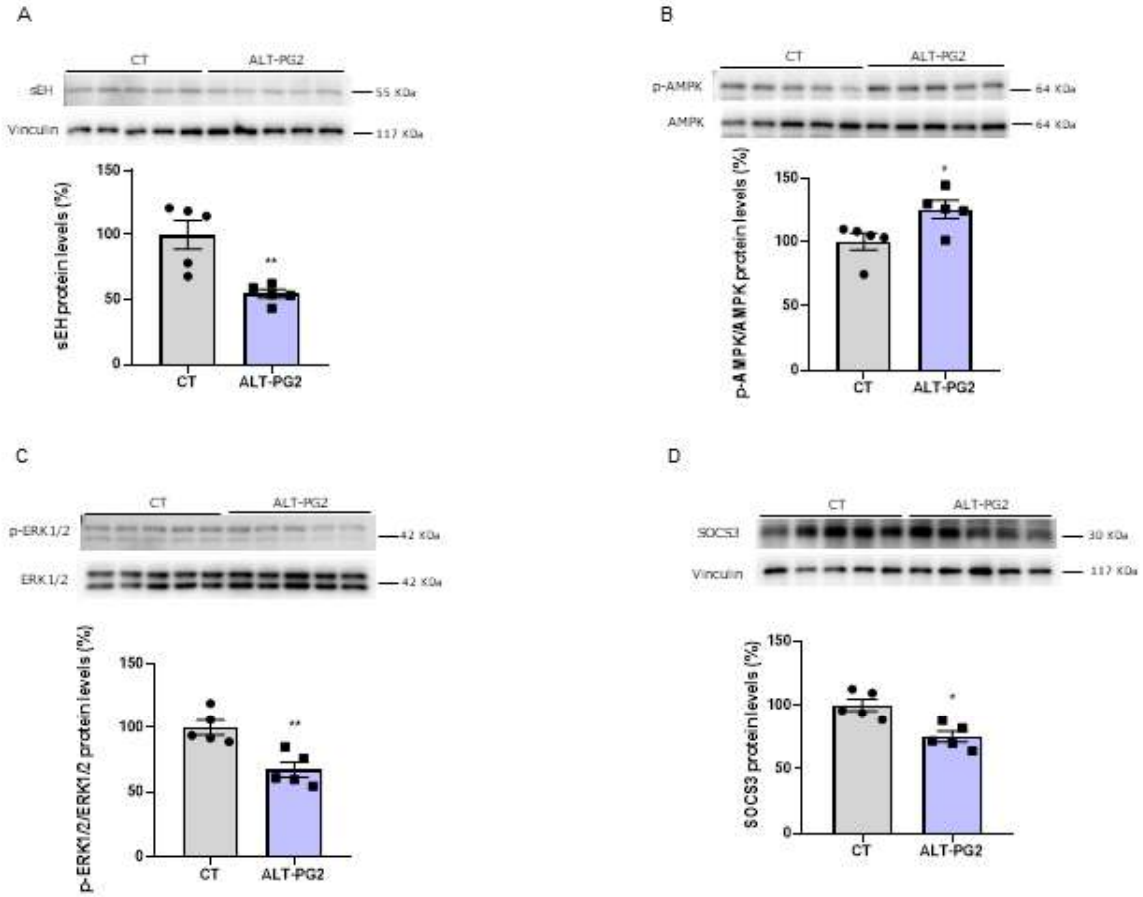

Figure 6. ALT-PG2 degrades sEH *in vivo*. Immunoblot analysis of (**A**) sEH, (**B**) total and phosphorylated AMPK, (**C**) total and phosphorylated ERK1/2, (**D**) SOCS3 in the liver of mice treated with vehicle or ALT-PG2 (30 mg/kg, i.p., twice a day for 1 day). Significant differences were established by Student's-t test. *$p < 0.05$ and **$p < 0.01$ *vs.* CT.

V. DISCUSSION

Because there are currently no fully effective treatments for all of the complications associated with MASLD, the condition has become a major global health concern in recent years (Younossi, et al.,2023). The substantial changes in lifestyle factors in the 21st century, especially in developed nations, have made MASLD a global problem. Furthermore, the accumulation of lipids in the liver causes chronic low-grade inflammation that not only makes MASLD, fibrosis, and even cirrhosis worse, but also may accelerate the progression of MASLD to HCC (Targher, et al. 2023). It is imperative to identify and develop new therapeutic targets for the more effective management of MASLD and its associated metabolic disturbances. Currently available pharmacological treatments for MASLD are associated with significant side effects and have limited efficacy (Yanai, et al. 2023). In the present study, we evaluated evaluated how the regulation of VLDLR by SIRT1 and a PROTAC molecule against sEH impact on ER-mediated hepatic steatosis.

ER stress is known to play a significant role in a number of pathological conditions, such as cancer, neurodegeneration, and metabolic disorders. ER stress is closely related to insulin action, glucose homeostasis, and lipid metabolism in the context of metabolic regulation. Research shows that ER stress affects important cellular pathways and signaling networks, which in turn affects the overall energy balance and influences these processes (Xiaoying, and Green.,2019).

The connection between ER stress and metabolic dysfunction is especially noticeable in conditions such as MASLD, where the severity and progression of the disease are greatly influenced by disturbed ER homeostasis (Yong, et al.,2021). These findings highlight the therapeutic potential of ER stress pathway targeting metabolic disorders.

V.1. Discussion of part 1: SIRT1 REGULATES HEPATIC VLDLR LEVELS THROUGH HIF-1α.

The accumulation of fat, mostly in the form of TGs within lipid droplets, in the liver is the defining characteristic of MASLD. A variety of complex mechanisms, such as changes in FAO, lipolysis, DNL, dietary fat intake, and the liver's ability to secrete lipoprotein particles, contribute to this condition (Badmus, et al.,2022). In addition to its complex physiopathology, with multiple processes intervene simultaneously, the complex nature of MASLD is linked to numerous metabolic changes and affects extrahepatic and liver-related conditions like cancer and cardiovascular diseases. For all these reasons, the search for new therapeutic targets that can slow the progression of this disease is essential (alenti, and Vittoria.2024).

The low expression of VLDLR receptor in the healthy liver has precluded the contribution of this receptor's uptake of triglyceride-enriched lipoproteins, which is another mechanism (Webb, et al.1994, Oka, et al.1994).

Studies suggest that VLDLR expression in the liver may rise in response to specific circumstances, such as dietary protein restriction, though this does not always result in the development of fatty liver in mice. This implies that although certain metabolic stressors may activate the VLDLR pathway, complex interactions beyond the direct uptake of TGs via this receptor may also play a role in the VLDLR pathway's contribution to lipid accumulation in the liver, particularly in the setting of MASLD (Oshio, et al.2021). Nevertheless, the finding that hepatic VLDLR expression was elevated in response to ER stress, which induced hepatic steatosis (Jo, et al.,2013) shown that a novel factor in hepatic steatosis is enhanced lipoprotein delivery to the liver. The function of VLDLR in the liver is in line with earlier research showing that elevated VLDLR causes cardiomyocytes to accumulate lipids (Perman, et al.,2011) and adipocytes (Takazawa, et al.,2009).

According to our research, fructose supplementation causes a decrease in hepatic SIRT1, which is linked to an increase in VLDLR levels. This relationship corroborates earlier research showing that fructose can cause the accumulation of liver fat by decreasing SIRT1 levels, among other pathways (Song, et al.,2019, Bai, et al.,2020). SIRT1 plays a critical role in metabolic regulation, especially when it comes to MASLD because it affects FA metabolism through a variety of nutrient sensors. The protective effects of SIRT1 against liver steatosis by regulating FA oxidation and decreasing lipogenesis have been demonstrated by hepatic overexpression of SIRT1, which has been shown to improve glucose intolerance and reduce steatosis in obese mice (Liu, et al.2021). Furthermore, fructose's relationship with SIRT1 has demonstrated its involvement in metabolic syndromes, including its role in insulin resistance (IR) and the induction of gluconeogenesis and lipogenesis (Caton, et al.2011). Consuming FR raises the production of glucose in the liver and promotes DNL, which raises cholesterol and TG levels. The metabolic response to dietary FR is mediated by a SIRT1-dependent mechanism, which highlights the significance of SIRT1 in this process. FR-induced gluconeogenesis and lipogenesis occur through a complex I-mediated increase in NAD^+/NADH ratio (Pixner, et al.2022).

Furthermore, it has been documented that liver biopsies from MASLD patients have lower SIRT1 levels (Wu, et al.,2014). The protective role of Sirt1 against hepatic steatosis is demonstrated by its critical role in reducing the harmful effects of HFD on the liver. Studies have demonstrated that hepatic steatosis in a mouse model of MASLD caused by a HFD can be alleviated by docosahexaenoic acid (DHA) supplementation via mechanisms involving Sirt1 activation (Luo, et al.2020). DHA promoted FAO, inhibited inflammation, and decreased lipid accumulation in the liver; these effects were reversed upon Sirt1 knockdown. This implies that DHA's advantageous effects on liver health in the setting of high dietary fat intake depend critically on Sirt1 activation (Yang, et al.2021).

SIRT1 reduces hepatic steatosis through a number of mechanisms, one of which is the deacetylation of PGC-1α (Lagouge, et al.,2006), which increases the activity of this transcriptional co-activator, activating PPARα and upregulating genes that code for FAO-related enzymes; activating LKB1 kinase and AMPK via deacetylation (Price, et al,.2012, Lan, Fan et al.,2008); and the suppression of SREBP-1c to lessen lipogenesis (Ponugoti, et al.,2010).

Our findings show that SIRT1 is important for controlling VLDLR levels, which in turn affects how fatty liver disease develops. In fact, mice lacking Sirt1 have higher levels of VLDLR in their livers, suggesting that the SIRT1-VLDLR might play a critical role in regulating lipid homeostasis in the liver (Dong,.2023). An increase in VLDLR levels in the liver, which typically has low expression of this receptor, could enhance the uptake of lipoproteins into the liver (Huang, et al.2021). This process might contribute to the accumulation of TGs within hepatic tissues, potentially leading to fatty liver. According to our research, HIF-1α drives an increase in VLDLR levels when SIRT1 expression or activity is reduced. Increased VLDLR expression resulted from inhibition of SIRT1 in liver cells, which encouraged higher VLDL uptake (Chu, et al.2022). Using an HIF-1α inhibitor lessened this effect, indicating a direct correlation between SIRT1 activity, HIF-1α expression, and the liver's VLDLR-mediated lipid uptake (Ryu, et al.2019). Prior research has indicated that SIRT1 directly deacetylates HIF-1α, resulting in the transcription factor's inactivation (Lim, Ji-Hong et al.2010).

Previous studies have reported that, VLDLR upregulation by ER stress increases lipoprotein delivery to the liver, exacerbating fatty liver and reducing serum TG levels as the result of lipoprotein delivery to the liver (Jo, et al.2013). Likewise, treatment with the ER stressor TM causes an accumulation of hepatic TG, confirming the causative role of ER in hepatic steatosis. Interestingly, the SIRT1 activator SRT1720, significantly reduces hepatic steatosis and prevents the increase in hepatic VLDLR levels in mice that received TM.

The upregulation of hepatic VLDLR, which increases the uptake of VLDL particles and consequently reduces serum TG levels, is one of the mechanisms underlying TM-induced hepatic steatosis (Fu, et al.2016). SIRT1 activation by SRT1720 inhibits this process by reducing the increase in VLDLR levels. This allows a partial recovery of serum TG levels and attenuates, hepatic steatosis. This suggests that SIRT1 activators may have a therapeutic role in the management of ER stress-induced liver fat accumulation (Sou Hyun et al.2022, Yanan et al.2020).

Overall, the findings of this study highlight a new regulatory mechanism by which SIRT1 regulates VLDLR levels. We propose that during the development of fatty liver, several stimuli such as fructose consumption, reduce hepatic SIRT1 levels, exacerbating this condition by increasing VLDLR levels and the subsequent delivery to the liver of triglyceride-enriched lipoproteins. In addition, SIRT1 activation can contribute to ameliorating fatty liver by reducing the increase in VLDLR levels caused by ER stress during MAFLD.

V.2. Discussion of part 2: Soluble epoxide hydrolase-targeting PROTAC activates AMPK and inhibits ER stress.

ALT-PG2 is a new PROTAC molecule that combines the thalidomide structure of the sEH inhibitor t-TUCB with thalidomide to act as a PEG linker-based recruiting agent for the E3 ligase cereblon. This novel PROTAC efficiently mediates the degradation of sEH in the liver tissue of mice, hepatocytes derived from primary mouse cultures, and the human Huh-7 hepatic cell line. This development highlights ALT-PG2 PROTAC's potential as a targeted therapeutic approach to cause the selective degradation of sEH. The results point to a potential treatment strategy that involves modifying sEH levels, which are important for a number of physiological and pathological processes in the liver.

Additionally, our study shows that sEH degradation by ALT-PG2 results in increase phosphorylated AMPK levels, while the phosphorylated levels of ERK1/2 are reduced (Peyman, et al.2023). These kinases play a crucial role in controlling ER stress, which is linked to a number of diseases because it affects protein folding and trafficking. The fact that ALT-PG2 successfully lowers ER stress markers' basal levels as well as their elevation in response to an ER stress-inducing agent adds further significance to our findings. Because of its dual action, ALT-PG2 has the potential to become a therapeutic agent. It presents a novel method of modulating ER stress pathways, making it a valuable target for treating diseases in which ER stress is a key factor. ALT-PG2 offers a viable route for investigating novel therapeutic approaches targeted at ameliorating pathologies associated with ER stress due to its influence on AMPK activation and ERK1/2 phosphorylation.

In addition to lowering ER stress, ALT-PG2's action also increases the expression of proteins essential to the insulin signaling pathway. These results suggest that ALT-PG2 may have therapeutic value in treating IR, T2DM, and other metabolic diseases associated with these conditions. Because of its potential to impact insulin signaling pathways and ER stress by modulating AMPK activity.

sEH degradation by ALT-PG2 provides a comprehensive strategy to address the intricate pathophysiology of T2DM and associated metabolic disorders by potentially enhancing insulin sensitivity and reducing the inflammatory responses linked to metabolic syndrome (Zhang, et al.2020).

In our study we have also assessed another PROTAC, ALT-PG3, which yielded a lower degradation of sEH than ALT-PG2. Indeed, ALT-PG3 was previously evaluated in a recent study designed as compound 1a (Wang et al., 2023). This study of ALT-PG2 and ALT-PG3 in comparison offers new information about the structure-activity relationship for targeting sEH degradation. The observed differential degradation efficiency emphasizes how crucial molecular design is to maximize PROTACs' therapeutic potential.

The study by Wang et al. also demonstrated that ALT-PG3 shows an exceptionally high degree of selectivity in cytosolic sEH degradation, while protecting the peroxisomal form of the enzyme. This nuanced finding explains why ALT-PG3 does not completely degrade sEH, which helps to explain the compound's observed partial degradation efficacy. A key feature of PROTAC function and design is highlighted by the specificity of ALT-PG3's action, which shows how these molecules can be engineered to target particular subcellular localizations of a protein. This selectivity shows promise for developing targeted therapies that minimize off-target effects by differentiating between different cellular pools of the same protein. It also advances our understanding of the molecular mechanisms underlying PROTAC activity (Simpson, et al.2022).

Given that ALT-PG2 and ALT-PG3 share structural similarities, it is plausible that ALT-PG2 would also prefer to target cytosolic sEH. This could explain why complete degradation of this enzyme is not accomplished.

According to this previous study, ALT-PG3-mediated sEH degradation was not rescued by the proteasome inhibitor MG132. However, they observed that the lysosomal pathway was involved in ALT-PG3-mediated degradation of sEH (Wang *et al.*, 2023).

In contrast, we report that MG132 rescues the degradation of sEH caused by ALT-PG2, indicating that ALT-PG2-mediated sEH degradation involves the ubiquitin-proteasome system. We do not know the reasons for these differences between ALT-PG2 and ALT-PG3, but the use of different cell lines (Huh-7 in our study *vs.* HepG2 and HEK293T) or concentrations (10 nM ALT-PG2 in our study *vs.* 250 nM ALT-PG3) might contribute.

We also show that sEH degradation by ALT-PG2 activates AMPK *in vitro* and *in vivo*. In fact, previous studies have observed AMPK activation in the sEH knockout mice (Mangels *et al.*, 2016; Wang *et al.*, 2021) and following treatment with sEH inhibitors (Luo *et al.*, 2019).

This finding has important therapeutic ramifications, especially when considering T2DM and IR, two conditions that are major contributors to the world's health issues (Wang, et al.2023). The fact that metformin, the drug most frequently prescribed to treat T2DM, mainly acts by activating AMPK, highlights the significance of our findings.

Due to the presence of an inhibitory crosstalk between AMPK and ERK1/2, activation of AMPK by ALT-PG2 might be responsible for the reduction of ER stress, since it has been reported that inhibition of ERK1/2 reverses ER stress-induced IR (Hwang *et al.*, 2013; Salvado *et al.*, 2014).

Our study clarifies a mechanistic insight: ER stress mitigation requires ALT-PG2 to activate AMPK. This conclusion is based on observations that the application of compound C, a well-known AMPK inhibitor, suppresses AMPK's activity, negating the protective effect of ALT-PG2 against ER stress.

It is well-known that ER stress contributes to IR and T2DM by activating inflammatory pathways and by reducing the protein levels of key proteins of the insulin-signaling pathway (Salvado *et al.*, 2015). In fact, our findings show that AMPK activation by ALT-PG2-mediated degradation of sEH results in a reduction of inflammatory markers. Since ER stress has been reported to reduce IRβ levels (Zhou *et al.*, 2009), the reduction in ER stress caused by ALT-PG2 might be responsible for the increase in the levels of this receptor.

Similarly, ALT-PG2 reduces the activation of STAT3 and the levels of its target gene SOCS3. Given that the STAT3-SOCS3 pathway reduces hepatic IRS1 levels (Serrano-Marco *et al.*, 2012), its attenuation by ALT-PG2 could be the underlying mechanism responsible for the increase in IRβ levels.

A previous study has reported that AMPK activation in the liver of sEH knockout mice was elicited by higher levels of the sEH substrate 12,13-epoxyoctadecenoic acid (Mangels et al., 2016). It is reasonable to assume that the accumulation of EETs, such as 12,13-epoxyoctadecenoic acid, could result from the reduction of sEH levels via ALT-PG2 treatment, even though our study did not specifically measure the concentrations of particular substrates affected by sEH degradation. Given that sEH plays a part in the metabolism of EETs—substances with well-known vasodilatory and anti-inflammatory effects—this accumulation is expected (Kelly, et al.2024). An important regulator of cellular energy homeostasis and metabolic function, AMPK, may become activated in response to an increase in EET levels, especially 12,13-epoxyoctadecenoic acid.

Moreover, as a result of AMPK activation following sEH degradation, p53 protein levels were also increased. This is relevant in IR since it has been reported that p53 modulates hepatic insulin sensitivity through NF-κB and p38/ERK- MAPK pathways (Geng et al., 2018).

As far as we know, this is the first study reporting the efficacy of PROTAC to promote the degradation of sEH *in vivo*. Further studies are necessary to better characterize the effects of PROTACs targeting sEH, but this first approach provides some interesting data. Our findings confirm that targeting sEH degradation by using PROTAC leads to AMPK activation after an acute treatment.

VI.CONCLUSIONS

The results obtained in the present doctoral thesis led to the following conclusions:

I.1. VLDLR is increased, while SIRT1 protein levels are reduced in the liver of rats supplemented with liquid fructose, suggesting a potential realtionship

I.2. Sirt1$^{-/-}$ mice show increased hepatic protein levels of VLDLR in the absence of ER stress.

I.3. SIRT1 inhibition leads to the upregulation of VLDLR via HIF-1α in hepatic cells.

I.4. SIRT1 activation ameliorates fatty liver and abolishes the increase in hepatic VLDLR caused by ER stress.

II.1. sEH degradation by ALT-PG2 activates AMPK and reduces the levels of ER stress markers in human Huh-7 hepatic cells.

II.2. sEH degradation by ALT-PG2 attenuates thapsigargin-induced ER stress in human Huh-7 hepatic cells and in mouse primary hepatocytes.

II.3. ALT-PG2 leads to sEH degradation in the liver of mice.

VII. BIBLIOGRAPHY

Adams, Christopher J et al. “Structure and Molecular Mechanism of ER Stress Signaling by the Unfolded Protein Response Signal Activator IRE1.” *Frontiers in molecular biosciences* vol. 6 11. 12 Mar. 2019, doi:10.3389/fmolb.2019.00011

Aguilar-Recarte, David et al. “GDF15 mediates the metabolic effects of PPARβ/δ by activating AMPK.” *Cell reports* vol. 36,6 (2021): 109501. doi:10.1016/j.celrep.2021.109501

Ahmed, Bulbul et al. “Adipose tissue and insulin resistance in obese.” *Biomedicine & pharmacotherapy = Biomedecine & pharmacotherapie* vol. 137 (2021): 111315. doi:10.1016/j.biopha.2021.111315

Ajoolabady, Amir et al. “ER stress in obesity pathogenesis and management.” *Trends in pharmacological sciences* vol. 43,2 (2022): 97-109. doi:10.1016/j.tips.2021.11.011

Al Bander, Zahraa et al. “The Gut Microbiota and Inflammation: An Overview.” International journal of environmental research and public health vol. 17,20 7618. 19 Oct. 2020, doi:10.3390/ijerph17207618

Alenti, Luca V C, and Vittoria Moretti. “Implications of the evolving knowledge of the genetic architecture of MASLD.” *Nature reviews. Gastroenterology & hepatology* vol. 21,1 (2024): 5-6. doi:10.1038/s41575-023-00866-0

Alkhouri, Naim et al. “Apoptosis in nonalcoholic fatty liver disease: diagnostic and therapeutic implications.” *Expert review of gastroenterology & hepatology* vol. 5,2 (2011): 201-12. doi:10.1586/egh.11.6

Andrikopoulos, S., Proietto, J., Görgün, C.Z., Carling, D., et al. (2006). Tumor necrosis factor alpha-induced skeletal muscle insulin resistance involves suppression of AMP-kinase signaling. Cell metabolism *4*, 465-474.

Anggreini, Putri et al. “Role of the AMPK/SIRT1 pathway in non-alcoholic fatty liver disease (Review).” *Molecular medicine reports* vol. 27,2 (2023): 35. doi:10.3892/mmr.2022.12922

Arab, Juan Pablo et al. “Recent Insights into the Pathogenesis of Nonalcoholic Fatty Liver Disease.” *Annual review of pathology* vol. 13 (2018): 321-350. doi:10.1146/annurev-pathol-020117-043617

Arai, Takatomo et al. “HIF-1-dependent lipin1 induction prevents excessive lipid accumulation in choline-deficient diet-induced fatty liver.” *Scientific reports* vol. 8,1 14230. 21 Sep. 2018, doi:10.1038/s41598-018-32586-w

Arora, Umang, et al. "MASLD screening and diagnostic algorithms are interchangeable from existing NAFLD literature." Journal of Hepatology (2023).

Arrese, Marco et al. “Innate Immunity and Inflammation in NAFLD/NASH.” *Digestive diseases and sciences* vol. 61,5 (2016): 1294-303. doi:10.1007/s10620-016-4049-x

Arvind, Ashwini et al. “Epoxygenase-Derived Epoxyeicosatrienoic Acid Mediators Are Associated with Nonalcoholic Fatty Liver Disease, Nonalcoholic Steatohepatitis, and Fibrosis.” Gastroenterology vol. 159,6 (2020): 2232-2234.e4. doi: 10.1053/j.gastro.2020.08.001

Atay, Kadri et al. “Apoptosis and Disease Severity is Associated with Insulin Resistance in Non-alcoholic Fatty Liver Disease.” *Acta gastro-enterologica Belgica* vol. 80,2 (2017): 271-277.

Athavale, Dipti et al. “Overexpression of HMGB1 in hepatocytes accelerates PTEN inactivation-induced liver cancer.” *Hepatology communications* vol. 7,12 e0311. 7 Dec. 2023, doi:10.1097/HC9.0000000000000311

Badmus, Olufunto O et al. “Molecular mechanisms of metabolic associated fatty liver disease (MAFLD): functional analysis of lipid metabolism pathways.” *Clinical science (London, England : 1979)* vol. 136,18 (2022): 1347-1366. doi:10.1042/CS20220572

Bagherieh, Molood et al. “Folic acid ameliorates palmitate-induced inflammation through decreasing homocysteine and inhibiting NF-κB pathway in HepG2 cells.” *Archives of physiology and biochemistry* vol. 129,4 (2023): 893-900. doi:10.1080/13813455.2021.1878539

Bai, Jing et al. “Multiscale integrative analyses unveil immune-related diagnostic signature for the progression of MASLD.” *Hepatology communications* vol. 7,11 e0298. 18 Oct. 2023, doi:10.1097/HC9.0000000000000298

Bai, Ruojun et al. “Apple pomace and rosemary extract ameliorates hepatic steatosis in fructose-fed rats: Association with enhancing fatty acid oxidation and suppressing inflammation.” *Experimental and therapeutic medicine* vol. 20,3 (2020): 1975-1986. doi:10.3892/etm.2020.8910

Ballester, Maria Pilar, et al. "Corrigendum to “Development and validation of the AMMON-OHE model to predict risk of overt hepatic encephalopathy occurrence in outpatients with cirrhosis”[J Hepatol 79 (4)(2023 Oct) 967–976]." *Journal of Hepatology* 79.6 (2023): 1571.

Basaranoglu, Metin et al. “Carbohydrate intake and nonalcoholic fatty liver disease: fructose as a weapon of mass destruction.” *Hepatobiliary surgery and nutrition* vol. 4,2 (2015): 109-16. doi:10.3978/j.issn.2304-3881.2014.11.05

Basu, Rita et al. “Nonalcoholic Fatty Liver Disease: Review of Management for Primary Care Providers.” *Mayo Clinic proceedings* vol. 97,9 (2022): 1700-1716. doi:10.1016/j.mayocp.2022.04.005

Bedossa, Pierre et al. “Histopathological algorithm and scoring system for evaluation of liver lesions in morbidly obese patients.” *Hepatology (Baltimore, Md.)* vol. 56,5 (2012): 1751-9. doi:10.1002/hep.25889

Békés, Miklós et al. “PROTAC targeted protein degraders: the past is prologue.” Nature reviews. Drug discovery vol. 21,3 (2022): 181-200. doi:10.1038/s41573-021-00371-6

Bell, Michelle C et al. “PERK-opathies: An Endoplasmic Reticulum Stress Mechanism Underlying Neurodegeneration.” *Current Alzheimer research* vol. 13,2 (2016): 150-63. doi:10.2174/1567205013666151218145431

Bendixen, Sofie M et al. “Single cell-resolved study of advanced murine MASH reveals a homeostatic pericyte signaling module.” *Journal of hepatology*, S0168-8278(23)05273-X. 14 Nov. 2023, doi:10.1016/j.jhep.2023.11.001

Besse-Patin, Aurèle, and Jennifer L Estall. “An Intimate Relationship between ROS and Insulin Signalling: Implications for Antioxidant Treatment of Fatty Liver Disease.” *International journal of cell biology* vol. 2014 (2014): 519153. doi:10.1155/2014/519153

Bessone, Fernando et al. “Molecular pathways of nonalcoholic fatty liver disease development and progression.” *Cellular and molecular life sciences : CMLS* vol. 76,1 (2019): 99-128. doi:10.1007/s00018-018-2947-0

Bezu, Lucillia et al. “eIF2α phosphorylation is pathognomonic for immunogenic cell death.” *Cell death and differentiation* vol. 25,8 (2018): 1375-1393. doi:10.1038/s41418-017-0044-9

Biesemann, Nadine et al. “Additive efficacy of a bispecific anti-TNF/IL-6 nanobody compound in translational models of rheumatoid arthritis.” *Science translational medicine* vol. 15,681 (2023): eabq4419. doi:10.1126/scitranslmed.abq4419

Blackwood, Erik A et al. “ATF6 Regulates Cardiac Hypertrophy by Transcriptional Induction of the mTORC1 Activator, Rheb.” *Circulation research* vol. 124,1 (2019): 79-93. doi:10.1161/CIRCRESAHA.118.313854

BLIGH, E G, and W J DYER. “A rapid method of total lipid extraction and purification.” *Canadian journal of biochemistry and physiology* vol. 37,8 (1959): 911-7. doi:10.1139/o59-099

Boucher, J., Kleinridders, A., and Kahn, C.R. (2014). Insulin receptor signaling in normal.

Boutari, Chrysoula et al. "Association of Adipokines with Development and Progression of Nonalcoholic Fatty Liver Disease." *Endocrinology and metabolism (Seoul, Korea)* vol. 33,1 (2018): 33-43. doi:10.3803/EnM.2018.33.1.33

Bouzakri, K., and Zierath, J.R. (2007). MAP4K4 gene silencing in human skeletal muscle prevents tumor necrosis factor-alpha-induced insulin resistance. The Journal of biological chemistry *282*, 7783-7789.

Boye, Erik, and Beáta Grallert. "eIF2α phosphorylation and the regulation of translation." *Current genetics* vol. 66,2 (2020): 293-297. doi:10.1007/s00294-019-01026-1

Brentnall, Matthew et al. "Caspase-9, caspase-3 and caspase-7 have distinct roles during intrinsic apoptosis." *BMC cell biology* vol. 14 32. 9 Jul. 2013, doi:10.1186/1471-2121-14-32

Bril, F. et al. (2017) Metabolic and histological implications of intrahepatic triglyceride content in nonalcoholic fatty live disease. Hepatology 65, 1132–1144

Broussy, Sylvain et al. "Biochemical mechanism and biological effects of the inhibition of silent information regulator 1 (SIRT1) by EX-527 (SEN0014196 or selisistat)." *Journal of enzyme inhibition and medicinal chemistry* vol. 35,1 (2020): 1124-1136. doi:10.1080/14756366.2020.1758691

Brown, Max et al. "Endoplasmic reticulum stress causes insulin resistance by inhibiting delivery of newly synthesized insulin receptors to the cell surface." *Molecular biology of the cell* vol. 31,23 (2020): 2597-2629. doi:10.1091/mbc.E18-01-0013

Bugianesi, E et al. "Insulin resistance in nonalcoholic fatty liver disease." *Current pharmaceutical design* vol. 16,17 (2010): 1941-51. doi:10.2174/138161210791208875

Bugianesi, E et al. "Insulin resistance in nonalcoholic fatty liver disease." *Current pharmaceutical design* vol. 16,17 (2010): 1941-51. doi:10.2174/138161210791208875

Buzzetti, Elena et al. "The multiple-hit pathogenesis of non-alcoholic fatty liver disease (NAFLD)." *Metabolism: clinical and experimental* 65 8 (2016): 1038-48

Cai, D., Yuan, M., Frantz, D.F., Melendez, P.A., Hansen, L., Lee, J., and Shoelson, S.E. (2005).

Caligiuri, Alessandra et al. "Molecular Pathogenesis of NASH." *International journal of molecular sciences* vol. 17,9 1575. 20 Sep. 2016, doi:10.3390/ijms17091575

Cariou, Bertrand. “The metabolic triad of non-alcoholic fatty liver disease, visceral adiposity and type 2 diabetes: Implications for treatment.” *Diabetes, obesity & metabolism* vol. 24 Suppl 2 (2022): 15-27. doi:10.1111/dom.14651

Carpi, Rodrigo Zamignan et al. “The Effects of Probiotics, Prebiotics and Synbiotics in Non-Alcoholic Fat Liver Disease (NAFLD) and Non-Alcoholic

Cartland, Siân P et al. “A "Western Diet" promotes symptoms of hepatic steatosis in spontaneously hypertensive rats.” *International journal of experimental pathology* vol. 101,5 (2020): 152-161. doi:10.1111/iep.12369

Casey, Georgina. “Diseases of the Liver.” *Nursing New Zealand (Wellington, N.Z. : 1995)* vol. 22,11 (2016): 20-24.

Castera, Laurent. “Diagnosis of non-alcoholic fatty liver disease/non-alcoholic steatohepatitis: Non-invasive tests are enough.” *Liver international : official journal of the International Association for the Study of the Liver* vol. 38 Suppl 1 (2018): 67-70. doi:10.1111/liv.13658

Castillo-Núñez, Yulino, Enrique Morales-Villegas, and Carlos A. Aguilar-Salinas. "Triglyceride-rich lipoproteins: their role in atherosclerosis." *Revista de investigación clínica* 74.2 (2022): 61-70.

Castro, Ana Valeria B et al. “Obesity, insulin resistance and comorbidities? Mechanisms of association.” *Arquivos brasileiros de endocrinologia e metabologia* vol. 58,6 (2014): 600-9. doi:10.1590/0004-2730000003223

Caton, Paul W et al. “Fructose induces gluconeogenesis and lipogenesis through a SIRT1-dependent mechanism.” *The Journal of endocrinology* vol. 208,3 (2011): 273-83. doi:10.1530/JOE-10-0190

Chalasani, Naga et al. “The diagnosis and management of nonalcoholic fatty liver disease: Practice guidance from the American Association for the Study of Liver Diseases.” *Hepatology (Baltimore, Md.)* vol. 67,1 (2018): 328-357. doi:10.1002/hep.29367

Chan, Wah-Kheong et al. “Metabolic Dysfunction-Associated Steatotic Liver Disease (MASLD): A State-of-the-Art Review.” *Journal of obesity & metabolic syndrome* vol. 32,3 (2023): 197-213. doi:10.7570/jomes23052

Chen, Hongdong et al. “Elucidation of the anti-β-cell dedifferentiation mechanism of a modified Da Chaihu Decoction by an integrative approach of network pharmacology and experimental verification.” *Journal of ethnopharmacology* vol. 321 (2024): 117481. doi:10.1016/j.jep.2023.117481

Chen, L., Chen, R., Wang, H., and Liang, F. (2015a). Mechanisms Linking Inflammation to Insulin Resistance. International Journal of Endocrinology *2015*, 508409.

Chen, Li et al. "Mechanisms Linking Inflammation to Insulin Resistance." *International journal of endocrinology* vol. 2015 (2015): 508409. doi:10.1155/2015/508409

Chen, Shaoting et al. "The application of PROTAC in HDAC." *European journal of medicinal chemistry* vol. 260 (2023): 115746. doi:10.1016/j.ejmech.2023.115746

Chen, Xingyi et al. "Endoplasmic reticulum stress: molecular mechanism and therapeutic targets." *Signal transduction and targeted therapy* vol. 8,1 352. 15 Sep. 2023, doi:10.1038/s41392-023-01570-w

Chen, Yanan et al. "Resveratrol Alleviates Endoplasmic Reticulum Stress-Associated Hepatic Steatosis and Injury in Mice Challenged with Tunicamycin." *Molecular nutrition & food research* vol. 64,14 (2020): e2000105. doi:10.1002/mnfr.202000105

Chen, Ze et al. "Role of oxidative stress in the pathogenesis of nonalcoholic fatty liver disease." *Free radical biology & medicine* vol. 152 (2020): 116-141. doi:10.1016/j.freeradbiomed.2020.02.025

Cherubini, Alessandro et al. "PNPLA3 as a therapeutic target for fatty liver disease: the evidence to date." *Expert opinion on therapeutic targets* vol. 25,12 (2021): 1033-1043. doi:10.1080/14728222.2021.2018418

Chevallet, M et al. "Metal homeostasis disruption and mitochondrial dysfunction in hepatocytes exposed to sub-toxic doses of zinc oxide nanoparticles." *Nanoscale* vol. 8,43 (2016): 18495-18506. doi:10.1039/c6nr05306h

Chitturi, Shivakumar et al. "NASH and insulin resistance: Insulin hypersecretion and specific association with the insulin resistance syndrome." *Hepatology (Baltimore, Md.)* vol. 35,2 (2002): 373-9. doi:10.1053/jhep.2002.30692

Choi, Yoon Kyung. "A positive circuit of VEGF increases Glut-1 expression by increasing HIF-1α gene expression in human retinal endothelial cells." *Archives of pharmacal research* vol. 40,12 (2017): 1433-1442. doi:10.1007/s12272-017-0971-5

Choudhury, M., Qadri, I., Rahman, S.M., Schroeder-Gloeckler, J., Janssen, R.C., and Friedman, J.E. (2011). C/EBPβ is AMP kinase sensitive and up-regulates

PEPCK in response to ER stress in hepatoma cells. Molecular and cellular endocrinology *331*,102-108.
Chu, Qingfei et al. “Regulatory mechanism of HIF-1α and its role in liver diseases: a narrative review.” *Annals of translational medicine* vol. 10,2 (2022): 109. doi:10.21037/atm-21-4222

Chu, Qingfei et al. “Regulatory mechanism of HIF-1α and its role in liver diseases: a narrative review.” *Annals of translational medicine* vol. 10,2 (2022): 109. doi:10.21037/atm-21-4222

Cobbina, Enoch, and Fatemeh Akhlaghi. “Non-alcoholic fatty liver disease (NAFLD) - pathogenesis, classification, and effect on drug metabolizing enzymes and transporters.” *Drug metabolism reviews* vol. 49,2 (2017): 197-211. doi:10.1080/03602532.2017.1293683

Croker, B.A., Kiu, H., and Nicholson, S.E. (2008). SOCS regulation of the JAK/STAT signalling pathway. Seminars in cell & developmental biology *19*, 414-422.
Cronin, Annette, et al. "The N-terminal domain of mammalian soluble epoxide hydrolase is a phosphatase." *Proce edings of the national academy of sciences* 100.4 (2003): 1552-1557.

Cullen, Sean P, and Seamus J Martin. “Fas and TRAIL 'death receptors' as initiators of inflammation: Implications for cancer.” *Seminars in cell & developmental biology* vol. 39 (2015): 26-34. doi:10.1016/j.semcdb.2015.01.012

Cusi, Kenneth et al. “American Association of Clinical Endocrinology Clinical Practice Guideline for the Diagnosis and Management of Nonalcoholic Fatty Liver Disease in Primary Care and Endocrinology Clinical Settings: Co-Sponsored by the American Association for the Study of Liver Diseases (AASLD).” *Endocrine practice : official journal of the American College of Endocrinology and the American Association of Clinical Endocrinologists* vol. 28,5 (2022): 528-562. doi:10.1016/j.eprac.2022.03.010

Dahik, Veronica D., Eric Frisdal, and Wilfried Le Goff. "Rewiring of lipid metabolism in adipose tissue macrophages in obesity: impact on insulin resistance and type 2 diabetes." *International journal of molecular sciences* 21.15 (2020): 5505.

Dai, Yuxuan et al. “Development of cell-permeable peptide-based PROTACs targeting estrogen receptor α.” *European journal of medicinal chemistry* vol. 187 (2020): 111967. doi:10.1016/j.ejmech.2019.111967

David, Deepu, and Chundamannil E Eapen. “What Are the Current Pharmacological Therapies for Nonalcoholic Fatty Liver Disease?.” *Journal of clinical and experimental hepatology* vol. 11,2 (2021): 232-238. doi:10.1016/j.jceh.2020.09.001

Davis, Caroline et al. “Mechanisms of substrate recognition by the 26S proteasome.” *Current opinion in structural biology* vol. 67 (2021): 161-169. doi: 10.1016/j.sbi.2020.10.010

De Sousa-Coelho, Ana Luísa et al. “Activating transcription factor 4-dependent induction of FGF21 during amino acid deprivation.” *The Biochemical journal* vol. 443,1 (2012): 165-71. doi:10.1042/BJ20111748

Del Campo, José A et al. “Role of inflammatory response in liver diseases: Therapeutic strategies.” *World journal of hepatology* vol. 10,1 (2018): 1-7. doi:10.4254/wjh.v10.i1.1

Delli Bovi, Anna Pia et al. “Oxidative Stress in Non-alcoholic Fatty Liver Disease. An Updated Mini Review.” *Frontiers in medicine* vol. 8 595371. 26 Feb. 2021, doi:10.3389/fmed.2021.595371

Deng, Ke-Qiong et al. “Role of hepatic lipid species in the progression of nonalcoholic fatty liver disease.” *American journal of physiology. Cell physiology* vol. 323,2 (2022): C630-C639. doi:10.1152/ajpcell.00123.2022

Deng, Lei et al. “Triacylglycerol uptake and handling by macrophages: From fatty acids to lipoproteins.” *Progress in lipid research* vol. 92 (2023): 101250. doi:10.1016/j.plipres.2023.101250

Devarbhavi, Harshad, et al. "Global burden of liver disease: 2023 update." *Journal of Hepatology* (2023).

Dey, Souvik et al. “Transcriptional repression of ATF4 gene by CCAAT/enhancer-binding protein β (C/EBPβ) differentially regulates integrated stress response.” *The Journal of biological chemistry* vol. 287,26 (2012): 21936-49. doi:10.1074/jbc.M112.351783

Diaconu, Cosmina-Theodora, and Cristian Guja. “Nonalcoholic Fatty Liver Disease and Its Complex Relation with Type 2 Diabetes Mellitus-From Prevalence to Diagnostic Approach and Treatment Strategies.” *Journal of clinical medicine* vol. 11,17 5144. 31 Aug. 2022, doi:10.3390/jcm11175144

Diehl, Kira L., et al. "Kupffer cells sense free fatty acids and regulate hepatic lipid metabolism in high-fat diet and inflammation." *Cells* 9.10 (2020): 2258.

DiNicolantonio, James J et al. “Added fructose as a principal driver of non-alcoholic fatty liver disease: a public health crisis.” *Open heart* vol. 4,2 e000631. 30 Oct. 2017, doi:10.1136/openhrt-2017-000631

DiStefano, Johanna K, and Gabriel Q Shaibi. “The relationship between excessive dietary fructose consumption and paediatric fatty liver disease.” *Pediatric obesity* vol. 16,6 (2021): e12759. doi:10.1111/ijpo.12759

Dlugosz, Paula, and Johannes Nimpf. "The reelin receptors apolipoprotein E receptor 2 (ApoER2) and VLDL receptor." *International journal of molecular sciences* 19.10 (2018): 3090.

Dong, X Charlie. “Sirtuin 6-A Key Regulator of Hepatic Lipid Metabolism and Liver Health.” *Cells* vol. 12,4 663. 19 Feb. 2023, doi:10.3390/cells12040663

Du, J., Guan, T., Zhang, H., Xia, Y., Liu, F., and Zhang, Y. (2008). Inhibitory crosstalk between ERK and AMPK in the growth and proliferation of cardiac fibroblasts. Biochemical and biophysical research communications *368*, 402-407.

Du, Jianhai et al. “Inhibitory crosstalk between ERK and AMPK in the growth and proliferation of cardiac fibroblasts.” *Biochemical and biophysical research communications* vol. 368,2 (2008): 402-7. doi:10.1016/j.bbrc.2008.01.099

Duan, Yamei et al. “Association of Inflammatory Cytokines With Non-Alcoholic Fatty Liver Disease.” *Frontiers in immunology* vol. 13 880298. 6 May. 2022, doi:10.3389/fimmu.2022.880298

Duseja, Ajay et al. “Non-alcoholic Fatty Liver Disease and Metabolic Syndrome-Position Paper of the Indian National Association for the Study of the Liver, Endocrine Society of India, Indian College of Cardiology and Indian Society of Gastroenterology.” *Journal of clinical and experimental hepatology* vol. 5,1 (2015): 51-68. doi:10.1016/j.jceh.2015.02.006

ElKhatib, Mohammed A W et al. “Effect of inflammation on cytochrome P450-mediated arachidonic acid metabolism and the consequences on cardiac hypertrophy.” *Drug metabolism reviews* vol. 55,1-2 (2023): 50-74. doi:10.1080/03602532.2022.2162075

Eskandari, Ebrahim, and Connie J Eaves. “Paradoxical roles of caspase-3 in regulating cell survival, proliferation, and tumorigenesis.” *The Journal of cell biology* vol. 221,6 (2022): e202201159. doi:10.1083/jcb.202201159

Eslam, Mohammed, et al. "A new definition for metabolic dysfunction-associated fatty liver disease: An international expert consensus statement." *Journal of hepatology* 73.1 (2020): 202-209.

Eslam, Mohammed, et al. "MAFLD: a consensus-driven proposed nomenclature for metabolic associated fatty liver disease." *Gastroenterology* 158.7 (2020): 1999-2014.

European Association for the Study of the Liver (EASL) et al. “EASL-EASD-EASO Clinical Practice Guidelines for the management of non-alcoholic fatty liver disease.” *Journal of hepatology* vol. 64,6 (2016): 1388-402. doi:10.1016/j.jhep.2015.11.004

Fang, Chunqiu et al. “The AMPK pathway in fatty liver disease.” *Frontiers in physiology* vol. 13 970292. 25 Aug. 2022, doi:10.3389/fphys.2022.970292

Farrell, Geoffrey C et al. “Pathogenesis of NASH: How Metabolic Complications of Overnutrition Favour Lipotoxicity and Pro-Inflammatory Fatty Liver Disease.” *Advances in experimental medicine and biology* vol. 1061 (2018): 19-44. doi:10.1007/978-981-10-8684-7_3

Ferguson, Daniel, and Brian N Finck. “Emerging therapeutic approaches for the treatment of NAFLD and type 2 diabetes mellitus.” *Nature reviews. Endocrinology* vol. 17,8 (2021): 484-495. doi:10.1038/s41574-021-00507-z

Fernández-Veledo, S., Vila-Bedmar, R., Nieto-Vazquez, I., and Lorenzo, M. (2009). c-Jun Nterminal kinase 1/2 activation by tumor necrosis factor-alpha induces insulin resistance in human visceral but not subcutaneous adipocytes: reversal by liver X receptor agonists. The Journal of clinical endocrinology and metabolism *94*, 3583-3593.

Filipovic, Branka et al. “Molecular Aspects of MAFLD-New Insights on Pathogenesis and Treatment.” *Current issues in molecular biology* vol. 45,11 9132-9148. 15 Nov. 2023, doi:10.3390/cimb45110573

Finer, Nick. “Weight loss interventions and nonalcoholic fatty liver disease: Optimizing liver outcomes.” *Diabetes, obesity & metabolism* vol. 24 Suppl 2 (2022): 44-54. doi:10.1111/dom.14569

Fiorentino, Teresa Vanessa et al. “SRT1720 counteracts glucosamine-induced endoplasmic reticulum stress and endothelial dysfunction.” *Cardiovascular research* vol. 107,2 (2015): 295-306. doi:10.1093/cvr/cvv169

Flamment, Mélissa et al. “New insights into ER stress-induced insulin resistance.” *Trends in endocrinology and metabolism: TEM* vol. 23,8 (2012): 381-90. doi:10.1016/j.tem.2012.06.003

Flessa, Christina-Maria et al. “Endoplasmic Reticulum Stress and Autophagy in the Pathogenesis of Non-alcoholic Fatty Liver Disease (NAFLD): Current Evidence and Perspectives.” *Current obesity reports* vol. 10,2 (2021): 134-161. doi:10.1007/s13679-021-00431-3

Fontes-Cal, Tereza C M et al. “Crosstalk Between Plasma Cytokines, Inflammation, and Liver Damage as a New Strategy to Monitoring NAFLD Progression.” *Frontiers in immunology* vol. 12 708959. 10 Aug. 2021, doi:10.3389/fimmu.2021.708959

Fouad, Yasser. “Metabolic-associated fatty liver disease: New nomenclature and approach with hot debate.” *World journal of hepatology* vol. 15,2 (2023): 123-128. doi:10.4254/wjh.v15.i2.123

Fu, Jihua et al. “Long-term Stress with Hyperglucocorticoidemia-induced Hepatic Steatosis with VLDL Overproduction Is Dependent on both 5-HT2 Receptor and 5-HT Synthesis in Liver.” *International journal of biological sciences* vol. 12,2 219-34. 1 Jan. 2016, doi:10.7150/ijbs.13062

Fujii, Hideki et al. “The Role of Insulin Resistance and Diabetes in Nonalcoholic Fatty Liver Disease.” *International journal of molecular sciences* vol. 21,11 3863. 29 May. 2020, doi:10.3390/ijms21113863

Galluzzi, Luca et al. “Endoplasmic reticulum stress and unfolded protein response in infection by intracellular parasites.” *Future science OA* vol. 3,3 FSO198. 12 May. 2017, doi:10.4155/fsoa-2017-0020

Gangopadhyay, Anwesha et al. “Non-alcoholic fatty liver disease (NAFLD) and mental illness: Mechanisms linking mood, metabolism and medicines.” *Frontiers in neuroscience* vol. 16 1042442. 15 Nov. 2022, doi:10.3389/fnins.2022.1042442

Gano, Lindsey B et al. “The SIRT1 activator SRT1720 reverses vascular endothelial dysfunction, excessive superoxide production, and inflammation with aging in mice.” *American journal of physiology. Heart and circulatory physiology* vol. 307,12 (2014): H1754-63. doi:10.1152/ajpheart.00377.2014

Ganz, Michal, and Gyongyi Szabo. “Immune and inflammatory pathways in NASH.” *Hepatology international* vol. 7 Suppl 2,Suppl 2 771-81. 30 Aug. 2013, doi:10.1007/s12072-013-9468-6

Gao, Yang et al. “Upregulation of hepatic VLDLR via PPARα is required for the triglyceride-lowering effect of fenofibrate.” *Journal of lipid research* vol. 55,8 (2014): 1622-33. doi:10.1194/jlr.M041988

Gao, Z., Hwang, D., Bataille, F., Lefevre, M., York, D., Quon, M.J., and Ye, J. (2002). Serine phosphorylation of insulin receptor substrate 1 by inhibitor kappa B kinase complex. The Journal of biological chemistry *277*, 48115-48121.

García-Monzón, Carmelo et al. “Hepatic insulin resistance is associated with increased apoptosis and fibrogenesis in nonalcoholic steatohepatitis and chronic hepatitis C.” *Journal of hepatology* vol. 54,1 (2011): 142-52. doi: 10.1016/j.jhep.2010.06.021

Gariani, Karim, and François R Jornayvaz. “Pathophysiology of NASH in endocrine diseases.” *Endocrine connections* vol. 10,2 (2021): R52-R65. doi:10.1530/EC-20-0490

Gastaldelli, Amalia, and Kenneth Cusi. “From NASH to diabetes and from diabetes to NASH: Mechanisms and treatment options.” *JHEP reports : innovation in hepatology* vol. 1,4 312-328. 19 Jul. 2019, doi:10.1016/j.jhepr.2019.07.002

Geng, Yana et al. “How does hepatic lipid accumulation lead to lipotoxicity in non-alcoholic fatty liver disease?.” *Hepatology international* vol. 15,1 (2021): 21-35. doi:10.1007/s12072-020-10121-2

Gerges, Samar H et al. “Non-alcoholic fatty liver disease: An overview of risk factors, pathophysiological mechanisms, diagnostic procedures, and therapeutic interventions.” *Life sciences* vol. 271 (2021): 119220. doi:10.1016/j.lfs.2021.119220

Ginsberg, Henry N., et al. "Triglyceride-rich lipoproteins and their remnants: metabolic insights, role in atherosclerotic cardiovascular disease, and emerging therapeutic strategies—a consensus statement from the European Atherosclerosis Society." *European Heart Journal* 42.47 (2021): 4791-4806.

Giridharan, Sivagami, and Mythily Srinivasan. “Mechanisms of NF-κB p65 and strategies for therapeutic manipulation.” *Journal of inflammation research* vol. 11 407-419. 30 Oct. 2018, doi:10.2147/JIR.S140188

Gofton, Cameron et al. “MAFLD: How is it different from NAFLD?.” *Clinical and molecular hepatology* vol. 29,Suppl (2023): S17-S31. doi:10.3350/cmh.2022.0367

Gonuguntla, Sumati et al. “Stress-induced pseudokinase TRB3 augments IL1β signaling by interacting with Flightless homolog 1.” *The Journal of biological chemistry* vol. 299,8 (2023): 104803. doi:10.1016/j.jbc.2023.104803

Grzych, Guillaume et al. “NASH-related increases in plasma bile acid levels depend on insulin resistance.” *JHEP reports : innovation in hepatology* vol. 3,2 100222. 16 Dec. 2020, doi:10.1016/j.jhepr.2020.100222

Gu, Shanshan et al. “PROTACs: An Emerging Targeting Technique for Protein Degradation in Drug Discovery.” *BioEssays : news and reviews in molecular, cellular and developmental biology* vol. 40,4 (2018): e1700247. doi:10.1002/bies.201700247

Guedeney, Nicolas et al. “PROTAC technology: A new drug design for chemical biology with many challenges in drug discovery.” *Drug discovery today* vol. 28,1 (2023): 103395. doi:10.1016/j.drudis.2022.103395

Hajifathalian, Kaveh et al. “Effect of Alcohol Consumption on Survival in Nonalcoholic Fatty Liver Disease: A National Prospective Cohort Study.” *Hepatology (Baltimore, Md.)* vol. 70,2 (2019): 511-521. doi:10.1002/hep.30226

Harris, Todd R et al. “Inhibition of soluble epoxide hydrolase attenuates hepatic fibrosis and endoplasmic reticulum stress induced by carbon tetrachloride in mice.” *Toxicology and applied pharmacology* vol. 286,2 (2015): 102-11. doi:10.1016/j.taap.2015.03.022

Hassani Zadeh, Shirin et al. “Relationship between dietary patterns and non-alcoholic fatty liver disease: A systematic review and meta-analysis.” *Journal of gastroenterology and hepatology* vol. 36,6 (2021): 1470-1478. doi:10.1111/jgh.15363

Hatok, Jozef, and Peter Racay. “Bcl-2 family proteins: master regulators of cell survival.” *Biomolecular concepts* vol. 7,4 (2016): 259-70. doi:10.1515/bmc-2016-0015

Hayden, M.S., and Ghosh, S. (2014). Regulation of NF-κB by TNF family cytokines. Semin Immunol *26*, 253-266.

He, Feng et al. “NRF2, a Transcription Factor for Stress Response and Beyond.” *International journal of molecular sciences* vol. 21,13 4777. 6 Jul. 2020, doi:10.3390/ijms21134777

He, Jiang et al. “Emerging mechanisms of the unfolded protein response in therapeutic resistance: from chemotherapy to Immunotherapy.” *Cell communication and signaling : CCS* vol. 22,1 89. 31 Jan. 2024, doi:10.1186/s12964-023-01438-0

He, Liuqin et al. “AMPK Regulation of Glucose, Lipid and Protein Metabolism: Mechanisms and Nutritional Significance.” *Current protein & peptide science* vol. 18,6 (2017): 562-570. doi:10.2174/1389203717666160627071125

He, Yan et al. “Silencing HIF-1α aggravates non-alcoholic fatty liver disease in vitro through inhibiting PPAR-α/ANGPTL4 singling pathway.” *Gastroenterologia y hepatologia* vol. 44,5 (2021): 355-365. doi:10.1016/j.gastrohep.2020.09.014

Heeren, Joerg, and Ludger Scheja. “Metabolic-associated fatty liver disease and lipoprotein metabolism.” *Molecular metabolism* vol. 50 (2021): 101238. doi:10.1016/j.molmet.2021.101238

Heida, Andries et al. “The hepatocyte IKK:NF-κB axis promotes liver steatosis by stimulating de novo lipogenesis and cholesterol synthesis.” *Molecular metabolism* vol. 54 (2021): 101349. doi:10.1016/j.molmet.2021.101349

Heidemann, Britt E., et al. "The relation between VLDL-cholesterol and risk of cardiovascular events in patients with manifest cardiovascular disease." *International Journal of Cardiology* 322 (2021): 251-257.

Helmstädter, Moritz et al. “Differential Therapeutic Effects of FXR Activation, sEH Inhibition, and Dual FXR/sEH Modulation in NASH in Diet-Induced Obese Mice.” *ACS pharmacology & translational science* vol. 4,2 966-979. 29 Mar. 2021, doi:10.1021/acsptsci.1c00041

Hin Tang, Justin Jit et al. “JAK/STAT signaling in hepatocellular carcinoma.” *Hepatic oncology* vol. 7,1 HEP18. 18 Mar. 2020, doi:10.2217/hep-2020-0001

Holmer, Magnus et al. “Treatment of NAFLD with intermittent calorie restriction or low-carb high-fat diet - a randomised controlled trial.” *JHEP reports : innovation in hepatology* vol. 3,3 100256. 17 Feb. 2021, doi:10.1016/j.jhepr.2021.100256

Holzner, Lorenz M W, and Andrew J Murray. “Hypoxia-Inducible Factors as Key Players in the Pathogenesis of Non-alcoholic Fatty Liver Disease and Non-alcoholic Steatohepatitis.” *Frontiers in medicine* vol. 8 753268. 6 Oct. 2021, doi:10.3389/fmed.2021.753268

Hong, Ting et al. “The Role and Mechanism of Oxidative Stress and Nuclear Receptors in the Development of NAFLD.” *Oxidative medicine and cellular longevity* vol. 2021 6889533. 27 Oct. 2021, doi:10.1155/2021/6889533

Honma, Midori et al. “Selective insulin resistance with differential expressions of IRS-1 and IRS-2 in human NAFLD livers.” *International journal of obesity (2005)* vol. 42,9 (2018): 1544-1555. doi:10.1038/s41366-018-0062-9

Hotamisligil, G.S., Shargill, N.S., and Spiegelman, B.M. (1993). Adipose expression of tumor necrosis factor-alpha: direct role in obesity-linked insulin resistance. Science (New York, N.Y.) *259*, 87-91.

Hu, Hai et al. “The C/EBP Homologous Protein (CHOP) Transcription Factor Functions in Endoplasmic Reticulum Stress-Induced Apoptosis and Microbial Infection.” *Frontiers in immunology* vol. 9 3083. 4 Jan. 2019, doi:10.3389/fimmu.2018.03083

Huang, Cheng et al. “Inhibition of Hepatic AMPK Pathway Contributes to Free Fatty Acids-Induced Fatty Liver Disease in Laying Hen.” *Metabolites* vol. 12,9 825. 1 Sep. 2022, doi:10.3390/metabo12090825

Huang, Hui et al. “EETs/sEH in diabetes and obesity-induced cardiovascular diseases.” *Prostaglandins & other lipid mediators* vol. 125 (2016): 80-9. doi: 10.1016/j.prostaglandins.2016.05.004

Huang, Jie et al. “Promising Therapeutic Targets for Treatment of Rheumatoid Arthritis.” *Frontiers in immunology* vol. 12 686155. 9 Jul. 2021, doi:10.3389/fimmu.2021.686155

Huang, Jih-Kai, and Hsiang-Chun Lee. “Emerging Evidence of Pathological Roles of Very-Low-Density Lipoprotein (VLDL).” *International journal of molecular sciences* vol. 23,8 4300. 13 Apr. 2022, doi:10.3390/ijms23084300

Huang, Jing et al. “Potential roles of AMP-activated protein kinase in liver regeneration in mice with acute liver injury.” *Molecular medicine reports* vol. 17,4 (2018): 5390-5395. doi:10.3892/mmr.2018.8522

Huang, Yiwei et al. “HIF-1α switches the functionality of TGF-β signaling via changing the partners of smads to drive glucose metabolic reprogramming in non-small cell lung cancer.” *Journal of experimental & clinical cancer research : CR* vol. 40,1 398. 20 Dec. 2021, doi:10.1186/s13046-021-02188-y

Huh, Jin Young, and Alan R Saltiel. “Roles of IκB kinases and TANK-binding kinase 1 in hepatic lipid metabolism and nonalcoholic fatty liver disease.” *Experimental & molecular medicine* vol. 53,11 (2021): 1697-1705. doi:10.1038/s12276-021-00712-

Humeau, Juliette et al. “EIF2α phosphorylation: a hallmark of both autophagy and immunogenic cell death.” *Molecular & cellular oncology* vol. 7,5 1776570. 19 Jun. 2020, doi:10.1080/23723556.2020.1776570

Hwang, Seung-Lark et al. “Inhibitory cross-talk between the AMPK and ERK pathways mediates endoplasmic reticulum stress-induced insulin resistance in skeletal muscle.” *British journal of pharmacology* vol. 169,1 (2013): 69-81. doi:10.1111/bph.12124

Hwang, Seung-Lark et al. “Inhibitory cross-talk between the AMPK and ERK pathways mediates endoplasmic reticulum stress-induced insulin resistance in skeletal muscle.” British journal of pharmacology vol. 169,1 (2013): 69-81. doi:10.1111/bph.12124

Ipsen, David Højland et al. “Molecular mechanisms of hepatic lipid accumulation in non-alcoholic fatty liver disease.” *Cellular and molecular life sciences : CMLS* vol. 75,18 (2018): 3313-3327. doi:10.1007/s00018-018-2860-6

Israelsen, Mads et al. “Validation of the new nomenclature of steatotic liver disease in patients with a history of excessive alcohol intake: an analysis of data from a prospective cohort study.” *The lancet. Gastroenterology & hepatology*, S2468-1253(23)00443-0. 10 Jan. 2024, doi:10.1016/S2468-1253(23)00443-0

Isse, Fadumo Ahmed et al. “The multifaceted role of cytochrome P450-Derived arachidonic acid metabolites in diabetes and diabetic cardiomyopathy.” *Drug metabolism reviews* vol. 54,2 (2022): 141-160. doi:10.1080/03602532.2022.2051045

Janochova, Karolina et al. “Visceral fat and insulin resistance - what we know?.” *Biomedical papers of the Medical Faculty of the University Palacky, Olomouc, Czechoslovakia* vol. 163,1 (2019): 19-27. doi:10.5507/bp.2018.062

Jeeyavudeen, Mohammad Sadiq et al. “Management of metabolic-associated fatty liver disease: The diabetology perspective.” *World journal of gastroenterology* vol. 29,1 (2023): 126-143. doi:10.3748/wjg.v29.i1.126

Jensen, Thomas et al. “Fructose and sugar: A major mediator of non-alcoholic fatty liver disease.” *Journal of hepatology* vol. 68,5 (2018): 1063-1075. doi:10.1016/j.jhep.2018.01.019

Jeong, Ha-Won et al. “Obesity-induced TRB3 negatively regulates Brown adipose tissue function in mice.” *Biochemical and biophysical research communications* vol. 547 (2021): 29-35. doi:10.1016/j.bbrc.2021.01.103

Jerez, Sofia et al. “Editorial: Chronic Liver Disease: New Targets and New Mechanisms, Volume II.” *Frontiers in molecular biosciences* vol. 10 1237824. 18 Jul. 2023, doi:10.3389/fmolb.2023.1237824

Jiao, P., Ma, J., Feng, B., Zhang, H., Diehl, J.A., Chin, Y.E., Yan, W., and Xu, H. (2011). FFAinduced adipocyte inflammation and insulin resistance: involvement of ER stress and IKKβ pathways. Obesity (Silver Spring, Md.) *19*, 483-491.

Jo, Hyunsun et al. “Endoplasmic reticulum stress induces hepatic steatosis via increased expression of the hepatic very low-density lipoprotein receptor.” *Hepatology (Baltimore, Md.)* vol. 57,4 (2013): 1366-77. doi:10.1002/hep.26126

Jo, Hyunsun et al. “Endoplasmic reticulum stress induces hepatic steatosis via increased expression of the hepatic very low-density lipoprotein receptor.” *Hepatology (Baltimore, Md.)* vol. 57,4 (2013): 1366-77. doi:10.1002/hep.26126

Ju, Cynthia et al. “Hypoxia-inducible factors as molecular targets for liver diseases.” *Journal of molecular medicine (Berlin, Germany)* vol. 94,6 (2016): 613-27. doi:10.1007/s00109-016-1408-1

Kalligeros, Markos et al. “Prevalence of Steatotic Liver Disease (MASLD, MetALD, and ALD) in the United States: NHANES 2017-2020.” *Clinical gastroenterology and hepatology : the official clinical practice journal of the American Gastroenterological Association*, S1542-3565(23)00914-X. 8 Nov. 2023, doi:10.1016/j.cgh.2023.11.003

Kanagaki, Shuhei et al. “Activation of AMP-activated protein kinase (AMPK) through inhibiting interaction with prohibitins.” *iScience* vol. 26,4 106293. 28 Feb. 2023, doi:10.1016/j.isci.2023.106293

Kanda, Tatsuo et al. “Apoptosis and non-alcoholic fatty liver diseases.” *World journal of gastroenterology* vol. 24,25 (2018): 2661-2672. doi:10.3748/wjg.v24.i25.2661

Kang, Hyunju et al. “Nicotinamide riboside, an NAD^+ precursor, attenuates inflammation and oxidative stress by activating sirtuin 1 in alcohol-stimulated macrophages.” *Laboratory investigation; a journal of technical methods and pathology* vol. 101,9 (2021): 1225-1237. doi:10.1038/s41374-021-00599-1

Kanwal, Fasiha et al. “Risk of Hepatocellular Cancer in Patients With Non-Alcoholic Fatty Liver Disease.” *Gastroenterology* vol. 155,6 (2018): 1828-1837.e2. doi: 10.1053/j.gastro.2018.08.024

Karkucinska-Wieckowska, Agnieszka et al. “Mitochondria, oxidative stress and nonalcoholic fatty liver disease: A complex relationship.” *European journal of clinical investigation* vol. 52,3 (2022): e13622. doi:10.1111/eci.13622

Kawano, Y. et al. (2015) Identification of lipid species linked to the progression of non-alcoholic fatty liver disease. Curr. Drug Targets 16, 1293–1300

Kawashima, Ichiro et al. “Negative regulation of the LKB1/AMPK pathway by ERK in human acute myeloid leukemia cells.” *Experimental hematology* vol. 43,7 (2015): 524-33.e1. doi:10.1016/j.exphem.2015.03.005

Kazankov, Konstantin, et al. "The role of macrophages in nonalcoholic fatty liver disease and nonalcoholic steatohepatitis." *Nature reviews Gastroenterology & hepatology* 16.3 (2019): 145-159.

Kciuk, Mateusz et al. “Doxorubicin-An Agent with Multiple Mechanisms of Anticancer Activity.” *Cells* vol. 12,4 659. 19 Feb. 2023, doi:10.3390/cells12040659

Kelly, Abigail G et al. “Enhancing cancer immunotherapy via inhibition of soluble epoxide hydrolase.” *Proceedings of the National Academy of Sciences of the United States of America* vol. 121,7 (2024): e2314085121. doi:10.1073/pnas.2314085121

Khader, Adam et al. “SRT1720, a sirtuin 1 activator, attenuates organ injury and inflammation in sepsis.” *The Journal of surgical research* vol. 219 (2017): 288-295. doi:10.1016/j.jss.2017.06.031

Khan, Shahzad, and Chang Hua Wang. “ER stress in adipocytes and insulin resistance: mechanisms and significance (Review).” *Molecular medicine reports* vol. 10,5 (2014): 2234-40. doi:10.3892/mmr.2014.2532

Kim, J.K., Fillmore, J.J., Sunshine, M.J., Albrecht, B., Higashimori, T., Kim, D.W., Liu, Z.X., Soos, T.J., Cline, G.W., O'Brien, W.R., et al. (2004). PKC-theta knockout mice are protected from fat-induced insulin resistance. The Journal of clinical investigation *114*, 823-827.

Kim, Ji Yong et al. "SIRT1 and Autophagy: Implications in Endocrine Disorders." *Frontiers in endocrinology* vol. 13 930919. 14 Jul. 2022, doi:10.3389/fendo.2022.930919

Kim, Kyung Soo et al. "Nonalcoholic Fatty Liver Disease and Diabetes: Part II: Treatment." *Diabetes & metabolism journal* vol. 43,2 (2019): 127-143. doi:10.4093/dmj.2019.0034

Kim, O.K., Jun, W., and Lee, J. (2015a). Mechanism of ER Stress and Inflammation for Hepatic Insulin Resistance in Obesity. Annals of Nutrition and Metabolism *67*, 218-227.

Kim, Seong Hun et al. "Fibroblast growth factor 21 participates in adaptation to endoplasmic reticulum stress and attenuates obesity-induced hepatic metabolic stress." *Diabetologia* vol. 58,4 (2015): 809-18. doi:10.1007/s00125-014-3475-6

Kim, Sou Hyun et al. "Taurine Ameliorates Tunicamycin-Induced Liver Injury by Disrupting the Vicious Cycle between Oxidative Stress and Endoplasmic Reticulum Stress." *Life (Basel, Switzerland)* vol. 12,3 354. 28 Feb. 2022, doi:10.3390/life12030354

Kitade, Hironori et al. "Nonalcoholic Fatty Liver Disease and Insulin Resistance: New Insights and Potential New Treatments." *Nutrients* vol. 9,4 387. 14 Apr. 2017, doi:10.3390/nu9040387

Klevstig, Martina et al. "Targeting acid sphingomyelinase reduces cardiac ceramide accumulation in the post-ischemic heart." *Journal of molecular and cellular cardiology* vol. 93 (2016): 69-72. doi:10.1016/j.yjmcc.2016.02.019

Klop, Boudewijn et al. "Dyslipidemia in obesity: mechanisms and potential targets." *Nutrients* vol. 5,4 1218-40. 12 Apr. 2013, doi:10.3390/nu5041218

Kodani, Sean D et al. "Identification and optimization of soluble epoxide hydrolase inhibitors with dual potency towards fatty acid amide hydrolase." *Bioorganic & medicinal chemistry letters* vol. 28,4 (2018): 762-768. doi: 10.1016/j.bmcl.2018.01.003

Kojta, Iwona et al. "Obesity, Bioactive Lipids, and Adipose Tissue Inflammation in Insulin Resistance." *Nutrients* vol. 12,5 1305. 3 May. 2020, doi:10.3390/nu12051305

Koo, Ja Hyun, and Chang Yeob Han. "Signaling nodes associated with endoplasmic reticulum stress during NAFLD progression." *Biomolecules* 11.2 (2021): 242.

Kountouras, Jannis et al. “Innate immunity and nonalcoholic fatty liver disease.” *Annals of gastroenterology* vol. 36,3 (2023): 244-256. doi:10.20524/aog.2023.0793

Koutny, Florian et al. “Prevalence of prediabetes and type 2 diabetes in children with obesity and increased transaminases in European German-speaking countries. Analysis of the APV initiative.” *Pediatric obesity* vol. 15,4 (2020): e12601. doi:10.1111/ijpo.12601

Kouyama, K., Miyake, K., Zenibayashi, M., Hirota, Y., Teranishi, T., Tamori, Y., Kanda, H., Sakaguchi, K., Ohara, T., and Kasuga, M. (2008). Association of serum MCP-1 concentration and MCP-1 polymorphism with insulin resistance in Japanese individuals with obese type 2 diabetes. The Kobe journal of medical sciences *53*, 345-354.

Kovarova, Marketa et al. “The Genetic Variant I148M in PNPLA3 Is Associated With Increased Hepatic Retinyl-Palmitate Storage in Humans.” *The Journal of clinical endocrinology and metabolism* vol. 100,12 (2015): E1568-74. doi:10.1210/jc.2015-2978

Kozako, Tomohiro et al. “SRT1720 induces SIRT1-independent cell death in adult T-cell leukemia/lymphoma.” *The FEBS journal* vol. 289,12 (2022): 3477-3488. doi:10.1111/febs.16353

Krauss, Ronald M et al. “VLDL receptor gene therapy for reducing atherogenic lipoproteins.” *Molecular metabolism* vol. 69 (2023): 101685. doi: 10.1016/j.molmet.2023.101685

Kroetz, Deanna L, and Darryl C Zeldin. “Cytochrome P450 pathways of arachidonic acid metabolism.” *Current opinion in lipidology* vol. 13,3 (2002): 273-83. doi:10.1097/00041433-200206000-00007

Kuo, Y. M., & Lee, Y. H. (2022). Epoxyeicosatrienoic acids and soluble epoxide hydrolase in physiology and diseases of the central nervous system. The Chinese journal of physiology, 65(1), 1–11. https://doi.org/10.4103/cjp.cjp_80_21

Lagouge, Marie et al. “Resveratrol improves mitochondrial function and protects against metabolic disease by activating SIRT1 and PGC-1alpha.” *Cell* vol. 127,6 (2006): 1109-22. doi:10.1016/j.cell.2006.11.013

Lan, Fan et al. “SIRT1 modulation of the acetylation status, cytosolic localization, and activity of LKB1. Possible role in AMP-activated protein kinase activation.” *The Journal of biological chemistry* vol. 283,41 (2008): 27628-27635. doi:10.1074/jbc.M805711200

Le, Michael H et al. “2019 Global NAFLD Prevalence: A Systematic Review and Meta-analysis.” *Clinical gastroenterology and hepatology : the official clinical practice journal of the American Gastroenterological Association* vol. 20,12 (2022): 2809-2817.e28. doi:10.1016/j.cgh.2021.12.002

Lebeaupin, Cynthia et al. “Endoplasmic reticulum stress signalling and the pathogenesis of non-alcoholic fatty liver disease.” *Journal of hepatology* vol. 69,4 (2018): 927-947. doi:10.1016/j.jhep.2018.06.008

Lebrun, P., and Van Obberghen, E. (2008). SOCS proteins causing trouble in insulin action. Acta physiologica (Oxford, England) *192*, 29-36.
Lebrun, P., Cognard, E., Bellon-Paul, R., Gontard, P., Filloux, C., Jehl-Pietri, C., Grimaldi, P., Samson, M., Pénicaud, L., Ruberte, J., et al. (2009). Constitutive expression of suppressor of cytokine signalling-3 in skeletal muscle leads to reduced mobility and overweight in mice. Diabetologia *52*, 2201-2212.
Lee, B.C., and Lee, J. (2014). Cellular and molecular players in adipose tissue inflammation in the development of obesity-induced insulin resistance. Biochimica et biophysica acta *1842*, 446-462.
Lee-Rueckert, Miriam, et al. "Lipid-Laden Macrophages and Inflammation in Atherosclerosi s and Cancer: An Integrative View." *Frontiers in Cardiovascular Medicine* 9 (2022): 777822.

Lefere, Sander, and Frank Tacke. “Macrophages in obesity and non-alcoholic fatty liver disease: Crosstalk with metabolism.” *JHEP reports : innovation in hepatology* vol. 1,1 30-43. 23 Feb. 2019, doi:10.1016/j.jhepr.2019.02.004

Lekakis, Vasileios, and George V Papatheodoridis. “Natural history of metabolic dysfunction-associated steatotic liver disease.” *European journal of internal medicine*, S0953-6205(23)00397-7. 6 Nov. 2023, doi:10.1016/j.ejim.2023.11.005

Lemmer, Imke L et al. “A guide to understanding endoplasmic reticulum stress in metabolic disorders.” *Molecular metabolism* vol. 47 (2021): 101169. doi:10.1016/j.molmet.2021.101169

Leuillier, Matthieu, et al. "CRISPR/Cas9-mediated inactivation of the phosphatase activity of soluble epoxide hydrolase prevents obesity and cardiac ischemic injury." *Journal of advanced research* 43 (2023): 163-174.

Li, Jie et al. “Prevalence, incidence, and outcome of non-alcoholic fatty liver disease in Asia, 1999-2019: a systematic review and meta-analysis.” *The lancet. Gastroenterology & hepatology* vol. 4,5 (2019): 389-398. doi:10.1016/S2468-1253(19)30039-1

Li, Juan et al. “HIF1A and VEGF regulate each other by competing endogenous RNA mechanism and involve in the pathogenesis of peritoneal fibrosis.” *Pathology, research and practice* vol. 215,4 (2019): 644-652. doi:10.1016/j.prp.2018.12.022

Li, Junhan et al. “Effect of aerobic exercise on GRP78 and ATF6 expressions in mice with non-alcoholic fatty liver disease.” *Sports medicine and health science* vol. 5,2 112-119. 22 Nov. 2022, doi:10.1016/j.smhs.2022.11.002

Li, Si et al. “Active ingredients of Erhuang Quzhi Granules for treating non-alcoholic fatty liver disease based on the NF-κB/NLRP3 pathway.” *Fitoterapia* vol. 171 (2023): 105704. doi:10.1016/j.fitote.2023.105704

Li, Songtao et al. “Activation of the AMPK-SIRT1 pathway contributes to protective effects of Salvianolic acid A against lipotoxicity in hepatocytes and NAFLD in mice.” *Frontiers in pharmacology* vol. 11 560905. 30 Nov. 2020, doi:10.3389/fphar.2020.560905

Li, Wei, and Reza Hakkak. “Feeding soy protein concentrates with low or high isoflavone decreases liver inflammation by reducing lipopolysaccharide translocation.” *Frontiers in nutrition* vol. 10 1278158. 20 Nov. 2023, doi:10.3389/fnut.2023.1278158

Li, Y., Soos, T.J., Li, X., Wu, J., Degennaro, M., Sun, X., Littman, D.R., Birnbaum, M.J., and Polakiewicz, R.D. (2004). Protein kinase C Theta inhibits insulin signaling by phosphorylating IRS1 at Ser (1101). The Journal of biological chemistry *279*, 45304-45307.

Li, Yiming et al. “New insights into the roles of CHOP-induced apoptosis in ER stress.” *Acta biochimica et biophysica Sinica* vol. 46,8 (2014): 629-40. doi:10.1093/abbs/gmu048

Li, Yu et al. “Hepatic SIRT1 attenuates hepatic steatosis and controls energy balance in mice by inducing fibroblast growth factor 21.” *Gastroenterology* vol. 146,2 (2014): 539-49.e7. doi:10.1053/j.gastro.2013.10.059

Lian, Cai-Yu et al. “High fat diet-triggered non-alcoholic fatty liver disease: A review of proposed mechanisms.” *Chemico-biological interactions* vol. 330 (2020): 109199. doi:10.1016/j.cbi.2020.109199

Lim, Ji-Hong et al. “Sirtuin 1 modulates cellular responses to hypoxia by deacetylating hypoxia-inducible factor 1alpha.” *Molecular cell* vol. 38,6 (2010): 864-78. doi:10.1016/j.molcel.2010.05.023

Lin, Yu-Cheng et al. “Genetic variants in GCKR and PNPLA3 confer susceptibility to nonalcoholic fatty liver disease in obese individuals.” *The*

American journal of clinical nutrition vol. 99,4 (2014): 869-74. doi:10.3945/ajcn.113.079749

Lindenmeyer, Christina C, and Arthur J McCullough. “The Natural History of Nonalcoholic Fatty Liver Disease-An Evolving View.” *Clinics in liver disease* vol. 22,1 (2018): 11-21. doi:10.1016/j.cld.2017.08.003

Liu, Jia et al. “The Role of JAK/STAT Pathway in Fibrotic Diseases: Molecular and Cellular Mechanisms.” *Biomolecules* vol. 13,1 119. 6 Jan. 2023, doi:10.3390/biom13010119

Liu, Xiaoying, and Richard M. Green. "Endoplasmic reticulum stress and liver diseases." *Liver research* 3.1 (2019): 55-64.

Liu, Yan et al. “Inhibition of soluble epoxide hydrolase attenuates high-fat-diet-induced hepatic steatosis by reduced systemic inflammatory status in mice.” *PloS one* vol. 7,6 (2012): e39165. doi:10.1371/journal.pone.0039165

Liu, Yang et al. “Hepatic Small Ubiquitin-Related Modifier (SUMO)-Specific Protease 2 Controls Systemic Metabolism Through SUMOylation-Dependent Regulation of Liver-Adipose Tissue Crosstalk.” *Hepatology (Baltimore, Md.)* vol. 74,4 (2021): 1864-1883. doi:10.1002/hep.31881

Liu, Yanqing, and Wei Gu. “The complexity of p53-mediated metabolic regulation in tumor suppression.” *Seminars in cancer biology* vol. 85 (2022): 4-32. doi:10.1016/j.semcancer.2021.03.010

Liu, Zi et al. “An overview of PROTACs: a promising drug discovery paradigm.” *Molecular biomedicine* vol. 3,1 46. 20 Dec. 2022, doi:10.1186/s43556-022-00112-0

Liu, Zi et al. “An overview of PROTACs: a promising drug discovery paradigm.” *Molecular biomedicine* vol. 3,1 46. 20 Dec. 2022, doi:10.1186/s43556-022-00112-0

Ludwig, J et al. “Nonalcoholic steatohepatitis: Mayo Clinic experiences with a hitherto unnamed disease.” *Mayo Clinic proceedings* vol. 55,7 (1980): 434-8.

Luo, Fei et al. “TM6SF2: A Novel Genetic Player in Nonalcoholic Fatty Liver and Cardiovascular Disease.” *Hepatology communications* vol. 6,3 (2022): 448-460. doi:10.1002/hep4.1822

Luo, Mingxiao et al. “The role of hypoxia-inducible factor 1α in hepatic lipid metabolism.” *Journal of molecular medicine (Berlin, Germany)* vol. 101,5 (2023): 487-500. doi:10.1007/s00109-023-02308-5

Luo, Xiao et al. “DHA Protects Against Hepatic Steatosis by Activating Sirt1 in a High Fat Diet-Induced Nonalcoholic Fatty Liver Disease Mouse

Model." *Diabetes, metabolic syndrome and obesity : targets and therapy* vol. 13 185-196. 22 Jan. 2020, doi:10.2147/DMSO.S232279

Luo, Ying et al. "Inhibition of soluble epoxide hydrolase attenuates a high-fat diet-mediated renal injury by activating PAX2 and AMPK." *Proceedings of the National Academy of Sciences of the United States of America* vol. 116,11 (2019): 5154-5159. doi:10.1073/pnas.1815746116

Luukkonen, P.K. et al. (2016) Hepatic ceramides dissociate steatosis and insulin resistance in patients with non-alcoholic fatty liver disease. J. Hepatol. 64, 1167–1175

Mair, Markus et al. "JAK-STAT signaling in hepatic fibrosis." *Frontiers in bioscience (Landmark edition)* vol. 16,8 2794-811. 1 Jun. 2011, doi:10.2741/3886

Malik, Vasanti S, and Frank B Hu. "The role of sugar-sweetened beverages in the global epidemics of obesity and chronic diseases." *Nature reviews. Endocrinology* vol. 18,4 (2022): 205-218. doi:10.1038/s41574-021-00627-6

Mangels, Nicole et al. "The soluble epoxide hydrolase determines cholesterol homeostasis by regulating AMPK and SREBP activity." *Prostaglandins & other lipid mediators* vol. 125 (2016): 30-9. doi:10.1016/j.prostaglandins.2016.05.003

Mann, Jake P et al. "Nonalcoholic Fatty Liver Disease in Children." *Seminars in liver disease* vol. 38,1 (2018): 1-13. doi:10.1055/s-0038-1627456

Manne, Vignan et al. "Pathophysiology of Nonalcoholic Fatty Liver Disease/Nonalcoholic Steatohepatitis." *Clinics in liver disease* vol. 22,1 (2018): 23-37. doi:10.1016/j.cld.2017.08.007

Mantovani, Alessandro et al. "Complications, morbidity and mortality of nonalcoholic fatty liver disease." *Metabolism: clinical and experimental* vol. 111S (2020): 154170. doi:10.1016/j.metabol.2020.154170

Marcondes-de-Castro, Ilitch Aquino et al. "AMPK/mTOR pathway significance in healthy liver and non-alcoholic fatty liver disease and its progression." *Journal of gastroenterology and hepatology* vol. 38,11 (2023): 1868-1876. doi:10.1111/jgh.16272

Maris, M., Overbergh, L., Gysemans, C., Waget, A., Cardozo, A.K., Verdrengh, E., Cunha, J.P.M., Gotoh, T., Cnop, M., Eizirik, D.L., et al. (2012). Deletion of C/EBP homologous protein (Chop) in C57Bl/6 mice dissociates obesity from insulin resistance. Diabetologia *55*, 1167-1178.

Martinou, Eirini et al. "Diagnostic Modalities of Non-Alcoholic Fatty Liver Disease: From Biochemical Biomarkers to Multi-Omics Non-Invasive

Approaches." *Diagnostics (Basel, Switzerland)* vol. 12,2 407. 4 Feb. 2022, doi:10.3390/diagnostics12020407

Marušić, Marinko et al. "NAFLD, Insulin Resistance, and Diabetes Mellitus Type 2." *Canadian journal of gastroenterology & hepatology* vol. 2021 6613827. 17 Feb. 2021, doi:10.1155/2021/6613827

Mashili, F., Chibalin, A.V., Krook, A., and Zierath, J.R. (2013). Constitutive STAT3 phosphorylation contributes to skeletal muscle insulin resistance in type 2 diabetes.

Matsuda, Tadashi. "The Physiological and Pathophysiological Role of IL-6/STAT3-Mediated Signal Transduction and STAT3 Binding Partners in Therapeutic Applications." *Biological & pharmaceutical bulletin* vol. 46,3 (2023): 364-378. doi:10.1248/bpb.b22-00887

Matsuzaka, Takashi, and Hitoshi Shimano. "Molecular mechanisms involved in hepatic steatosis and insulin resistance." *Journal of diabetes investigation* vol. 2,3 (2011): 170-5. doi:10.1111/j.2040-1124.2011.00111.x

Matulewicz, Natalia, and Monika Karczewska-Kupczewska. "Insulin resistance and chronic inflammation." *Postepy higieny i medycyny doswiadczalnej (Online)* vol. 70,0 1245-1258. 20 Dec. 2016

McPherson, Stuart, et al. "Quality standards for the management of non-alcoholic fatty liver disease (NAFLD): consensus recommendations from the British Association for the Study of the Liver and British Society of Gastroenterology NAFLD Special Interest Group." *The lancet Gastroenterology & hepatology* (2022).

Meares, Gordon P et al. "PERK-dependent activation of JAK1 and STAT3 contributes to endoplasmic reticulum stress-induced inflammation." *Molecular and cellular biology* vol. 34,20 (2014): 3911-25. doi:10.1128/MCB.00980-14

Méndez-Sánchez, Nahum, and Shreya C. Pal. "New terms for fatty liver disease other than MAFLD: Time for a reality check." Journal of Hepatology 77.6 (2022): 1716-1717.

Miao, Mengqiu et al. "Clinical Potential of Hypoxia Inducible Factors Prolyl Hydroxylase Inhibitors in Treating Nonanemic Diseases." *Frontiers in pharmacology* vol. 13 837249. 24 Feb. 2022, doi:10.3389/fphar.2022.837249

Mirza, Agha Zeeshan et al. "Role of PPAR receptor in different diseases and their ligands: Physiological importance and clinical implications." *European journal of medicinal chemistry* vol. 166 (2019): 502-513. doi:10.1016/j.ejmech.2019.01.067

Mitsuyoshi, Hironori et al. “Hepatic nucleotide binding oligomerization domain-like receptors pyrin domain-containing 3 inflammasomes are associated with the histologic severity of non-alcoholic fatty liver disease.” *Hepatology research : the official journal of the Japan Society of Hepatology* vol. 47,13 (2017): 1459-1468. doi:10.1111/hepr.12883

Mocciaro, Gabriele, and Amalia Gastaldelli. “Obesity-Related Insulin Resistance: The Central Role of Adipose Tissue Dysfunction.” Handbook of experimental pharmacology vol. 274 (2022): 145-164. doi:10.1007/164_2021_573

Modanloo, Mona, and Mohammad Shokrzadeh. “Analyzing Mitochondrial Dysfunction, Oxidative Stress, and Apoptosis: Potential Role of L-carnitine.” *Iranian journal of kidney diseases* vol. 13,2 (2019): 74-86.

Mongraw-Chaffin, Morgana et al. “Association of Visceral Adipose Tissue and Insulin Resistance with Incident Metabolic Syndrome Independent of Obesity Status: The IRAS Family Study.” *Obesity (Silver Spring, Md.)* vol. 29,7 (2021): 1195-1202. doi:10.1002/oby.23177

Moosavian, Seyedeh Alia et al. “The Emerging Role of Nanomedicine in the Management of Nonalcoholic Fatty Liver Disease: A State-of-the-Art Review.” *Bioinorganic chemistry and applications* vol. 2021 4041415. 8 Oct. 2021, doi:10.1155/2021/4041415

Musio, Alessandra et al. “Osteosarcopenia in NAFLD/MAFLD: An Underappreciated Clinical Problem in Chronic Liver Disease.” *International journal of molecular sciences* vol. 24,8 7517. 19 Apr. 2023, doi:10.3390/ijms24087517

Mzimela, Nomusa Christina et al. “Investigation into changes in inflammatory and immune cell markers in pre-diabetic patients from Durban, South Africa.” *Journal of immunotoxicology* vol. 21,1 (2024): 2290282. doi:10.1080/1547691X.2023.2290282

Naeem, Zumer et al. “Role of the soluble epoxide hydrolase in keratinocyte proliferation and sensitivity of skin to inflammatory stimuli.” *Biomedicine & pharmacotherapy = Biomedecine & pharmacotherapie* vol. 171 (2024): 116127. doi:10.1016/j.biopha.2024.116127

Nalawansha, Dhanusha A, and Craig M Crews. “PROTACs: An Emerging Therapeutic Modality in Precision Medicine.” *Cell chemical biology* vol. 27,8 (2020): 998-1014. doi: 10.1016/j.chembiol.2020.07.020

Namba, Takushi et al. “Loss of p53 enhances the function of the endoplasmic reticulum through activation of the IRE1α/XBP1 pathway.” *Oncotarget* vol. 6,24 (2015): 19990-20001. doi:10.18632/oncotarget.4598

Napper, Andrew D et al. “Discovery of indoles as potent and selective inhibitors of the deacetylase SIRT1.” *Journal of medicinal chemistry* vol. 48,25 (2005): 8045-54. doi:10.1021/jm050522v

Nassir, Fatiha. “NAFLD: Mechanisms, Treatments, and Biomarkers.” *Biomolecules* vol. 12,6 824. 13 Jun. 2022, doi:10.3390/biom12060824

Nath, Preetam, and Shivaram P Singh. “Nonalcoholic Fatty Liver Disease: Time to Take the Bull by the Horns.” *Euroasian journal of hepato-gastroenterology* vol. 8,1 (2018): 47-51. doi:10.5005/jp-journals-10018-1257

Nguyen, Andrew et al. “Very low density lipoprotein receptor (VLDLR) expression is a determinant factor in adipose tissue inflammation and adipocyte-macrophage interaction.” *The Journal of biological chemistry* vol. 289,3 (2014): 1688-703. doi:10.1074/jbc.M113.515320

Nguyen, Long T et al. “Parental SIRT1 Overexpression Attenuate Metabolic Disorders Due to Maternal High-Fat Feeding.” *International journal of molecular sciences* vol. 21,19 7342. 5 Oct. 2020, doi:10.3390/ijms21197342

Nguyen, Long The et al. “SRT1720 attenuates obesity and insulin resistance but not liver damage in the offspring due to maternal and postnatal high-fat diet consumption.” *American journal of physiology. Endocrinology and metabolism* vol. 315,2 (2018): E196-E203. doi:10.1152/ajpendo.00472.2017

Nguyen, M.T., Favelyukis, S., Nguyen, A.K., Reichart, D., Scott, P.A., Jenn, A., Liu-Bryan, R., Glass, C.K., Neels, J.G., and Olefsky, J.M. (2007). A subpopulation of macrophages infiltrates hypertrophic adipose tissue and is activated by free fatty acids via Toll-like receptors 2 and 4 and JNK-dependent pathways. The Journal of biological chemistry *282*,35279-35292.

Ogawa, Chie et al. “Hypoxia-Inducible Factor Prolyl Hydroxylase Inhibitors and Iron Metabolism.” *International journal of molecular sciences* vol. 24,3 3037. 3 Feb. 2023, doi:10.3390/ijms24033037

Oh, Hyunwoo et al. “The effects of moderate alcohol consumption on non-alcoholic fatty liver disease.” *Clinical and molecular hepatology* vol. 29,Suppl (2023): S261-S267. doi:10.3350/cmh.2022.0393

Oh, You-Take, and Shi-Yong Sun. “Regulation of Cancer Metastasis by TRAIL/Death Receptor Signaling.” *Biomolecules* vol. 11,4 499. 26 Mar. 2021, doi:10.3390/biom11040499

Oka, K et al. “Mouse very-low-density-lipoprotein receptor (VLDLR) cDNA cloning, tissue-specific expression and evolutionary relationship with the low-density-lipoprotein receptor.” *European journal of biochemistry* vol. 224,3 (1994): 975-82. doi:10.1111/j.1432-1033.1994.00975.x

olyzos, Stergios A et al. “Obesity and nonalcoholic fatty liver disease: From pathophysiology to therapeutics.” *Metabolism: clinical and experimental* vol. 92 (2019): 82-97. doi:10.1016/j.metabol.2018.11.014

Ong, Agnes L C, and Thamil Selvee Ramasamy. “Role of Sirtuin1-p53 regulatory axis in aging, cancer and cellular reprogramming.” *Ageing research reviews* vol. 43 (2018): 64-80. doi:10.1016/j.arr.2018.02.004

Oshio, Yui et al. “Very low-density lipoprotein receptor increases in a liver-specific manner due to protein deficiency but does not affect fatty liver in mice.” *Scientific reports* vol. 11,1 8003. 13 Apr. 2021, doi:10.1038/s41598-021-87568-2

Oshio, Yui et al. “Very low-density lipoprotein receptor increases in a liver-specific manner due to protein deficiency but does not affect fatty liver in mice.” *Scientific reports* vol. 11,1 8003. 13 Apr. 2021, doi:10.1038/s41598-021-87568-2

Ota, Tsuguhito. “Molecular Mechanisms of Nonalcoholic Fatty Liver Disease (NAFLD)/Nonalcoholic Steatohepatitis (NASH).” *Advances in experimental medicine and biology* vol. 1261 (2021): 223-229. doi:10.1007/978-981-15-7360-6_20

Overby, Haley et al. “Soluble Epoxide Hydrolase Inhibition by *t*-TUCB Promotes Brown Adipogenesis and Reduces Serum Triglycerides in Diet-Induced Obesity.” *International journal of molecular sciences* vol. 21,19 7039. 24 Sep. 2020, doi:10.3390/ijms21197039

Packard, Chris J., Jan Boren, and Marja-Riitta Taskinen. "Causes and consequences of hypertriglyceridemia." *Frontiers in endocrinology* 11 (2020): 252.

Palma, Rossella et al. “The Role of Insulin Resistance in Fueling NAFLD Pathogenesis: From Molecular Mechanisms to Clinical Implications.” *Journal of clinical medicine* vol. 11,13 3649. 24 Jun. 2022, doi:10.3390/jcm11133649

Pan, Xiongfeng et al. “Gut metabolites and inflammation factors in non-alcoholic fatty liver disease: A systematic review and meta-analysis.” *Scientific reports* vol. 10,1 8848. 1 Jun. 2020, doi:10.1038/s41598-020-65051-8

Parra-Vargas, Marcela et al. “Nutritional Approaches for the Management of Nonalcoholic Fatty Liver Disease: An Evidence-Based Review.” *Nutrients* vol. 12,12 3860. 17 Dec. 2020, doi:10.3390/nu12123860

Parthasarathy, Gopanandan, and Harmeet Malhi. “Assessment of Lipotoxic Endoplasmic Reticulum (ER) Stress in Nonalcoholic Steatohepatitis (NASH).” *Methods in molecular biology (Clifton, N.J.)* vol. 2455 (2022): 243-254. doi:10.1007/978-1-0716-2128-8_19

Pennisi, Grazia et al. “Risk of liver-related events in metabolic dysfunction-associated steatohepatitis (MASH) patients with fibrosis: A comparative analysis of various risk stratification criteria.” *Hepatology (Baltimore, Md.)*, 10.1097/HEP.0000000000000616. 2 Oct. 2023, doi:10.1097/HEP.0000000000000616

Perazzo, Hugo, et al. "Changing from NAFLD through MAFLD to MASLD: Similar prevalence and risk factors in a large Brazilian cohort." *Journal of Hepatology* (2023).

Perman, Jeanna C et al. “The VLDL receptor promotes lipotoxicity and increases mortality in mice following an acute myocardial infarction.” *The Journal of clinical investigation* vol. 121,7 (2011): 2625-40. doi:10.1172/JCI43068

Petersen, M.C., and Shulman, G.I. (2017). Roles of Diacylglycerols and Ceramides in Hepatic Insulin Resistance. Trends Pharmacol Sci *38*, 649-665.

Pettersson, Mariell, and Craig M Crews. “PROteolysis TArgeting Chimeras (PROTACs) - Past, present and future.” *Drug discovery today. Technologies* vol. 31 (2019): 15-27. doi:10.1016/j.ddtec.2019.01.002

Peyman, Mona et al. “Soluble epoxide hydrolase-targeting PROTAC activates AMPK and inhibits endoplasmic reticulum stress.” *Biomedicine & pharmacotherapy = Biomedecine & pharmacotherapie* vol. 168 (2023): 115667. doi:10.1016/j.biopha.2023.115667

Piazzolla, Valeria Annarita, and Alessandra Mangia. “Noninvasive Diagnosis of NAFLD and NASH.” *Cells* vol. 9,4 1005. 17 Apr. 2020, doi:10.3390/cells9041005

Pipitone, Rosaria Maria et al. “MAFLD: a multisystem disease.” *Therapeutic advances in endocrinology and metabolism* vol. 14 20420188221145549. 28 Jan. 2023, doi:10.1177/20420188221145549

Pixner, Thomas et al. “The Role of Macronutrients in the Pathogenesis, Prevention and Treatment of Non-Alcoholic Fatty Liver Disease (NAFLD) in the Paediatric Population-A Review.” *Life (Basel, Switzerland)* vol. 12,6 839. 5 Jun. 2022, doi:10.3390/life12060839

Planavila, A et al. “Dilated cardiomyopathy and mitochondrial dysfunction in Sirt1-deficient mice: a role for Sirt1-Mef2 in adult heart.” *Journal of molecular and cellular cardiology* vol. 53,4 (2012): 521-31. doi:10.1016/j.yjmcc.2012.07.019

Plaza-Díaz, Julio et al. “Insights into the Impact of Microbiota in the Treatment of NAFLD/NASH and Its Potential as a Biomarker for Prognosis and

Diagnosis." *Biomedicines* vol. 9,2 145. 3 Feb. 2021, doi:10.3390/biomedicines9020145

Ponugoti, Bhaskar et al. "SIRT1 deacetylates and inhibits SREBP-1C activity in regulation of hepatic lipid metabolism." *The Journal of biological chemistry* vol. 285,44 (2010): 33959-70. doi:10.1074/jbc.M110.122978

Porteiro, Begoña et al. "Pharmacological stimulation of p53 with low-dose doxorubicin ameliorates diet-induced nonalcoholic steatosis and steatohepatitis." *Molecular metabolism* vol. 8 (2018): 132-143. doi:10.1016/j.molmet.2017.12.005

Powell, Elizabeth E et al. "Non-alcoholic fatty liver disease." *Lancet (London, England)* vol. 397,10290 (2021): 2212-2224. doi:10.1016/S0140-6736(20)32511-3

Poznyak, Anastasia V., et al. "Overview of OxLDL and its impact on cardiovascular health: focus on atherosclerosis." *Frontiers in Pharmacology* (2021): 2248.

Price, Nathan L et al. "SIRT1 is required for AMPK activation and the beneficial effects of resveratrol on mitochondrial function." *Cell metabolism* vol. 15,5 (2012): 675-90. doi:10.1016/j.cmet.2012.04.003

Purushotham, Aparna et al. "Hepatocyte-specific deletion of SIRT1 alters fatty acid metabolism and results in hepatic steatosis and inflammation." *Cell metabolism* vol. 9,4 (2009): 327-38. doi:10.1016/j.cmet.2009.02.006

Qi, Si-Min et al. "PROTAC: An Effective Targeted Protein Degradation Strategy for Cancer Therapy." *Frontiers in pharmacology* vol. 12 692574. 7 May. 2021, doi:10.3389/fphar.2021.692574

Qian, Shanna et al. "The role of BCL-2 family proteins in regulating apoptosis and cancer therapy." *Frontiers in oncology* vol. 12 985363. 12 Oct. 2022, doi:10.3389/fonc.2022.985363

Qin, Qiu-Fang et al. "AMPK-ERK/CARM1 Signaling Pathways Affect Autophagy of Hepatic Cells in Samples of Liver Cancer Patients." Frontiers in oncology vol. 9 1247. 14 Nov. 2019, doi:10.3389/fonc.2019.01247

Qing, Bowen et al. "Crosstalk between endoplasmic reticulum stress and multidrug-resistant cancers: hope or frustration." *Frontiers in pharmacology* vol. 14 1273987. 18 Sep. 2023, doi:10.3389/fphar.2023.1273987

Quesada-Vázquez, Sergio, et al. "Diet, gut microbiota and non-alcoholic fatty liver disease: three parts of the same axis." *Cells* 9.1 (2020): 176.

Rada, Patricia et al. “Understanding lipotoxicity in NAFLD pathogenesis: is CD36 a key driver?.” *Cell death & disease* vol. 11,9 802. 25 Sep. 2020, doi:10.1038/s41419-020-03003-w

Rahman, M.M., and McFadden, G. (2011). Modulation of NF-κB signalling by microbial pathogens. Nature Reviews Microbiology *9*, 291-306.

Rajesh, Yetirajam, and Devanand Sarkar. “Association of Adipose Tissue and Adipokines with Development of Obesity-Induced Liver Cancer.” *International journal of molecular sciences* vol. 22,4 2163. 22 Feb. 2021, doi:10.3390/ijms22042163

Ramms, Bastian, et al. "ApoC-III ASO promotes tissue LPL activity in the absence of apoE-mediated TRL clearance." *Journal of lipid research* 60.8 (2019): 1379-1395.

Ramos-Tovar, Erika, and Pablo Muriel. “NLRP3 inflammasome in hepatic diseases: A pharmacological target.” *Biochemical pharmacology* vol. 217 (2023): 115861. doi:10.1016/j.bcp.2023.115861

Rana, Sandeep, et al. "Inhibitors, PROTACs and molecular glues as diverse therapeutic modalities to target cyclin-dependent kinase." *Cancers* 13.21 (2021): 5506.

Ratziu, Vlad, et al. "The times they are a-changin'(for NAFLD as well)." *Journal of Hepatology* 73.6 (2020): 1307-1309.

Rebollo, Alba et al. “Liquid fructose downregulates Sirt1 expression and activity and impairs the oxidation of fatty acids in rat and human liver cells.” *Biochimica et biophysica acta* vol. 1841,4 (2014): 514-24. doi:10.1016/j.bbalip.2014.01.002

Remmerie, Anneleen, and Charlotte L. Scott. "Macrophages and lipid metabolism." *Cellular immunology* 330 (2018): 27-42.

Rieusset, J., Bouzakri, K., Chevillotte, E., Ricard, N., Jacquet, D., Bastard, J.P., Laville, M., and Vidal, H. (2004). Suppressor of cytokine signaling 3 expression and insulin resistance in skeletal muscle of obese and type 2 diabetic patients. Diabetes *53*, 2232-2241.

Rinella, Mary E et al. “A multisociety Delphi consensus statement on new fatty liver disease nomenclature.” *Hepatology (Baltimore, Md.)* vol. 78,6 (2023): 1966-1986. doi:10.1097/HEP.0000000000000520

Rinella, Mary E et al. “A multisociety Delphi consensus statement on new fatty liver disease nomenclature.” *Annals of hepatology* vol. 29,1 (2024): 101133. doi:10.1016/j.aohep.2023.101133

Rinella, Mary E., et al. "A multi-society Delphi consensus statement on new fatty liver disease nomenclature." *Annals of Hepatology* (2023): 101133.

Rivera-Esteban, Jesús et al. “Prevalence and Risk Factors of MASLD and Liver Fibrosis amongst the Penitentiary Population in Catalonia: The PRISONAFLD Study.” *Journal of clinical medicine* vol. 12,23 7276. 24 Nov. 2023, doi:10.3390/jcm12237276

Rives, Clémence et al. “Oxidative Stress in NAFLD: Role of Nutrients and Food Contaminants.” *Biomolecules* vol. 10,12 1702. 21 Dec. 2020, doi:10.3390/biom10121702

Rodríguez-Calvo, R., Serrano, L., Coll, T., Moullan, N., Sánchez, R.M., Merlos, M., Palomer, X., Laguna, J.C., Michalik, L., Wahli, W., et al. (2008). Activation of peroxisome proliferatoractivated receptor beta/delta inhibits lipopolysaccharide-induced cytokine production in adipocytes by lowering nuclear factor-kappaB activity via extracellular signal-related kinase 1/2. Diabetes *57*, 2149-2157.

Roeb, Elke, and Ralf Weiskirchen. “Fructose and Non-Alcoholic Steatohepatitis.” *Frontiers in pharmacology* vol. 12 634344. 8 Feb. 2021, doi:10.3389/fphar.2021.634344

Rojas, Yesmi A Ortega et al. “Non-alcoholic fatty liver disease prevalence in Latin America: A systematic review and meta-analysis.” *Annals of hepatology* vol. 27,6 (2022): 100706. doi:10.1016/j.aohep.2022.100706

Ron, D., and Walter, P. (2007). Signal integration in the endoplasmic reticulum unfolded protein response. Nature reviews. Molecular cell biology *8*, 519-529.

Rosca, Mariana G et al. “Oxidation of fatty acids is the source of increased mitochondrial reactive oxygen species production in kidney cortical tubules in early diabetes.” *Diabetes* vol. 61,8 (2012): 2074-83. doi:10.2337/db11-1437

Roth, Katherine J, and Bryan L Copple. “Role of Hypoxia-Inducible Factors in the Development of Liver Fibrosis.” *Cellular and molecular gastroenterology and hepatology* vol. 1,6 589-597. 25 Sep. 2015, doi:10.1016/j.jcmgh.2015.09.005

Rupasinghe, Kushila et al. “Updates in Metabolic Dysfunction-Associated Fatty Liver Disease (MAFLD) in Children.” *Journal of pediatric gastroenterology and nutrition* vol. 77,5 (2023): 583-591. doi:10.1097/MPG.0000000000003919

Rusli, Fenni et al. “Fibroblast growth factor 21 reflects liver fat accumulation and dysregulation of signalling pathways in the liver of C57BL/6J mice.” *Scientific reports* vol. 6 30484. 29 Jul. 2016, doi:10.1038/srep30484

Russo, Maria Francesca et al. “Insulin Resistance Is Central to Long-Term Reversal of Histologic Nonalcoholic Steatohepatitis After Metabolic

Surgery." *The Journal of clinical endocrinology and metabolism* vol. 106,3 (2021): 750-761. doi:10.1210/clinem/dgaa892

Ryu, Dong Ryeol et al. "Sirt1-hypoxia-inducible factor-1α interaction is a key mediator of tubulointerstitial damage in the aged kidney." *Aging cell* vol. 18,2 (2019): e12904. doi:10.1111/acel.12904

Sakamoto, K M et al. "Protacs: chimeric molecules that target proteins to the Skp1-Cullin-F box complex for ubiquitination and degradation." Proceedings of the National Academy of Sciences of the United States of America vol. 98,15 (2001): 8554-9. doi:10.1073/pnas.141230798

Sakurai, H., Suzuki, S., Kawasaki, N., Nakano, H., Okazaki, T., Chino, A., Doi, T., and Saiki, I. (2003). Tumor Necrosis Factor-α-induced IKK Phosphorylation of NF-κB p65 on Serine 536 Is Mediated through the TRAF2, TRAF5, and TAK1 Signaling Pathway*. Journal of Biological Chemistry *278*, 36916-36923.

Sakurai, Yoshitaka et al. "Role of Insulin Resistance in MAFLD." *International journal of molecular sciences* vol. 22,8 4156. 16 Apr. 2021, doi:10.3390/ijms22084156

Salminen, A., Hyttinen, J.M.T., and Kaarniranta, K. (2011). AMP-activated protein kinase inhibits NF-κB signaling and inflammation: impact on healthspan and lifespan. J Mol Med (Berl) *89*, 667-676.

Salminen, Antero et al. "AMP-activated protein kinase inhibits NF-κB signaling and inflammation: impact on healthspan and lifespan." *Journal of molecular medicine (Berlin, Germany)* vol. 89,7 (2011): 667-76. doi:10.1007/s00109-011-0748-0

Salvadó, L., Barroso, E., Gómez-Foix, A.M., Palomer, X., Michalik, L., Wahli, W., and

Salvado, L., Palomer, X., Barroso, E., and Vazquez-Carrera, M. (2015). Targeting endoplasmic reticulum stress in insulin resistance. Trends in endocrinology and metabolism: TEM *26*, 438-448.

Salvado, L., Palomer, X., Barroso, E., and Vazquez-Carrera, M. (2015). Targeting endoplasmic reticulum stress in insulin resistance. Trends in endocrinology and metabolism: TEM *26*, 438-448.

Salvadó, Laia et al. "PPARβ/δ prevents endoplasmic reticulum stress-associated inflammation and insulin resistance in skeletal muscle cells through an AMPK-dependent mechanism." *Diabetologia* vol. 57,10 (2014): 2126-35. doi:10.1007/s00125-014-3331-8

Salvadó, Laia et al. "Targeting endoplasmic reticulum stress in insulin resistance." *Trends in endocrinology and metabolism: TEM* vol. 26,8 (2015): 438-48. doi:10.1016/j.tem.2015.05.007

Salva-Pastor, Nicolás et al. “The diagnostic and initial approach of the patient with non-alcoholic fatty liver disease: role of the primary care provider.” *Gastroenterology and hepatology from bed to bench* vol. 12,4 (2019): 267-277.

Salvoza, Noel et al. “The potential role of omentin-1 in obesity-related metabolic dysfunction-associated steatotic liver disease: evidence from translational studies.” *Journal of translational medicine* vol. 21,1 906. 11 Dec. 2023, doi:10.1186/s12967-023-04770-8

Santos, João Paulo Margiotti Dos et al. “Non-Alcoholic Steatohepatitis (NASH) and Organokines: What Is Now and What Will Be in the Future.” *International journal of molecular sciences* vol. 23,1 498. 2 Jan. 2022, doi:10.3390/ijms23010498

Sawada, Keisuke et al. “The bidirectional immune crosstalk in metabolic dysfunction-associated steatotic liver disease.” *Cell metabolism* vol. 35,11 (2023): 1852-1871. doi:10.1016/j.cmet.2023.10.009

Scheuner, D., Vander Mierde, D., Song, B., Flamez, D., Creemers, J.W., Tsukamoto, K., Ribick,M., Schuit, F.C., and Kaufman, R.J. (2005). Control of mRNA translation preserves endoplasmic reticulum function in beta cells and maintains glucose homeostasis. Nature medicine *11*, 757-764.

Schilcher, Katharina et al. “Saturated Fat-Mediated Upregulation of IL-32 and CCL20 in Hepatocytes Contributes to Higher Expression of These Fibrosis-Driving Molecules in MASLD.” *International journal of molecular sciences* vol. 24,17 13222. 25 Aug. 2023, doi:10.3390/ijms241713222

Schmitz-Peiffer, C., and Biden, T.J. (2008). Protein kinase C function in muscle, liver, and beta-cells and its therapeutic implications for type 2 diabetes. Diabetes *57*, 1774-1783.

Schröder, M., and Kaufman, R.J. (2005). The mammalian unfolded protein response. Annual review of biochemistry *74*, 739-789.

Schuck, Robert N et al. “The cytochrome P450 epoxygenase pathway regulates the hepatic inflammatory response in fatty liver disease.” *PloS one* vol. 9,10 e110162. 13 Oct. 2014, doi: 10.1371/journal.pone.0110162

Schüler, Rita et al. “VEGF and GLUT1 are highly heritable, inversely correlated and affected by dietary fat intake: Consequences for cognitive function in humans.” *Molecular metabolism* vol. 11 (2018): 129-136. doi:10.1016/j.molmet.2018.02.004

Schuster, Susanne et al. “Triggering and resolution of inflammation in NASH.” *Nature reviews. Gastroenterology & hepatology* vol. 15,6 (2018): 349-364. doi:10.1038/s41575-018-0009-6

Schwartz, Brian E et al. “Discovery and Targeting of the Signaling Controls of *PNPLA3* to Effectively Reduce Transcription, Expression, and Function in Pre-Clinical NAFLD/NASH Settings.” *Cells* vol. 9,10 2247. 7 Oct. 2020, doi:10.3390/cells9102247

Schwartz, Brian E et al. “Discovery and Targeting of the Signaling Controls of *PNPLA3* to Effectively Reduce Transcription, Expression, and Function in Pre-Clinical NAFLD/NASH Settings.” *Cells* vol. 9,10 2247. 7 Oct. 2020, doi:10.3390/cells9102247

Schwertheim, Suzan et al. “Higher pNRF2, SOCS3, IRF3, and RIG1 Tissue Protein Expression in NASH Patients versus NAFL Patients: pNRF2 Expression Is Concomitantly Associated with Elevated Fasting Glucose Levels.” *Journal of personalized medicine* vol. 13,7 1152. 18 Jul. 2023, doi:10.3390/jpm13071152

Serrano-Marco, L et al. “The peroxisome proliferator-activated receptor (PPAR) β/δ agonist GW501516 inhibits IL-6-induced signal transducer and activator of transcription 3 (STAT3) activation and insulin resistance in human liver cells.” *Diabetologia* vol. 55,3 (2012): 743-51. doi:10.1007/s00125-011-2401-4

Sharma, Ankita et al. “AMP-activated protein kinase: An energy sensor and survival mechanism in the reinstatement of metabolic homeostasis.” *Experimental cell research* vol. 428,1 (2023): 113614. doi:10.1016/j.yexcr.2023.113614

Sharma, Ashish. and Shivaraj Nagalli. “Chronic Liver Disease.” *StatPearls*, StatPearls Publishing, 3 July 2023.

Sharma, Priyanka et al. “Reactive oxygen species (ROS)-mediated oxidative stress in chronic liver diseases and its mitigation by medicinal plants.” *American journal of translational research* vol. 15,11 6321-6341. 15 Nov. 2023

Sheka, Adam C et al. “Nonalcoholic Steatohepatitis: A Review.” *JAMA* vol. 323,12 (2020): 1175-1183. doi:10.1001/jama.2020.2298

Shen, Hao et al. “Hepatocyte-derived VEGFA accelerates the progression of non-alcoholic fatty liver disease to hepatocellular carcinoma via activating hepatic stellate cells.” *Acta pharmacologica Sinica* vol. 43,11 (2022): 2917-2928. doi:10.1038/s41401-022-00907-5

Shen, Katie et al. “Therapies for non-alcoholic fatty liver disease: A 2022 update.” *World journal of hepatology* vol. 14,9 (2022): 1718-1729. doi:10.4254/wjh.v14.i9.1718

Shin, Soyeon et al. “Mitochondrial Quality Control: Its Role in Metabolic Dysfunction-Associated Steatotic Liver Disease (MASLD).” *Journal of obesity &*

metabolic syndrome, 10.7570/jomes23054. 5 Dec. 2023, doi:10.7570/jomes23054

Shoelson, Steven E et al. "Inflammation and insulin resistance." *The Journal of clinical investigation* vol. 116,7 (2006): 1793-801. doi:10.1172/JCI29069

Shrestha, Ayush et al. "Soluble epoxide hydrolase inhibitor, t-TUCB, protects against myocardial ischaemic injury in rats." *The Journal of pharmacy and pharmacology* vol. 66,9 (2014): 1251-8. doi:10.1111/jphp.12251

Simon, Tracey G et al. "Incident cardiac arrhythmias associated with metabolic dysfunction-associated steatotic liver disease: a nationwide histology cohort study." Cardiovascular diabetology vol. 22,1 343. 13 Dec. 2023, doi:10.1186/s12933-023-02070-5

Simpson, Luke M et al. "Target protein localization and its impact on PROTAC-mediated degradation." *Cell chemical biology* vol. 29,10 (2022): 1482-1504.e7. doi:10.1016/j.chembiol.2022.08.004

Singuru, Gajalakshmi et al. "Therapeutic efficacy of mitochondria-targeted esculetin in the improvement of NAFLD-NASH via modulating AMPK-SIRT1 axis." *International immunopharmacology* vol. 124,Pt B (2023): 111070. doi:10.1016/j.intimp.2023.111070

Smagris, Eriks et al. "Pnpla3I148M knockin mice accumulate PNPLA3 on lipid droplets and develop hepatic steatosis." *Hepatology (Baltimore, Md.)* vol. 61,1 (2015): 108-18. doi:10.1002/hep.27242

Smith, Erin Vanessa LaRae et al. "Maternal Fructose Intake, Programmed Mitochondrial Function and Predisposition to Adult Disease." *International journal of molecular sciences* vol. 23,20 12215. 13 Oct. 2022, doi:10.3390/ijms232012215

Smith, Gordon I et al. "Insulin resistance drives hepatic de novo lipogenesis in nonalcoholic fatty liver disease." *The Journal of clinical investigation* vol. 130,3 (2020): 1453-1460. doi:10.1172/JCI134165

Song, Aqian et al. "GLUT5: structure, functions, diseases and potential applications." *Acta biochimica et biophysica Sinica* vol. 55,10 (2023): 1519-1538. doi:10.3724/abbs.2023158

Song, Lin et al. "Pterostilbene prevents hepatocyte epithelial-mesenchymal transition in fructose-induced liver fibrosis through suppressing miR-34a/Sirt1/p53 and TGF-β1/Smads signalling." *British journal of pharmacology* vol. 176,11 (2019): 1619-1634. doi:10.1111/bph.14573

Song, Myeong Jun, and Harmeet Malhi. "The unfolded protein response and hepatic lipid metabolism in non alcoholic fatty liver disease." *Pharmacology &*

therapeutics vol. 203 (2019): 107401. doi:10.1016/j.pharmthera.2019.107401

Stauffer, Winston T et al. "The ER Unfolded Protein Response Effector, ATF6, Reduces Cardiac Fibrosis and Decreases Activation of Cardiac Fibroblasts." *International journal of molecular sciences* vol. 21,4 1373. 18 Feb. 2020, doi:10.3390/ijms21041373

Steatohepatitis (NASH): A Systematic Review." *International journal of molecular sciences* vol. 23,15 8805. 8 Aug. 2022, doi:10.3390/ijms23158805

Strey, Cláudia B M et al. "Impact of Diabetes Mellitus and Insulin on Nonalcoholic Fatty Liver Disease in the Morbidly Obese." *Annals of hepatology* vol. 17,4 (2018): 585-591. doi:10.5604/01.3001.0012.0922

Sun, Cheng-Peng et al. "Discovery of Soluble Epoxide Hydrolase Inhibitors from Chemical Synthesis and Natural Products." *Journal of medicinal chemistry* vol. 64,1 (2021): 184-215. doi: 10.1021/acs.jmedchem.0c01507

Sun, Shao-Cong. "The non-canonical NF-κB pathway in immunity and inflammation." *Nature reviews. Immunology* vol. 17,9 (2017): 545-558. doi:10.1038/nri.2017.52

Tak, Eunyoung et al. "Protective role of hypoxia-inducible factor-1α-dependent CD39 and CD73 in fulminant acute liver failure." *Toxicology and applied pharmacology* vol. 314 (2017): 72-81. doi:10.1016/j.taap.2016.11.016

Takahashi, Sadao. "Triglyceride Rich Lipoprotein -LPL-VLDL Receptor and Lp(a)-VLDL Receptor Pathways for Macrophage Foam Cell Formation." *Journal of atherosclerosis and thrombosis* vol. 24,6 (2017): 552-559. doi:10.5551/jat.RV17004

Takaki, Akinobu et al. "Molecular mechanisms and new treatment strategies for non-alcoholic steatohepatitis (NASH)." *International journal of molecular sciences* vol. 15,5 7352-79. 29 Apr. 2014, doi:10.3390/ijms15057352

Takazawa, Takeshi et al. "Peroxisome proliferator-activated receptor gamma agonist rosiglitazone increases expression of very low density lipoprotein receptor gene in adipocytes." *The Journal of biological chemistry* vol. 284,44 (2009): 30049-57. doi:10.1074/jbc.M109.047993

Takeuchi, Tadashi et al. "Gut microbial carbohydrate metabolism contributes to insulin resistance." *Nature* vol. 621,7978 (2023): 389-395. doi:10.1038/s41586-023-06466-x

Tan, Darren Jun Hao et al. "Clinical characteristics, surveillance, treatment allocation, and outcomes of non-alcoholic fatty liver disease-related

hepatocellular carcinoma: a systematic review and meta-analysis." *The Lancet. Oncology* vol. 23,4 (2022): 521-530. doi:10.1016/S1470-2045(22)00078-X

Tanase, Daniela Maria et al. "The Intricate Relationship between Type 2 Diabetes Mellitus (T2DM), Insulin Resistance (IR), and Nonalcoholic Fatty Liver Disease (NAFLD)." *Journal of diabetes research* vol. 2020 3920196. 31 Jul. 2020, doi:10.1155/2020/3920196

Taniguchi, C.M., Emanuelli, B., and Kahn, C.R. (2006). Critical nodes in signalling

Targher, Giovanni et al. "MASLD: a systemic metabolic disorder with cardiovascular and malignant complications." *Gut*, gutjnl-2023-330595. 16 Jan. 2024, doi:10.1136/gutjnl-2023-330595

Targher, Giovanni et al. "The complex link between NAFLD and type 2 diabetes mellitus - mechanisms and treatments." *Nature reviews. Gastroenterology & hepatology* vol. 18,9 (2021): 599-612. doi:10.1038/s41575-021-00448-y

Teske, Brian F et al. "The eIF2 kinase PERK and the integrated stress response facilitate activation of ATF6 during endoplasmic reticulum stress." *Molecular biology of the cell* vol. 22,22 (2011): 4390-405. doi:10.1091/mbc. E11-06-0510

Tian, Jing et al. "JianPi-QingHua formula attenuates nonalcoholic fatty liver disease by regulating the AMPK/SIRT1/NF-κB pathway in high-fat-diet-fed C57BL/6 mice." *Pharmaceutical biology* vol. 61,1 (2023): 647-656. doi:10.1080/13880209.2023.2188549

Tincopa, Monica A, and Rohit Loomba. "Non-invasive diagnosis and monitoring of non-alcoholic fatty liver disease and non-alcoholic steatohepatitis." *The lancet. Gastroenterology & hepatology* vol. 8,7 (2023): 660-670. doi:10.1016/S2468-1253(23)00066-3

Tokushige, Katsutoshi, et al. "Evidence-based clinical practice guidelines for nonalcoholic fatty liver disease/nonalcoholic steatohepatitis 2020." Journal of Gastroenterology 56.11 (2021): 951-963.

Torres, Sandra et al. "The Specific NLRP3 Antagonist IFM-514 Decreases Fibrosis and Inflammation in Experimental Murine Non-Alcoholic Steatohepatitis." *Frontiers in molecular biosciences* vol. 8 715765. 13 Aug. 2021, doi:10.3389/fmolb.2021.715765

Tsankof, Alexandra et al. "Which is the optimal antiobesity agent for patients with nonalcoholic fatty liver disease?." *Frontiers in endocrinology* vol. 13 984041. 2 Sep. 2022, doi:10.3389/fendo.2022.984041

Tshivhase, Abegail Mukhethwa et al. "Resveratrol attenuates high glucose-induced inflammation and improves glucose metabolism in HepG2

cells." *Scientific reports* vol. 14,1 1106. 11 Jan. 2024, doi:10.1038/s41598-023-50084-6

Tsuchida, T. and Friedman, S.L. (2017) Mechanisms of hepatic stellate cell activation. Nat. Rev. Gastroenterol. Hepatol. 14,397–411

Ueki, K., Kondo, T., and Kahn, C.R. (2004). Suppressor of cytokine signaling 1 (SOCS-1) and SOCS-3 cause insulin resistance through inhibition of tyrosine phosphorylation of insulin receptor substrate proteins by discrete mechanisms. Molecular and cellular biology *24*, 5434-5446.

Utzschneider, Kristina M et al. "Hepatic Insulin Extraction in NAFLD Is Related to Insulin Resistance Rather Than Liver Fat Content." *The Journal of clinical endocrinology and metabolism* vol. 104,5 (2019): 1855-1865. doi:10.1210/jc.2018-01808

Vallée, Déborah et al. "La réponse au stress du réticulum endoplasmique dans la physiopathologie des maladies chroniques du foie" [Endoplasmic reticulum stress response and pathogenesis of non-alcoholic steatohepatitis]. *Medecine sciences : M/S* vol. 36,2 (2020): 119-129.

van Dierendonck, Xanthe AMH, et al. "Triglyceride breakdown from lipid droplets regulates the inflammatory response in macrophages." *Proceedings of the National Academy of Sciences* 119.12 (2022): e2114739119.

Vasudevan, Deepika et al. "Translational induction of ATF4 during integrated stress response requires noncanonical initiation factors eIF2D and DENR." *Nature communications* vol. 11,1 4677. 16 Sep. 2020, doi:10.1038/s41467-020-18453-1

Vaziri, H et al. "hSIR2(SIRT1) functions as an NAD-dependent p53 deacetylase." *Cell* vol. 107,2 (2001): 149-59. doi:10.1016/s0092-8674(01)00527-x

Vázquez-Carrera, M. (2014). PPARβ/δ prevents endoplasmic reticulum stress-associated inflammation and insulin resistance in skeletal muscle cells through an AMPK-dependent mechanism. Diabetologia *57*, 2126-2135.

Villalobos-Labra, Roberto et al. "Endoplasmic reticulum stress and development of insulin resistance in adipose, skeletal, liver, and foetoplacental tissue in diabesity." *Molecular aspects of medicine* vol. 66 (2019): 49-61. doi:10.1016/j.mam.2018.11.001

Villalva, Marisol et al. "Polyphenols as NLRP3 inflammasome modulators in cardiometabolic diseases: a review of *in vivo* studies." *Food & function* vol. 14,21 9534-9553. 30 Oct. 2023, doi:10.1039/d3fo03015f

Viollet, Benoit et al. “Activation of AMP-activated protein kinase in the liver: a new strategy for the management of metabolic hepatic disorders.” *The Journal of physiology* vol. 574,Pt 1 (2006): 41-53. doi:10.1113/jphysiol.2006.108506

Wagner, Karen M et al. “Soluble epoxide hydrolase as a therapeutic target for pain, inflammatory and neurodegenerative diseases.” *Pharmacology & therapeutics* vol. 180 (2017): 62-76. doi: 10.1016/j.pharmthera.2017.06.006

Walter, Franziska et al. “ER stress signaling has an activating transcription factor 6α (ATF6)-dependent "off-switch".” *The Journal of biological chemistry* vol. 293,47 (2018): 18270-18284. doi:10.1074/jbc.RA118.002121

Wan, Xingyong et al. “Role of NLRP3 Inflammasome in the Progression of NAFLD to NASH.” *Canadian journal of gastroenterology & hepatology* vol. 2016 (2016): 6489012. doi:10.1155/2016/6489012

Wang, Bei et al. “Metabolism pathways of arachidonic acids: mechanisms and potential therapeutic targets.” *Signal transduction and targeted therapy* vol. 6,1 94. 26 Feb. 2021, doi:10.1038/s41392-020-00443-w

Wang, Doudou et al. “Targeting AMPK Signaling in the Liver: Implications for Obesity and Type 2 Diabetes Mellitus.” *Current drug targets* vol. 23,11 (2022): 1057-1071. doi:10.2174/1389450123666220429082702

Wang, Feixue et al. “Activated Natural Killer Cell Promotes Nonalcoholic Steatohepatitis Through Mediating JAK/STAT Pathway.” *Cellular and molecular gastroenterology and hepatology* vol. 13,1 (2022): 257-274. doi:10.1016/j.jcmgh.2021.08.019

Wang, Haojie et al. “The Upstream Pathway of mTOR-Mediated Autophagy in Liver Diseases.” *Cells* vol. 8,12 1597. 9 Dec. 2019, doi:10.3390/cells8121597

Wang, Hua et al. “Immunological mechanisms and therapeutic targets of fatty liver diseases.” *Cellular & molecular immunology* vol. 18,1 (2021): 73-91. doi:10.1038/s41423-020-00579-3

Wang, Kang et al. “FXR agonists for MASH therapy: Lessons and perspectives from obeticholic acid.” *Medicinal research reviews*, 10.1002/med.21991. 30 Oct. 2023, doi:10.1002/med.21991

Wang, Luyun et al. “Soluble epoxide hydrolase deficiency attenuates lipotoxic cardiomyopathy via upregulation of AMPK-mTORC mediated autophagy.” *Journal of molecular and cellular cardiology* vol. 154 (2021): 80-91. doi:10.1016/j.yjmcc.2020.12.013

Wang, Qi et al. “AMPK-Mediated Regulation of Lipid Metabolism by Phosphorylation.” *Biological & pharmaceutical bulletin* vol. 41,7 (2018): 985-993. doi:10.1248/bpb.b17-00724

Wang, Sheng et al. “The role of the CD39-CD73-adenosine pathway in liver disease.” *Journal of cellular physiology* vol. 236,2 (2021): 851-862. doi:10.1002/jcp.29932

Wang, Tong-Hao et al. “Association of TNF-α, IGF-1, and IGFBP-1 levels with the severity of osteopenia in mice with nonalcoholic fatty liver disease.” *Journal of orthopaedic surgery and research* vol. 18,1 915. 1 Dec. 2023, doi:10.1186/s13018-023-04385-1

Wang, Xi et al. “Blocking the JAK2/STAT3 and ERK pathways suppresses the proliferation of gastrointestinal cancers by inducing apoptosis.” *Journal of Zhejiang University. Science. B* vol. 22,6 (2021): 492-503. doi:10.1631/jzus.B2000842

Wang, Xiaojing et al. “Macrophage-Specific Hypoxia-Inducible Factor-1α Contributes to Impaired Autophagic Flux in Nonalcoholic Steatohepatitis.” *Hepatology (Baltimore, Md.)* vol. 69,2 (2019): 545-563. doi:10.1002/hep.30215

Wang, Yuxin et al. “PROTAC-Mediated Selective Degradation of Cytosolic Soluble Epoxide Hydrolase Enhances ER Stress Reduction.” *ACS chemical biology* vol. 18,4 (2023): 884-896. doi:10.1021/acschembio.3c00017

Wang, Zhigang et al. “Nuclear factor (erythroid-derived 2)-like 2 activation-induced hepatic very-low-density lipoprotein receptor overexpression in response to oxidative stress contributes to alcoholic liver disease in mice.” *Hepatology (Baltimore, Md.)* vol. 59,4 (2014): 1381-92. doi:10.1002/hep.26912

Wasilewska, Natalia, and Dariusz Marek Lebensztejn. “Non-alcoholic fatty liver disease and lipotoxicity.” *Clinical and experimental hepatology* vol. 7,1 (2021): 1-6. doi:10.5114/ceh.2021.104441

Webb, J C et al. “Characterization and tissue-specific expression of the human 'very low density lipoprotein (VLDL) receptor' mRNA.” *Human molecular genetics* vol. 3,4 (1994): 531-7. doi:10.1093/hmg/3.4.531

Welsh, Sarah et al. “Antitumor activity and pharmacodynamic properties of PX-478, an inhibitor of hypoxia-inducible factor-1alpha.” *Molecular cancer therapeutics* vol. 3,3 (2004): 233-44.

Weng, Gong, and Winston Dunn. “Effect of alcohol consumption on nonalcoholic fatty liver disease.” *Translational gastroenterology and hepatology* vol. 4 70. 17 Sep. 2019, doi:10.21037/tgh.2019.09.02

Wiering, Leke et al. “Hepatic Stellate Cells: Dictating Outcome in Nonalcoholic Fatty Liver Disease.” *Cellular and molecular gastroenterology and hepatology* vol. 15,6 (2023): 1277-1292. doi:10.1016/j.jcmgh.2023.02.010

Wieser, Verena et al. “Inflammation, cytokines and insulin resistance: a clinical perspective.” *Archivum immunologiae et therapiae experimentalis* vol. 61,2 (2013): 119-25. doi:10.1007/s00005-012-0210-1

Wilson, Claire H, and Sharad Kumar. “Caspases in metabolic disease and their therapeutic potential.” *Cell death and differentiation* vol. 25,6 (2018): 1010-1024. doi:10.1038/s41418-018-0111-x

Wree, Alexander et al. “NLRP3 inflammasome activation is required for fibrosis development in NAFLD.” *Journal of molecular medicine (Berlin, Germany)* vol. 92,10 (2014): 1069-82. doi:10.1007/s00109-014-1170-1

Wu, H et al. “Peroxisome proliferator-activated receptor gamma in white and brown adipocyte regulation and differentiation.” *Physiological research* vol. 69,5 (2020): 759-773. doi:10.33549/physiolres.934411

Wu, Tao et al. “Direct evidence of sirtuin downregulation in the liver of non-alcoholic fatty liver disease patients.” *Annals of clinical and laboratory science* vol. 44,4 (2014): 410-8.

Wu, Zhenhua et al. “Induction of Liver Steatosis in BAP31-Deficient Mice Burdened with Tunicamycin-Induced Endoplasmic Reticulum Stress.” *International journal of molecular sciences* vol. 19,8 2291. 4 Aug. 2018, doi:10.3390/ijms19082291

Xia, Si-Wei et al. “Endoplasmic reticulum stress and protein degradation in chronic liver disease.” *Pharmacological research* vol. 161 (2020): 105218. doi:10.1016/j.phrs.2020.105218

Xian, Ying-Xin et al. “MAFLD vs. NAFLD: shared features and potential changes in epidemiology, pathophysiology, diagnosis, and pharmacotherapy.” *Chinese medical journal* vol. 134,1 8-19. 14 Dec. 2020, doi:10.1097/CM9.0000000000001263

Xin, Xiaofei et al. “ROS-scavenging nanomedicine for "multiple crosstalk" modulation in non-alcoholic fatty liver disease.” *Biomaterials science* vol. 11,10 3709-3725. 16 May. 2023, doi:10.1039/d2bm02161g

Xu, Fen et al. “Lack of SIRT1 (Mammalian Sirtuin 1) activity leads to liver steatosis in the SIRT1+/- mice: a role of lipid mobilization and inflammation.” *Endocrinology* vol. 151,6 (2010): 2504-14. doi:10.1210/en.2009-1013

Xu, Xuan et al. “Phosphorylation of NF-κBp65 drives inflammation-mediated hepatocellular carcinogenesis and is a novel therapeutic target.” *Journal of*

experimental & clinical cancer research : CR vol. 40,1 253. 11 Aug. 2021, doi:10.1186/s13046-021-02062-x

Xue, Wan-Ying et al. “Research progress on the relationship between TM6SF2 rs58542926 polymorphism and non-alcoholic fatty liver disease.” *Expert review of gastroenterology & hepatology* vol. 16,2 (2022): 97-107. doi:10.1080/17474124.2022.2032661

Yamazaki, Yu et al. “Treatment with SRT1720, a SIRT1 activator, ameliorates fatty liver with reduced expression of lipogenic enzymes in MSG mice.” *American journal of physiology. Endocrinology and metabolism* vol. 297,5 (2009): E1179-86. doi:10.1152/ajpendo.90997.2008

Yan, Jiawei, and Tiffany Horng. "Lipid metabolism in regulation of macrophage functions." *Trends in cell biology* 30.12 (2020): 979-989.

Yanai, Hidekatsu et al. “Metabolic-Dysfunction-Associated Steatotic Liver Disease-Its Pathophysiology, Association with Atherosclerosis and Cardiovascular Disease, and Treatments.” *International journal of molecular sciences* vol. 24,20 15473. 23 Oct. 2023, doi:10.3390/ijms242015473

Yang, Aruhan et al. “Transitioning from NAFLD to MAFLD and MASLD: Consistent prevalence and risk factors in a Chinese cohort.” *Journal of hepatology*, S0168-8278(23)05161-9. 10 Oct. 2023, doi:10.1016/j.jhep.2023.09.033

Yang, Fan et al. “Restraint stress promotes nonalcoholic steatohepatitis by regulating the farnesoid X receptor/NLRP3 signaling pathway.” *Acta biochimica et biophysica Sinica* vol. 55,12 (2023): 1961-1971. doi:10.3724/abbs.2023240

Yang, Hongying et al. “SIRT1 activators suppress inflammatory responses through promotion of p65 deacetylation and inhibition of NF-κB activity.” *PloS one* vol. 7,9 (2012): e46364. doi:10.1371/journal.pone.0046364

Yang, Jinchunzi et al. “Effects of Long-Term DHA Supplementation and Physical Exercise on Non-Alcoholic Fatty Liver Development in Obese Aged Female Mice.” *Nutrients* vol. 13,2 501. 3 Feb. 2021, doi:10.3390/nu13020501

Yang, Yuan et al. “Transcription Factor C/EBP Homologous Protein in Health and Diseases.” *Frontiers in immunology* vol. 8 1612. 27 Nov. 2017, doi:10.3389/fimmu.2017.01612

Yang, Yunshu et al. “Regulation of SIRT1 and Its Roles in Inflammation.” *Frontiers in immunology* vol. 13 831168. 11 Mar. 2022, doi:10.3389/fimmu.2022.831168

Yao, Pengyu, and Yajuan Liu. “Terpenoids: Natural Compounds for Non-Alcoholic Fatty Liver Disease (NAFLD) Therapy.” *Molecules (Basel, Switzerland)* vol. 28,1 272. 29 Dec. 2022, doi:10.3390/molecules28010272

Yekollu, S.K., Thomas, R., and O'Sullivan, B. (2011). Targeting curcusomes to inflammatory dendritic cells inhibits NF-κB and improves insulin resistance in obese mice. Diabetes *60*,2928-2938.

Yin, Huquan et al. “Deletion of SIRT1 from hepatocytes in mice disrupts lipin-1 signaling and aggravates alcoholic fatty liver.” *Gastroenterology* vol. 146,3 (2014): 801-11. doi:10.1053/j.gastro.2013.11.008

Yong, Jing, et al. "Therapeutic opportunities for pancreatic β-cell ER stress in diabetes mellitus." *Nature Reviews Endocrinology* 17.8 (2021): 455-467.

Yoo, Wonbaek et al. “HIF-1α expression as a protective strategy of HepG2 cells against fatty acid-induced toxicity.” *Journal of cellular biochemistry* vol. 115,6 (2014): 1147-58. doi:10.1002/jcb.24757

Younossi, Zobair M et al. “The global epidemiology of nonalcoholic fatty liver disease (NAFLD) and nonalcoholic steatohepatitis (NASH): a systematic review.” *Hepatology (Baltimore, Md.)* vol. 77,4 (2023): 1335-1347. doi:10.1097/HEP.0000000000000004

Younossi, Zobair M. “The epidemiology of nonalcoholic steatohepatitis.” *Clinical liver disease* vol. 11,4 92-94. 20 Apr. 2018, doi:10.1002/cld.710

Younossi, Zobair M., et al. "Global epidemiology of nonalcoholic fatty liver disease—meta-analytic assessment of prevalence, incidence, and outcomes." *Hepatology* 64.1 (2016): 73-84.

Younossi, Zobair, et al. "Global burden of NAFLD and NASH: trends, predictions, risk factors and prevention." *Nature reviews Gastroenterology & hepatology* 15.1 (2018): 11-20.

Yun, Chawon et al. “Doxorubicin Attenuates Free Fatty Acid-Induced Lipid Accumulation via Stimulation of p53 in HepG2 Cells.” *Biomolecules & therapeutics* vol. 32,1 (2024): 94-103. doi:10.4062/biomolther.2023.200

Žáček, Petr et al. “Dietary saturated fatty acid type impacts obesity-induced metabolic dysfunction and plasma lipidomic signatures in mice.” *The Journal of nutritional biochemistry* vol. 64 (2019): 32-44. doi:10.1016/j.jnutbio.2018.10.005

Zand, Hamid et al. “Signaling pathways linking inflammation to insulin resistance.” *Diabetes & metabolic syndrome* vol. 11 Suppl 1 (2017): S307-S309. doi: 10.1016/j.dsx.2017.03.006

Zarei, Mohammad et al. “Hepatic regulation of VLDL receptor by PPARβ/δ and FGF21 modulates non-alcoholic fatty liver disease.” *Molecular metabolism* vol. 8 (2018): 117-131. doi:10.1016/j.molmet.2017.12.008

Zarei, Mohammad et al. “Targeting FGF21 for the Treatment of Nonalcoholic Steatohepatitis.” Trends in pharmacological sciences vol. 41,3 (2020): 199-208. doi:10.1016/j.tips.2019.12.005

Zhang, Chen-Song et al. “Metformin Activates AMPK through the Lysosomal Pathway.” *Cell metabolism* vol. 24,4 (2016): 521-522. doi:10.1016/j.cmet.2016.09.003

Zhang, Jianan et al. “Soluble epoxide hydrolase as a therapeutic target for obesity-induced disorders: roles of gut barrier function involved.” *Prostaglandins, leukotrienes, and essential fatty acids* vol. 162 (2020): 102180. doi:10.1016/j.plefa.2020.102180

Zhang, L., Chen, Z., Wang, Y., Tweardy, D.J., and Mitch, W.E. (2020a). Stat3 activation

Zhang, R., Liu, S., Guo, B., Chang, L., and Li, Y. (2014a). Chemerin induces insulin resistance in rat cardiomyocytes in part through the ERK1/2 signaling pathway. Pharmacology *94*, 259-264.

Zhang, Shumin et al. “Dietary fiber-derived short-chain fatty acids: A potential therapeutic target to alleviate obesity-related nonalcoholic fatty liver disease.” *Obesity reviews : an official journal of the International Association for the Study of Obesity* vol. 22,11 (2021): e13316. doi:10.1111/obr.13316

Zhang, Wenyan et al. “Exosome GLUT1 derived from hepatocyte identifies the risk of non-alcoholic steatohepatitis and fibrosis.” *Hepatology international* vol. 17,5 (2023): 1170-1181. doi:10.1007/s12072-023-10520-1

Zhao, Huimin et al. “Association Between Dietary Fiber Intake and Non-alcoholic Fatty Liver Disease in Adults.” *Frontiers in nutrition* vol. 7 593735. 19 Nov. 2020, doi:10.3389/fnut.2020.593735

Zhao, Jianhong et al. “p53 promotes peroxisomal fatty acid β-oxidation to repress purine biosynthesis and mediate tumor suppression.” *Cell death & disease* vol. 14,2 87. 7 Feb. 2023, doi:10.1038/s41419-023-05625-2

Zhao, Jie et al. “STAT3: A key regulator in liver fibrosis.” *Annals of hepatology* vol. 21 (2021): 100224. doi:10.1016/j.aohep.2020.06.010

Zhao, Peng et al. “An AMPK-caspase-6 axis controls liver damage in nonalcoholic steatohepatitis.” *Science (New York, N.Y.)* vol. 367,6478 (2020): 652-660. doi:10.1126/science.aay0542

Zheng, Youwei et al. “Mitochondrial metabolic dysfunction and non-alcoholic fatty liver disease: new insights from pathogenic mechanisms to clinically

targeted therapy." *Journal of translational medicine* vol. 21,1 510. 28 Jul. 2023, doi:10.1186/s12967-023-04367-1

Zhou, Lijun et al. "Autophagy-mediated insulin receptor down-regulation contributes to endoplasmic reticulum stress-induced insulin resistance." *Molecular pharmacology* vol. 76,3 (2009): 596-603. doi:10.1124/mol.109.057067

Zhou, Zhou et al. "Intestinal SIRT1 Deficiency Protects Mice from Ethanol-Induced Liver Injury by Mitigating Ferroptosis." *The American journal of pathology* vol. 190,1 (2020): 82-92. doi:10.1016/j.ajpath.2019.09.012

Zhu, Xiaopeng et al. "Update on genetics and epigenetics in metabolic associated fatty liver disease." *Therapeutic advances in endocrinology and metabolism* vol. 13 20420188221132138. 28 Oct. 2022, doi:10.1177/20420188221132138

Zhu, Yu et al. "Dietary fiber intake and non-alcoholic fatty liver disease: The mediating role of obesity." *Frontiers in public health* vol. 10 1038435. 6 Jan. 2023, doi:10.3389/fpubh.2022.1038435

Ziolkowska, Sylwia et al. "The Interplay between Insulin Resistance, Inflammation, Oxidative Stress, Base Excision Repair and Metabolic Syndrome in Nonalcoholic Fatty Liver Disease." *International journal of molecular sciences* vol. 22,20 11128. 15 Oct. 2021, doi:10.3390/ijms222011128

Zordoky, B. N., & El-Kadi, A. O. (2010). Effect of cytochrome P450 polymorphism on arachidonic acid metabolism and their impact on cardiovascular diseases. *Pharmacology & therapeutics*, *125*(3), 446-463.

Biomedicine & Pharmacotherapy 168 (2023) 115667

Contents lists available at ScienceDirect

Biomedicine & Pharmacotherapy

journal homepage: www.elsevier.com/locate/biopha

Soluble epoxide hydrolase-targeting PROTAC activates AMPK and inhibits endoplasmic reticulum stress

Mona Peyman [a,b,c,d,1], Emma Barroso [a,b,c,d,1], Andreea L. Turcu [b,e], Francesc Estrany Jr. [a,b,c,d], Dáire Smith [a,b,c,d], Javier Jurado-Aguilar [a,b,c,d], Patricia Rada [c,f], Christophe Morisseau [g], Bruce D. Hammock [g], Ángela M. Valverde [c,f], Xavier Palomer [a,b,c,d], Carles Galdeano [b,h], Santiago Vázquez [b,e], Manuel Vázquez-Carrera [a,b,c,d,*]

[a] Department of Pharmacology, Toxicology and Therapeutic Chemistry, Faculty of Pharmacy and Food Sciences, Spain
[b] Institute of Biomedicine of the University of Barcelona (IBUB), University of Barcelona, 08028 Barcelona, Spain
[c] Spanish Biomedical Research Center in Diabetes and Associated Metabolic Diseases (CIBERDEM)-Instituto de Salud Carlos III, 28029 Madrid, Spain
[d] Pediatric Research Institute-Hospital Sant Joan de Déu, 08950 Esplugues de Llobregat, Spain
[e] Laboratori de Química Farmacèutica (Unitat Associada al CSIC), Facultat de Farmàcia i Ciències de l'Alimentació, Universitat de Barcelona, Av. Joan XXIII, 27-31, 08028 Barcelona, Spain
[f] Instituto de Investigaciones Biomédicas Alberto Sols (CSIC/UAM), Madrid, Spain
[g] Department of Entomology and Nematology, and UC Davis Comprehensive Cancer Center, University of California, Davis, CA 95616, United States
[h] Department of Pharmacy and Pharmaceutical Technology and Physical Chemistry, Faculty of Pharmacy and Food Sciences, University of Barcelona, 08028 Barcelona, Spain

ARTICLE INFO

Keywords:
SEH
PROTAC
AMPK
ER stress
Hepatocyte

ABSTRACT

Soluble epoxide hydrolase (sEH) is a drug target with the potential for therapeutic utility in the areas of inflammation, neurodegenerative disease, chronic pain, and diabetes, among others. Proteolysis-targeting chimeras (PROTACs) molecules offer new opportunities for targeting sEH, due to its capacity to induce its degradation. Here, we describe that the new ALT-PG2, a PROTAC that degrades sEH protein in the human hepatic Huh-7 cell line, in isolated mouse primary hepatocytes, and in the liver of mice. Remarkably, sEH degradation caused by ALT-PG2 was accompanied by an increase in the phosphorylated levels of AMP-activated protein kinase (AMPK), while phosphorylated extracellular-signal-regulated kinase 1/2 (ERK1/2) was reduced. Consistent with the key role of these kinases on endoplasmic reticulum (ER) stress, ALT-PG2 attenuated the levels of ER stress and inflammatory markers. Overall, the findings of this study indicate that targeting sEH with degraders is a promising pharmacological strategy to promote AMPK activation and to reduce ER stress and inflammation.

1. Introduction

Proteolysis-targeting chimeras (PROTACs) molecules have changed the landscape for drug discovery and design [1]. PROTACs are bifunctional molecules consisting of a ligand targeting a protein of interest, a ligand recruiting an E3 ligase, and a connecting linker [1]. Compared to classical inhibitors, PROTACs not only inhibit their targets, but also induce their degradation through the ubiquitin-proteasome system. This offers several advantages over merely inhibiting proteins, including the use of lower doses [2], and additional layer of selectivity [3], cumulative efficacy [4], and the potential to degrade undruggable targets and domains [5].

Soluble epoxide hydrolase (sEH) is a bifunctional enzyme with C-terminal hydrolase and N-terminal phosphatase activities [6]. This enzyme is highly expressed in the liver [6], a vital organ with important metabolic, secretory and excretory functions. sEH hydrolase activity converts epoxyeicosatrienoic acids (EETs) and other epoxy fatty acids (EpFAs) to their corresponding diols. The products of hydrolysis of the EETs and other EpFAs are dihydroxyeicosatrienoic acids. These diols are much less bioactive than their parents epoxides. As a result, compounds that inhibit sEH significantly increase levels of EETs and other EpFAs, which are opposing counterparts to the largely pro-inflammatory

* Correspondence to: Unitat de Farmacologia, Facultat de Farmàcia i Ciències de l'Alimentació, Av. Joan XXIII 27–31, E-08028 Barcelona, Spain.
E-mail address: mvazquezcarrera@ub.edu (M. Vázquez-Carrera).
[1] Both authors contributed equally.

https://doi.org/10.1016/j.biopha.2023.115667
Received 26 July 2023; Received in revised form 30 September 2023; Accepted 6 October 2023
Available online 10 October 2023

prostanoids and leukotrienes, providing therapeutic efficacy for the treatment of neurodegenerative diseases, inflammation, chronic pain, cardiovascular disease, pulmonary diseases, and diabetes [7–9]. Many of these chronic diseases are also the result of persistent endoplasmic reticulum (ER) stress due to its potential to elicit aberrant inflammatory signaling and facilitate cell death [10,11]. Thus, targeting ER stress has emerged as a therapeutic strategy for many disorders. ER stress develops in part because of the accumulation of misfolded and unfolded proteins in the ER lumen. This disrupts the homeostasis of this organelle and activates the unfolded protein response (UPR), intended to restore the ER's folding capacity, and mitigate stress [12]. However, if ER homeostasis cannot be restored, inflammation and cell death are induced. Therefore, although the UPR forms part of an acute mechanism to re-establish the cellular homeostasis, when sustained chronically activated this response contributes to disease. The UPR involves the activation of three transmembrane proteins: inositol-requiring enzyme 1 (IRE-1), activating transcription factor 6 (ATF6), and protein kinase R (PKR)-like ER kinase (PERK). The latter phosphorylates the eukaryotic initiation factor (eIF2α) and attenuates protein translation, thereby reducing the number of new proteins entering the ER lumen. If UPR cannot restore ER homeostasis, apoptosis is induced by the PERK-eIF2α pathway and the subsequent increase in ATF4 activity, which upregulates the expression of C/EBP homologous protein (CHOP). Moreover, the three branches of the UPR intersect with a variety of inflammatory and stress signaling systems, including the nuclear factor-κB (NF-κB) pathway [12] or the signal transducer and activator of transcription 3 (STAT3) pathway [13], thereby stimulating inflammation.

Since the liver has a large requirement for protein synthesis and folding, hepatocytes are enriched in ER and, thus, are more susceptible to ER perturbation and ER stress [14]. Excessive ER stress contributes to the development of insulin resistance and type 2 diabetes mellitus [12] and activation of adenosine monophosphate-activated protein kinase (AMPK) has been reported to protect against insulin resistance by reducing ER stress [15,16]. In addition, the presence of an inhibitory crosstalk between AMPK and extracellular-signal-regulated kinase 1/2 (ERK1/2) contributes to the development of ER stress, since inhibition of ERK1/2 was found to improve AMPK pathway and to reverse ER stress-induced insulin resistance [15,16].

In this work, we describe that the sEH-targeting PROTAC ALT-PG2 degrades this protein at low nanomolar concentration in the human hepatoma-derived Huh-7 cell line and in primary mouse hepatocytes. The degradation of the sEH protein in these cells was accompanied by AMPK activation, while phosphorylated ERK1/2 was reduced. Moreover, these changes resulted in a basal reduction of both ER stress and inflammatory markers, whereas an increase was observed in the levels of proteins involved in the insulin signaling pathway. Likewise, ALT-PG2 prevented the increase in ER stress induced by thapsigargin, an ER stressor which induces ER stress by inhibiting SERCA (sarco/endoplasmic reticulum Ca^{2+} ATPase) and, consequently, blocking the calcium entry into the ER lumen. Finally, two intraperitoneal administrations of ALT-PG2 for one single day resulted in rapid and robust degradation of sEH in the liver of mice, as well as the activation of AMPK and the reduction of the phosphorylated levels of ERK1/2. Overall, these findings indicate that targeting sEH with PROTACs leads to the degradation of this protein *in vitro* and *in vivo*, which in turn results in the activation of AMPK and the reduction of ER stress and inflammatory markers.

2. Materials and methods

2.1. General

Commercially available reagents and solvents were used without further purification unless stated otherwise. 400 MHz ^{1}H and 100.6 MHz ^{13}C NMR spectra were recorded on a Bruker 400 Avance III spectrometers. The chemical shifts are reported in ppm (δ scale) relative to internal tetramethylsilane, and coupling constants are reported in Hertz (Hz). High resolution mass spectrometry (HRMS) analyses were performed with an LC/MSD TOF Agilent Technologies spectrometer. HPLC / MS were determined with a HPLC Agilent 1260 Infinity II LC/MSD coupled to a photodiode array and mass spectrometer. Samples (5 μl, 0.5 mg/mL) in a 1:1 mixture of water with 0.05% formic acid (A) and acetonitrile with 0.05% formic acid (B) were injected using an Agilent Poroshell 120 EC-C18 (2.7 μm, 50 mm × 4.6 mm) column at 40 °C. The mobile phase was a mixture of A and B, with a flow 0.6 mL/min, using the following gradients: from 95% A–5% B to 100% B in 3 min; 100% B for 3 min; from 100% B to 95% A–5% B in 1 min; and 95% A–5% B for 3 min. Purity is given as % of absorbance at 254 nm. All compounds that were subjected to pharmacological evaluation are > 95% pure by HPLC.

2.2. Synthesis procedure for PROTAC molecules

Synthesis of ALT-PG2. To a solution of *trans*-4-[4-(3-trifluoromethoxyphenyl-1-ureido)cyclohexyloxy]benzoic acid (*t*-TUCB) (26 mg, 0.055 mmol) in dimethylformamide (DMF) (0.5 mL) was added the recruiter molecule (thalidomide-PEG3-NH_2·HCl, 25 mg, 0.046 mmol), and the solution was stirred at room temperature. N,N-diisopropylethylamine (DIPEA) (24 μl, 0.138 mmol) was added dropwise, and the mixture was stirred for 5 min at room temperature. Hexafluorophosphate azabenzotriazole tetramethyl uronium (HATU) (35 mg, 0.092 mmol) was added, and the mixture was stirred at room temperature overnight. Water was added, and the mixture was extracted with ethyl acetate (3 ×). The combined organic phases were washed with $NaHCO_3$ (twice), dried over anhydrous Na_2SO_4, filtered, and evaporated under reduced pressure to give a crude. Column chromatography [SiO_2, 100% dichloromethane (DCM) to 90% DCM / 10% methanol mixtures] yielded ALT-PG2 (23 mg, 54% yield) as a white solid.

^{1}H-RMN (400 MHz, DMSO-d_6) δ: 1.32 – 1.40 (cs, 2 H), 1.44 – 1.53 (cs, 2 H), 1.91 – 1.95 (cs, 2 H), 2.00 – 2.06 (cs, 3 H), 2.51 – 2.50 (cs, 2 H), 2.89 (ddd, J = 17.6, J'= 13.9, J'' = 5.5 Hz, 1 H), 3.30 (s, 2 H), 3.38 (q, J = 6.0 Hz, 2 H), 3.44 (t, J = 5.6 Hz, 2 H), 3.48–3.50 (cs, 12 H), 4.42 (m, 1 H), 4.78 (s, 2 H), 5.11 (dd, J = 13.2 Hz, J' = 3.6 Hz, 1 H), 6.18 (d, J = 7.4 Hz, 1 H), 6.99 (d, J = 8.8 Hz, 2 H), 7.21 (d, J = 8.4 Hz, 2 H), 7.39 (d, J = 8.4 Hz, 1 H), 7.45–7.50 (cs, 3 H), 7.77–7.82 (cs, 3 H), 8.00 (t, J = 5.6 Hz, 1 H), 8.32 (t, J = 5.6 Hz, 1 H), 8.5 (s, 1 H), 11.11 (brs, 1 H).

^{13}C-RMN (100.6 MHz, DMSO-d_6) δ: 22.0, 29.7, 30.0, 30.9, 38.4, 47.2, 48.8, 67.5, 68.8, 69.0, 69.6, 69.7, 74.1, 114.8, 116.0, 116.8, 118.5, 120.3, 121.6, 126.4, 129.0, 133.0, 136.9, 139.8, 141.9, 154.4, 155.0, 159.7, 165.4, 165.7, 166.7, 166.9, 169.9, 172.8.

HRMS-ESI- m/z [M-]$^-$ calcd for $[C_{44}H_{48}F_3N_6O_{13}]^-$: 925.3237, found: 925.3225.

Synthesis of ALT-PG3. To a solution of *t*-TUCB (22 mg, 0.051 mmol) in DMF (0.5 mL) was added the recruiter molecule (thalidomide-PEG4-NH_2·HCl, 25 mg, 0.043 mmol), and the solution was stirred at room temperature. DIPEA (23 μl, 0.129 mmol) was added dropwise, and the mixture was stirred for 5 min at room temperature. HATU (33 mg, 0.086 mmol) was added, and the mixture was stirred at room temperature overnight. Water was added, and the mixture was extracted with ethyl acetate (3 ×). The combined organic phases were washed with $NaHCO_3$ (twice), dried over anhydrous Na_2SO_4, filtered, and evaporated under reduced pressure to give a crude. Column chromatography (SiO_2, 100% DCM to 90% DCM / 10% methanol mixtures) yielded ALT-PG3 (15 mg, 36% yield) as a white solid which spectroscopic data matched the described in the literature [17].

2.3. In vitro determination of the inhibitory activities toward human and mouse sEH

The *in vitro* inhibitory activity toward human and mouse sEH was determined as previously described [18].

2.4. Animal treatment

Male C57BL/6 mice (10–12 weeks old) were purchased from Envigo (Barcelona, Spain). After an acclimation period of 10 days, mice were randomly distributed into two experimental groups (n = 5 each). One of the groups received one i.p. injection of vehicle (0.9% NaCl containing 5% Kolliphor HS15 (42966, Sigma-Aldrich, St. Louis, MO, USA)) and the other ALT-PG2 (30 mg/kg, i.p., twice a day for 1 day) dissolved in the vehicle. Mice were sacrificed, and liver samples were frozen in liquid nitrogen and then stored at − 80ºC.

Animal experimentation complied with the Guide for the Care and Use of Laboratory Animals published by the US National Institutes of Health (8th edition: National Academies Press; 2011). All procedures were approved by the Bioethics Committee of the University of Barcelona, as stated in Law 5/21 July 1995 passed by the Generalitat de Catalunya. The animals were treated humanely, and all efforts were made to minimize both animal numbers and suffering.

2.5. Cell culture

Human Huh-7 hepatoma cells (kindly donated by Dr. Mayka Sanchez from the Josep Carreras Leukemia Research Institute, Barcelona) were cultured in DMEM supplemented with 10% fetal bovine serum and 1% penicillin-streptomycin, at 37 °C under 5% CO_2.

Primary mouse hepatocytes were isolated from non-fasting male C57BL/6 mice (10–12 weeks old) by perfusion with collagenase as described elsewhere [19]. Compounds ALT-PG2 and ALT-PG3 were dissolved in DMSO.

Huh-7 and mouse primary hepatocytes were exposed to ALT-PG2 for 48 h and co-incubated with vehicle (DMSO) or the ER stressor thapsigargin (1 μM) for the last 24 h.

2.6. Immunoblotting

Isolation of total protein extracts was performed as described elsewhere [20]. Immunoblotting was performed with antibodies against AMPKα (#2532, Cell Signaling Technology, Danvers, MA, USA), phosphorylated AMPK Thr^{172} (#2531, Cell Signaling Technology), β-Actin (A5441, Sigma), CHOP (GTX112827, Genetex, Irvine, CA, USA), eIF2α (#9722, Cell Signalling Technology), phosphorylated eIF2α Ser^{51} (#9721, Cell Signalling Technology); ERK1/2 (44/42 MAPK) (#9102, Cell Signaling Technology), phosphorylated ERK1/2 (44/42 MAPK) Thr^{202}/Tyr^{204} (#9101, Cell Signalling Technology), IRβ (#3025, Cell Signaling Technology), IRS-1 (#2382, Cell Signaling Technology), NF-κB p65 (sc-109, Santa Cruz Biotechnology Inc., Dallas, TX, USA), phosphorylated NF-κB p65 Ser^{536} (#3036 s, Cell Signalling Technology), PP2A (#2259, Cell Signaling Technology), p53 (2524 T, Cell Signaling Technology), sEH (sc-25797, Santa Cruz Biotechnology Inc.), SOCS3 (sc-9023, Santa Cruz Biotechnology Inc.), STAT3 (sc-482X, Santa Cruz Biotechnology Inc.), phosphorylated STAT3 Tyr^{705} (#9131, Cell Signaling Technology), TNF-α (AF410-NA, R&D Systems, Minneapolis, MN, USA), TRB3 (sc-365842, Santa Cruz Biotechnology Inc.), vinculin (sc-25336, Santa Cruz Biotechnology Inc.), VLDLR (AF2258, R&D Systems). Signal acquisition was performed using the Amersham Imager 680 apparatus and quantification of the immunoblot signal was performed with the Bio-Rad Image Lab software. The results for protein quantification were normalized to the levels of a control protein to avoid unwanted sources of variation.

2.7. Statistical analysis

Results are expressed as the mean ± SEM. Significant differences were assessed by either Student's t-test or one-way ANOVA, according to the number of groups compared, using the GraphPad Prism program (version 9.0.2) (GraphPad Software Inc., San Diego, CA, USA). When significant variations were found by ANOVA, Tukey's post-hoc test for multiple comparisons was performed only if F achieved a p value < 0.05. Differences were considered significant at $p < 0.05$.

3. Results

3.1. Synthesis and characterization of the sEH PROTAC ALT-PG2

Two sEH PROTACs were evaluated, ALT-PG2 and ALT-PG3. These compounds consist of the sEH competitive inhibitor *t*-TUCB [21] (Table 1) as binder to the enzyme, while incorporating the thalidomide-based cereblon ligand (as E3 ligase ligand) and two different polyethylene glycol (PEG) linkers. The synthesis of the targeted PROTACs was carried out by a coupling reaction of *t*-TUCB [21] and either thalidomide-PEG3-NH2 for ALT-PG2, or thalidomide-PEG4-NH2 for ALT-PG3, in the presence of HATU and DIPEA in DMF (Table 1). First, we examined the inhibitory activity of these compounds against the human and murine enzymes. Consistent with previous studies [17], and despite the presence of the bulky recruiter linked to the *t*-TUCB unit, the two compounds showed activity in the low nanomolar or even subnanomolar ranges in both the human and murine enzymes (Table 1). As a control, we first examined the effects of different concentrations of the sEH inhibitor *t*-TUCB on the protein levels of sEH in the human hepatoma-derived Huh-7 cell line. As expected, exposure to this compound did not cause sEH degradation (Fig. 1A). In contrast, ALT-PG2 caused a robust degradation of sEH protein levels at concentrations ranging from 1 nM to 1 μM (Fig. 1B). At 1 μM concentration some U-shaped concentration-response curve or hook effect was observed, a known phenomenon in PROTACs [22]. This effect was not observed with ALT-PG3, although it caused a weaker degradation of sEH. Thus, we selected the ALT-PG2 PROTAC at 10 nM for further studies. When we conducted a time-course study, we observed that significant sEH degradation occurred after only 1 h of treatment, but exposure for longer periods (8, 12, and 24 h) provided greater degradation (Fig. 1D). To determine whether ALT-PG2-induced proteasome-mediated degradation, cells were treated with the proteasome inhibitor MG132 prior PROTAC application. Inhibition of proteasome with MG132 completely abrogated the ALT-PG2-mediated degradation of sEH (Fig. 2A), indicating that this degradation depends on the ubiquitin-proteasome system. Moreover, addition of the cereblon ligand lenalidomide effectively rescued the degradation of sEH by ALT-PG2, confirming that it requires the binding of ALT-PG2 to the E3 ligase cereblon (Fig. 2B). One of the potential advantages of PROTACs over inhibitors is the potential development of cumulative efficacy after repeated administration when the target protein has a slow turnover. To assess the presence of this potential effect for ALT-PG2, repeated administrations were conducted in cells. Exposure to 2 concentrations for 24 h or 4 concentrations for 12 h of 10 nM ALT-PG2 yielded similar degradations of sEH than a single concentration treatment (Fig. 2C), suggesting that ALT-PG2 does not develop cumulative efficacy following repeated administrations, at least during the periods assessed.

3.2. sEH degradation by ALT-PG2 activates AMPK and reduces the levels of ER stress markers in human Huh-7 hepatic cells

Previous studies have reported that the reduction in cardiac AMPK caused by a high-fat diet (HFD) is prevented in sEH knockout mice [23], that hepatocytes from sEH knockout mice show activation of AMPK [24], as well as that sEH inhibition significantly attenuates the HFD-induced renal injury, partially by activating AMPK [25]. Since these findings suggested that both the absence of sEH or its inhibition resulted in AMPK activation, we next examined whether sEH degradation by ALT-PG2 activated AMPK in human Huh-7 hepatic cells. Moreover, given that AMPK activation mitigates ER stress [15,16], we also examined if ALT-PG2 attenuated ER stress and inflammatory markers. As expected, exposure of Huh-7 cells to 10 nM ALT-PG2 for 16 h caused a rapid and robust degradation of sEH (Fig. 3A). This was accompanied

Table 1
PROTACs and *t*-TUCB structures and inhibitory potency against sEH.

Compound	Structure	Human sEH IC_{50} nM[a]	Murine sEH IC_{50} nM[a]
t-TUCB	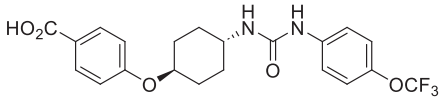	0.4	3.6
ALT-PG2	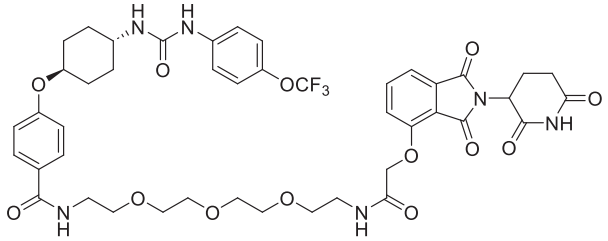	0.4	2.5
ALT-PG3	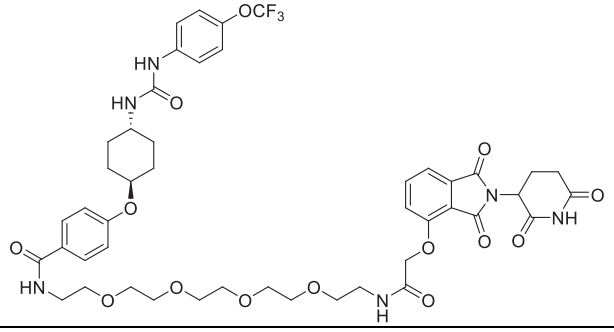	0.4	0.4

IC_{50} in human and murine sEH of *t*-TUCB, ALT-PG2 and ALT-PG3. [a]The inhibition potencies were measured using recombinant purified human or murine sEH and a fluorescent substrate for hydrolase activity (Jones et al., 2005). Reported IC_{50} values are the average of triplicate with at least two data points above and at least two below the IC_{50}. The fluorescent based assay has a standard error between 10% and 20%, suggesting that differences of 2-fold or greater are significant.

by AMPK activation (Fig. 3B), and consistent with the reported inhibitory crosstalk between AMPK and ERK1/2, the phosphorylated levels of the latter kinase were reduced (Fig. 3C). The fact that the sEH inhibitor *t*-TUCB increased the phosphorylated levels of AMPK (Fig. 3D) suggests that AMPK activation caused by ALT-PG2 is mediated by the reduction of the hydrolase levels, while further studies are needed to evaluate whether the phosphatase activity of the enzyme contributes to AMPK activation. AMPK is known to inhibit the p53 negative regulator, murine double minute X (MDMX), resulting in increased p53 levels [26]. Consistent with this, AMPK activation caused by ALT-PG2 was accompanied by an increase in p53 protein levels (Fig. 3E) supporting that ALT-PG2 activates AMPK. Likewise, treatment with ALT-PG2 reduced the levels of ER stress marker phosphorylated eIF2α (Fig. 3F), while no changes were observed in the levels of inflammatory transcription factor NF-κB or its phosphorylation status (Fig. 3G). Despite this latter finding, the levels of phosphorylated STAT3, which is activated by ER stress [13] and is the primary downstream regulator of interleukin (IL)− 6 signaling with a prominent role in regulating inflammation [27], were attenuated by ALT-PG2 (Fig. 3H). Since activation of the STAT3 pathway has been reported to reduce insulin receptor substrate 1 (IRS1) protein levels in hepatocytes [28] and ER stress reduces the levels of insulin receptor β (IRβ) [29], we examined the levels of these two proteins involved in the insulin signaling pathway. Remarkably, the protein levels of both IRβ and IRS1 were upregulated by ALT-PG2 (Fig. 3I). Collectively, these findings indicate that the degradation of sEH by ALT-PG2 activates AMPK, reduces ER stress and inflammatory markers and increases the levels of proteins involved in the insulin signaling pathway in hepatocytes.

3.3. sEH degradation by ALT-PG2 attenuates thapsigargin-induced ER stress in human Huh-7 hepatic cells

To confirm that ALT-PG2 ameliorates ER stress, we used the ER stressor thapsigargin. Exposure of Huh-7 cells to thapsigargin did not significantly increase sEH protein levels (Fig. 4A). Moreover, ALT-PG2 treatment resulted in sEH degradation independently of the presence of thapsigargin. Interestingly, ALT-PG2 abolished the thapsigargin-mediated increase in the ER stress markers CHOP (Fig. 4A), phosphorylated eIF2α (Fig. 4B), tribbles 3 (TRB3) and very low-density lipoprotein receptor (VLDLR) (Fig. 4C). Consistent with these effects of ALT-PG2, this PROTAC prevented the increase in the levels of suppressor of cytokine signaling 3 (SOCS3) (Fig. 4A), a STAT3-target gene, and of the inflammatory markers p65-NF-κB and TNF-α (Fig. 4C). These findings indicate that ALT-PG2 reduces the levels of ER stress and inflammatory markers in thapsigargin-stimulated cells. Since AMPK activation prevents ER stress [15,16], we examined whether the increase in AMPK activity caused by ALT-PG2 was responsible for the reduction of ER stress by using the AMPK inhibitor compound C. Remarkably, the reduction in CHOP protein levels caused by ALT-PG2 in thapsigargin-stimulated cells was prevented when cells were co-incubated with compound C (Fig. 4D). This finding suggests that the inhibition of ER stress provoked by ALT-PG2 is mediated by AMPK.

3.4. sEH degradation by ALT-PG2 activates AMPK and reduces the levels of ER stress markers in mouse primary hepatocytes

Since primary hepatocytes are the gold standard for physiologically relevant *in vitro* liver models as they retain *in vivo*-like functions and morphologies, we next evaluated the effects of the ALT-PG2 PROTAC in this model. Exposure of mouse primary hepatocytes to ALT-PG2 led to significant sEH degradation (Fig. 5A), which was accompanied by an increase in phosphorylated AMPK (Fig. 5B). Likewise, and in agreement with the activation of AMPK, phosphorylated ERK1/2 was reduced (Fig. 5C). In addition, ALT-PG2 reduced basal CHOP protein levels (Fig. 5E), as well as the levels of SOCS3, while the protein levels of IRβ were increased (Fig. 5E). Likewise, when mouse primary hepatocytes

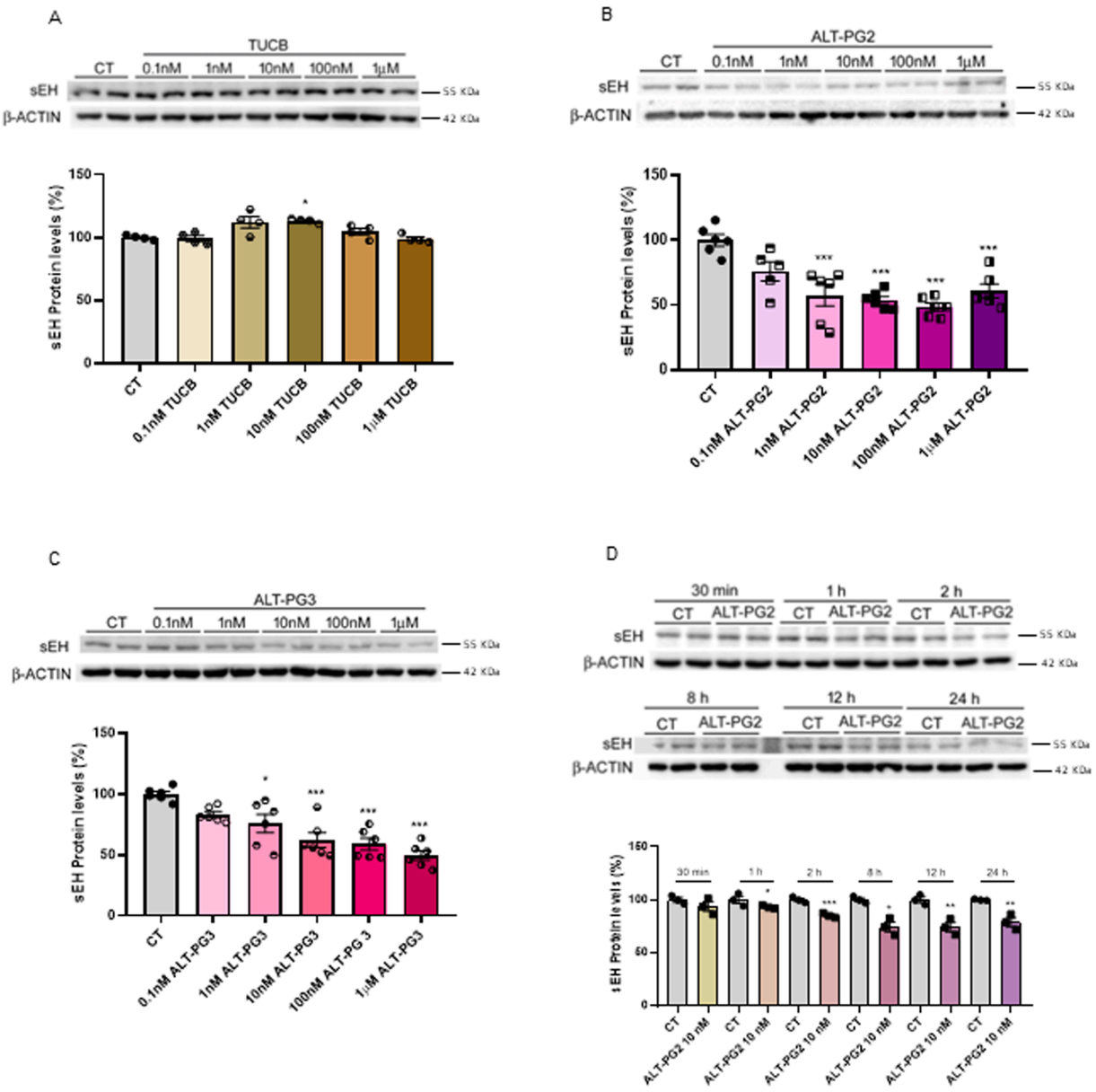

Fig. 1. ALT-PG2 PROTAC degrades sEH in Huh-7 hepatic cells. (**A**) Immunoblot analysis of sEH in Huh-7 hepatic cells exposed to different concentrations of *t*-TUCB for 24 h. Immunoblot analysis of sEH in Huh-7 hepatic cells exposed to different concentrations of (**B**) ALT-PG2 or (**C**) ALT-PG3 for 24 h. (**D**) Time-course of the effects of 10 nM ALT-PG2 on sEH protein levels. Data are presented as the mean ± SEM. one-way ANOVA with Tukey's *post hoc* test. *p < 0.05, * *p < 0.01 and * **p < 0.001 *vs.* control (CT).

were stimulated with thapsigargin, co-incubation of the cells with ALT-PG2 attenuated the increase in CHOP caused by the ER stressor (Fig. 5F). In agreement with the reduction in ER stress, ALT-PG2 also reduced the levels of the inflammatory marker TNF-α (Fig. 5G).

3.5. ALT-PG2 leads to sEH degradation in the liver of mice

We conducted a first approach to evaluate the effect of ALT-PG2 on sEH degradation *in vivo*. Mice treated with ALT-PG2 (30 mg/kg, twice a day for 1 day) showed a significant degradation in hepatic sEH protein levels (Fig. 6A). Consistent with previous studies *in vitro*, ALT-PG2 increased the phosphorylated levels of AMPK in the liver (Fig. 6B). The activation of AMPK was confirmed by the reduction in phosphorylated ERK1/2 (Fig. 6C) and SOCS3 (Fig. 6D). Collectively, these findings suggest that the PROTAC ALT-PG2 causes a potent and rapid degradation of sEH *in vivo* after only 24 h that results in the activation of AMPK.

4. Discussion

In the present study we show that the ALT-PG2 PROTAC (based on the scaffold of the sEH inhibitor *t*-TUCB connected to thalidomide-like ligand as the recruiter of the E3 ligase cereblon and a PEG linker) degrades sEH in the human Huh-7 hepatic cell line, in mouse primary hepatocytes and in mouse liver. In addition, sEH degradation results in the activation of AMPK and the reduction of phosphorylated ERK1/2, which are important regulators of ER stress. In fact, ALT-PG2 reduces basal ER stress markers after stimulation with an ER stressor. Moreover, the inhibition of ER stress caused by ALT-PG2 seems to be mediated by the activation of AMPK. The effects of ALT-PG2 also contribute to attenuate inflammation and the increase in the levels of proteins involved in the insulin signaling pathway, suggesting that ALT-PG2 might be a potential treatment of insulin resistance and type 2 diabetes mellitus as well as metabolic diseases associated with these conditions. In our study we have also assessed another PROTAC, ALT-PG3,

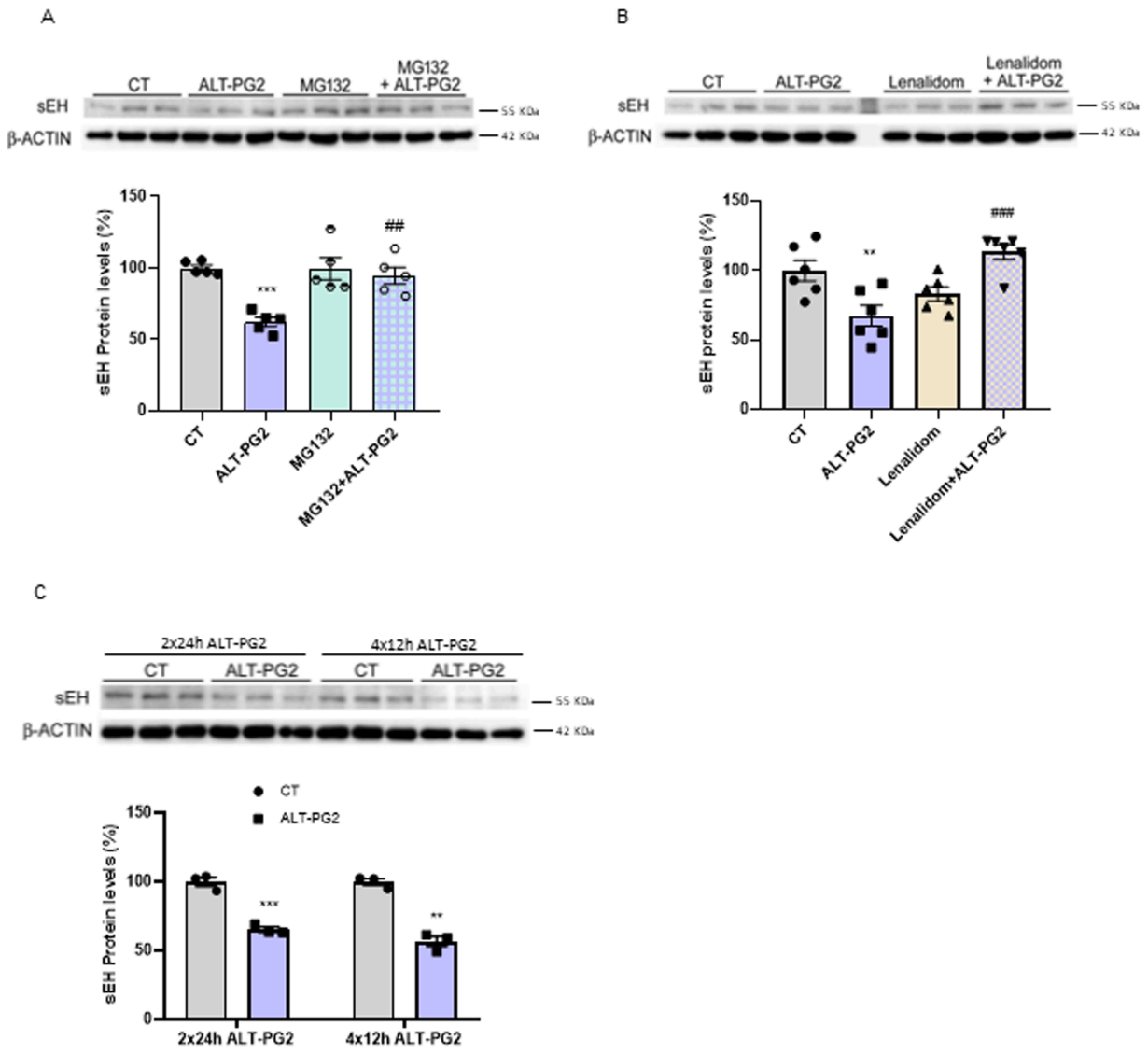

Fig. 2. ALT-PG2 degrades sEH *via* the ubiquitin–proteasome system in Huh-7 hepatic cells. (**A**) Immunoblot analysis of sEH in Huh-7 hepatic cells exposed to 10 nM ALT-PG2 for 24 h in the presence or in the absence of 10 μM of the proteasome inhibitor MG132 (added 3 h prior ALT-PG2). (**B**) Immunoblot analysis of sEH in Huh-7 hepatic cells exposed to 10 nM ALT-PG2 for 24 h in the presence or in the absence of 100 μM of the cereblon ligand lenalidomide (added 3 h prior ALT-PG2). (**C**) sEH protein levels in Huh-7 hepatic cells exposed to the addition of 2 concentrations of ALT-PG2, each one every 24 h, and 4 concentrations of ATL-PG2, each one every 12 h. Data are presented as the mean ± SEM. Significant differences were established by Student's-t test or one-way ANOVA with Tukey's *post hoc* test. *$p < 0.05$, * *$p < 0.01$ and * **$p < 0.001$ *vs.* CT. $^{\#}p < 0.05$, and $^{\#\#}p < 0.01$ *vs.* ALT-PG2.

which yielded a slightly lower degradation of sEH than ALT-PG2. Indeed, ALT-PG3 has been previously evaluated in a recent study designed as compound **1a** [17]. Interestingly, this study elegantly demonstrated that ALT-PG3 selectively targeted the degradation of cytosolic but not peroxisomal sEH. It is also reported that the lack of effect of ALT-PG3 on peroxisomal sEH explained the apparent lack of total degradation of sEH. Given the structural similarities between ALT-PG2 and ALT-PG3, it is likely that ALT-PG2 may also show selectivity against cytosolic sEH, thereby explaining the lack of total degradation of this protein. However, despite the structural similarities, some differences may exist between ALT-PG2 and ALT-PG3. In fact, according to this previous study, ALT-PG3-mediated sEH degradation was not rescued by the proteasome inhibitor MG132. However, they observed that the lysosomal pathway was involved in the ALT-PG3-mediated degradation of sEH [17]. In contrast, we report that MG132 rescues completely the degradation of sEH caused by ALT-PG2, indicating that ALT-PG2-mediated sEH degradation involves the proteasome system. We do not know the reasons for these differences between ALT-PG2 and ALT-PG3, but the use of different cell lines (Huh-7 in our study *vs.* HepG2 and HEK293T) or concentrations (10 nM ALT-PG2 in our study *vs.* 250 nM ALT-PG3) might contribute, since, for instance, it is well-known in the field the influence of the cell line in the degradation patterns.

We also show that sEH degradation by ALT-PG2 activates AMPK *in vitro* and *in vivo*. In fact, previous studies have observed AMPK activation in the sEH knockout mice [23,24] and following treatment with sEH inhibitors [25]. Our findings confirm that sEH degradation by PROTAC is also a valid strategy to activate AMPK in hepatic cells. This has implications for the treatment of insulin resistance and type 2 diabetes mellitus, since the most prescribed drug for the treatment of type 2 diabetes mellitus, metformin, activates AMPK. Moreover, due to the presence of an inhibitory crosstalk between AMPK and ERK1/2, activation of AMPK by ALT-PG2 might be responsible for the reduction of ER stress, since it has been reported that inhibition of ERK1/2 reverses ER stress-induced insulin resistance [15,16]. Actually, our findings demonstrate that AMPK activation by ALT-PG2 is required for the

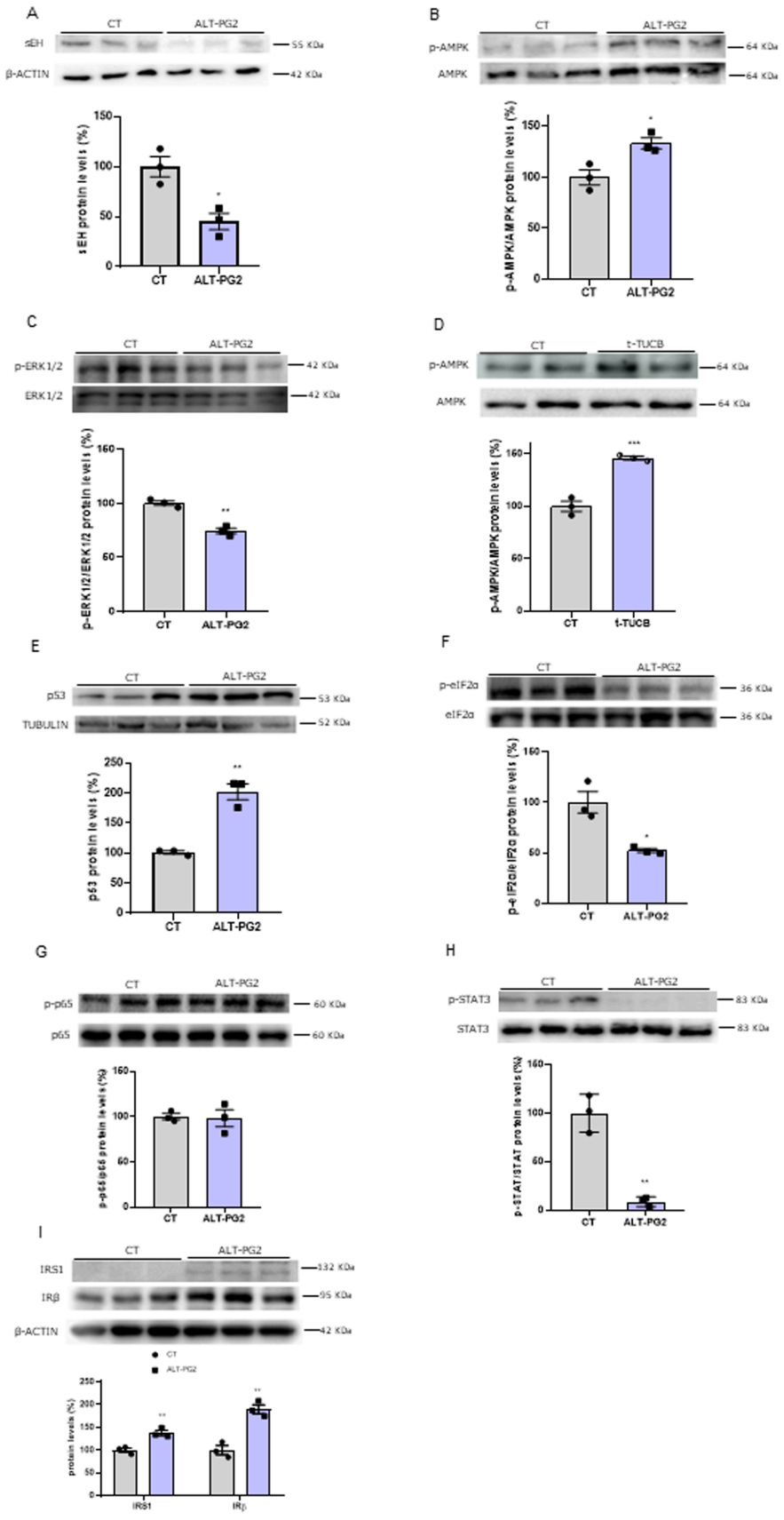

(caption on next page)

Fig. 3. sEH degradation by ALT-PG2 activates AMPK and reduces basal levels of ER stress markers in Huh-7 hepatic cells. Immunoblot analysis of (**A**) sEH in Huh-7 hepatic cells exposed to 10 nM ALT-PG2 for 16 h. (**B**) Total and phosphorylated AMPK and (**C**) total and phosphorylated ERK1/2 in Huh-7 hepatic cells exposed to 10 nM ALT-PG2 for 48 h. (**D**) Immunoblot analysis of total and phosphorylated AMPK in Huh-7 hepatic cells exposed to 1 μM *t*-TUCB for 4 h. Immunoblot analysis of (**E**) p53, (**F**) total and phosphorylated eIF2α, (**G**) total and phosphorylated levels of the p65 subunit of NF-κB, (**H**) total and phosphorylated (Tyr^{705}) levels of STAT3 and (**I**) IRβ and IRS1 in Huh-7 hepatic cells exposed to 10 nM ALT-PG2 for 16 h. Significant differences were established by Student's-t test. *p < 0.05, * *p < 0.01 and * **p < 0.001 *vs.* CT.

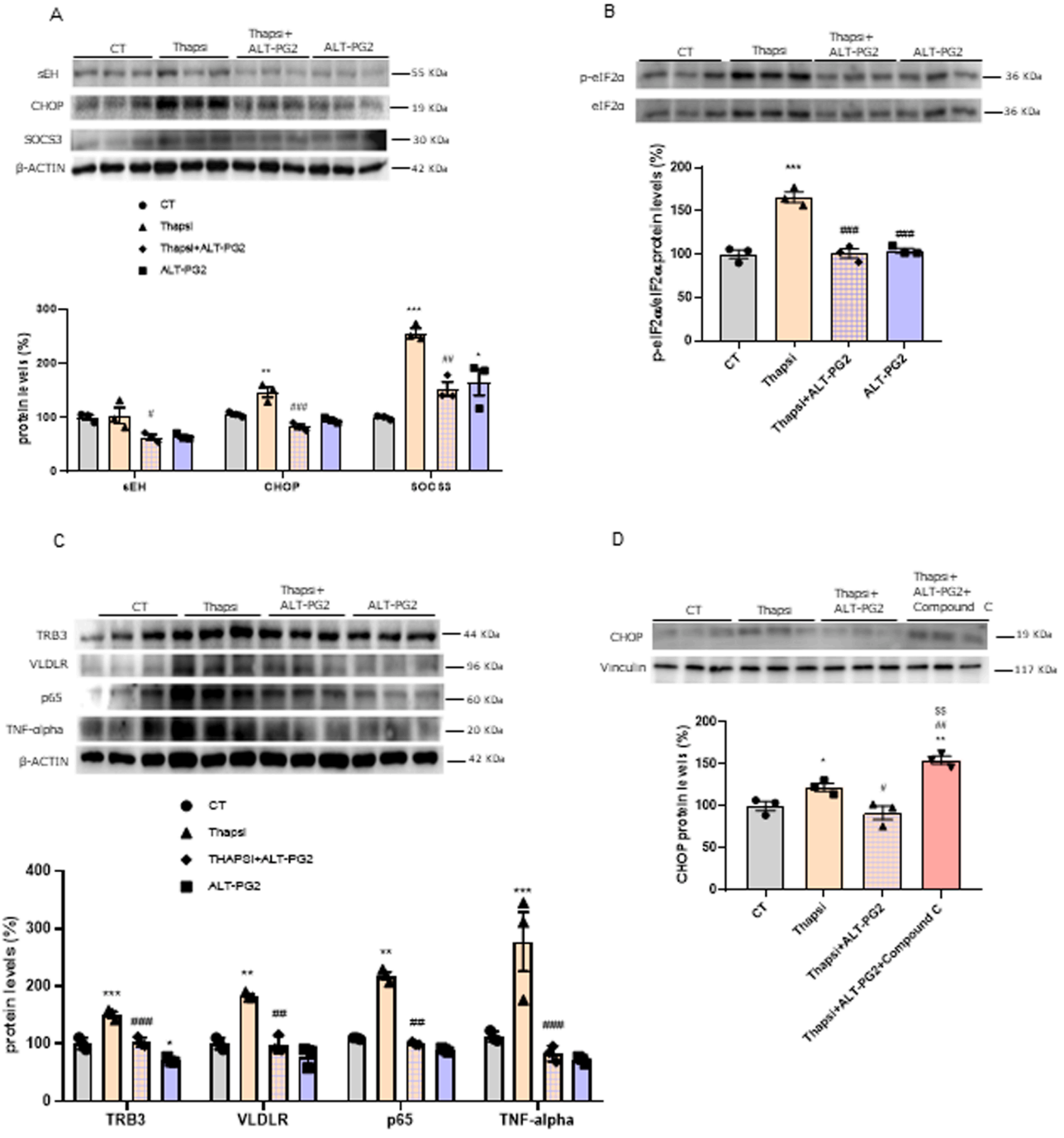

Fig. 4. sEH degradation by ALT-PG2 attenuates thapsigargin-induced ER stress in Huh-7 hepatic cells. Immunoblot analysis of (**A**) sEH, CHOP, SOCS3 and (**B**) total and phosphorylated eIF2α in Huh-7 hepatic cells exposed to 10 nM ALT-PG2 for 48 h co-incubated with vehicle or the ER stressor thapsigargin (1 μM) for the last 24 h. (**C**) TRB3, VLDLR, p65 and TNF-α in Huh-7 hepatic cells exposed to 10 nM ALT-PG2 for 48 h co-incubated with vehicle or the ER stressor thapsigargin (1 μM) for the last 24 h. (**D**) Immunoblot analysis of CHOP in Huh-7 hepatic cells exposed to 10 nM ALT-PG2 for 48 h co-incubated with vehicle or the ER stressor thapsigargin (1 μM) for the last 24 h with or without the AMPK inhibitor compound C (15 μM). Data are presented as the mean ± SEM. Significant differences were established by one-way ANOVA with Tukey's *post hoc* test. *p < 0.05, * *p < 0.01 and * **p < 0.001 *vs.* CT. $^{\#}$p < 0.05, $^{\#\#}$p < 0.01 and $^{\#\#\#}$p < 0.001 *vs.* thapsigargin. $^{\$\$}$p < 0.01 *vs.* Thapsi+ALT-PG2.

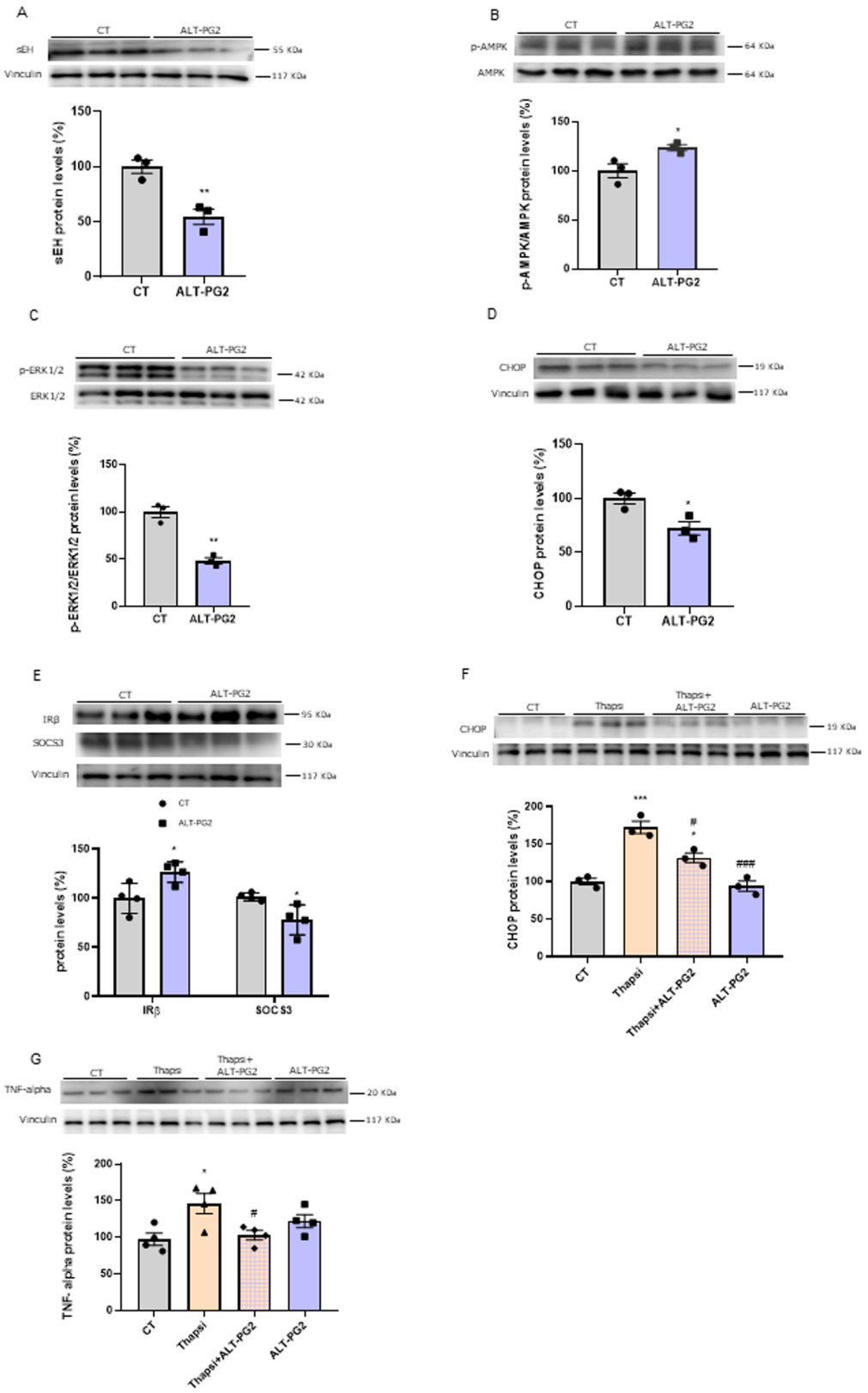

Fig. 5. sEH degradation by ALT-PG2 attenuates ER stress in mouse primary hepatocytes. Immunoblot analysis of (**A**) sEH, (**B**) total and phosphorylated AMPK, (**C**) total and phosphorylated ERK1/2, (**D**) CHOP, (**E**) IRβ and SOCS3 in mouse primary hepatocytes exposed to 10 nM ALT-PG2 for 48 h. Immunoblot analysis of (**F**) CHOP and (**G**) TNF-α in mouse primary hepatocytes exposed to 10 nM ALT-PG2 for 48 h co-incubated with vehicle or the ER stressor thapsigargin (1 μM) for the last 24 h. Data are presented as the mean ± SEM. Significant differences were established by Student's-t test or one-way ANOVA with Tukey's *post hoc* test. *$p < 0.05$, * **$p < 0.01$ and * **$p < 0.001$ *vs.* CT. $^{\#}p < 0.05$ and $^{\#\#\#}p < 0.001$ *vs.* thapsigargin.

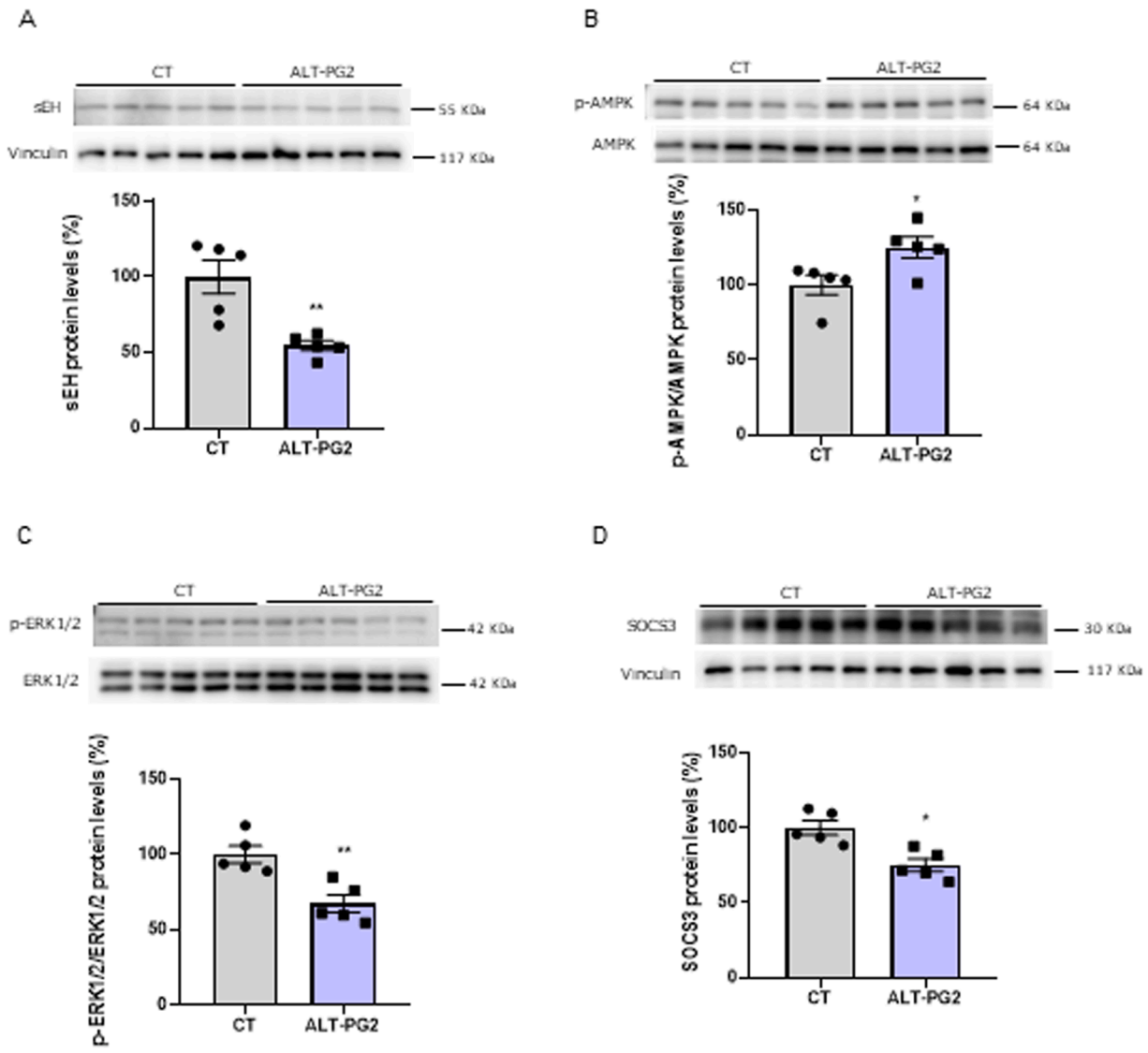

Fig. 6. ALT-PG2 degrades sEH *in vivo*. Immunoblot analysis of (**A**) sEH, (**B**) total and phosphorylated AMPK, (**C**) total and phosphorylated ERK1/2, (**D**) SOCS3 in the liver of mice treated with vehicle or ALT-PG2 (30 mg/kg, i.p., twice a day for 1 day). Significant differences were established by Student's-t test. *$p < 0.05$ and * *$p < 0.01$ *vs.* CT.

inhibition of ER stress, since the AMPK inhibitor compound C abolished this effect. It is well-known that ER stress contributes to insulin resistance and type 2 diabetes by activating inflammatory pathways and by reducing the protein levels of key proteins of the insulin-signaling pathway [12]. In fact, our findings show that AMPK activation by ALT-PG2-mediated degradation of sEH results in a reduction of inflammatory markers. Since ER stress has been reported to reduce IRβ levels [29], the reduction in ER stress caused by ALT-PG2 might be responsible for the increase in the levels of this receptor. Similarly, ALT-PG2 reduces the activation of STAT3 and the levels of its target gene SOCS3. Given that the STAT3-SOCS3 pathway reduces hepatic IRS1 levels [28], its attenuation by ALT-PG2 could be the underlying mechanism responsible for the increase in IRβ levels. Moreover, because of AMPK activation following sEH degradation, p53 protein levels were also increased. This result is relevant since it has been reported that p53 modulates hepatic insulin sensitivity through NF-κB and p38/ERK-mitogen activated protein kinase (MAPK) pathways [30].

As far as we know, this is the first study reporting the efficacy of a PROTAC to promote the degradation of sEH *in vivo*. Further studies are necessary to better characterize the effects of PROTACs targeting sEH, but this first approach provides some interesting data. Our findings confirm that targeting sEH degradation by using degraders leads to AMPK activation after an acute treatment. Likewise, the activation of AMPK by ALT-PG2 in the liver results in a reduction of phosphorylated ERK1/2 and SOCS3 levels, indicating that ALT-PG2 shows beneficial effects similar to those observed in Huh-7 cells and in primary hepatocytes. A previous study has reported that AMPK activation in the liver of sEH knockout mice was elicited by higher levels of the sEH substrate 12,13-epoxyoctadecenoic acid [24]. Although we have not examined the levels of this substrate, it is likely that the level of degradation of sEH caused by ALT-PG2 might be sufficient to increase the levels of 12, 13-epoxyoctadecenoic acid, eventually leading to the activation of AMPK.

Altogether, the findings of this study demonstrate that the ALT-PG2 PROTAC degrades sEH protein in human Huh-7 hepatic cells, mouse primary hepatocytes, and in the liver of mice. In these three models the degradation of sEH was accompanied by the activation of AMPK and the reduction of phosphorylated ERK1/2 as well as the reduction of ER stress and inflammatory markers. These findings indicate that targeting sEH with a PROTAC molecule is an effective strategy to activate AMPK and to prevent ER stress and inflammation in hepatic cells.

Funding

This study was partly supported by grants RTI2018-093999-B-100 and PID2021-122116OB-I00 (M.V-C.), PID2020-118127RB-I00 (S.V.), PID2021-127693OB-I00 (C.G.) and PID2021-122766OB-I00 (A.M.V.) funded by MCIN/AEI/10.13039/501100011033 and by "ERDF A way of making Europe". CIBER de Diabetes y Enfermedades Metabólicas Asociadas (CIBERDEM) is a Carlos III Health Institute project. CERCA Programme/Generalitat de Catalunya. Partial support was provided by NIH – NIEHS (RIVER Award) R35 ES030443-01, NIH – NIEHS (Superfund Award) P42 ES004699 and NIH Counter Act Award U54 NS127758 (B. H.).

CRediT authorship contribution statement

MP, EB, FE, DS, JJ, PR, CM, BH, AMV, and MVC performed the experiments; ALT and SV conducted the synthesis of the compounds, EB, ALT, XP, CM, BH, CG, SV and MVC analyzed the data, reviewed the results and wrote the manuscript; EB, CG, SV and MVC designed the experiments. MVC is the guarantor of this work and, as such, had full access to all of the data in the study and takes responsibility for the integrity of the data and the accuracy of the data analysis.

Declaration of Competing Interest

None.

Data Availability

Data will be made available on request.

Acknowledgements

We would like to thank the Language Services of the University of Barcelona for revising the manuscript.

References

[1] M. Bekes, D.R. Langley, C.M. Crews, PROTAC targeted protein degraders: the past is prologue, Nat. Rev. Drug Discov. 21 (3) (2022) 181–200.
[2] Y. Zou, D. Ma, Y. Wang, The PROTAC technology in drug development, Cell Biochem Funct. 37 (1) (2019) 21–30.
[3] S. Rana, M. Bendjennat, S. Kour, H.M. King, S. Kizhake, M. Zahid, A. Natarajan, Selective degradation of CDK6 by a palbociclib based PROTAC, Bioorg. Med Chem. Lett. 29 (11) (2019) 1375–1379.
[4] A. Mares, A.H. Miah, I.E.D. Smith, M. Rackham, A.R. Thawani, J. Cryan, P.A. Haile, B.J. Votta, A.M. Beal, C. Capriotti, M.A. Reilly, D.T. Fisher, N. Zinn, M. Bantscheff, T.T. MacDonald, A. Vossenkamper, P. Dace, I. Churcher, A.B. Benowitz, G. Watt, J. Denyer, P. Scott-Stevens, J.D. Harling, Extended pharmacodynamic responses observed upon PROTAC-mediated degradation of RIPK2. Commun, Biol 3 (1) (2020) 140.
[5] R.B. Kargbo, PROTAC-mediated degradation of KRAS protein for anticancer therapeutics, ACS Med Chem. Lett. 11 (1) (2020) 5–6.
[6] J.W. Newman, C. Morisseau, T.R. Harris, B.D. Hammock, The soluble epoxide hydrolase encoded by EPXH2 is a bifunctional enzyme with novel lipid phosphate phosphatase activity, Proc. Natl. Acad. Sci. USA 100 (4) (2003) 1558–1563.
[7] F.C.G. van Bussel, W.H. Backes, P.A.M. Hofman, R.J. van Oostenbrugge, M.P.J. van Boxtel, F.R.J. Verhey, H.W.M. Steinbusch, M.T. Schram, C.D.A. Stehouwer, J. E. Wildberger, J.F.A. Jansen, Cerebral pathology and cognition in diabetes: the merits of multiparametric neuroimaging, Front Neurosci. 11 (2017) 188.
[8]] K.M. Wagner, C.B. McReynolds, W.K. Schmidt, B.D. Hammock, Soluble epoxide hydrolase as a therapeutic target for pain, inflammatory and neurodegenerative diseases, Pharm. Ther. 180 (2017) 62–76.
[9] S.D. Kodani, B.D. Hammock, The 2014 Bernard B. Brodie award lecture-epoxide hydrolases: drug metabolism to therapeutics for chronic pain, Drug Metab. Dispos. 43 (5) (2015) 788–802.
[10] S.R. Chadwick, P. Lajoie, Endoplasmic reticulum stress coping mechanisms and lifespan regulation in health and diseases, Front Cell Dev. Biol. 7 (2019) 84.
[11] A. Bettaieb, N. Nagata, D. AbouBechara, S. Chahed, C. Morisseau, B.D. Hammock, F.G. Haj, Soluble epoxide hydrolase deficiency or inhibition attenuates diet-induced endoplasmic reticulum stress in liver and adipose tissue, J. Biol. Chem. 288 (20) (2013) 14189–14199.
[12] L. Salvado, X. Palomer, E. Barroso, M. Vazquez-Carrera, Targeting endoplasmic reticulum stress in insulin resistance, Trends Endocrinol. Metab. 26 (8) (2015) 438–448.
[13] G.P. Meares, Y. Liu, R. Rajbhandari, H. Qin, S.E. Nozell, J.A. Mobley, J.A. Corbett, E.N. Benveniste, PERK-dependent activation of JAK1 and STAT3 contributes to endoplasmic reticulum stress-induced inflammation, Mol. Cell Biol. 34 (20) (2014) 3911–3925.
[14] X. Liu, R.M. Green, Endoplasmic reticulum stress and liver diseases, Liver Res. 3 (1) (2019) 55–64.
[15] S.L. Hwang, Y.T. Jeong, X. Li, Y.D. Kim, Y. Lu, Y.C. Chang, I.K. Lee, H.W. Chang, Inhibitory cross-talk between the AMPK and ERK pathways mediates endoplasmic reticulum stress-induced insulin resistance in skeletal muscle, Br. J. Pharm. 169 (1) (2013) 69–81.
[16] L. Salvado, E. Barroso, A.M. Gomez-Foix, X. Palomer, L. Michalik, W. Wahli, M. Vazquez-Carrera, PPARbeta/delta prevents endoplasmic reticulum stress-associated inflammation and insulin resistance in skeletal muscle cells through an AMPK-dependent mechanism, Diabetologia 57 (10) (2014) 2126–2135.
[17] Y. Wang, C. Morisseau, A. Takamura, D. Wan, D. Li, S. Sidoli, J. Yang, D.W. Wolan, B.D. Hammock, S. Kitamura, PROTAC-mediated selective degradation of cytosolic soluble epoxide hydrolase enhances ER stress reduction, ACS Chem. Biol. 18 (4) (2023) 884–896.
[18] P.D. Jones, N.M. Wolf, C. Morisseau, P. Whetstone, B. Hock, B.D. Hammock, Fluorescent substrates for soluble epoxide hydrolase and application to inhibition studies, Anal. Biochem 343 (1) (2005) 66–75.
[19] R. Benveniste, T.M. Danoff, J. Ilekis, H.R. Craig, Epidermal growth factor receptor numbers in male and female mouse primary hepatocyte cultures, Cell Biochem Funct. 6 (4) (1988) 231–235.
[20] D. Aguilar-Recarte, E. Barroso, M. Zhang, P. Rada, J. Pizarro-Delgado, L. Pena, X. Palomer, A.M. Valverde, W. Wahli, M. Vazquez-Carrera, A positive feedback loop between AMPK and GDF15 promotes metformin antidiabetic effects, Pharm. Res 187 (2022), 106578.
[21] S.H. Hwang, H.J. Tsai, J.Y. Liu, C. Morisseau, B.D. Hammock, Orally bioavailable potent soluble epoxide hydrolase inhibitors, J. Med Chem. 50 (16) (2007) 3825–3840.
[22] M. Pettersson, C.M. Crews, PROteolysis targeting chimeras (PROTACs) - past, present and future, Drug Discov. Today Technol. 31 (2019) 15–27.
[23] L. Wang, D. Zhao, L. Tang, H. Li, Z. Liu, J. Gao, M.L. Edin, H. Zhang, K. Zhang, J. Chen, X. Zhu, D. Wang, D.C. Zeldin, B.D. Hammock, J. Wang, H. Huang, Soluble epoxide hydrolase deficiency attenuates lipotoxic cardiomyopathy via upregulation of AMPK-mTORC mediated autophagy, J. Mol. Cell Cardiol. 154 (2021) 80–91.
[24] N. Mangels, K. Awwad, A. Wettenmann, L.R. Dos Santos, T. Fromel, I. Fleming, The soluble epoxide hydrolase determines cholesterol homeostasis by regulating AMPK and SREBP activity, Prostaglandins Other Lipid Mediat. 125 (2016) 30–39.
[25] Y. Luo, M.Y. Wu, B.Q. Deng, J. Huang, S.H. Hwang, M.Y. Li, C.Y. Zhou, Q.Y. Zhang, H.B. Yu, D.K. Zhao, G. Zhang, L. Qin, A. Peng, B.D. Hammock, J.Y. Liu, Inhibition of soluble epoxide hydrolase attenuates a high-fat diet-mediated renal injury by activating PAX2 and AMPK, Proc. Natl. Acad. Sci. USA 116 (11) (2019) 5154–5159.
[26] D. Aguilar-Recarte, E. Barroso, A. Guma, J. Pizarro-Delgado, L. Pena, M. Ruart, X. Palomer, W. Wahli, M. Vazquez-Carrera, GDF15 mediates the metabolic effects of PPARbeta/delta by activating AMPK, Cell Rep. 36 (6) (2021), 109501.
[27] T. Matsuda, The physiological and pathophysiological role of IL-6/STAT3-mediated signal transduction and STAT3 binding partners in therapeutic applications, Biol. Pharm. Bull. 46 (3) (2023) 364–378.
[28] L. Serrano-Marco, E. Barroso, I. El Kochairi, X. Palomer, L. Michalik, W. Wahli, M. Vazquez-Carrera, The peroxisome proliferator-activated receptor (PPAR) beta/delta agonist GW501516 inhibits IL-6-induced signal transducer and activator of transcription 3 (STAT3) activation and insulin resistance in human liver cells, Diabetologia 55 (3) (2012) 743–751.
[29] L. Zhou, J. Zhang, Q. Fang, M. Liu, X. Liu, W. Jia, L.Q. Dong, F. Liu, Autophagy-mediated insulin receptor down-regulation contributes to endoplasmic reticulum stress-induced insulin resistance, Mol. Pharm. 76 (3) (2009) 596–603.
[30] S. Geng, W. Zhu, S. Wang, C. Xie, X. Li, J. Wu, Y. Li, Y. Chen, X. Wang, Y. Meng, Q. Zhang, J. Chen, C. Zhong, P53 modulates hepatic insulin sensitivity through NF-kappaB and p38/ERK MAPK pathways, Biochem Biophys. Res Commun. 495 (3) (2018) 2139–2144.

Barroso *et al.*
Cell Communication and Signaling (2023) 21:326
https://doi.org/10.1186/s12964-023-01352-5

Cell Communication and Signaling

RESEARCH Open Access

CHOP upregulation and dysregulation of the mature form of the SNAT2 amino acid transporter in the placentas from small for gestational age newborns

Emma Barroso[1,2,3], Marta Díaz[2,3,4], Ana Cristina Reguera[1,2,3], Mona Peyman[1,2,3], Jesús Balsinde[2,5], Javier Jurado-Aguilar[1,2,3], Meijian Zhang[1,2,3], Adel Rostami[1,2,3], Xavier Palomer[1,2,3], Lourdes Ibáñez[2,3,4] and Manuel Vázquez-Carrera[1,2,3*]

Abstract

Background The placentas from newborns that are small for gestational age (SGA; birth weight < -2 SD for gestational age) may display multiple pathological characteristics. A key determinant of fetal growth and, therefore, birth weight is placental amino acid transport, which is under the control of the serine/threonine kinase mechanistic target of rapamycin (mTOR). The effects of endoplasmic reticulum (ER) stress on the mTOR pathway and the levels of amino acid transporters are not well established.

Methods Placentas from SGA and appropriate for gestational age (AGA) newborns and the human placental BeWo cell line exposed to the ER stressor tunicamycin were used.

Results We detected a significant increase in the levels of C/EBP homologous protein (CHOP) in the placentas from SGA newborns compared with those from AGA newborns, while the levels of other ER stress markers were barely affected. In addition, placental mTOR Complex 1 (mTORC1) activity and the levels of the mature form of the amino acid transporter sodium-coupled neutral amino acid transporter 2 (SNAT2) were also reduced in the SGA group. Interestingly, CHOP has been reported to upregulate growth arrest and DNA damage-inducible protein 34 (GADD34), which in turn suppresses mTORC1 activity. The GADD34 inhibitor guanabenz attenuated the increase in CHOP protein levels and the reduction in mTORC1 activity caused by the ER stressor tunicamycin in the human placental cell line BeWo, but it did not recover mature SNAT2 protein levels, which might be reduced as a result of defective glycosylation.

Conclusions Collectively, these data reveal that GADD34A activity and glycosylation are key factors controlling mTORC1 signaling and mature SNAT2 levels in trophoblasts, respectively, and might contribute to the SGA condition.

Keywords Placenta, CHOP, SNAT2, mTORC1, ER stress, GADD34

*Correspondence:
Manuel Vázquez-Carrera
mvazquezcarrera@ub.edu
Full list of author information is available at the end of the article

Background

Newborns with a birth weight for gestational age less than -2 SD are considered to be small for gestational age (SGA) [1]. SGA infants, particularly those who experience a rapid and significant catch-up in weight, have an increased risk of developing metabolic disorders later in life, including visceral obesity, hypertension, insulin resistance, type 2 diabetes, and cardiovascular disease [2]. The SGA condition has been associated with multiple placental pathological characteristics [3–5]. A feature of placental pathophysiology is endoplasmic reticulum (ER) stress, which is considered a target for pregnancy complications [6, 7]. The ER has key functions within cells, including the synthesis, folding, and transport of proteins. The accumulation of misfolded and unfolded proteins in the ER lumen disrupts the homeostasis of this organelle and leads to ER stress, which activates the unfolded protein response (UPR) [8]. This is an adaptive response that involves the activation of a signaling pathway in order to restore the folding capacity. The UPR involves the activation of three transmembrane proteins: inositol-requiring enzyme 1 (IRE-1), activating transcription factor 6 (ATF6), and protein kinase RNA (PKR)-like ER kinase (PERK). PERK phosphorylates eukaryotic initiation factor 2α (eIF2α) and attenuates protein translation, thereby reducing the amounts of new proteins entering the ER lumen. However, if the UPR cannot restore ER homeostasis, apoptosis is induced by the PERK-eIF2α pathway and the subsequent increase in ATF4 activity, which upregulates the expression of C/EBP homologous protein (CHOP) and growth arrest and DNA damage-inducible protein 34 (GADD34). Remarkably, CHOP upregulation has been associated with compromised placental development and function in vivo and in vitro [9–11].

A key determinant of fetal growth and, therefore, birth weight is placental nutrient transfer. This is highly dependent on the levels of nutrient transporters in the epithelium of the placenta, the syncytiotrophoblast [12]. A reduction in the placental activity of system A, a sodium-dependent transporter mediating the uptake of non-essential amino acids, has been associated with decreased birth weight in humans [13, 14] and in animal models [15, 16]. System A includes several subtypes of sodium-coupled neutral amino acid transporters (SNATs) with similar substrate specificities: SNAT1, SNAT2, and SNAT4 [17]. Similar reductions have been reported in the levels of transporters of essential amino acids, such as system L, which includes L-type amino acid transporter 1 (LAT1) and LAT2 [18, 19]. Trophoblast system A and system L amino acid transporter activities are under the control of the serine/threonine kinase mechanistic target of rapamycin (mTOR) [20]. mTOR forms two distinct complexes, mTORC1 and mTORC2. The function of mTORC1 is mediated by the phosphorylation of downstream targets, mainly eukaryotic initiation factor 4E-binding protein 1 (4E-BP1) and p70 S6 kinase (S6K), the latter catalyzing the phosphorylation of ribosomal protein (RP)S6. Activation of mTORC2 promotes the phosphorylation of protein kinase B (Akt), protein kinase Cα (PKCα), and serum and glucocorticoid-regulated kinase 1 (SGK1). Notably, the silencing of mTORC1 and/or mTORC2 results in a marked inhibition of trophoblast system A and system L amino acid transporter activities [20], thereby indicating that the inhibition of placental mTOR is involved in decreased placental amino acid uptake and fetal growth. However, little is known about how the activation of the ER stress/UPR process results in a reduction in mTOR signaling and in the levels of amino acid transporters in the placenta and trophoblasts.

Here, we show that the ER stress marker CHOP is upregulated in the placentas from SGA newborns, which is accompanied by reduced mTORC1 activity and a significant decrease in the mature form of the amino acid transporter SNAT2. Interestingly, inhibition of GADD34A in a human placental cell line by the ER stressor tunicamycin attenuates the reduction in mTORC1 activity, but does not recover mature SNAT2 protein levels, which might be reduced as a result of defective glycosylation. These findings suggest that the dysregulation of CHOP and of the processing/maturation of SNAT2 may contribute to the SGA condition.

Methods

Reagents

Guanabenz and tunicamycin were purchased from Sigma-Aldrich (Madrid, Spain).

Study population

The study cohort consisted of 40 mother-newborn pairs recruited at the Hospital Sant Joan de Déu of Barcelona (Spain) from a prenatal cohort study of mothers and infants. Twenty infants were born AGA (10 girls, 10 boys) and 20 SGA (10 girls, 10 boys). The inclusion criteria were: (i) infants born at term (37–42 weeks) from singleton pregnancies and with a birth weight between -1.0 and + 1.0 SD (range 2.9–3.8 kg) for AGA and below -2 SD (range 1.9–2.6 kg) for SGA; (ii) placenta collected at delivery; and (iii) written informed consent obtained in the third trimester of pregnancy. The exclusion criteria were: (i) maternal disease (hypertension, preeclampsia, gestational diabetes, or preexisting type 1 and type 2 diabetes mellitus), alcohol abuse or drug addiction; and (ii) fetal malformations or complications at birth. The SGA babies included in the present study had normal

umbilical flow indices, and none of them had oligohydramnios or neonatal complications.

The study was approved by the Institutional Review Board of the Hospital Sant Joan de Déu at the University of Barcelona.

Clinical, endocrine-metabolic and body composition assessments

Information on maternal age at conception, height, pregestational weight, and gestational weight gain were retrieved from the mother's clinical records. Gestational age was calculated from the last menses and was confirmed by a first-trimester ultrasound.

The weight and length of the newborns were measured in the delivery room and transformed into Z-scores according to country and sex-specific growth charts [21]. Blood samples were obtained at birth from the umbilical cord, before placental separation.

Serum glucose levels were measured with the glucose oxidase method. Insulin and insulin-like growth factor-1 (IGF-1) were assessed by immunechemiluminescence (DPC, IMMULITE 2500, Siemens, Erlangen, Germany), with the intra- and inter-assay coefficient of variation (CVs) being < 10%.

Homeostatic model assessment for insulin resistance (HOMA-IR) was calculated as fasting insulin (mU/L) x fasting glucose (mmol/L)/22.5. Circulating high molecular weight (HMW)-adiponectin was measured with a specific enzyme-linked immunosorbent assay (R&D Systems, Minneapolis, USA), with the intra- and inter-assay CVs being < 9%. Glucagon-like peptide-1 (GLP-1) was assessed by an enzyme-linked immunosorbent assay (Millipore, Billerica, MA, USA). The antibody pair in the assay binds to GLP-1 (7–36) and (9–36) and has no cross-reactivity with GLP-2, GIP, glucagon or oxyntomodulin. The intra-assay and inter-assay CVs were < 2% and < 10%, respectively, and the detection limit was 1.5 pM.

Body composition was assessed at the age of 15 days by dual X-ray absorciometry with a Lunar Prodigy system coupled to Lunar software (Lunar Corp, Madison, WI, USA) adapted for infants. CVs were < 3% for fat and lean mass [22].

Placenta collection

Placentas were collected after childbirth in the delivery room and weighed immediately. Placental tissue encompassing the decidua and the upper side of the chorionic villous proximal to the decidua was dissected to obtain placental maternal biopsies. Three pieces of 1-cm^3 cuboidal sections were collected from the maternal side after removal of the amniotic and chorionic layers. Placental samples were washed three times with physiological saline to remove all maternal blood and immediately frozen in liquid nitrogen and stored at − 80 °C until analysis. The personnel always wore face masks and sterile gloves and used a sterile scalpel and instruments.

For the studies of mRNA and protein expression in the placentas from AGA and SGA infants, only girls were selected (as specified in the Results section).

Cell culture

BeWo cells (kindly donated by Dr. Vicente Andreu Fernández from the Universidad Internacional de Valencia, Valencia) were cultured in Ham's F12 medium (Gibco-Invitrogen) supplemented with 10% fetal bovine serum (FBS) (Sigma-Aldrich) and 1% penicillin–streptomycin (Gibco-Invitrogen). Cells were seeded and, 72 h later, differentiated into syncytiotrophoblasts by incubation with 40 μM forskolin (Santa Cruz Biotechnology) for 48 h. Once differentiated, cells were treated with 0.1 μg/ml of tunicamycin (TM) (Sigma-Aldrich) and 5 μM guanabenz (GB) (Sigma-Aldrich), which was added 1 h before tunicamycin, for 24 h.

Reverse transcription-polymerase chain reaction and quantitative polymerase chain reaction

Isolated RNA was reverse transcribed to obtain 1 μg of complementary DNA (cDNA) using Random Hexamers (Thermo Scientific), 10 mM deoxynucleotide (dNTP) mix, and the reverse transcriptase enzyme derived from the Moloney murine leukemia virus (MMLV, Thermo Fisher). The experiment was run in a thermocycler (Bio-Rad) and consisted of a program with different steps and temperatures: 65 °C for 5 min, 4 °C for 5 min, 37 °C for 2 min, 25 °C for 10 min, 37 °C for 50 min, and 70 °C for 15 min. The relative levels of specific mRNAs were assessed by real-time RT-PCR in a mini 48-well T100™ thermal cycler (Bio-Rad), using the SYBR Green Master Mix (Applied Biosystems), as previously described [23]. Briefly, samples had a final volume of 20 μl, containing 20 ng of total cDNA, 0.9 μM of the primer mix, and 10 μl of 2 × SYBR Green Master Mix. The thermal cycler protocol for real-time PCR included a first step of denaturation at 95 °C for 10 min followed by 40 repeated cycles of 95 °C for 15 s, 60 °C for 30 s, and 72 °C for 30 s for denaturation, primer annealing, and amplification, respectively. Primer sequences were designed using the Primer-BLAST tool (NCBI), based on the full mRNA sequences to find the optimal primers for amplification, and evaluated with the Oligo-Analyzer Tool (Integrated DNA Technologies) to ensure an optimal melting temperature (Tm) and avoid the formation of homo/heterodimers or non-specific structures that can interfere with the interpretation of the results. The primer sequences were designed specifically to span the junction between the exons. The primer sequences used were: *CHOP*, 5'-GGAAATGAA

GAGGAAGAATCAAAAAT-3' and 5'-GTTCTGGCT CCTCCTCAGTCA-3'; *GRP78/BiP*, 5'- ACTATTGCT GGCCTAAATGTTATGAG-3' and 5'-TTATCCAGG CCATAAGCAATAGC-3'; *SLC7A5/LAT1*, 5'-CAGTAC ATCGTGGCCCTGGT-3' and 5'-TGAGCAGCAGCA CGCAGAG-3'; *SLC38A1/SNAT1*, 5'-GTGTATGCTTTA CCCACCATTGC-3' and 5'- GCACGTTGTCATAGA ATGTCAAGT-3'; *SLC38A2/SNAT2*, 5'- ACGAAACAA TAAACACCACCTTAA-3' and 5'-AGATCAGAATTG GCACAGCATA-3'; and *TBP*, 5'-CCACTCACAGAC TCTCACAAC-3' and 5'-CTGCGGTACAATCCCAGA ACT-3'. Values were normalized to the expression levels of TATA-box-binding protein (TBP), and measurements were performed in triplicate. All changes in expression were normalized to the untreated control.

Immunoblotting

The isolation of total protein extracts was performed as described elsewhere [24]. For the isolation of total cell membranes, cell suspensions or placenta tissues were resuspended in 3 ml of ice-cold buffer I (250 mM sucrose, 20 mM HEPES, 5 mM NaN_3, 2 mM EGTA, 100 µM phenylmethylsulfonyl fluoride, 10 µM L-trans-epoxysuccinyl-leucylamido(4-guanidino)butane, 1 µM pepstatin A, and 1 µM leupeptin; pH 7.4) and homogenized. The resulting homogenate was centrifuged at 177,000 g for 1 h at 4 °C. The pellet, containing the total membranes, was resuspended in 50 µl of buffer I supplemented with a protease inhibitor and stored at -20 °C.

Immunoblotting was performed with antibodies against β-actin (Sigma, A5441), 4EBP1 (Cell Signalling, 9452), AKT (Cell Signalling, 9272), AMPKα (Cell Signalling, 2532), ATF4 (Santa Cruz Biotechnology, sc-200), ATF6 (Santa Cruz Biotechnology, sc-22799), BiP/GRP78 (Cell Signalling, 3183), CHOP (Cell Signalling, 2895), eIF2α (Cell Signalling, 9722), ERK1/2 (44/42 MAPK) (Cell Signalling, 9102), GADD34 (Cell Signalling, sc-46661), GAPDH (Millipore, MAB374), GRASP55 (Proteintech, 66,627–1-Ig), LAT1 (Cell Signalling, 5347), mTOR (Cell Signalling, 2972), Na–K-ATPase (Santa Cruz Biotechnology, sc-514614), NEDD4-L (Cell Signalling, sc-514954), phospho-4EBP1 $Thr^{37/46}$ (Cell Signalling, 2855), phospho-AKT Ser^{473} (Cell Signalling, 9271), phospho-AMPKα Thr^{172} (Cell Signalling, 2531), phospho-ERK1/2 (44/42 MAPK) Thr^{202}/Tyr^{204} (Cell Signalling, 9101), phospho-IRE Ser^{724} (Novus Biologicals, NB100-2323), phospho-mTOR Ser^{2448} (Santa Cruz Biotechnology, sc-101738), phospho-ribosomal protein S6 (Cell Signalling, 2211), ribosomal protein S6 (Cell Signalling, 2317), SNAT1 (Novus Biologicals, NBP-2–59311), SNAT2 (MBL, BMP081), and vinculin (Santa Cruz Biotechnology, sc-73614). Signal acquisition was conducted using the Bio-Rad ChemiDoc apparatus and the quantification of the immunoblot signal was performed with the Bio-Rad Image Lab software. The results for protein quantification were normalized to the levels of a control protein (GAPDH, β-actin, vinculin, or Na–K-ATPase) to avoid unwanted sources of variation.

Statistical analysis

Results are expressed as the mean ± SEM. Significant differences were assessed by either Student's t-test or one-way ANOVA, according to the number of groups compared, using the GraphPad Prism program (version 9.0.2) (GraphPad Software Inc., San Diego, CA, USA). When significant variations were found by ANOVA, Tukey's post-hoc test for multiple comparisons was performed only if F achieved a p value < 0.05. Differences were considered significant at $p < 0.05$.

Results

Maternal and newborn characteristics

Table 1 shows the anthropometric parameters of the women and their newborns according to the birth weight

Table 1 Characteristics of the studied population

	AGA ($n=20$)	SGA ($n=20$)	*P* value
Mothers			
Age	33.8 ± 1.2	31.9 ± 1.2	0.266
Height (cm)	163.7 ± 1.1	160.2 ± 1.3	0.051
Weight (Kg)[a]	63.1 ± 2.6	54.1 ± 1.7	**0.005**
BMI (Kg/m^2)	23.5 ± 0.8	21.0 ± 0.5	**0.016**
Ponderal index (Kg/m^3)	14.3 ± 0.5	13.1 ± 0.3	**0.045**
Gestational weight gain (Kg)	15.0 ± 1.3	12.3 ± 0.8	0.084
Newborns			
Sex (% females)	50	50	
Gestational age (weeks)	39.8 ± 0.2	38.8 ± 0.4	**0.029**
Caesarean section (%)	5	35	**0.018**
Placental weight (g)	554 ± 13	474 ± 10	**< 0.0001**
Birth weight (Kg)	3.3 ± 0.1	2.3 ± 0.1	**< 0.0001**
Birth length (cm)	50.0 ± 0.4	46.1 ± 0.4	**< 0.0001**
Ponderal index (Kg/m^3)	26.7 ± 0.5	24.0 ± 0.3	**< 0.0001**
Endocrine-metabolic variables			
HOMA-IR	0.6 ± 0.1	0.8 ± 0.4	0.515
IGF-1 (ng/mL)	59.6 ± 4.8	34.6 ± 2.5	**< 0.0001**
HMW-adiponectin (mg/L)	34.7 ± 2.7	36.7 ± 3.2	0.645
GLP-1 (pmol/L)	17.7 ± 2.3	27.0 ± 6.7	0.150
Body composition (DXA)[b]			
Fat mass (g)	617 ± 38	482 ± 37	**0.015**
Abdominal fat (g)	24.8 ± 2.7	18.1 ± 2.7	0.091
Lean mass (Kg)	3.1 ± 0.1	2.3 ± 0.1	**< 0.0001**

Results are mean ± sem

[a] Pre-gestational weight

[b] Assessed at 15 days of life

groups. No significant differences were observed between the appropriate-for-gestational-age (AGA) and SGA groups regarding maternal age at conception, maternal height, and the pregestational weight gain, while the maternal weight, ponderal index and BMI were reduced in the SGA group (Table 1). As expected, caesarean sections were more frequent among SGA babies and SGA infants at birth showed reductions in the length of gestation, placental weight, birth weight, birth length and ponderal index (Table 1). No differences were found in birth weight when the data were separated by sex (Fig. 1A). Fat mass and lean mass were reduced in the SGA group compared with the AGA group, whereas no differences were observed for abdominal fat (Table 1). Homeostatic model assessment for insulin resistance (HOMA-IR), high molecular weight (HMW)-adiponectin, and glucagon-like peptide 1 (GLP-1) did not show differences between the AGA and SGA groups (Fig. 1B, C and D). However, insulin-like growth factor 1 (IGF-1) levels were significantly lower in the SGA group (Fig. 1E).

SGA is associated with increased placental levels of CHOP and inhibition of the mTORC1 pathway

Since placental development differs between female and male newborns [25], we selected placental samples from newborn girls to examine the levels of proteins involved in ER stress. First, we assessed the protein levels of 78-kDa glucose-regulated protein (GRP78), which is also referred to as binding immunoglobulin protein (BiP). This protein is induced by ER stress and is a master regulator for this process through its role as a major ER chaperone with antiapoptotic properties, as well as its ability to control the activation of UPR signaling [8]. Placental GRP78 mRNA (Fig. 2A) and protein levels (Fig. 2B) were higher in the SGA than in the AGA group. Upon ER stress, GRP78 is released from the ER transmembrane, and IRE1, PERK, and ATF6 are activated. After the dissociation from GRP78, PERK dimerizes and undergoes autophosphorylation and activation. Activated PERK then phosphorylates eIF2α, which in turn increases the activity of ATF4, a transcription factor that upregulates the expression of CHOP. ATF6 is a large 90 kDa protein anchored at the ER membrane, which translocates to the Golgi apparatus in response to ER stress. Once in the Golgi, it is cleaved to release a smaller 50 kDa active protein, which enters the nucleus and acts as a transcription factor. No significant changes were observed in the levels of phospho-IRE1α and phospho-eIF2α (Fig. 2C, D). Likewise, ATF4 (Fig. 2E) or ATF6 (Fig. 2F) protein levels were not significantly different between the SGA and AGA groups. The expression of CHOP was not affected (Fig. 2G), while its protein levels were increased in the SGA group (Fig. 2H). Although *GADD34* transcription has been reported to be activated by ATF4 and CHOP [24], no significant changes were observed in its protein levels, which is likely to be the result of the reported transient increase in this protein under ER stress conditions [26] (Fig. 2I). Although ER stress has been associated with a reduction in the activity of AMP-activated protein kinase (AMPK) and the subsequent increase in the activity of extracellular signal-regulated kinase (ERK)1/2 [27], no differences were observed in the phosphorylated levels of AMPK and ERK1/2 between the AGA and SGA groups (Supplementary Fig. 1A, B), making it unlikely that these kinases were involved in the development of placental ER stress in the SGA group.

Placental mTORC1 activity was assessed by quantifying the phosphorylated levels of mTOR, 4E-BP1, and RPS6. Although mTOR phosphorylation was not different between the two groups, the phosphorylation of both 4E-BP1 and RPS6 was markedly reduced in the SGA group when compared with the AGA group (Fig. 3A-C), suggesting that the mTORC1 pathway was inhibited. By contrast, no differences were observed in the phosphorylated levels of Akt between the AGA and SGA groups, indicating that mTORC2 activity was not affected

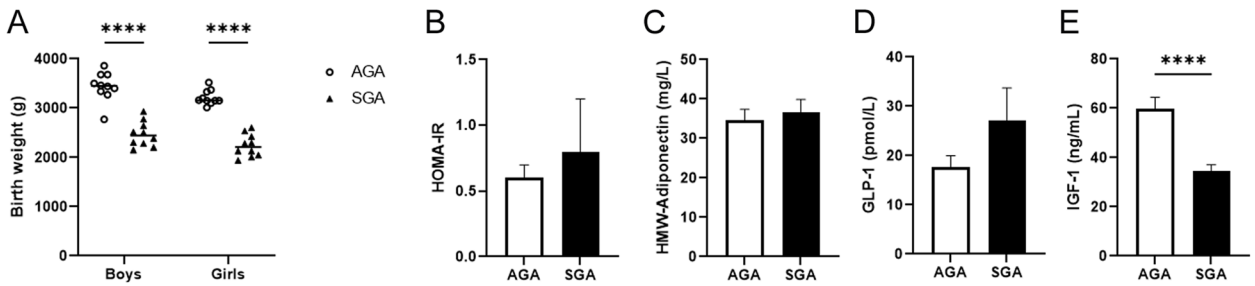

Fig. 1 Selected anthropometric and endocrine-metabolic parameters in infants born appropriate (AGA) or small for gestational age (SGA). **A** Birth weight of newborns split by sex ($N = 10$). Serum HOMA-IR (**B**), serum high molecular weight (HMW)-adiponectin (**C**), GLP-1 (**D**) and circulating insulin-like growth factor 1 (IGF-1) (**E**) ($N = 20$). Data are presented as the mean ± SEM. **** $p < 0.0001$ *versus* the AGA group. *P*-values determined by two-tailed unpaired Student's t-test

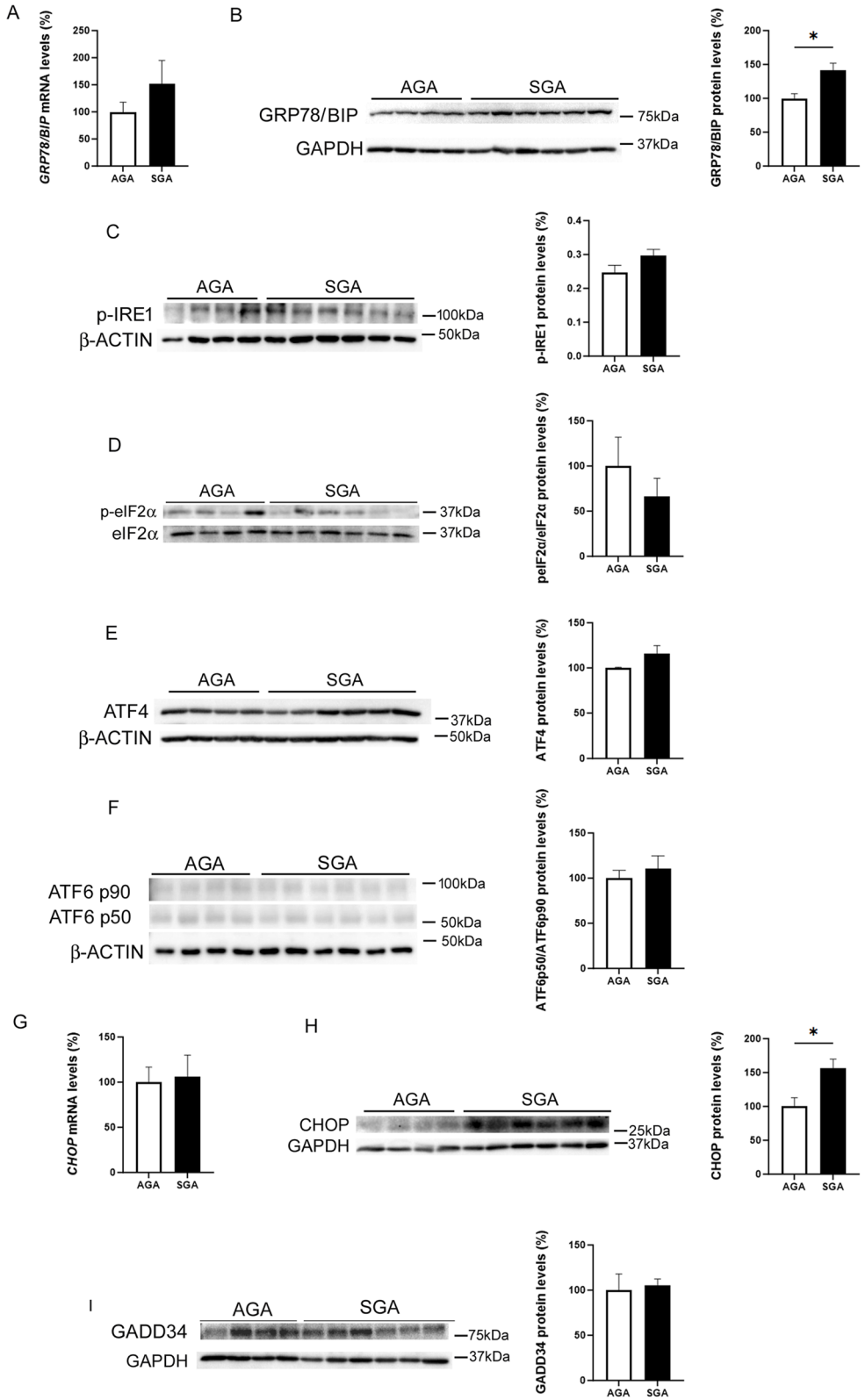

Fig. 2 Placental CHOP protein levels are increased in SGA newborns. Placental GRP78/BiP mRNA (**A**) and protein (**B**) levels in the AGA and SGA groups. Placental cell lysate extracts were assayed via western blot analysis with antibodies against phosphorylated IRE (**C**), phosphorylated eIF2α (**D**), ATF4 (**E**) and ATF6 (**F**). Placental CHOP mRNA (**G**) and protein (**H**) levels in the AGA and SGA groups. **I** GADD34 protein levels. Data ($N = 10$) are presented as the mean ± SEM. * $p < 0.05$ *versus* the AGA group. *P*-values determined by two-tailed unpaired Student's t-test

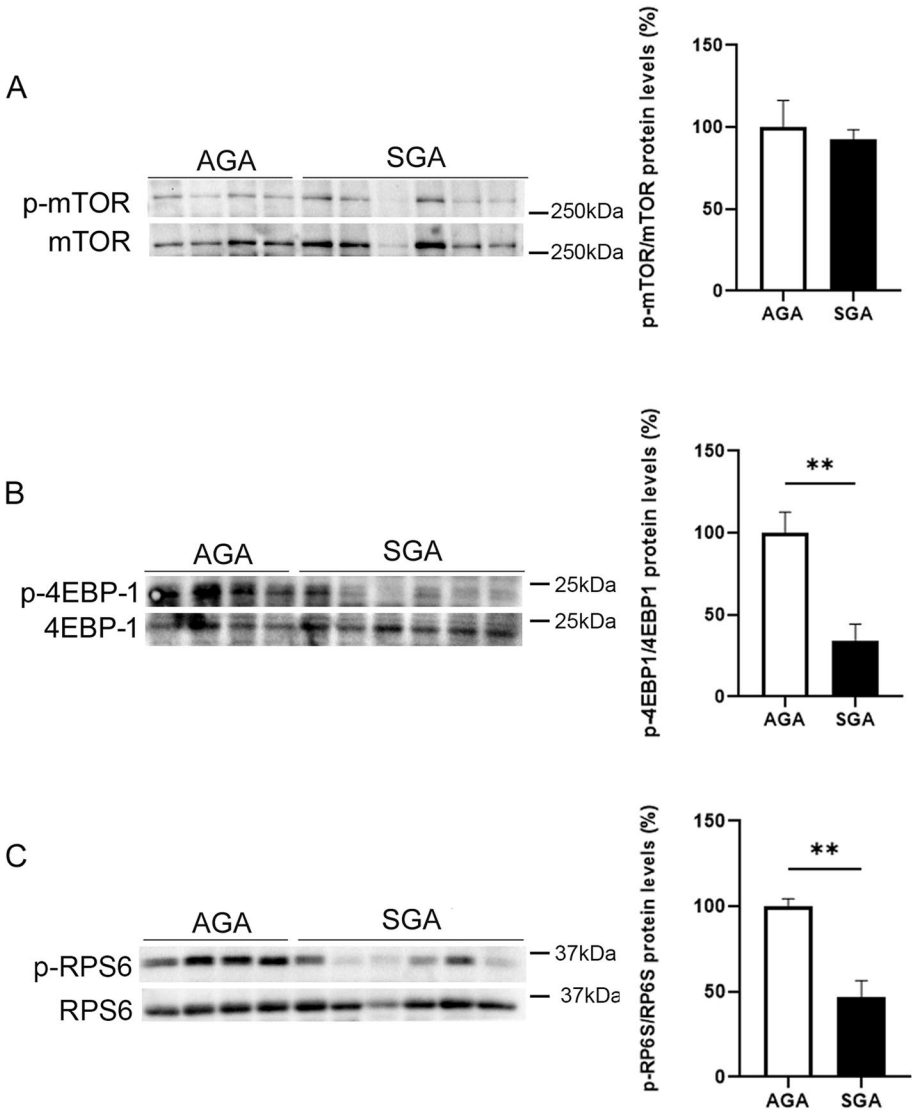

Fig. 3 mTORC1 activity is reduced in SGA newborns. Placental cell lysate extracts were assayed via western blot analysis with antibodies against total and phosphorylated mTOR (**A**), total and phosphorylated 4EBP-1 (**B**), and total and phosphorylated RPS6 (**C**). Data ($N = 10$) are presented as the mean ± SEM. ** $p < 0.01$ *versus* the AGA group. *P*-values determined by two-tailed unpaired Student's t-test

(Supplementary Fig. 1C). Overall, these findings indicate that the SGA condition is associated with increased levels of the ER stress marker CHOP and a reduction in mTORC1 activity.

Levels of placental amino acid transporters are altered in SGA newborns

Since a reduction in the activity of mTORC1 has been reported to inhibit trophoblast system A and system L amino acid transporter activities [20], we next evaluated whether the placentas from SGA newborns were accompanied by a reduction in the expression and protein levels of *SLC38A1* (encodes the protein SNAT1), *SLC38A2* (SNAT2), and *SLC7A5* (LAT1). Interestingly, the mRNA levels of *SLC38A1*, *SLC38A2*, and *SLC7A5* were significantly reduced in the placentas from SGA newborns when compared with the AGA group (Fig. 4A-C). When we examined the protein levels of SNAT1 in the isolated total membranes, we did not observe differences between the groups (Fig. 4D). Regarding SNAT2, it is worth mentioning that system A transporter activity depends on the processing/maturation and delivery of SNAT2 to the cell surface [28]. Antibodies against this protein detect two bands, one corresponding to the slower-migrating mature glycosylated transporter (~60 kDa) and the other corresponding to the faster-migrating immature SNAT2

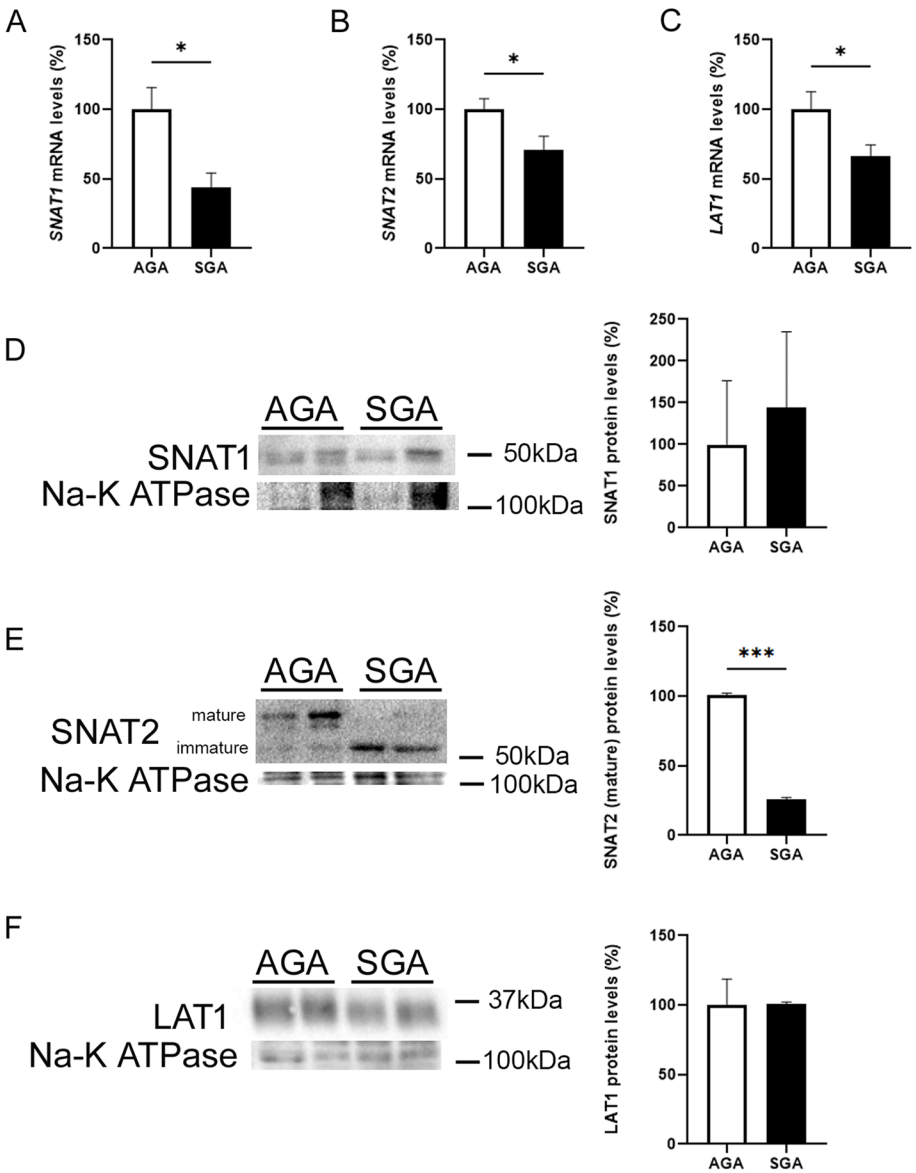

Fig. 4 Levels of the placental mature form of the SNAT2 protein are reduced in SGA newborns. Placental mRNA levels of SNAT1 (*SLC38A1*) (**A**), SNAT2 (*SLC38A2*) (**B**), and LAT1 (*SLC7A5*) (**C**). Placental membrane cell lysate extracts were assayed via western blot analysis with antibodies against SNAT1 (**D**), SNAT2 (**E**), and LAT1 (**F**). Data ($N = 10$) are presented as the mean ± SEM. * $p < 0.05$ and *** $p < 0.001$ *versus* the AGA group. *P*-values determined by two-tailed unpaired Student's t-test

protein that is partially processed in the ER (not or partially glycosylated, ~ 50 kDa) [29]. Interestingly, the SGA group showed a significant reduction in the levels of the mature SNAT2 protein, which was associated with increased levels of the immature form of this protein (Fig. 4E), thereby suggesting the involvement of post-transcriptional mechanisms. Finally, LAT1 protein levels were similar in both groups (Fig. 4F). Although the E3 ubiquitin-protein ligase neural precursor cell-expressed developmentally down-regulated protein 4-like 2 (NEDD4-2) (NEDD4L in humans) has been reported to be involved in the ubiquitination-mediated protein degradation of SNAT2 and LAT1 caused by mTORC1 inhibition [30], we did not observe differences in the levels of this ligase between the SGA and AGA newborns (Supplementary Fig. 1D), suggesting that this mechanism was unlikely to be involved. Since Golgi fragmentation has been reported to play a role in SNAT2 maturation [31] and given that this process is also essential for regulating the mTOR pathway [32], we examined the potential occurrence of

this alteration in the placenta. Golgi re-assembly and stacking protein 65 (GRASP65) [33] and GRASP55 [34] play essential roles in the assembly and membrane stacking of the Golgi apparatus and in maintaining the Golgi structure formation. However, phosphorylation of GRASP55 has been reported to induce Golgi fragmentation [35]. We thus investigated whether the placentas from SGA newborns showed increased levels of phosphorylated GRASP55. In Phos-tag gels, the GRASP55 protein migrates as a doublet, with the upper band representing the phosphorylated form [36]. However, the placentas from SGA infants did not show differences from those of the AGA newborns (Supplementary Fig. 1E), suggesting that Golgi fragmentation is not involved in the reduced mTORC1 activity.

GADD34 inhibition prevents the reduction of mTORC1 activity in BeWo cells

To assess the mechanisms by which increased CHOP levels are associated with the reductions in mTORC1 activity and in the levels of amino acid transporters, we used the human placental BeWo cell line, which originated from a choriocarcinoma [37] and has been widely used as an in vitro model to study placental amino acid transporters [38, 39]. Stimulation of cells with the ER stressor tunicamycin reduced the levels of phosphorylated RPS6, indicating that mTORC1 activity was inhibited (Fig. 5A). Notably, it has been reported that GADD34 links ER stress and mTOR inactivation in the liver [26]. In fact, GADD34-knockout mice show enhanced phosphorylated mTOR signaling upon nutrient depletion, suggesting that GADD34 negatively regulates mTOR [40]. Consistent with this, incubation of the BeWo cells with tunicamycin and the GADD34 inhibitor guanabenz restored the levels of phosphorylated RPS6, thus confirming that GADD34 inhibits mTORC1 signaling. Likewise, GADD34 inhibition by guanabenz attenuated the increase in CHOP protein levels caused by tunicamycin (Fig. 5B), which is consistent with the findings of previous studies [41]. Next, we examined the effects of tunicamycin and guanabenz on the levels of SNAT1 and SNAT2. SNAT1 protein levels were not affected either by tunicamycin or guanabenz (Fig. 5C). By contrast, tunicamycin caused a marked reduction in the levels of the mature form of SNAT2 and this reduction was not restored by guanabenz, suggesting that additional mechanisms are involved in the regulation of this amino acid transporter (Fig. 5D).

Discussion

The placenta is an organ with major endocrine and/or exocrine activity. It is more vulnerable to ER stress due to its constitutively high levels of protein translation. In fact, sustained ER stress results in compromised placental development and function [9]. Thus, it has been reported that the administration of a single dose of tunicamycin to pregnant dams causes lower placental and fetal weight, partly through placental abnormalities in nutrient transport [6]. Here, we examined placental levels of different ER stress markers in AGA and SGA newborns. A significant increase in CHOP protein levels was observed in the SGA group. The levels of GRP78 were also increased in the SGA group, while no changes were observed in the other ER stress markers. Thus, our findings suggest that low-level ER stress develops in the placentas from SGA newborns. It has been reported an increase in ER stress markers in human placenta when delivered at term by standard vaginal delivery compared to elective non-laboring caesarean section [42], with increases in the protein levels of p-eIF2α, GRP78 and X-box-binding protein 1 (XBP-1). Since caesarean sections were more frequent among SGA babies, differences in the delivery seem not to contribute to the changes in ER stress markers. The robust increase in CHOP protein levels observed in the placenta from SGA newborns might be not related to ER stress since the levels of ATF4 and ATF6, which upregulate CHOP expression under ER stress conditions, and the mRNA levels of CHOP, were not affected. The occurrence of increased CHOP levels in the placenta might be a crucial event in the reduction of birth weight by reducing mTORC1 activity, which in turn downregulates the levels of amino acid transporters. Interestingly, CHOP has been reported to upregulate GADD34 [24], which suppresses mTORC1 activity [26, 40]. Therefore, our findings suggest that the increased CHOP levels in the SGA group might contribute to the reduction in mTORC1 signaling via GADD34. mTOR is an important regulator of protein synthesis and mTOR signaling is suppressed by stressors, such as energy depletion, nutrient deprivation, and hypoxia, via the activation of tuberous sclerosis complex (TSC) 1/2. GADD34 has been reported to form a stable complex with TSC1/2, dephosphorylating TSC2, and leading to the inhibition of mTORC1 signaling [40, 43]. Consistent with this, we observed that the inhibition of GADD34 by guanabenz prevented the reduction in the mTORC1 activity caused by the ER stressor tunicamycin in BeWo cells. In addition, the reduction of the tunicamycin-mediated increase in CHOP protein levels caused by the inactivation of GADD34 by guanabenz is in accordance with the findings of a previous study conducted in HEK293T cells [41]. However, we did not observe an increase in GADD34 levels in the placentas from the SGA group compared with the AGA group. As mentioned above, GADD34 is transiently activated during ER stress [26], suggesting that this might be the reason for the absence of the increase in the levels of this protein. In line with this, a recent study has reported that GADD34

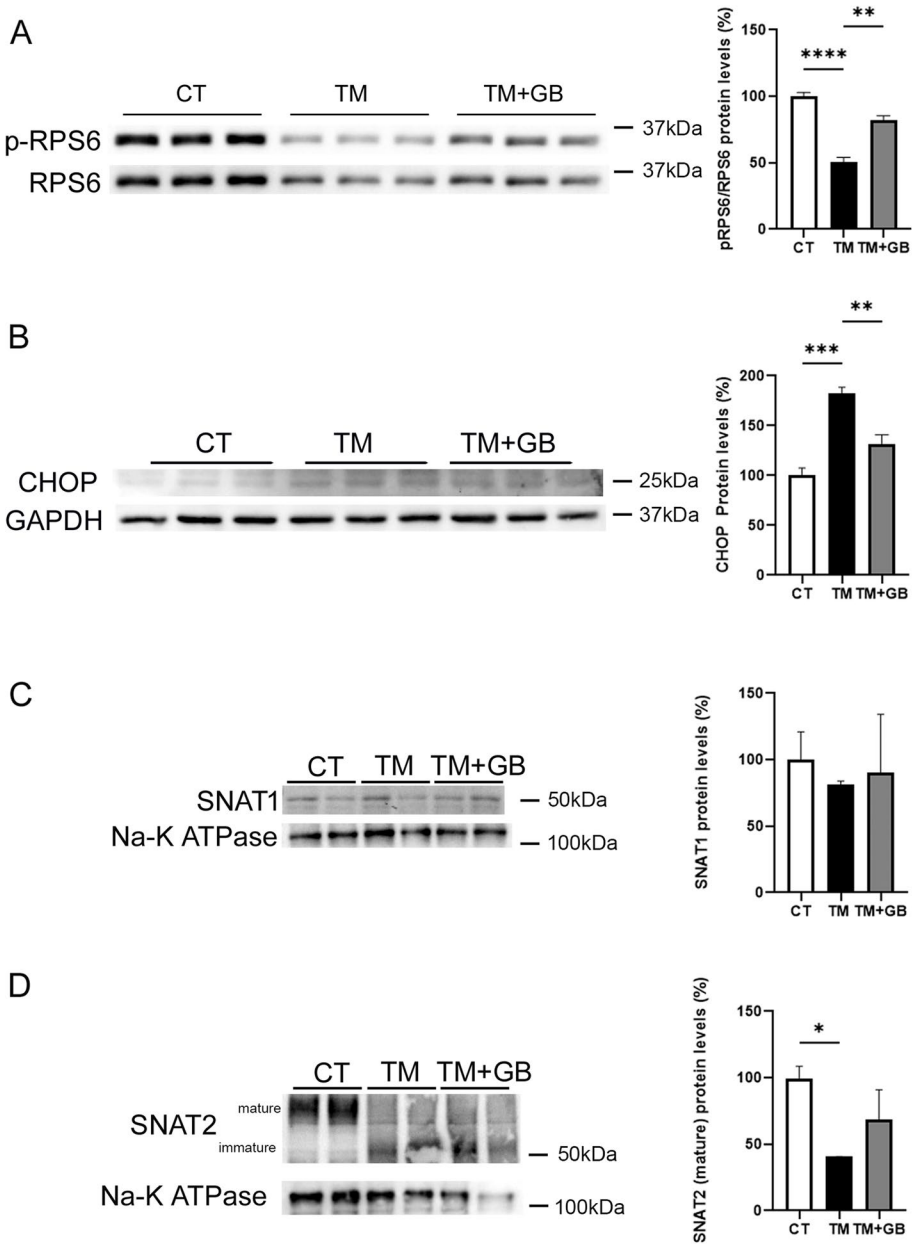

Fig. 5 GADD34 inhibition by guanabenz attenuates the reduction in mTORC1 activity and the increase in CHOP levels caused by ER stress in the human placental cell line BeWo. BeWo cells were stimulated with 0.1 µg/ml of tunicamycin (TM) either in the presence or absence of 5 µM guanabenz (GB) for 24 h and the protein levels of total and phosphorylated RPS6 (**A**), CHOP (**B**), SNAT1 (**C**), and SNAT2 (**D**) were assessed. Data ($N = 3$) are presented as the mean ± SEM. * $p < 0.05$, ** $p < 0.01$, *** $p < 0.001$ and **** $p < 0.0001$ *versus* the AGA group. *P*-values determined by two-tailed unpaired Student's t-test

is extremely sensitive to degradation, with an estimated half-life of approximately 37 min [44]. Overall, these findings suggest that the CHOP-GADD34 pathway plays a role in the reduction of mTOR activity in the placentas from SGA newborns.

A previous study by Yung et al. reported the first evidence that placental protein synthesis inhibition and ER stress play key roles in intrauterine growth restriction (IUGR) pathophysiology [9]. This study found that decreased AKT protein reduced mTOR signaling and impaired murine placental growth. In our study we did not find changes in AKT phosphorylation in the placentas from SGA newborns. Since IUGR reflects fetal distress and SGA could represent an attenuated subtype

of IUGR, these differences could be attributed to the different stages of progression of SGA and IUGR. Likewise, while Yung et al. [9] found a general induction of ER stress makers in IUGR, we only observed a robust increase in CHOP in the placentas from SGA newborns, which was accompanied by reduced mTORC1 activity and a significant decrease in the mature form of the amino acid transporter SNAT2. These findings suggest that CHOP upregulation might pull the trigger for the reduction in mTORC1 activity in the placentas from SGA newborns, while the contribution of high-grade ER stress might not be necessary. Finally, our in vitro data point to GADD34 as a potential player in the reduction in mTORC1 activity. Therefore, our findings point to the dysregulation of CHOP and of the processing/maturation of SNAT2 as key contributors to the SGA condition.

Inhibition of placental mTOR activity is associated with a reduced placental amino acid uptake and a lower birth weight [16, 45]. The SGA group exhibited a reduced expression of *SLC38A1*, *SLC38A2*, and *SLC7A5*. As mTORC1 can regulate *SLC38A2* and *SLC38A2* expression [46, 47], their reduction is likely to be the result of the inactivation of mTORC1 signaling in the placentas of the SGA group. However, the reduction in the expression of *SLC38A1* and *SLC7A5* was not accompanied by a decrease in their protein levels, suggesting that the reduction in transcription was not sufficient to attenuate their protein levels.

The regulation of *SLC38A2* transcription contributes to overall changes in SNAT2 protein levels, although post-transcriptional modifications involving the stabilization of the SNAT2 protein also play an important role [48]. A strong reduction was observed in the protein levels of the mature glycosylated SNAT2 protein in the SGA group, while the levels of the immature SNAT2 protein (not or partially glycosylated) were increased. Quantification of SNAT2 was conducted in total membrane fractions, but not in syncytiotrophoblast microvillous and basal plasma membranes, thereby preventing the study of post-translational modifications that affect the trafficking of placental SNAT2 to and from the plasma membrane. The E3 ubiquitin ligase NEDD4L has been previously implicated in the polyubiquitination and degradation of SNAT2 through the ubiquitin–proteasome system [28, 49]. However, we did not observe changes in the levels of the NEDD4L protein in the SGA group, suggesting that it was not involved in the changes observed for SNAT2. Likewise, although Golgi fragmentation may affect SNAT2 maturation [31] and controls the mTOR pathway [32], no changes were observed in the levels of phosphorylated GRASP55, a marker of this process. This therefore confirmed that Golgi fragmentation was not involved.

A limitation of this study is that it does not provide an explanation for the increase in CHOP protein in the placentas from SGA newborns independent of a high-level ER stress. Interestingly, protein N-glycosylation is a widespread post-translational modification. N-linked glycosylation is initiated in the ER and completed in the Golgi complex [50]. Alterations in glycosylation affect the proteins required for trophoblast function and have been associated with pathological conditions, including fetal growth restriction [51]. Remarkably, CHOP has been reported to be induced in the cells defective in N-glycosylation [52]. This suggests that most of the increase in the CHOP protein levels observed in the SGA newborns might be more related to defective glycosylation than to the increase in ER stress. Consistent with this, it has been reported that the increase in CHOP levels under Golgi stress is independent from the canonical UPR [53]. The strong reduction in the levels of the mature SNAT2 protein caused by the ER stressor tunicamycin in the BeWo cells seems to contradict the idea that ER stress is not the main stimulus leading to the increase in CHOP protein levels in the SGA group. However, tunicamycin is not considered a good inducer of ER stress because it blocks the assembly of N-linked glycans in the ER, causing the accumulation of the fastest migrating (immature) form of SNAT2, which is consistent with the inhibition of N-linked glycosylation [31]. Therefore, this suggests that the inhibition of glycosylation might be responsible for the reduction in the levels of the mature form of SNAT2 in the SGA group.

Another limitation of this study is that placental tissue used in our experiments contained decidua and the upper side of the chorionic villous proximal to the decidua. Since trophoblast villi (fetal tissue) and decidua (maternal tissue) are different tissues with respect to their origin, function and responses to various stimuli, the analysis of these samples may restrict the interpretation of the data.

Overall, here we unveil that the placentas from SGA newborns show low-level ER stress, with an increase in CHOP protein levels being accompanied by a reduction in mTORC1 activity and decreases in the expression of several amino acid transporters. The increase in CHOP levels contributes to the reduction of mTOR signaling in trophoblasts via GADD34. The placentas from SGA newborns also display increased levels of the immature form of SNAT2 and a consequent reduction in the levels of the mature form of this protein, which might be the result of the inhibition of N-linked glycosylation.

Conclusions

Collectively, these results suggest that the increase in CHOP levels and the reduction in the mature form of SNAT2 contribute to a reduction in amino acid transport and, eventually, to a decreased birth weight in humans.

Supplementary Information

The online version contains supplementary material available at https://doi.org/10.1186/s12964-023-01352-5.

Additional file 1: Supplementary Figure 1. Placental cell lysate extracts were assayed via western blot analysis with antibodies against total and phosphorylated AMPK (A), total and phosphorylated ERK1/2 (B), and total and phosphorylated Akt (C), NEDD4-L (D) and GRASP55 (E) in either a standard (bar graph quantification corresponds to this image) or a Phos-tag gel where the GRASP55 protein migrates as a doublet, with the upper band representing the phosphorylated form. The absence of a doublet in the samples from the SGA newborns as well as in the AGA newborns indicates the absence of phosphorylated GRASP55. Data ($N = 10$) are presented as the mean ± SEM.

Acknowledgements
We would like to thank the Language Services of the University of Barcelona for revising the manuscript.

Authors' contributions
E.B., M.D., A.C.R., J.B., M.P., J.J-A., M.Z., and A.R. performed the experiments; E.B., M.D., J.B., X.P., L.I., and M.V.-C. analyzed the data and reviewed the results; E.B., M.D., L.I., and M.V.-C. designed the experiments and reviewed the results; M.V.-C. was primarily responsible for writing the manuscript. All authors reviewed the manuscript.

Funding
This study was partly supported by the grants RTI2018-093999-B-I00 and PID2021-122116OB-I00 (M.V.-C.) from MCIN/AEI/10.13039/501100011033 and "ERDF, A Way of Making Europe". CIBER de Diabetes y Enfermedades Metabólicas Asociadas (CIBERDEM) is a Carlos III Health Institute project. Support was also received from the CERCA Programme/Generalitat de Catalunya.

Availability of data and materials
The source data for this study are available as a Source Data file or from the corresponding author upon reasonable request.

Declarations

Consent for publication
Not applicable.

Competing interests
The authors declare no competing interests.

Author details
[1]Unitat de Farmacologia, Facultat de Farmàcia I Ciències de L'Alimentació, Institute of Biomedicine of the University of Barcelona (IBUB), University of Barcelona, Av. Joan XXIII 27-31, 08028 Barcelona, Spain. [2]Spanish Biomedical Research Center in Diabetes and Associated Metabolic Diseases (CIBERDEM)-Instituto de Salud Carlos III, Madrid, Spain. [3]Pediatric Research Institute-Hospital Sant Joan de Déu, Esplugues de Llobregat, Spain. [4]Endocrinology, Pediatric Research Institute, Sant Joan de Déu Children's Hospital, Barcelona, Esplugues, Spain. [5]Instituto de Biología y Genética Molecular, Consejo Superior de Investigaciones Científicas, Valladolid, Spain.

Received: 21 June 2023 Accepted: 10 October 2023
Published online: 13 November 2023

References

1. Clayton PE, et al. Management of the child born small for gestational age through to adulthood: a consensus statement of the international societies of pediatric endocrinology and the growth hormone research society. J Clin Endocrinol Metab. 2007;92:804–10. https://doi.org/10.1210/jc.2006-2017.
2. Hong YH, Chung S. Small for gestational age and obesity related comorbidities. Ann Pediatr Endocrinol Metab. 2018;23:4–8. https://doi.org/10.6065/apem.2018.23.1.4.
3. Thorne J, et al. Placental pathology associated with small for gestational age infants. Ir Med J. 2014;107:249–50.
4. Chisholm KM, Folkins AK. Placental and clinical characteristics of term small-for-gestational-age neonates: a case-control study. Pediatr Dev Pathol. 2016;19:37–46. https://doi.org/10.2350/15-04-1621-OA.1.
5. Battarbee AN, et al. Association of Isolated Single Umbilical Artery with Small for gestational age and preterm birth. Obstet Gynecol. 2015;126:760–4. https://doi.org/10.1097/AOG.0000000000001037.
6. Kawakami T, et al. Prolonged endoplasmic reticulum stress alters placental morphology and causes low birth weight. Toxicol Appl Pharmacol. 2014;275:134–44. https://doi.org/10.1016/j.taap.2013.12.008.
7. Mizuuchi M, et al. Placental endoplasmic reticulum stress negatively regulates transcription of placental growth factor via ATF4 and ATF6beta: implications for the pathophysiology of human pregnancy complications. J Pathol. 2016;238:550–61. https://doi.org/10.1002/path.4678.
8. Salvado L, et al. Targeting endoplasmic reticulum stress in insulin resistance. Trends Endocrinol Metab. 2015;26:438–48. https://doi.org/10.1016/j.tem.2015.05.007.
9. Yung HW, et al. Evidence of placental translation inhibition and endoplasmic reticulum stress in the etiology of human intrauterine growth restriction. Am J Pathol. 2008;173:451–62. https://doi.org/10.2353/ajpath.2008.071193.
10. Yung HW, et al. Endoplasmic reticulum stress exacerbates ischemia-reperfusion-induced apoptosis through attenuation of Akt protein synthesis in human choriocarcinoma cells. FASEB J. 2007;21:872–84. https://doi.org/10.1096/fj.06-6054com.
11. Yung HW, et al. Placental endoplasmic reticulum stress in gestational diabetes: the potential for therapeutic intervention with chemical chaperones and antioxidants. Diabetologia. 2016;59:2240–50. https://doi.org/10.1007/s00125-016-4040-2.
12. Roos S, et al. Placental mTOR links maternal nutrient availability to fetal growth. Biochem Soc Trans. 2009;37:295–8. https://doi.org/10.1042/BST0370295.
13. Glazier JD, et al. Association between the activity of the system A amino acid transporter in the microvillous plasma membrane of the human placenta and severity of fetal compromise in intrauterine growth restriction. Pediatr Res. 1997;42:514–9. https://doi.org/10.1203/00006450-199710000-00016.
14. Jansson T, et al. Alterations in the activity of placental amino acid transporters in pregnancies complicated by diabetes. Diabetes. 2002;51:2214–9. https://doi.org/10.2337/diabetes.51.7.2214.
15. Jansson N, et al. Down-regulation of placental transport of amino acids precedes the development of intrauterine growth restriction in rats fed a low protein diet. J Physiol. 2006;576:935–46. https://doi.org/10.1113/jphysiol.2006.116509.
16. Rosario FJ, et al. Maternal protein restriction in the rat inhibits placental insulin, mTOR, and STAT3 signaling and down-regulates placental amino acid transporters. Endocrinology. 2011;152:1119–29. https://doi.org/10.1210/en.2010-1153.
17. Mackenzie B, Erickson JD. Sodium-coupled neutral amino acid (System N/A) transporters of the SLC38 gene family. Pflugers Arch. 2004;447:784–95. https://doi.org/10.1007/s00424-003-1117-9.
18. Norberg S, et al. Intrauterine growth restriction is associated with a reduced activity of placental taurine transporters. Pediatr Res. 1998;44:233–8. https://doi.org/10.1203/00006450-199808000-00016.
19. Jansson T, et al. Placental transport of leucine and lysine is reduced in intrauterine growth restriction. Pediatr Res. 1998;44:532–7. https://doi.org/10.1203/00006450-199810000-00011.
20. Rosario FJ, et al. Mammalian target of rapamycin signalling modulates amino acid uptake by regulating transporter cell surface abundance in

primary human trophoblast cells. J Physiol. 2013;591:609–25. https://doi.org/10.1113/jphysiol.2012.238014.
21. Ferrández-Longas A, Mayayo E, Labarta JI, Bagué L, Puga B, Rueda C. Estudio longitudinal de crecimiento y desarrollo. Centro Andrea Prader. Zaragoza 1980–2002. (Patrones de crecimiento y desarrollo en España); 2004.
22. Diaz M, et al. Placental and cord blood methylation of genes involved in energy homeostasis: association with fetal growth and neonatal body composition. Diabetes. 2017;66:779–84. https://doi.org/10.2337/db16-0776.
23. Salvado L, et al. PPARbeta/delta prevents endoplasmic reticulum stress-associated inflammation and insulin resistance in skeletal muscle cells through an AMPK-dependent mechanism. Diabetologia. 2014;57:2126–35. https://doi.org/10.1007/s00125-014-3331-8.
24. Marciniak SJ, et al. CHOP induces death by promoting protein synthesis and oxidation in the stressed endoplasmic reticulum. Genes Dev. 2004;18:3066–77. https://doi.org/10.1101/gad.1250704.
25. Bulka CM, et al. Sex-based differences in placental DNA methylation profiles related to gestational age: an NIH ECHO meta-analysis. Epigenetics. 2023;18:2179726. https://doi.org/10.1080/15592294.2023.2179726.
26. Holczer M, et al. GADD34 keeps the mTOR pathway inactivated in endoplasmic reticulum stress related autophagy. PLoS ONE. 2016;11:e0168359. https://doi.org/10.1371/journal.pone.0168359.
27. Du J, et al. Inhibitory crosstalk between ERK and AMPK in the growth and proliferation of cardiac fibroblasts. Biochem Biophys Res Commun. 2008;368:402–7. https://doi.org/10.1016/j.bbrc.2008.01.099.
28. Nardi F, et al. Proteasomal modulation of cellular SNAT2 (SLC38A2) abundance and function by unsaturated fatty acid availability. J Biol Chem. 2015;290:8173–84. https://doi.org/10.1074/jbc.M114.625137.
29. Hyde R, et al. Insulin promotes the cell surface recruitment of the SAT2/ATA2 system A amino acid transporter from an endosomal compartment in skeletal muscle cells. J Biol Chem. 2002;277:13628–34. https://doi.org/10.1074/jbc.M108609200.
30. Rosario FJ, et al. Regulation of amino acid transporter trafficking by mTORC1 in primary human trophoblast cells is mediated by the ubiquitin ligase Nedd4-2. Clin Sci (Lond). 2016;130:499–512. https://doi.org/10.1042/CS20150554.
31. Krokowski D, et al. GADD34 function in protein trafficking promotes adaptation to hyperosmotic stress in human corneal cells. Cell Rep. 2017;21:2895–910. https://doi.org/10.1016/j.celrep.2017.11.027.
32. Gosavi, P. et al. The Golgi ribbon in mammalian cells negatively regulates autophagy by modulating mTOR activity. J Cell Sci. 2018;131. https://doi.org/10.1242/jcs.211987
33. Wang Y, et al. A direct role for GRASP65 as a mitotically regulated Golgi stacking factor. EMBO J. 2003;22:3279–90. https://doi.org/10.1093/emboj/cdg317.
34. Xiang Y, Wang Y. GRASP55 and GRASP65 play complementary and essential roles in Golgi cisternal stacking. J Cell Biol. 2010;188:237–51. https://doi.org/10.1083/jcb.200907132.
35. Ireland S, et al. Cytosolic Ca(2+) Modulates Golgi Structure Through PKCalpha-Mediated GRASP55 Phosphorylation. iScience. 2020;23:100952. https://doi.org/10.1016/j.isci.2020.100952.
36. Nuchel J, et al. An mTORC1-GRASP55 signaling axis controls unconventional secretion to reshape the extracellular proteome upon stress. Mol Cell. 2021;81:3275–93. https://doi.org/10.1016/j.molcel.2021.06.017. e3212.
37. Pattillo RA, Gey GO. The establishment of a cell line of human hormone-synthesizing trophoblastic cells in vitro. Cancer Res. 1968;28:1231–6.
38. Eaton BM, Sooranna SR. In vitro modulation of L-arginine transport in trophoblast cells by glucose. Eur J Clin Invest. 1998;28:1006–10. https://doi.org/10.1046/j.1365-2362.1998.00409.x.
39. Eaton BM, Sooranna SR. Transport of large neutral amino acids into BeWo cells. Placenta. 2000;21:558–64. https://doi.org/10.1053/plac.2000.0507.
40. Uddin MN, et al. Gadd34 induces autophagy through the suppression of the mTOR pathway during starvation. Biochem Biophys Res Commun. 2011;407:692–8. https://doi.org/10.1016/j.bbrc.2011.03.077.
41. Marton M, et al. A systems biological analysis of the ATF4-GADD34-CHOP regulatory triangle upon endoplasmic reticulum stress. FEBS Open Bio. 2022;12:2065–82. https://doi.org/10.1002/2211-5463.13484.
42. Veerbeek JH, et al. Endoplasmic reticulum stress is induced in the human placenta during labour. Placenta. 2015;36:88–92. https://doi.org/10.1016/j.placenta.2014.11.005.
43. Watanabe R, et al. GADD34 inhibits mammalian target of rapamycin signaling via tuberous sclerosis complex and controls cell survival under bioenergetic stress. Int J Mol Med. 2007;19:475–83.
44. Klein P, et al. Temporal control of the integrated stress response by a stochastic molecular switch. Sci Adv. 2022;8:eabk2022. https://doi.org/10.1126/sciadv.abk2022.
45. Dimasuay KG, et al. Inhibition of placental mTOR signaling provides a link between placental malaria and reduced birthweight. BMC Med. 2017;15:1. https://doi.org/10.1186/s12916-016-0759-3.
46. Deldicque L, et al. ER stress induces anabolic resistance in muscle cells through PKB-induced blockade of mTORC1. PLoS ONE. 2011;6:e20993. https://doi.org/10.1371/journal.pone.0020993.
47. Liu XM, et al. Platelet-derived growth factor stimulates LAT1 gene expression in vascular smooth muscle: role in cell growth. FASEB J. 2004;18:768–70. https://doi.org/10.1096/fj.03-0886fje.
48. Hyde R, et al. Distinct sensor pathways in the hierarchical control of SNAT2, a putative amino acid transceptor, by amino acid availability. J Biol Chem. 2007;282:19788–98. https://doi.org/10.1074/jbc.M611520200.
49. Hatanaka T, et al. Regulation of amino acid transporter ATA2 by ubiquitin ligase Nedd4-2. J Biol Chem. 2006;281:35922–30. https://doi.org/10.1074/jbc.M606577200.
50. Yung HW, et al. Perturbation of placental protein glycosylation by endoplasmic reticulum stress promotes maladaptation of maternal hepatic glucose metabolism. iScience. 2023;26:105911. https://doi.org/10.1016/j.isci.2022.105911.
51. Sgambati E, et al. Lectin histochemistry in the human placenta of pregnancies complicated by intrauterine growth retardation based on absent or reversed diastolic flow. Placenta. 2002;23:503–15. https://doi.org/10.1053/plac.2002.0793.
52. Wang XZ, et al. Signals from the stressed endoplasmic reticulum induce C/EBP-homologous protein (CHOP/GADD153). Mol Cell Biol. 1996;16:4273–80. https://doi.org/10.1128/MCB.16.8.4273.
53. Eisenberg-Lerner A, et al. Golgi organization is regulated by proteasomal degradation. Nat Commun. 2020;11:409. https://doi.org/10.1038/s41467-019-14038-9.

Publisher's Note